BIO-INSPIRED ROBOTIC CONTROL SCHEMES USING BIOLOGICALLY PLAUSIBLE NEURAL STRUCTURES

Niceto Rafael Luque Sola

A Thesis submitted for the degree of:

"Philosophiae Doctor (Ph. D.)"

"In Automation & Electronics"

University of Granada

2013

Declaración

Dr. Eduardo Ros Vidal, Catedrático de Universidad del Departamento de Arquitectura y Tecnología de Computadores de la Universidad de Granada, y Dr. Richard Rafael Carrillo Sánchez, investigador contratado bajo el Programa Juan de la Cierva del Departamento de Arquitectura de Computadores y Electrónica de la Universidad de Almería,

CERTIFICAN:

Que la memoria titulada " Bio-Inspired Robotic Control Schemeses Using Biologically Plausible Neural Structures", ha sido realizada por D. Niceto Rafael Luque Sola bajo nuestra dirección en el Departamento de Arquitectura y Tecnología de Computadores de la Universidad de Granada para optar al grado de Doctor por la Universidad de Granada.

Granada, de Mayo de 2013

Fdo. Eduardo Ros Vidal

Fdo. Richard Rafael Carrillo Sánchez

TABLE OF CONTENTS

ABSTRACT

The cerebellar circuitry belonging to the Central Nervous System (CNS) consists of a set of neurons and synapses that present rich dynamical properties. In the field of traditional artificial neural network (ANN), most approaches are based on very simplistic connectivity rules between very simplified neuron models which produce an output in each propagation cycle (the time domain is not introduced in the simulation). Nevertheless, if we want to study computational neuroscience and consider biological nervous systems, we need a higher degree of detail. For instance the cerebellum does not consist only of very complex neurons in a sophisticated network but also this cerebellum network deals with non-continuous signals called spikes. Hence, it is clear that in order to understand the foundations of cerebellar processing (from a computational neuroscience perspective); it is mandatory to work with a realistic cerebellar spiking neural network.

In the case of the Cerebellum, its functionality has been studied for decades and it is well accepted that it plays a fundamental role in human motor control loops by means of regulating movement and also cognitive processes. The cerebellum is able to dynamically regulate its activity (it can present a highly non-linear behavior) and it is also able to tune its synaptic connections by distributed and heterogeneous forms of synaptic plasticity. Along this thesis, we have focused on studying the cerebellar functionality and how it is related with its structure (network topology), neuron models and synaptic adaptation mechanisms. To that aim, we have developed a biologically inspired cerebellar like network (based on neurophysiological findings) embedded into a robotic system in order to evaluate circuit functioning under closed-loop conditions. According to the embodiment concept, we have developed a complete framework that allows researchers to contrast different experimental cerebellar hypotheses.

This work was partly supported by the Spanish Subprogram FPU 2007 (MICINN), and the EU projects SENSOPAC (IST-028056), and REALNET (IST-270434).

RESUMEN

Como es bien sabido, la circuitería cerebelar perteneciente al sistema nervioso central está conformada por una serie de neuronas y sinapsis que presentan un conjunto de propiedades dinámicas tremendamente ricas. Si se echa un vistazo a lo largo de la literatura concerniente a redes neuronales artificiales tradicionales, es fácil comprobar que la mayoría de ellas están basadas en reglas de conectividad de algún modo simplistas entre modelos de neurona simplificados, los cuales son evaluados en ciclos de propagación (la dimensión de tiempo no está contemplada en la simulación). Sin embargo, lo que encontramos en el cerebelo no sólo se corresponde con neuronas de extraordinaria complejidad dinámica insertas en una sofisticada red, sino también se puede constatar un tratamiento por parte de dicha red cerebelar de señales no continuas, señales llamadas impulsos (impulsos eléctricos) o en su forma anglosajona "spikes". Por lo tanto, resulta evidente que, con el fin de entender los fundamentos de la circuitería cerebelar, resulta imprescindible implementar una red neuronal cerebelar realista donde las características funcionales del cerebelo se vean reflejadas.

Por otro lado, la comunidad científica asume que el cerebelo juega un rol fundamental en los circuitos de control motor humano mediante la regulación del movimiento, en los procesos cognitivos y en el control de emociones. El cerebelo es capaz de regular de forma dinámica su actividad (que puede presentar un comportamiento fuertemente no lineal) siendo capaz también de modificar sus conexiones sinápticas mediante diferentes formas de plasticidad sináptica distribuida. A lo largo de esta tesis, hemos tratado de arrojar algo de luz sobre la funcionalidad (no solo estructural) del cerebelo, un campo que, a día de hoy, aún sigue siendo poco conocido. Con este objetivo, hemos construido una red neuronal cerebelar bio-inspirada (haciendo uso de hallazgos neurofisiológicos) la cual se integra en un sistema robótico con el fin de evaluar su funcionamiento bajo condiciones de control en bucle cerrado, desarrollándose para ello un completo entorno de trabajo que permite a distintos tipo de investigadores contrastar diferentes hipótesis cerebelares experimentales.

Este trabajo ha sido parcialmente cofinanciado tanto por el programa español FPU 2007 (MICINN), como por los proyectos europeos SENSOPAC (IST-028056) y REALNET (IST-270434).

ACKNOWLEDGEMENTS

I would like to show my gratitude to my supervisor, Prof. Eduardo Ros, who shared with me a lot of his expertise and research insight. He quickly became for me in the paradigm of a successful researcher to follow. I would also like to thank Dr. Richard Carrillo, whose sharp intelligence has often served to give me a sense of direction during my PhD studies.

It has been an honor for me to work shoulder to shoulder with my college and also friend Jesús Garrido. There is no doubt that thanks to his hard work this thesis has come to light. His friendship has made Science more human in my eyes.

I thank my colleagues from CIE/CITIC Jarno Ralli, Mauricio Vanegas, Silvia Tolu, Juanma Gomez, Francisco Barranco, Jose Miguel Urquiza, Matteo Tomassi, Juan Pedro Cobos, Sara Granados, Luca Leonardo Bologna, Jean Baptiste Passot, Karl Pauwels, Leonardo Rubio, Juanlu Jiménez, Jose Luís Gutiérrez, whom I have shared much more than just a workplace. Moreover I would like to thank my friends in college from my lovely Córdoba, Mario, Paco y Rafa whom I have spent almost an entire life sharing experiences.

I wish to thank my brother and sister for providing a loving environment for me.

I owe my loving thanks to my girlfriend Beatriz, without her optimism, encouragement, understanding and common sense, it would have been impossible for me to finish this thesis. She brought me some light to the darkness.

Last but not least, I wish to thank my parents, Niceto R. Luque and Francisca Sola. They raised me, supported me, taught me, and loved me. I owe you all what I am; to them I dedicate this thesis.

Satius est supervacua scire quam nihil.

(Seneca the younger; Letter LXXXVIII: On liberal and vocational studies.)

FIGURE LIST

TABLES

GLOSSARY

Axon - extension from the cell that carries nerve impulses from the cell body to other neurons.

Afferent fibers - any of the nerve fibers that convey impulses to a ganglion or to a nerve center in the brain or spinal cord.

Basal ganglia - group of neural structures involved in movement control, procedural learning and cognitive functions; located in the forebrain (telencephalon).

Brain - the major organ of the central nervous system. It exerts a centralized control over the organs of the body.

Brainstem - also known as the hindbrain; region of the brain that consists of the midbrain (tectum, tegmentum), ponds, and medulla; responsible for functions such as breathing, heart rate, and blood pressure.

Cell Body - region of the neuron defined by the presence of a nucleus.

Central nervous system (CNS) - portion of the nervous system that includes the brain and the spinal cord.

Cerebellum - structure located in the back of the brain (dorsal to the pons) involved in central regulation of movement, such as basic movement, balance, and posture; comes from the Latin word meaning "little brain"; is divided into two hemispheres and has a cortex.

Cerebral cortex - the outer covering of the cerebral hemispheres consisting mostly of nerve cell bodies and branches; involved in functions such as thought, voluntary movement, language, reasoning, and perception; the right and left sides of the cerebral cortex are connected by a thick band of nerve fibers (corpus callosum); highly grooved or "gyrencephalic" in mammals.

Climbing fibers (CFs) - arise from cells in the inferior olive and provide an extraordinarily strong, 'climbing' multi-synaptic contact on Purkinje cells. However, branches of the olivo-cerebellar axon contact not only Purkinje cells but also other neuron types of the cerebellum.

Control system - a term that was originally used to refer to a mechanical or chemical system equipped with a mechanism for manipulating an object or regulating a process. The term now broadly applies to an informational, biological, neural, psychological or social system.

Controlled object - in an object manipulation scenario, the controlled object is conceived as plant+object under manipulation. It translates motor commands in actual movements of plant+object (in a manipulation task).

Controller - a key part of a control system, a controller converts a given instruction into a command. For example, the brain converts an instructed spatial position of a target into a command, which consists of signals in the nerves that innervate muscles.

Deep Cerebellar Nuclei (DCN) - the nuclei at the base of the cerebellum that relay information from the cerebellar cortex to the thalamus.

Dendrite - one of the extensions of the cell body that are reception surfaces of the neuron.

Diencephalon - part of the midbrain; consists of the thalamus and hypothalamus.

Dorsal - anatomical term referring to structures toward the back of the body or top of the brain.

Efferent fibers - nerve fibers that take messages from the brain to the peripheral nervous system; motor fibers are efferent.

Engineering control theory - a branch of engineering science concerned with the control of dynamic systems (including aircraft, chemical reactions and robots).

Error signals - signals representing errors in a system. The errors are discrepancies in the performance of a control system from either the instruction (consequence errors) or the prediction by an internal model (internal errors).

Eyeblink conditioning - in this experiment, a conditional stimulus (CS) is presented a certain time before an unconditional stimulus (US). Typically, a tone is used as a CS, and an air puff directed to one eye as the US. After repeating this training for some iterations, the subject learns to close its eye (called conditioned response, CR) a little time after the CS and just before the air puff reaches the eye).

Forebrain - the frontal division of the brain which contains cerebral hemispheres, the thalamus, and the hypothalamus.

Glial cells - non-neuronal brain cells that provide structural, nutritional, and other supports to the brain.

Golgi cells (GoCs) - inhibitory interneurons in the granular layer that synapse with granule cells. They receive excitatory input from mossy fibers and parallel fibers.

Granule cells (GrCs) - integrate excitatory mossy fiber inputs from external sources and local inhibitory input from Golgi cells.

Gray matter - areas of the brain that are dominated by cell bodies and have no myelin covering (in contrast to white matter).

Gyrencephalic - when the cerebral cortex is highly folded and convoluted (due to gyri and sulci).

Gyrus - raised portion of convoluted brain surface.

Hindbrain - the rear division of the brain includes the cerebellum, ponds, and medulla (also called the rhomb encephalon).

Hippocampus - the portion of the cerebral hemispheres in basal medial part of the temporal lobe. This part of the brain is important for learning and memory for converting short term memory to more permanent memory, and for recalling spatial relationships in the world about us.

Hypothalamus - part of the diencephalon, ventral to the thalamus. The structure is involved in functions including homeostasis, emotion, thirst, hunger, circadian rhythms, and control of the autonomic nervous system. In addition, it controls the pituitary.

Internal model - a functional dummy of a body part or of a mental representation in the cerebral cortex. Internal models are encoded in the neuronal circuitry of the cerebellum and mimic the essential properties of a body part or mental representation.

Inferior olivary nucleus (IO) - Prominent nucleus in the ventral medulla located just lateral and dorsal to the medullary pyramids; source of climbing fibers that provide a critical input to the cerebellum, involved in Purkinje cell plasticity and motor learning

Kinesthesia - feedback from muscle spindles (a more specific term than proprioception)

Lateral - anatomical term meaning toward the side (versus medial).

Long-term potentiation (LTP) - the prolonged strengthening of synaptic transmission, which is thought to be involved in learning and memory formation.

Long-term depression (LTD) - a persistent reduction of synaptic strength caused, for example, by specific neural activity.

Medulla Oblongata/ Myelencephalon - this structure is the caudal-most part of the brain stem, between the pons and spinal cord. It is responsible for maintaining vital body functions, such as breathing and heart rate. See overall NS organization.

Metencephalon - subdivision of the hindbrain, which includes the cerebellum and pons.

Midbrain/ Mesencephalon - middle division of the brain, which includes the tectum and tegmentum; involved in functions such as vision, hearing, eye movement, and body movement.

Molecular layer - the outermost layer of the cerebellar cortex; it contains the parallel fibers, Purkinje cell dendritic trees, stellate cells and basket cells.

Mossy fibers (MFs) - provide the bulk of the afferent input to the cerebellum and originate from numerous sources in the spinal cord, brain stem and pontine nuclei.

Motor cortex - a region of the cerebral cortex whose activity influences muscular movements; involved in planning and control of movement; found in the frontal lobe.

Myelencephalon - caudal part of the hindbrain includes the medulla oblongata.

Microzone - a narrow longitudinal strip (a sagittal region of Purkinje cells within a cerebellar zone that is approximately 50 to 100 μm wide) of the cerebellar cortex, just a few Purkinje cells wide but up to hundreds of Purkinje cells long, in which all the Purkinje cells receive climbing fibers driven by the same input (climbing fibers from a cluster of coupled olivary neurons).

Myelin - fatty insulation around an axon which improves the speed of conduction of nerve impulses.

Nervous System - extends throughout the entire body and connects every organ to the brain; can be divided into the central nervous system (CNS) and the peripheral nervous system (PNS); the basic building blocks of the nervous system are nerve cells or neurons.

Neuron - the basic building block of the brain; these cells receive input from other nerve cells and distribute information to other neurons; the information integration underlies the simplest and most complex of our thoughts and behaviors.

Neuroscience - the science of the nervous system.

Neurotransmitter - chemical substance which is released by the presynaptic neuron at synapses that transmits information to the next neuron.

Occipital lobe - the posterior lobe of the brain; involved with vision (the "occipital cortex" is also referred to as the "visual cortex").

Parallel fibers (PFs) - arise from granule cells and provide excitatory input to Purkinje cells and molecular layer interneurons.

Parietal lobe - located behind the frontal cortex (and central sulcus); involved in perception of stimuli related to touch, pressure, temperature, and pain.

Peripheral nervous system (PNS) - portion of the nervous system that includes all the nerves and neurons OUTSIDE the brain and spinal cord.

Pons - part of the metencephalon in the hindbrain. It relays signals related to respiration, sleep, hearing, arousal, etc. For example; information from the ear first enters the brain in the pons. It has parts involved in consciousness and dreaming. Some structures within the pons are linked to the cerebellum, thus are involved in movement and posture.

Prefrontal cortex - the most anterior region of the frontal cortex; involved in problem solving, emotion, and complex thought.

Presynaptic - the region of a synapse that releases the neurotransmitter (in contrast to postsynaptic).

Primary motor cortex - motor cortex region whose activity controls the execution of movements. It participates in motor learning and possibly in cognitive events. Some of its parts are suggested to be important for initiation of voluntary movement.

Primary somatosensory cortex - region which receives tactile information from the body.

Primary visual cortex - the region of the occipital cortex where most visual information first arrives. It performs visual processing such as pattern recognition.

Proprioception - sensory information about pressure, movement, vibration, position, muscle pain, and equilibrium that is received by the brain from the muscle spindles and other sensory receptors.

Prosencephalon - the forebrain; lies rostral to the midbrain (mesencephalon); consists of the telencephalon (cerebral cortex & hippocampus) and diencephalon (thalamus and hypothalamus).

Purkinje cell - by far the largest neuron of the cerebellum and the sole output of the cerebellar cortex. Receives climbing fiber input and integrates inputs from parallel fibers and interneurons.

Rhombencephalon - the hindbrain; lies caudal to the midbrain (mesencephalon); made of the metencephalon and myelencephalon.

Sagittal - the plane that bisects the body or brain into right and left halves.

Spinal cord - the part of the central nervous system that lies below the magnum foramen and that extends downward to just above the cauda equina; it contains the cell bodies of the spinal nerves and their afferent and efferent fibers

Sulcus - a furrow of convoluted brain surface (opposite of gyrus).

Synapse - the area between one neuron and the next through which neurotransmitters are passed transmitting neural messages.

Synaptic plasticity - the ability of certain synapses to increase or decrease their synaptic strength.

Tectum - the dorsal portion of the midbrain (mesencephalon).

Tegmentum - ventral part of the midbrain (mesencephalon).

Telencephalon - the frontal subdivision of the forebrain includes the cerebral hemispheres and the hippocampus, basal ganglia, and amygdale.

Temporal lobe - located below the frontal and parietal lobes; involved in perception and recognition of auditory stimuli, memory, emotions and comprehending language.

Thalamus - a large mass of gray matter deeply situated in the forebrain at the topmost portion of the diencephalon. It relays sensory information and motor signals. Almost all sensory information enters this structure where neurons send that information to the cerebral cortex. Axons from many sensory systems (except olfaction) synapse here as the last relay site before the information reaches the cerebral cortex.

Visual cortex - located in the occipital lobe; is responsible for processing visual information.

White matter - the white parts underneath the cortex that consists mostly of axons with white myelin sheaths and glia cells (in contrast to gray matter).

Zone - a sagittal region of Purkinje cells in the cerebellar cortex that is up to 500 μm wide and that receives climbing fibers from a particular olivary subnucleus.

CHAPTER 1

Introduction

In the scientific community, it is accepted the relation between the cerebellum and different motor control features that humans present. In fact, it is well-known that the cerebellum plays a fundamental role in controlling fast and accurate movements [1] [2] [3] [4]; for example, it supervises ballistic movement timing [5], it is able to establish the duration of those movements in advance and supplies corrective motor commands [6] [7].

These characteristics are supported by the feedback mechanism which is present in the cerebellum structure [8] [9]. In this way, the cerebellum can make efficient use of mechanisms and properties such as elasticity in muscular movements and help the central nervous system to predict the movement of the body parts [10]. This set of features seems to fit well in the robotic field, where the cerebellum could be used as an "artificial biologically plausible controller" that drives robotic motor activity [11] [12] [13] [14] [15] [16] [17] [18] [19].

The relationship between cerebellum operation and many of the different types of local plasticity mechanisms is not well-known and even less known is its implication in what it is called "high level functions" [20] [21]. In the mid-eighties, some experimental findings in several research fields began to show that the cerebellum was involved not only in motor tasks but also in spatial cognition and other high level functions [22] [23] [24]. Neuro-image studies have shown the cerebellar activation in several processes such as, word generation [25], comprehension and semantic processing [26] [27], verbal recognition and non-verbal recognition [28], immediate verbal memory [29], cognitive planning [30], motor imagination [30], sensorial acquisition and discrimination [31] or cognitive attention [32]. Even more, some evidence has been obtained from patients with focal lesions [33] [34]: alterations on processing speed in complex spatial movements and operational planning tasks, word generation in relation to a set point or a reference value, planning and flexibility in abstract reasoning, operative memory or perception and motor timing. Personality changes have been also observed, agrammatism, dysprosody, and difficulties in fast and precise voluntary changes to focus attention.

During the last decade, an important amount of evidence supporting the hypothesis of cerebellum acting in cognitive functions has been shown to be true, however, some researchers are skeptic [35] [36]

due to the fact that the conducted experiments are not free of doubts. Cerebellar activation in certain tasks does not allow researchers to directly ensure a fundamental role of the cerebellum in the cognitive process under study, the clinic results presents inconsistencies and contradictions, it is not easy to control the motor problem effects, the tasks are complex and the observed deficits are difficult to be interpreted, etc. Therefore, the role of the cerebellum in different cognitive and non-cognitive features and how it is supported by its intrinsic characteristics is an open issue.
Keeping in mind this idea of the cerebellum being involved in multiple tasks, cognitive and non-cognitive processes, we can consider the following points:

- The cerebellar cortex uniform synaptic organization suggests that both motor-related and cognitive cerebellar functions might be emulated by using the same computational principles.

- Biologically plausible robot control field seems to be a good candidate to work with to reveal cerebellar functionality.

Consequently a combination of both fields (computational cerebellar principles and computational robot control theory) should give us a powerful tool to find out the cerebellar functionality. These two points constitute the grounds of this dissertation and it will be extended in the incoming sections.

The main objective of this thesis is to bring some light to the functional roles of the cerebellum in both motor and spatial cognitive processes by exploiting computational rules that allow inferring how those processes could take place in the cerebellum.

I. THE CEREBELLUM

The human brain has (estimate) 100 billion neurons. Some sources say between 10 and 100 billion [37] [38]. The cerebellum takes up 10 % of the brain's total volume and contains roughly 50% of all the neurons in the brain [39].

The cerebellum looks like an independent structure attached right to the bottom of the brain, located underneath the cerebral hemispheres. The cerebellum is encased by a highly convoluted sheet of tissue called the cerebellar cortex, which contains almost all of the neurons in the cerebellum being Purkinje and granule cells the most important [37] [39] . Such a quantity of neurons and their interconnections allow the cerebellum to develop massive signal-processing capabilities [40] (Even though most of the

cerebellum outputs are driven to a set of small deep cerebellar nuclei lying in the interior of the cerebellum)

The cerebellum is a region of the brain which plays a main role in motor control. In addition it is also related to some cognitive functions such as attention and language, and probably in some emotional functions as we have already mentioned [41].

The cerebellum is involved in a feedback loop for muscle movement [42] [43]. When the cortex sends a message for motor movement to the lower motor neurons in the brain stem and spinal cord it also sends a copy of this message to the cerebellum [44]. This is conveyed from pyramidal fibers in the cortex on the cortico-pontine-cerebellar tract to the cerebellum. In addition, information reaches to the cerebellum from muscle spindles (Kinesthesia), joints and tendons (Proprioception) [45]. This information allows the cerebellum to determine how well motor commands coming from the cortex are being carried out and then, it can coordinate the muscle activity for the production of smooth movement through its connections with the pyramidal and extra pyramidal systems and the descending reticular formation [46] [47].

In the framework of this coordination of fine motor movements the cerebellum makes important contributions to the control of rapid, alternating muscle movements necessary for high speed tasks.

Moreover the cerebellum is not only involved in direct motor control but also with several types of motor learning, being the most relevant one the learning of adjusting changes in sensorimotor primitives [48]. Along last decades an enormous theoretical modeling effort has been done to explain sensorimotor calibration in terms of synaptic plasticity within the cerebellum (for a deeper review the reader is referred to chapter 2 section 4). Most of those theoretical models are based on early models formulated by Marr-Albus [49] [50], where each cerebellar Purkinje cell receive two dramatically different types of input: on one hand, thousands of inputs from parallel fibers, each individually very weak; on the other hand, inputs from one single climbing fiber, which is, however, so strong that a single climbing fiber action potential will reliably cause a target Purkinje cell to fire a complex action potential. The basic concept of the Marr-Albus theory is that the climbing fiber serves as a "teaching signal" [51], which induces a long-lasting change in the strength of synchronously activated parallel fiber inputs [52]. Observations of long-term depression in parallel fiber inputs have provided support for theories of this type, but their validity remains controversial. [53]

A theoretical cerebellar model based on spiking neural network has been implemented and evolved along this thesis and it is presented in the included journal papers.

II. THE CEREBELLUM IN MOTOR CONTROL

Biological control systems (which deal with non-stiff-joint plants, as a human arm is) have evolved during millions of years and have become into an interesting paradigm to emulate in robotic controller construction [54]. The cerebellum is known to be involved in control and learning of smooth coordinated movements [6]. Furthermore, an accurate understanding of how this advance control engine works should have a strong impact in controlling biomorphic robots.

Human arm, as a mechanic manipulator, consists of rigid organs, bones, which are joined with flexible unions with respect to objects to be manipulated. Both, bones and joints are actuated by muscles; these muscles act as high performance effectors (high relationship between effort/mass). These effectors produce a contraction effort when nervous stimuli arrive, and in order to allow bidirectional rotational movements in each joint, they are disposed in opposite pairs [55].

The whole set; arm-forearm-hand does not possess an exceptional mechanic accuracy but it has a great mobility (27 Degrees Of Freedom: 4 in each finger, 3 for extension and flexion and one for abduction and adduction; the thumb is more complicated and has 5 DOF, leaving 6 DOF for the rotation and translation of the wrist [56] plus 7 DOF [57] of the arm) and a great amount of effort sensors to compensate for this lack of accuracy helping in the control tasks. Our high handling performance is in part, a consequence of the cerebellum working as a control system which is able to develop highly complex tasks with unreachable results by any other current robot control system.

In a biological control scenario with touch sensing, the transmission delay of the generated spike from the finger contact with any surface and the arrival time of this spike into the cerebellum cortex is around 70ms, that is, the control loop presents a delay between 100-150ms [58](Actually standard industrial control loops cannot deal with such delays in transmission paths) [59]. This means that our handy human arm is not able to develop contact tasks which requires correction torques with a frequency higher than 6 or 10 times per second (about 100-150ms delay). The response to very fast events is usually attenuated by the hand, but when the contact takes place with a stiff arm-element, such as fist is, the presented error is high. [60]

Then, how human beings have an extraordinarily manual ability when interacting with different scenarios? In fact, the arm (prior contact), presents a certain stiffness modulated by muscles. The simultaneous muscle pair activation allows increasing the joint stiffness. For instance the elbow can increase its stiffness in a ratio of 200 to 1 [60], by using biceps and triceps muscle. The proper arm stiffness is set using the previous task knowledge; afterwards this stiffness is modified before contact (before suffering position error muscles adjust and keep the proper stiffness without the intervention of the entire control loop) in order to optimize this task in terms of the specific task parameters (position, velocity, acceleration, torque value, etc.)

Through this thesis, it is assumed that agonist-antagonist muscle pair is able to modify stiffness but, in fact, from a global point of view, which is modified is not the stiffness but the mechanic arm impedance. In a simple scenario, we can consider that the arm impedance has three parameters per D.O.F: stiffness, mass and damping. Thus, this impedance provides the static and dynamic relations between force and motion.

It is clear enough that a control implementation which modifies the mechanic robot impedance allows having an approximation to human arm behavior.

To that aim, this thesis has evolved a biological plausible cerebellar controller in a robot control scenario which is showed in the included journal papers.

III. MOTIVATION

The cerebellar architecture has been studied for more than a century, however its functional role and operation remains being an open issue [21] [61]. It is well known that cerebellum plays an important role in motor control making a fundamental contribution to the coordination, precision, and accurate timing of movements [62]. The cerebellum receives inputs from sensory systems and from other parts of the brain and spinal cord, and integrates them with motor commands in order to modulate the motor activity and improve the movement performance [46] [47]. Many theories have been proposed to explain the operation of this region of the brain, and some of them have achieved a remarkable success [46,47,63,64]. However, several specific types of neurons, connections and plasticity mechanisms have been discovered in the cerebellum. Each of them possesses concrete properties which confer different information-processing capabilities. And even so, when modeling large nervous circuits to investigate

their operation, these specific properties are usually not properly considered; either because they are not implemented (simple neural models and networks) or they are implemented (computationally-costly biological models) but their contribution to the entire network computation is not clearly understood. Consequently, in order to clarify how the computation is done in our cerebellum and to prove hypotheses about its operation, nervous circuit simulations seems to be a test bench. Applying those cerebellar hypotheses to a demanding motor control task scenario gives us the chance to discover how the sensorimotor and cognitive information could be managed by a computational cerebellar like architecture and to determine which the key functional properties of the neural processing are and how they contribute to the resultant computation performed by the entire network.

From the control theory point of view, the best system is the one that achieves the best performance in terms of accuracy, speed and stability. This idea can be extrapolated to neuroscience, in a sense that the best performing biologically inspired system possible should give clues, and deeper understanding, about the real biological system. In this way, the network parameters that allow us to discern which architecture presents a better behavior can be studied. On the other hand, generating efficient functional large-or-medium-scale networks can be exploited in a practical task. Specifically, these realistic networks can be applicable to robotic control. An understanding of the theoretical principles underlying the simplicity, flexibility and robustness of biological control schemes is therefore of interest to control engineers. More specifically the cerebellar learning mechanism is capable of producing predictive responses statistically tuned to the demands of the environment so that an understanding of its control properties will be of direct benefit to those designing moving robots. This application may have major impact if the forecasted large growth in all robotics areas occurs. Cerebellar-inspired control schemes will be especially important for the new generation of 'soft' robots, designed for safe interaction with humans in clinical and home settings. Because of the high dimensionality that a realistic neural network has and the timing constraints a simulated/realistic robot control scenario presents, an ultra-fast simulator of biologically realistic neural networks is mandatory, the performance requirements demand an efficient simulator (EDLUT) able to perform even in real time [65] [66]. The combination of both fields, these biological architectures and robot control theory, involves a cutting-edge challenge.

A whole cerebellum model simulation embedded into a control loop to accurately control a robotic arm constitutes a demanding test bench for the developed biological system. It is necessary to address all the inconveniences of working in between of two worlds; biology processing is written in spike terms, robot control processing is written in analog control signal terms, a Rosetta stone has to be found out.

IV. OBJECTIVES

The main aim of this work lies in the study and implementation of functional cerebellar like models working in a robot control scenario, taking full advantage of the capabilities of the cerebellar architecture. This implementation aims at contributing to a better understanding of the central nervous system (essentially the cerebellum) from a computational approximation and to assess its application in the robotic domain.

The design of a cerebellar model embedded in a control loop is not straight forward. Reaching this aim demands a continuous developing process which has been divided into different stages according to the journal papers included in order to give a gradual overview of the whole developed work.

- ✓ The first objective is the study of how an adaptive cerebellum-like module embedded in the control loop can build up corrective models to compensate deviations in the target trajectory when the dynamics of the controlled plant (arm-hand-object in the case of a human operator) are altered due to manipulation of heavy objects (whose mass significantly affects the basic model dynamics). We address the study of how this corrective model is inferred through a biologically plausible local adaptation mechanism using a simplified cerebellar architecture.

  Through the development of this simple cerebellar module, we can monitor how the synaptic weight's space adapts to a distributed stable model that depends on the basic network topology, the target trajectory, and model deviations.

  This is covered in [14] (paper included in the fourth chapter).

- ✓ The second objective is to describe how a more realistic spiking neural network (a granular layer is now implemented) mimicking a cerebellar micro-structure allows internal corrective model inference. By adopting a cerebellar-like network, we explore how different sensor representations can be efficiently used for a corrective model abstraction corresponding to different manipulated objects. It has been done in two steps:

  i. We address a biologically relevant task which consists in an accurate manipulation of objects which affect a base (kinematic and dynamic) model of the plant using low power actuators.

ii. We define and implement a spiking-neuron based cerebellum model to evaluate how different properties of the cerebellar model affect the functional performance of the system.

This is covered in [12] (paper included in the fourth chapter).

- ✓ Thirdly, we aim at studying how an adaptive spiking cerebellum-like module which includes long-term depression (LTD) and long-term potentiation (LTP) at parallel-fiber to Purkinje-cell synapses (PF→PC) is embedded in diverse control loops (forward, recurrent, and a combination of both architectures) to infer corrective models which compensate deviations in the robot trajectory when the dynamics and kinematics of the controlled robotic arm are altered and noise (related to the inherent noise of the muscle spindle signal) is introduced in the cerebellar input (MFs). The main goal at this point is to make a comparative evaluation of these control architectures which shows how forward and recurrent architectures complement each other in the framework of a manipulation task and how robustly they behave in the presence of noise.

  This is covered in [13] (paper included as fourth chapter).

- ✓ The last objective is to study the best way in which sensori-motor information in a common robot scenario can be encoded to investigate an optimal representation of somatosensory information.

  This is covered by the last paper included in the fourth chapter.

V. PROJECT FRAMEWORK

This work has been developed in the framework of two European projects "SENSOrimotor structuring of Perception and Action for emergent Cognition" (SENSOPAC) and "Realistic Real-time Networks: computation dynamics in the cerebellum" (REALNET (IST-270434)).

The SENSOPAC (IST-028056) project (belonging to the EU Framework 6 IST Cognitive Systems Initiative) extended from January, 2006 to July, 2010 in collaboration with 12 institutions from 9

different countries. The SENSOPAC (IST-028056) project combines machine learning techniques and modeling of biological systems to develop a machine capable of abstracting cognitive notions from sensorimotor relationships during interactions with its environment, and of generalizing this knowledge to novel situations. In particular, SENSOPAC (IST-028056) has combined robot dynamic models with sensory causal relationships in a haptic exploration task, in order to grasp and decide. Detailed neural models of key brain areas have been embedded into functional models of perception, decision making, planning, and control, effectively bridging and contributing to neuroscience and engineering.

Sensory feedback including tactile sensory arrays, proprioceptive feedback, and motor command afferents have been employed for manipulation tasks under various contexts allowing the study of efficient representations, encoding/decoding mechanisms and abstractions; both in human haptic manipulation as well as artificial robotic sensor systems.

Our research group at the University of Granada has been mainly involved in the development of the spiking neuron computation environment (EDLUT) following neuroscientist findings in order to design biologically inspired control systems capable of carrying out manipulating tasks.

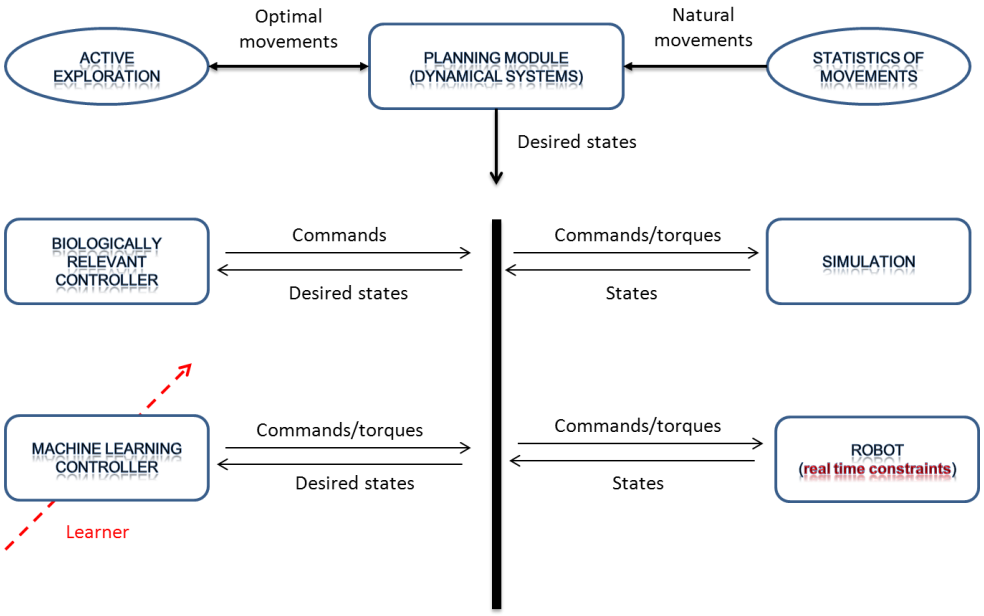

Figure 1.1 Module organization of the SENSOPAC

Our work as a partner is focused in biological relevant controller and simulation module provide a bridge between neurophysiologist and control theory in robotic systems.

More recently our research group is involved with the REALNET (IST-270434) project as a continuation of SENSOPAC (IST-028056) project. REALNET (IST-270434) project (funded under the EU Framework 7 Information and Communication Technologies work program) started in February, 2011 and will last until February, 2014. The main goal of this project is to understand the circuits of the central nervous system from the functional level to the molecular/neuronal level. In order to understand circuit computations a different approach is needed: it aims to elaborate realistic spiking networks and use them, together with experimental recordings of network activity, to investigate the theoretical basis of central network computation. As a benchmark this project will use the cerebellar circuit. Based on experimental data, this project will develop the very first realistic real-time model of the cerebellum. This cerebellar model will connect to a biomorphic robotic system to evaluate circuit functioning under closed-loop conditions. The data deriving from recordings, large-scale simulations and robots will be used to explain circuit functioning through the adaptable filter theory.

Because of the multidisciplinary properties these projects require each of the members of our research group to focus their research in a particular area. The present work mainly presents results where a cerebellum-like simulated architecture has been used in order to manipulate tools with a robotic arm. This work implies dealing with robotic system; developing a robotic arm simulator, studying the biologically plausible control loops, conversion from/to spiking signals, embedded the EDLUT simulator in the control loop, studying the spike/analog connection… etc. All these issues focus my research but it is mandatory to point out that all this work would not have been possible without the hard work of Jesus Alberto Garrido who is in charge of evolving the EDLUT simulator environment and performing simulations of more realistic biological structures. Our hard work shoulder to shoulder trying to bring some light to the motor control theory; from the biology findings through the implementation in realistic spike simulator to a robot control loop, has made this thesis possible.

VI. CHAPTER ORGANIZATION

In order to facilitate the reading and utilization of this dissertation we provide a concise summary of the information presented in each chapter:

- ✓ In chapter 1 (the present chapter), a brief introduction of state of the art in computational neuroscience applied in robot control scenarios is described. The motivation of this dissertation is presented and the work carried out is summarized.

- ✓ In chapter 2, a proper contextualization of the research area in which this thesis has been done is presented. Although journal papers are self-contained, a previous overview on the research field aims to make easier the task of getting deep into details through the journal papers.

- ✓ In chapter 3, we briefly enumerate the main contributions and future work plans.

- ✓ Finally in chapter 4, all the related papers are included with a brief remark about the source journals, their impact factor and the quartile to which they belong. In addition other publications associated to this work (conference articles and cooperative journal articles) are also indicated.

CHAPTER 2

Thesis Contextualization

In this chapter, we try to contextualize the research area in which this thesis has been developed. Due to the "journal article structure" used in this thesis, we first briefly introduce the research area related to this thesis. Therefore, we hope that the rest will be easier to follow for the reader and, in general, will facilitate to have a global picture of the work accomplished.

I. ANATOMY OF THE MEMORY

One of the most important aspects that the brain presents is its learning ability and its storage capacity of dynamic entry patterns. The way in which our experiences are structured and stored by our brain and how these experiences have an effect in our behavior, is strongly related with the nature of this storage process [67]. The memory is not something tangible which is stored as an image in a computer and it is invoked on demand. The experiences change the way in which we perceive, we think, we plan and we act. These experiences physically modify the nervous system structure, changing those neuronal circuits which are involved in perception, thinking and planning [68]. For example, an unpleasant or disturbing experience will tend to be avoided; in contrast, we will try to repeat those experiences which gave us satisfaction or pleasure.

One of the main brain functionalities is to activate the muscles in order to produce useful operating conducts. The learning capability is the result of developing useful operating conducts which are adapted to our surrounded dynamic environment. The learning shows up in different ways (Fig. 2):

- ***Perceptual learning:*** ability to learn to recognize stimuli that have been seen before [69].
    - ✓ Primary function is to identify and categorize objects and situations
    - ✓ Changes within the sensory systems of the brain
- ***Stimulus-response learning:*** ability to learn to perform a particular behavior when a certain stimulus is present. Establishment of connections between sensory systems and motor systems.

- ***Motor learning:*** establishment of changes within the motor system [70] [71].
- ***Relational learning:*** involves connections between different areas of the association cortex [72].
- ***Spatial learning:*** involves learning about the relations among many stimuli [73] [74].
- ***Episodic learning:*** remembering sequences of events that we witness [75].
- ***Observational learning:*** learning by watching and imitation other people [76].

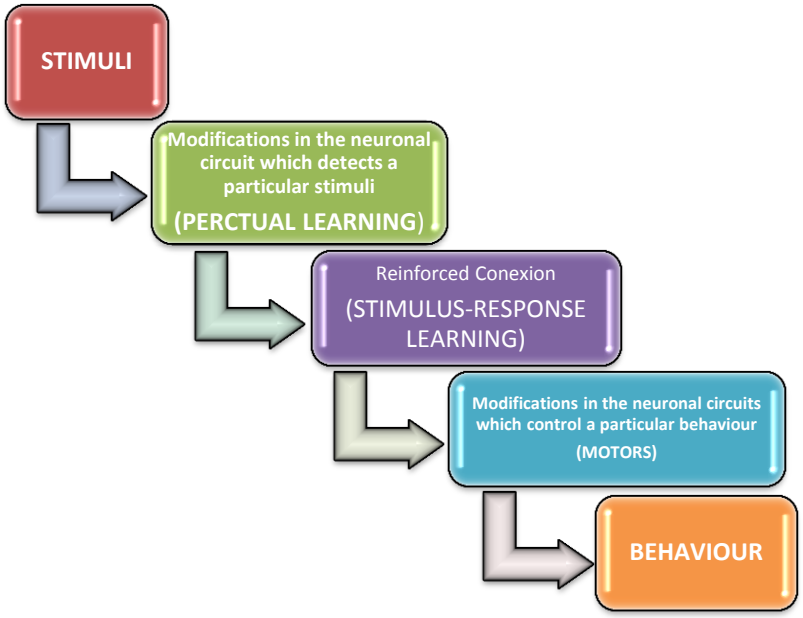

Figure 2.1. A general view of perceptual behaviorism learning: stimulus response learning and motor learning [67].

II. BEHAVIORISM. PSYCHOLOGICAL BEHAVIORISM

The psychologist F.B Skinner [67], in the seventieths, developed a fundamental research; the behavior analysis in terms of stimuli and responses. Considering behaviorism as "the observable activity that an individual performs" (activity that basically consists of movements) then what we called behaviorism is

based on a set of rules that regulates the dependency between behavioral elements (mainly stimuli and responses) by means of finding out functional relationships. Considering the organism as a black box in which only inputs and outputs are well known; being the functional correlation between stimuli and responses a "reflex", and finally taking into consideration a reflex action as an instrument to describe the behaviorism (classical behaviorism), but just as a behavioral action not as a neurological concept, so then, we can described the Psychological behaviorism [77] as a kind of behaviorism that examines behavioral changes in relation to the results (experience) focusing its attention in the learning process.

For instance, when a hungry rat is placed in a cage for the first time, it is very unlikely the rat activates the feeding mechanism. Nevertheless, when the rat activates the mechanism and receives a piece of meal, after that, the probability that the rat activates again the mechanism, increases. But ¿how does psychological behaviorism work? Figure 2 shows a possible model. The visual system of the previous rat has two neurons. One of them fires when the rat sees the feeding mechanism the other one fires when the rat sees a bottle of water. The motor system has three neurons, each of them has a specific functionality (moving the ears, standing only on the hind legs, and activating the feeding mechanism). Another neuron is part of the reinforcement system. This one fires when the rat is hungry and receives some food. Initially, the M synapsis (Mechanism) is too weak for firing the motor neuron. However, the rat explores the cage and, by chance, activates the feeding mechanism. This positive fact is detected by the reinforcement system which synapses onto all moto-neurons. When the reinforcement synapsis R (Reinforcement) fires makes all the synapsis recently activated stronger. On this case, the synapsis M is responsible of reinforcing the learning when the mechanism is activated. When this last synapsis has been reinforced enough, just the mechanism vision provoke the behavior of activate that mechanism.

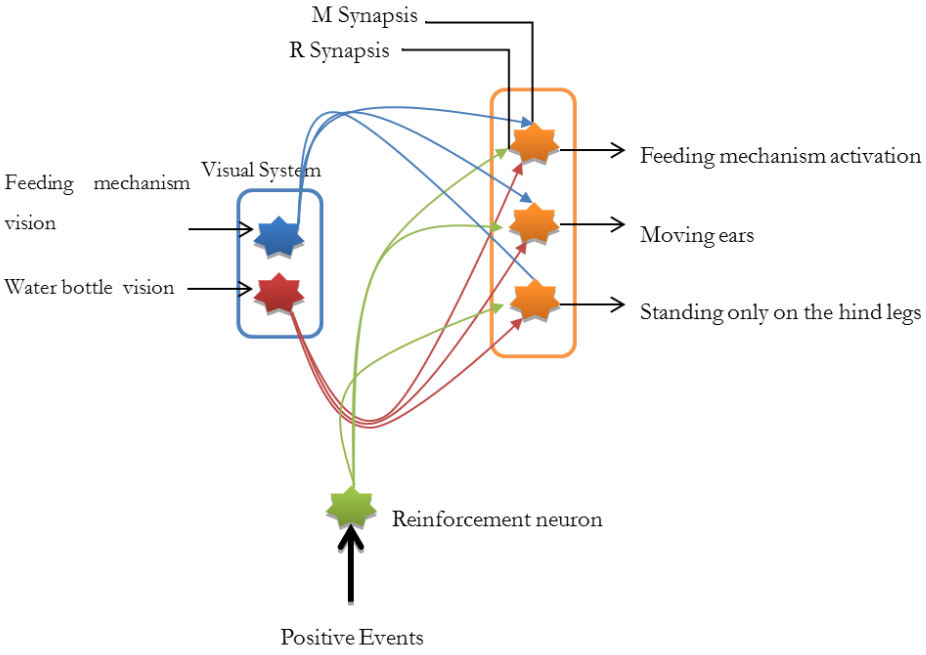

Figure 2.2. A simple reinforcement neuronal model of physiological behaviorism.
When the animal sees the feeding mechanism, and then activates it, a positive event happens. The activity of the reinforcement system makes the synapsis M stronger.

III. NEURAL NETWORKS, MODELING THE LEARNING CAPABILITY OF THE BRAIN

The experience modifies the neural connections of our brain, and these modifications, these changes, represent what it is already learned [78] [79]. But ¿why does a new sensorial stimulus modify the way in which neurons respond to the stimuli already learned? One possible answer can be deduced from the functional models of the neural circuits, that is, the neural networks. Each "element" has computational properties as neurons have; these "elements" are connected to each other through connections which are similar to a synapsis. These connections can be excitatory or inhibitory as real synapses are.

When one of these "elements" receives a *critic* amount of excitation, it sends a message to those elements to which it is connected. The elements of the network have inputs that can receive "external" signals, representing a sensorial organ or received information from other network, for example as a feedback of our network. Other "elements" have outputs which control muscles or connect with other

network producing particular behaviors. That means, particular patterns in the inputs can represent particular stimuli and particular output patterns can represent particular responses.

It is possible to "teach" neural networks to recognize particular stimuli. These networks receive a single input pattern, being the inhibitory and excitatory elements of the neural circuit those that refine the response of the network when it is faced to a defined input pattern. The first time a defined stimulus is presented, the output "elements" response in a weak and unspecific way; but after several trials, a strong and reliable response pattern emerges. More stimuli can be presented to the network and then more corresponding specific output patterns can be generated. The functional properties of the neural network are quite similar to those which can be found in real nervous system, and this is the reason why Scientifics are interested on the fundamental principles of the neural learning. For instance, neural networks show generalization, discrimination and soft degradation. Generalization in this case, should be understood as the capacity of recognizing similarities between stimuli. For instance, let assume that our network has learnt some different stimuli, if we show to the network a stimuli similar to that one that it has already learnt, the network response pattern will be very close to that response which is produced when the already known stimulus was shown. What we understand for discrimination is the capability of recognizing differences between stimuli. If several similar stimuli are presented to a neural network, the network will learn to distinguish them and it will produce different output patterns for each stimuli. Finally the term soft degradation is used to indicate that the apoptosis (the malfunctioning of different elements or connections, synapses, in the neural network) do not make the whole neural network stop totally working. Instead of stopping working, the processing progressively deteriorates depending on the rate of deterioration that the neural network presents. All of these three phenomena; generalization, discrimination and soft degradation also characterize the behavior of our brain.

Our cerebellum is built up by neural networks which involves that our learning takes place within these neural networks. The question relies on the possibility of replicating the brain functionality with these neural networks. Knowing the neural circuits' anatomy in detail and the physiological characteristics of single neurons and their synapse connections is the only way to give answer to that question. The more we learn about this issue, the more realistic neural network model we can build up.

As a first step, this research field tries to study what it is called microstructure, of the brain, that is, brain functions which are performed by individual modules. The brain presents a huge amount of neural networks (it seems to be thousands), where each of these neural networks has it corresponding functionality. It is likely that those neural networks present a hierarchical structure where some of them

control the functionality of other ones and regulate the information exchange between them. Therefore, the individual comprehension of the operations that happen in a specific neural network will not reveal all we need to know about the brain functions. We will also need to know the brain organization (relationship between individual neural networks which compose the brain). Then the brain macrostructure need to be also known. Developing and improving neural networks is linked to brain macro and microstructure research; macro-microstructure research supplies a fundamental physiological base which supports the artificial neural network develop.

IV. CEREBELLAR CONTROL

1. Distributed Motor System

The cerebral motor system is a complex controller. A good way to realize of this could be shown by using an example. Let's suppose we see on the corner of our eye something that is moving. Quickly turn our head and look towards the source of motion, and we found that someone has taken a blow to a vase of flowers and it is about to fall off the table. Quickly we extend the arm, grab the vase and try to put in a stable position.

The rapid movement of the head and eyes is controlled by mechanisms involving the superior colliculus and some nearby nuclei. The head and trunk movements are driven by the tectospinal tract. We note how the vase was tilted by the activity of neurons in the visual cortex. The same visual cortex also provides information on depth to the right parietal lobe, which is able to determine the spatial location of the vase. Our left parietal lobe uses the spatial information, along with its own record of the location of the hand to determine the path it has to do to intercept the vase. The information is sent to the left frontal lobe, where the associative motor cortex begins with the movement. Since this movement has to be ballistic, the temporal pattern control is based on the information received from the associative cortex of the frontal and parietal lobes. Our hand stops at the instant it touches the vase, and the connections between the somatosensory cortex and primary motor cortex start the reflex of closing the hand to grasp the vase.

The hand movement is controlled by the cooperation of the corticospinal, rubrospinal and ventromedial tract. Even before our hand begins to move, the ventral corticospinal tract and the

ventromedial pathway begin to adjust our posture to avoid our falling when we go to pick it up. Depending on how far we are away from the jar, the reticulospinal tract can even make us take a step to keep balance (adapted from [80]).

2. The Cerebellum. Introduction

The cerebellum is an important part of the motor system [1] [81] [82] [63] [83]. It consists of two hemispheres that contain several deep nuclei located just below its folded and wrinkled cortex. Thus, the cerebellum looks like a miniaturized brain [37].

The cerebellum cortex receives inputs from the brain cortex encoding extrinsic and intrinsic movement parameters. [84] In fact, the cerebellum contributes both to control rapid and accurate movements and to control the temporal development of fast ballistic movements, movements which are too fast to be modified by feedback circuits [85] [86]. Because of that, the sequence of muscle movements must be programmed in advance, so then, individual muscles should be activated at the right time. Considering the distance between our hand and the aim to reach, our cerebellum calculates the timing that muscles should be active [64] [42] [9]. After that time, the cerebellum briefly activates the antagonistic muscles to stop the movement. [46] [47]

Another main function of the cerebellum is programming the duration of rapid movement. The cerebellum monitors and provides corrective adjustments to motor activities triggered by other parts of the brain. The cerebellum continuously receives current information from the peripheral body parts to determine the instantaneous state of each of its areas (position, rate of motion, forces acting on it, and so on) [21] [87]. The cerebellum compares the actual physical condition of each body part as indicated by the sensory information with the state the motor system is trying to produce. If these two values do not instantly match, then the appropriate corrective signals are transmitted to the motor system, increasing or decreasing the activity of specific muscles [46] [47].

The cerebellum communicates with the brain through a cord of fibers called superior cerebellar peduncles, with the pons through the middle cerebellar peduncles and with the medulla oblongata through the inferior cerebellar peduncles [88].

The gray matter contains cells that constitute the origin of the fibers that synapses with those fibers which enters into the cerebellum coming from other parts of the brain. The impulses from the motor centers of the brain, from the semicircular canals of the inner ear and from striated muscles get into the cerebellum by the peduncles. Cerebellar motor impulses are transmitted from the motor centers of the brain and the spinal cord to the muscles [88].

3. The Cerebellum Entry System (Cerebellar Afferent Pathways)

The cerebellum is divided into three lobes: flocculonodular lobe, anterior and posterior lobe. The vermis is located in the anterior and posterior lobe. Most of the nerve signals which are originated in the somatic areas of the body end in the vermis [37] [88]. The vermis plays a role in the integration of subconscious postural mechanisms. Most of the signals coming from the highest levels of the brain, especially the motor areas of the cortex, finish in the cerebellar hemispheres [89].

Cortico-cerebellar tract is born in the motor cortex and directly links with the cerebellar cortex. In addition, major afferents arise from the brain stem, the inferior olive, motor-cortex, basal ganglia and finally scattered areas of the reticular formation and spinal cord [88] [90].

The cerebellum also receives important sensory signals directly from the body periphery. The signals from these body parts arise from the muscle spindles, Golgi tendon organs, and large tactile receptors both on skin and joints, which informs the cerebellum of the current state of muscle contraction, the degree of tension in the tendons, the body part positions, and the acting forces on the surfaces of the body. All this information is processed in the cerebellum which is constantly informed of the instantaneous physical state of the body [88] [90].

Spinocerebellar tract can transmit impulses with latencies of less than 100 ms; that is the faster transmission in any impulse transmission path throughout the central nervous system. This extremely fast transmission allows the cerebellum to quickly know the changes taking place in the state of the muscles. The cerebellum continuously receives information from all body parts, despite of these body parts are working at a subconscious level.

TABLE I. The cerebellar afferent pathways [88].

Pathway	***Function***	***Origin***	***Destination***
Afferents from the cerebral cortex			
Cortico-ponto-cerebellar	*Conveys control from cerebral cortex*	*Frontal, parietal, occipital & temporal lobes*	*Cerebellar cortex*
Cerebro-olivo-cerebellar			
Cerebro-reticulo-cerebellar		*Sensorimotor areas*	*Via reticular formation to cerebellar cortex*
Afferents from the spinal cord			
Anterior-spino-cerebellar	*Conveys information form muscles & joints*	1. *Muscle spindles* 2. *Tendon organs* 3. *Joint receptors*	*Cerebellar cortex*
Posterior-spino-cerebellar			
Cuneo cerebellar	*Conveys information from muscles & joints of upper limbs*		
Afferents from the vestibular nerve			
Vestibular nerve	*Conveys information on*	1. Utricle 2. Saccule	*Cortex of the Flocculonodular*

	head position & movements	3. Semi circular canals	*lobe*
Other afferents	*Conveys information from the mid brain*	1. *Red nucleus* 2. *Tectum*	*Cerebellar cortex*

The main entrance to the cerebellum is carried out by mossy fibers [87] [91]. Mossy fibers carry information from sources that control the balance (vestibular system), warning (reticular formation), motor activity (cerebral cortex), sensory organs and location of the tendon positions, contraction speed of muscles, and skin pressure [92] [93] [94] [95] [96] [97] [98].

Mossy fibers can be classified according to the origin of the information that they carry in two classes:

1. Those which carry information from higher hierarchical levels.

2. Those which carry feedback information about the results corresponding to the motor control output.

Once in the cerebellum, these two classes are mixed, in an indistinguishable way.

4. The Cerebellum Output System (Cerebellar Efferent Pathways)

There are four deep cerebellar nuclei located deep in the cerebellar mass, being these cerebellar deep nuclei, the sole outputs of the cerebellum. These nuclei receive signals from two different sources: the cerebellar cortex, and all the sensory afferent pathways to the cerebellum. The cerebellar input is carried by the mossy fibers. Three major efferent pathways can be found [88]:

1. A pathway that starts in the cortex of both cerebellar hemispheres, which goes to the motor cortex.

2. A pathway that starts in the structures of the midline cerebellum (vermis) and targets at bulbar and pontine regions of the brainstem. This circuit works in close relationship with the apparatus of balance and postural attitudes of the body.

3. A pathway that originates in the intermediate areas on each side of the cerebellum, connecting the vermis and cerebellar hemispheres, the motor cortex, the basal ganglia, the red nucleus and reticular formation of the upper brain stem. This circuit works for coordinate activities between the two first mentioned output cerebellar pathways, that is, to help coordinate the interfaces between postural control subconscious bodies and voluntary conscious control of the motor cortex.

In addition to these inputs, all cerebellar nuclei and all regions of cerebellum get special inputs from the **inferior olive** of the medulla.

Cerebellar peduncles. Three fiber bundles carry the input and output of the cerebellum [88].

1. The inferior cerebellar peduncle (also called the restiform body) primarily contains afferent fibers from the medulla, as well as efferents to the vestibular nuclei.
2. The middle cerebellar peduncle (also called the brachium pontis) primarily contains afferents from the pontine nuclei.
3. The superior cerebellar peduncle (also called the brachium conjunctivum) primarily contains efferent fibers from the cerebellar nuclei, as well as some afferents from the spino-cerebellar tract.

Thus, the inputs to the cerebellum are conveyed primarily through the inferior and middle cerebellar peduncles, whereas the outputs are conveyed primarily through the superior cerebellar peduncle.

5. The Cerebellum Cortex

The cerebellar cortex is divided into three layers: Molecular, Purkinje cell, and granular layer and at least seven or more types of neurons connected in a very specific and uniform way can be differentiated [99].

The molecular layer is located at the surface of the cerebellar cortex, it contains:

- ✓ Two types of interneurons: stellate and basket cells
- ✓ The parallel fibers
- ✓ The Purkinje cell's dendritic tree.

Below the molecular layer, the Purkinje cell layer gathers the somas of the Purkinje cells. Finally, the granular layer — the deepest of the cerebellar cortex — contains the somas of granular cells, an ascending section of granular cell's axons, the Golgi cells, the Lugaro cells, the unipolar brush cells, and the glomeruli, an intricate formation that receives contacts from mossy fibers and inhibitory cells from the same layer [100].

Furthermore, the cerebellum contains a large quantity of glial cells which are located in the gray and white matter.

In the following section, we will give an overview on the cytoarchitecture of the cerebellar cortex and describe the internal circuitry and cellular components of the cerebellar micro-complex.

6. Micro-complex Theory

The functional units of the cerebellar cortex are identified as longitudinal zones, zones which are usually divided into smaller microzones consisting of [101] about 1000 Purkinje longitudinally located in a narrow strip (200mm). This group of Purkinje cells presents the same somatotopic receptive field [102]. Each micro-zone of the cerebellar cortex receives climbing fibers from a different group of olivary neurons [103].

Each longitudinal zone of the cerebellar cortex targets a specific cerebellar nucleus. That involves that each micro-zone is also combined with a small group of neurons in a cerebellar or vestibular nucleus. The combination of a micro-zone with a set of subcortical structures (cerebellar or vestibular nucleus, the inferior olive and the red nucleus) constitutes which is called a corticonuclear micro-complex, or cerebellar micro-complex. These micro-complexes are hypothesized to be the operational unit of the cerebellum [81] [104]. It is believed that human cerebellum presents thousands of micro-complexes which play different roles by interacting with a functional system at the spinal cord, the brainstem, the subcortical structures and the cerebral cortex.

7. Internal Circuitry. The Human Control Loop

The three main layers of the cerebellar cortex are: the molecular layer, Purkinje cell layer and granular cell layer [99]. In addition to these layers, the deep cerebellar nuclei are located inside the cerebellar mass and surrounded by white matter. Most of the output of the cerebellar processing units comes from deep nuclei cells. The output information from the cerebellum is driven by the axons of our deep nuclei cells and flocculonodular lobe cells, which project onto different areas of the central nervous system. These cells are continually under the influence of both types of stimulation, excitatory and inhibitory. The output of the cerebellar cortex is conveyed by the inhibitory axons of the Purkinje cells. These Purkinje cells receive two major excitatory inputs; Purkinje cell receives the excitatory input of single climbing fibers, and at the same time, through the numerous synapses with parallel fibers [37] [105].

The inputs in the cerebellum are of two types, one called climbing fibers and the other mossy fibers. There is a climbing fiber per 10 Purkinje cells approximately. The information path begins with mossy fibers. Mossy fibers reach the cerebellum and target both the deep cerebellar nuclei and the granular layer. Most of granule cells and, to a lesser proportion, Golgi cells are contacted. Climbing fibers also create collaterals innervations with deep cerebellar nuclei with a few synapses and it is thought that they might also be sparsely projected to some types of neurons in the cerebellar cortex (such as Golgi cells) [37] [105].

As it is said, a single Purkinje cell receives hundred thousands of synapses from parallel fibers. Those parallel fibers also handle inhibitory basket and stellate cells activity, which in turn project to Purkinje cells. Finally, closing the loop, granule cells receive excitatory signals from the same mossy fibers that innervate deep cerebellar nuclei. Granule cells and mossy fibers also send projection to Golgi cells, which in turn inhibit the granular cells [37] [105].

Summarizing, the stimulation of a single mossy fiber never triggers an action potential in Purkinje cell; thus, a large number of mossy cells must be simultaneously stimulated to activate a Purkinje cell.

Golgi cells are also contacted by parallel fibers. These cells have a dense dendritic tree. Each Golgi cell has an axon with extensive branches. This axon makes inhibitory contact with about 100,000 granule cells in their immediate neighborhood, including some granule cells (granule cells which are branched in parallel fibers) that previously excited them. Golgi cells suppress all granule cell outputs which are not

maximally stimulated. As a result, each pattern or input vector is transformed by the granular layer into a small and a relatively fixed percentage of active parallel fibers. Each Purkinje cell performs a "summation" of their inputs (synapses), producing more specific outputs. The basket and stellate cells are essentially inhibitors that provide "negative weights" to Purkinje cells, which are added to the "positive weights" of the parallel fibers.

The climbing fibers cells are the second set of incoming fibers to the cerebellar cortex. Typically there is a climbing fiber per Purkinje cell. The output of the Purkinje cell depends on the input of the climbing fiber (each single spike produces an output spike on the Purkinje cell) and also on the inputs of the parallel fibers (whose contribution depends on the parallel fiber - Purkinje cell weights). These weights seem to be altered with the correlation between the inputs from the climbing fiber and from parallel fibers. Climbing cells may provide the necessary information for learning.

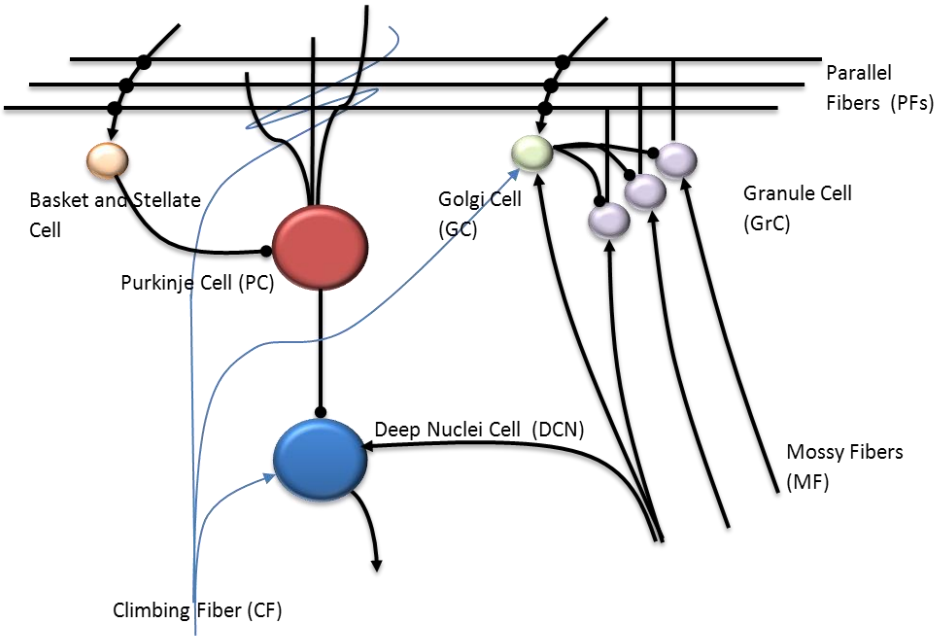

Figure 2.3. Major cells in the cerebellum.

8. Models of Cerebellar Control (Computational Models)

a. The Marr-Albus Model

In the Marr-Albus Model [49] [50] the cerebellum works as a classifier of sensory-motor patterns which are received through the MFs. Just a small portion of parallel fibers (PF) are activated when a Purkinje cell (PC) fires thus driving the motor neuron output. In this model, the error signal is supplied by the climbing fibers (CF), because they are specific to each PC. These error signals (encoded in activity through CFs) will affect the weights between PFs and PCs, improving the PC firing response to specific PF patterns. In this model CF activity was hypothesized to have a debilitating effect in PF/PC synapses. This weakening of active synapses (known as Marr-Albus Model) still remains being the reference model of nowadays studies of synaptic plasticity of the cortex. In this model each PC is considered as a perceptron whose task is to control an elemental movement. This very first approximation constituted the starting point of different cerebellar models where cerebellar plasticity plays a key role.

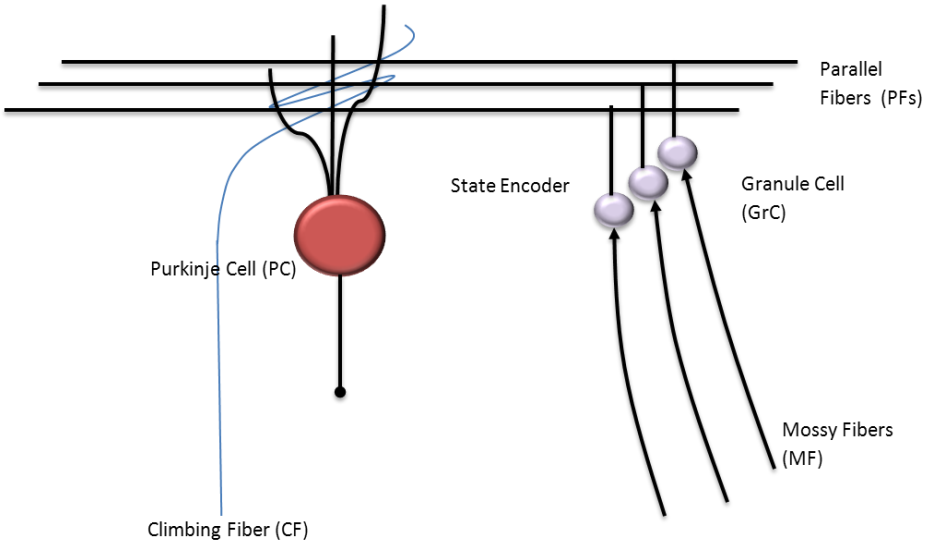

Figure 2.4. Cells in the Marr-Albus model.

b. The Cerebellar Model Articulation Controller (CMAC)

One of the well-known early computational models of the cerebellum is the CMAC: This artificial model is based on Marr-Albus [49] [50] conception of the cerebellum, but it was not initially proposed as a biological plausible approximation [16]. This model considers MFs to be responsible of the discretization of the input values, that means, when a signal on a MF is in the receptive field of a particular GrC, it fires onto a PF. The process in which the inputs are "mapped" in binary states constituted the working principle of the CMAC. Learning signal is supplied by CFs. CMAC in essence consists of a large set of overlapping multidimensional receptive fields with finite boundaries. A local receptive fields is activated when an input is presented, the global output is formed by the average of the responses of the receptive fields activated by that input.

The basic idea of CMAC is to store data within a region in such a way where those data can be easily recovered and the storage space is minimal, so the CMAC network presents multiple inputs and outputs. L1 layer presents the entry variable set $s = s_1, s_{2,}..., s_n$, the entry space is divided in segments which are called resolute elements r_s, each entry space has an allowed value range, so each analog entry s_i is quantified and transformed into a discrete value. These new two values will be used to generate a memory address.
In the L2 layer, the previously selected memory address is associated with other memories located in its neighborhood. The associative space is constituted when this neighborhood is projected into the resolution elements, r_s, per each entry s_i. For the same memory address, different memory positions can be assigned, each group constituted by this different memory positions is called hyper-cube. The value of all the hyper cubes will be modified according to a learning law.

L3 layer finally is the sum of the value of all the memory positions of the hyper cubes.

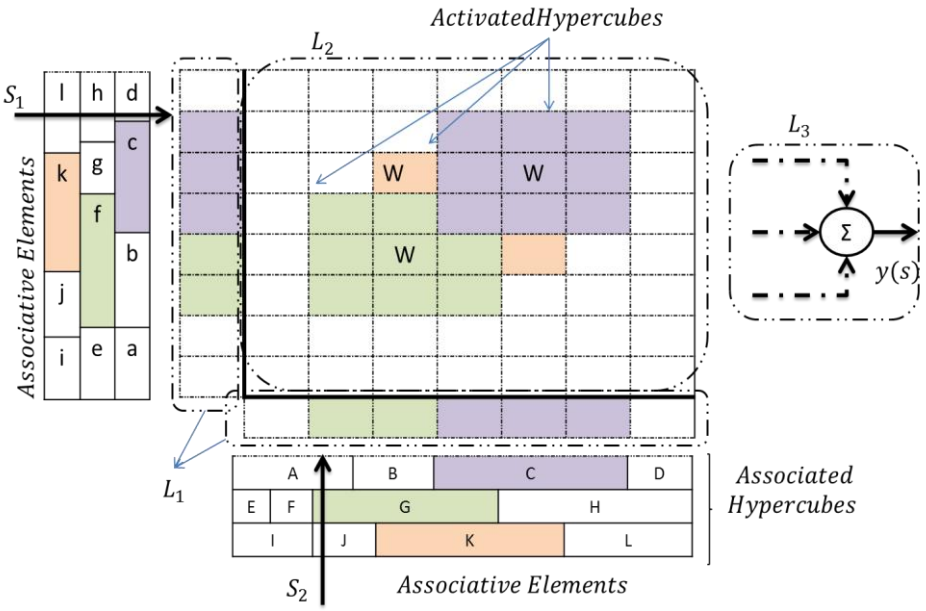

Figure 2.5. Internal structure in CMAC model (Inspired by [16]).

c. The APG Model. Adjustable Pattern Generator

Houk and colleagues proposed this model in 1986 [17]. He was convinced from experimental studies that movement signals constituted the output of pattern generators in the brain rather than the effect of continuous feedback from periphery. In this model, the cerebellum is modeled as an array of adjustable pattern generators (APGs), each of which generate a "burst command" with varying intensity and duration. APG model operation relies on the same principles of MFs→GrC→PF structure as CMAC presents. The state encoder works in the same way, but deep nuclei cells play a fundamental role. Each nucleus cell is connected to a motor cell in a positive feedback circuit; a reciprocal relationship between Purkinje cell responses and motor commands is established. The generated motor patterns are assumed to be under the control of Purkinje cells which are also taken to be the site of learning of the motor pattern. The learning rule determines which of the PF→PC synapses will be updated to improve the generated movement using training signals derived from sensory information. These training signals are conveyed by CFs to direct the adaptation of PF synapses and, after learning, selection of the motor patterns initiated by a trigger mechanism is controlled by basket cells.

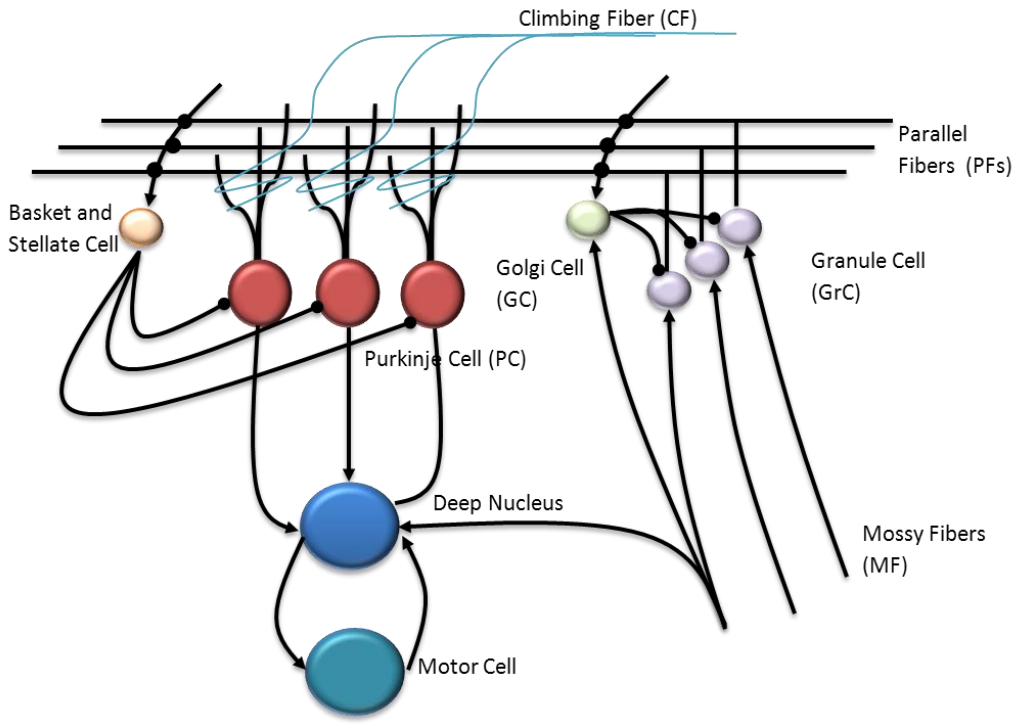

Figure 2.6. Internal structure in APG model.

d. The Schweighofer-Arbib Model

This model is strongly biologically inspired [19]; it tries to copy biology avoiding the idea of using an encoder of different status in granule cells. The model is constrained severely with anatomical data and based on the micro-complex hypothesis proposed by Ito (1984). Many assumptions are made:

- ✓ Mossy fibers drive an afferent copy of actual and desire state of the controlled plant. A mossy fiber diverges in an average of sixteen branches.
- ✓ GrC has an average of four synapses coming from the MF inputs through a glomerulus.
- ✓ Three Golgi cells synapse on a granule cell through glomeruli, the synaptic strength depends on the "geometric" distance between cells.
- ✓ There is no connection between CFs and DCN.

The learning process relies on the error information given by CFs from the inferior olive (IO).A kind of STDP is considered where LTD (long term depression) is supplied when the IO firing rate provides an

error signal for a certain synapse. LTP (Long term potentiation) is represented by a slower constant increase in synaptic strength when no error signal occurs.

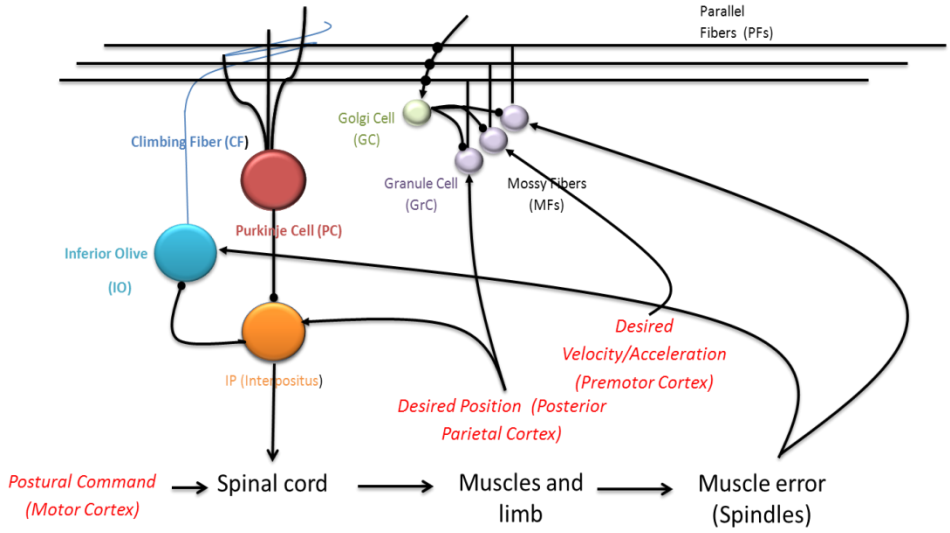

Figure 2.7. Internal structure in Schweighofer-Arbib Model. (Adapted from [47])

e. The MPFIM Model. Multiple Paired Forward-Inverse Model

The basic idea of this model conceives the cerebellum containing multiple pairs (modules) of forward (predictors) and inverse (controllers) models (MPFIM) [106]. Within each module, the forward and inverse model are coupled both during the acquisition and use, in which the forward model determines the contribution of each inverse model's output to the final motor command. This architecture simultaneously learns the multiple inverse models necessary for control. This model is based on the indirect/direct model approach by Kawato and at the same time the micro-complex theory previously described. As previously described, a microzone is a group of PCs and a micro-complex combines these PCs with a small group of neurons in a cerebellar or vestibular nucleus. Establishing and analogy, in MPFIM a micro-zone is built up by a set of modules which control the same degree of freedom, modules whose adaption is controlled by a single climbing fiber. Each module presents three types of PCs which compute a forward model, an inverse model or a responsibility predictor, but all of these three receive the same input. A single internal model acts as a controller which generates a motor command and a predictor which predicts the current state of the plant. Each predictor is a forward model of the controlled system, while a controller consists of an inverse model of the system

particularized for a specific region. There are also a set of responsibility signals which determines the weight contribution that a particular model will make to the overall output of the micro-zone.

Finally the control motor command consists of the output of the single models adjusted by the sum of responsibility signal: and planning.

$$\tau_{Forward} = \frac{\sum r_i \cdot \tau_i}{\sum r_i}; i = number\ \ of\ \ models \quad (1)$$

Where $\tau_{Forward}$ the forward motor command, τ_i is the motor command response of the model i, and finally r_i corresponds to the responsibility of model i.

The PCs are considered to have a linear response, MFs carry all necessary information (state information, efference copies of the last motor commands and desired states), GrCs transform the state information (even non-linearities) into a rich set of basic functions through PFs. Finally while a CF carries a scalar error signal a PF cell encodes a scalar output. Responsibilities, predictions and controller outputs are all of them one-dimensional values.

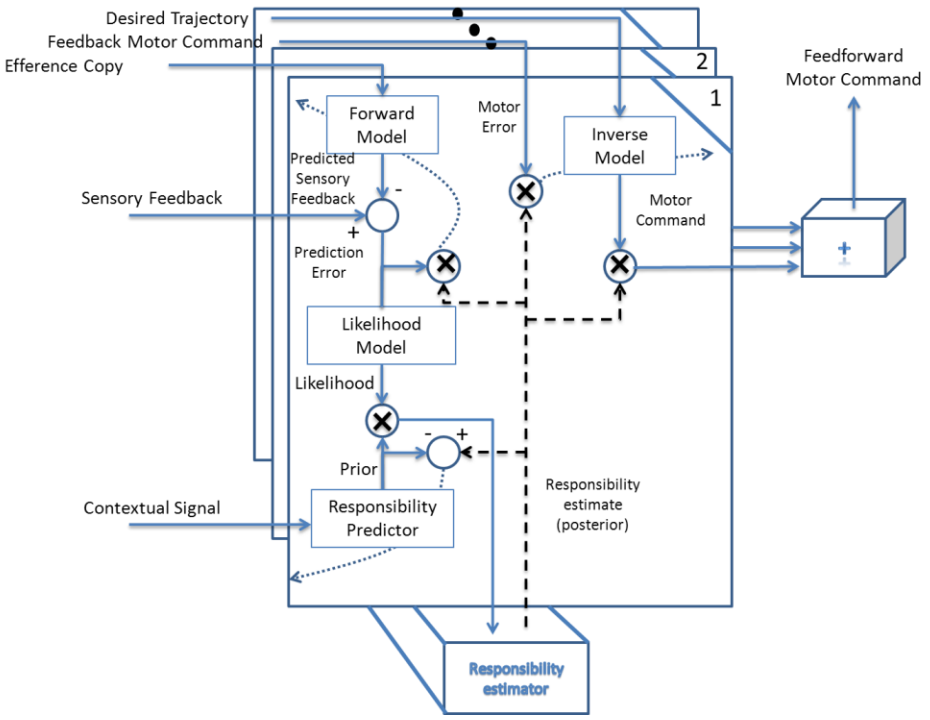

Figure 2.8. MPFIM Model. The thick dashed line shows the central role of the responsibility estimators' signals. Dotted lines passing through models are training signals for learning (adapted from [106]).

f. The Adaptive Filter Model

This cerebellar model was firstly proposed by Fujita [107]. Subsequent studies by Dean and Porril developed this theory in the last years [108] [109] [110].

Adaptive filters are used in cerebellar model functions as a response of Marr-Albus cerebellum theories [49] [50]. It was a response coming from control theory towards a better understanding of the "obscure" biological control. It was a successful attempt to apply a very well-known field to an unexplored/unexploited field [107].

Adaptive filters present parameters which can be self-adjusted to modify the output form. The input signal is decomposed into component signals by means of a set of filters. Filter set outputs are weighted and summed up to obtain the desired output. The self-adjustment is driven by a learning rule consistent with the well-known Hebbian covariance rule [111]. The learning rule modifies the weights according to the relation between the corresponding component signal and the teaching signal. This is called the Analysis-Synthesis filter model proposed by Dean and Porril [108] [110]. The system analyses and separates the frequency components of the input signal, correlates these individual components and the

system error and is able to synthesize (through local adaptation at the parallel fibers) the appropriate filtered responses towards a desired output.

To establish a comparison between this Analysis-Synthesis filter model and the cerebellar microcircuitry the reader is referred to Fig 9 (Adapted from [108])

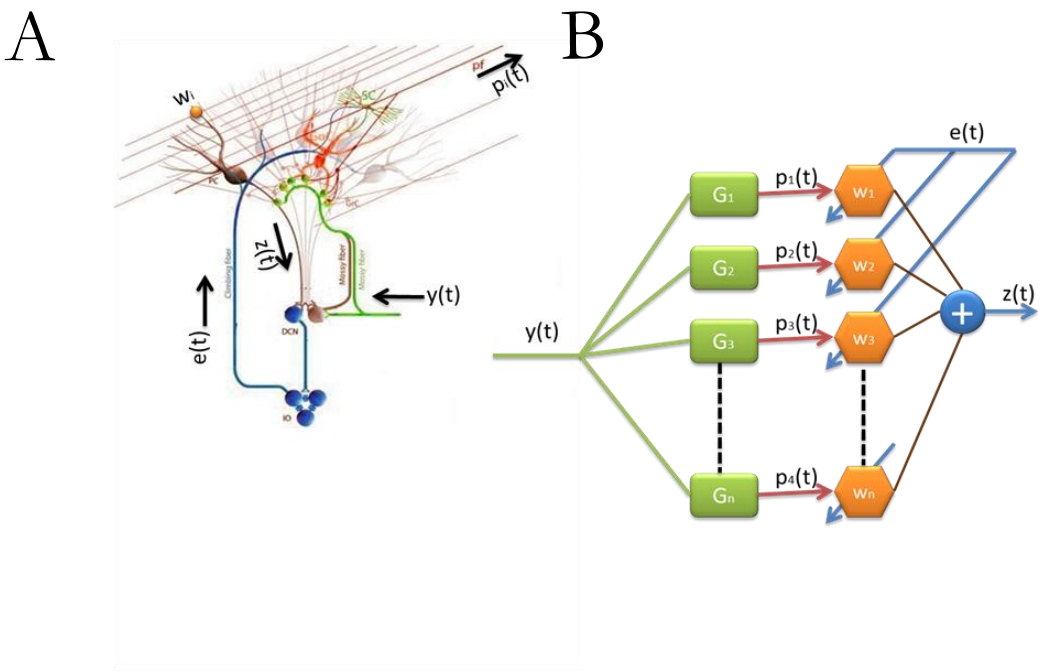

Figure 2.9. Adaptive Filter. This scheme shows the most relevant connections within a cerebellar module and its relation with an adaptive filter.
A) The cerebellar module presents different connections communicating different circuit elements in closed loops. Mossy fibers (MFs) contact granule cells (GrC) and DCN cells which, in turn, receive inhibition from the same common set of Purkinje cells (PC). Moreover, the IO cells project climbing fibers that contact PC which also are projected to DCN cells. B) Filter inputs correspond to MF firing. These incoming inputs are conveyed by GrC into parallel fibers. The component weights act as the synapses made by parallel fibers on PCs. PCs add the component weights signals obtaining the output. The correlation between climbing-fiber inputs and parallel fiber climbing is used by the correlation learning law, the strength of the synapse is increased if the correlation is negative and it is increased when the correlation is positive (Long Term Potentiation/Long Term Depression).

Climbing fiber and Teaching Signal.

It is well known that these climbing fibers carry information from various sources (spinal cord, vestibular system, red nucleus, sensory and motor cortices…etc). One widely assumed hypothesis is that their activation carries motor error signal sent to the cerebellum, and it seems to be also an important signal for motor timing but the way in which the error is translated into a climbing fiber signal is still an

open issue [112] [113] [114] [115]. In the very first approach to cerebellum as an adaptive filter made by Fujita [107] it was assumed that the climbing fiber response acted as a teaching signal in which its variable impulse rate was given by the difference between the output signal and a desired response. The weights can be adjusted increasing or decreasing iteratively their values in order to obtain the desired output signal, if the correlation between de "error signal" (climbing fiber) and the component weights (mimicking the synapses made by parallel fibers on PCs) was positive the weight was increased otherwise it was decreased. Fujita proposes an equivalent way to use the error signal learning principle as it is the case in the adaptive filter theory. Although this proposal does not consider nowadays biological climbing fiber known characteristics, it is an inspiring source which is used in different applications [1] [116] [11] (This Fujita approach has been evolved along last decade [108] [110] [109]).

Golgi-Granule Scheme

In order to understand a functional scheme of this theory, different general assumptions have to be made:

a) Golgi cells acts a leaky integrator. According to discharge pattern observations [117], it is assumed that Golgi cells act as temporal filters, with a transfer function given by $G(s) = k/(1+Ts)$, that is, a low pass filter in which $k > 0$, s represents Laplace transform of complex frequency and T represents cut-off frequency. That means that Golgi cells, in these models, show an integrator-like pattern with a time constant T on the order of several seconds. The corresponding parallel fiber signals have a similar response. That means that we obtain a bank of low pass filters that responds to a range of frequencies. Their output is convoluted with different weight (PC/PF synapses) according to a teaching signal driven by the error; the global response is a sum of different analog frequency signals as a response of input stimuli.

b) Adaptive filter breaks down the input signal into different components (that is supposed to be done in granular layer [118] [119]) ensuring a diversification in parallel fiber signals. This diversification is a phase diversification; this cerebellum model uses spikes as simple activity carriers.

c) Identical mossy fiber input signals should hit onto identical Golgi-granule cell areas. This is a controversial point. Although in [109] this fact is justified by means of biological records, until nowadays, recording granule activity has been a troublesome task, and the debate is opened. There

is no a consensus along adaptive filter cerebellum theory [107] [108] [110] [109] on how the mossy fibers codification is done. Mossy fiber inputs are treated as a signal given by a "transducer", transmission information spike theory [120] [121] is not taken into account; interspike/intraspike distance [122], population neural coding [121] or first spike information [122] are not included in the general adaptive filter behavior [123] though some research efforts are being currently done [124].

Purkinje Cells

Output signals from Golgi-granule cell are conveyed to PCs. The connection pathways to Purkinje are simplified, only the direct synaptic contact PF/PC is represented by a positive synaptic weight and an inhibitory interneuron per Purkinje is responsible of the negative synaptic weight. Both contributions are summed into a final output.

g. The Synchronous System Cerebellar Model

Maex and De Schutter published in 1998, their granular layer simulation model [125] consisting of Golgi cells, granule cells and mossy fibers all based in physiological findings. In their model the populations of both Golgi and granule cells became entrained in a single synchronous oscillation as a response to random mossy fiber stimulation and were robust over different parameters such as synaptic connection strengths, mossy fiber firing rates or the spiking propagation speed in parallel fibers.
Nevertheless, de-synchronization could happen in this implemented network under different conditions:

- Very low mossy fiber input activity. A very low activity rate at mossy fibers (and therefore at the GrCs) generates almost no excitation at the GoCs, and in this way, the synchronization path (GrC → GoC →GrC) is disabled.
- Strong dominant excitation of Golgi cells through mossy fiber synapses (in relation to parallel fiber synapses). This MFs → GoCs activity destabilizes the synchronism in the granule cells.
- Tonic activation of GrC inhibition [126] decrements the level of average activity in GrC. Thus, the synchronization elements (the Golgi cells) remain nearly inactive and do not produce such synchronism.

S. Solinas in 2010 [127] evolved this cerebellar model solving all the established restrictions because of the simulation capabilities in 1998. This evolved model simulates a more realistic large-scale model of

the cerebellar granular layer and verifies some spatio-temporal filtering properties founded in physiological studies. This model implements the main granular layer properties which make the cerebellum being such an important part of the nervous system.

The main weakness that this model presents is that it has not been clarified how the properties which the implemented granular layer has, can be efficiently used for a functional signal processing and how these properties can solve specific problems in a relevant task framework such as movement correction or eye blink conditioning.

h. The Yamazaki and Tanaka Cerebellar Model (Liquid State Machine)

This model assumes that the cerebellum generates activity patterns without temporal recurrence representing the passage of time [128]. The granular layer acts as an event-driven internal clock triggered by an initial activity pattern. Each time step can be represented with combinations of active granule cells.

According to that point of view, the cerebellum can be interpreted as a liquid state machine. The presentation of finite sequences of active neuron populations without recurrence as the response to different combinations of binary inputs can be compared to a liquid state machine [129] with high power of information processing.

Neuro-physiological findings support the hypothesis that the neural clock could be implemented by the inhibitory loop composed of GrCs and GoCs s [130]. That is, GrCs would excite GoCs (through PFs) thanks to their input stimuli, and subsequently, these GoCss would inhibit some of the granule cells, thus obtaining the transition between active and inactive states and therefore representing the passage of time.

One of the main critics that this model could have is related to its application field. This simple model has been successfully applied to eye blink conditioning problem. By contrast, this model has never been put into practice in more difficult scenarios such as coordination of body-movements where the cerebellum is involved.

The eye blink conditioning solution should correlate the inter-stimulus interval and the unconditional stimulus, but, in this problem, the cerebellar output, supplied by the deep cerebellar nuclei cells (DCN) presents just two different states; active DCN (closed eyelid) or inactive DCN (open eyelid). In other motor tasks (i.e. target reaching or fast ballistic movements) a continuous error correction in time is mandatory in order to execute properly the desired planned movement, that is, DCN output must be

more than just a bi-stable output, DCN output has to supply as many temporal states as the temporal correction demands.

Summarizing, this model proposes a cerebellar architecture composed of two different sub-circuits. The first one (where GrCs, GoCs and MFs are located) represents a liquid state machine, and generates non recurrent sequences of activity. The second one (where MFs and cerebellar nucleus cells are located) represents a simple perceptron. This cerebellar architecture receives a teaching signal from the inferior olive.

9. Discussion and Comparison

Summing up, the presented models can be categorized as follows:

- State-encoder-driven models: These kinds of models present a granule cell layer where on/off types of entities are located. These on/off entities divide the state space (Marr-Albus Model, CMAC model, APG model or Yamazaki and Tanaka).These models fit well in simple function approximations, and suffer strongly from the curse of dimensionality.
- Functional models: these models have been developed based on the functionality that the cerebellar architecture seems to possess. These models just take into account the functional understanding of the cells. In this case, it is obtained only a basic insight into the functions of the parts and finally it is applied as a crude approximation (MPFIM model, Adaptive Filter model or APG model). This kind of approximation derive from an engineering point of view and can solve most of the tasks that the cerebellum seems to perform, such as the eye blink conditioning or the movement correction, but in contrast, the lack of realistic implementations, and the suppositions that these models assume with little neuro-finding backup make these models not be still well established among the neurophysiology community.
- Cellular-level models: Obviously, the most realistic simulations would be at the cellular level. Although these models fully fit from a neuro-physiological point of view, yet their application in the context of a whole cerebellum model and the modeling and computing of just only a few Purkinje /Granular/ Mossy Fibers/Golgi / Inferior Olive/ Deep Cerebellar Nuclei cells at realistic conditions, remains unclear. Still, from the biological point of view these kinds of models are the most important since they allow obtaining insight into cerebellar function at cellular level. The first steps in this direction were taken by the Schweighofer–Arbib model (e.g. Synchronous System Cerebellar Model and Scheweighofer-Arbib model [19] [46] [47]).

The contribution of this work is also related to this level of detail but keeping in mind the cerebellar functionality in a manipulation task scenario that the proposed models must present. For a further overview the reader is referred to [1] [11] [12] [13] [14] [131]

In this thesis contextualization chapter, it is demonstrated the importance of multidisciplinary studies where both neurophysiologists and engineers are involved.

Neurophysiologists have studied and proposed very detailed models according to physiological findings; however actual modeled physiological systems are usually not ready to carry out complex and specific tasks at a system level. By contrast, engineers have proposed machine-like systems that try to solve particular biological problems assuming an engineered point of view.

Thus, both, neurophysiologists and system engineers need to work shoulder to shoulder towards a perfect understanding of how specific problems are solved using biologically plausible computational principles.

SpikeFORCE, SENSOPAC and REALNET are European projects (FP5, FP6 and FP7) in which our research group has been involved during more than a decade (and it is still involved) where the understanding of the relationship between neuroscience, computational neuroscience and classical control theory has represented and represents the philosopher's stone of our research.

CHAPTER 3

Discussion and Conclusions

This chapter shows a summary of the main contributions of the presented work as well as future lines of work raised from the proposal work made in this memory. Finally a brief resume of the obtained researched results in terms of international conferences and scientific journals is included.

I. DISCUSSION

- ✓ As a first step, this thesis (chapter 4 section 1) presents how a simple spiking cerebellum-like architecture can infer corrective models in the framework of a motor control task when manipulating objects that significantly affect the dynamics model of the base robotic system. This initial approximation evaluates a simplified bio-mimetic approach during a manipulation task. It focuses on how the model inference is carried out by a cerebellar module within a forward control loop and on how these inferred internal models are built up by means of biologically plausible synaptic adaptation mechanisms. A basic temporal-correlation kernel including a specific long-term depression (LTD) and a non-specific long-term potentiation (LTP) at parallel fiber-Purkinje cell synapses can effectively infer corrective models. It is also evaluated how this spike-timing-dependent plasticity correlates sensorimotor activity arriving through the parallel fibers with teaching signals (dependent on error estimates) arriving through the climbing fibers from the inferior olive. This first approximation to a functional bio-inspired cerebellar model brought some light about how these LTD and LTP components need to be well balanced with each other to achieve accurate learning. Furthermore, it is illustrated how the temporal-correlation kernel (used for the LTD computation) can also work in the presence of transmission delays in sensorimotor pathways.

  This kind of investigations may provide clues on how biology achieves accurate control of non-stiff-joint robot with low-power actuators which involve controlling systems with high inertial components.

  The associated journal article to this point is:

N. R. Luque, J. A. Garrido, R. R. Carrillo, O. J. M. D. Coenen, E. Ros, " Cerebellar-like Corrective Model Inference Engine for Manipulation Tasks ", *IEEE Transactions on Systems, Man, and Cybernetics, Part B: Cybernetics*, **41**(5), 2011.

- ✓ Secondly this thesis (chapter 4 section 2) evaluates a way in which a spiking cerebellar-like structure (an evolution of the previous model) can store a model in the granular-molecular layers. As it was explained in contextualization chapter the cerebellum is assumed to be one of the main nervous centers involved in correcting and refining planned movement and accounting for disturbances occurring during the movement, for instance due to the manipulation of objects which affect the kinematics and dynamics of the robot-arm plant model, so it is interesting to study not only the molecular layer storage capability but also how the cerebellar microstructure and its input representations (context labels and sensor signals) can efficiently support model abstraction towards delivering accurate corrective torques for increasing precision during different-object manipulation. This work also described how the explicit (object-related input labels) and implicit state input representations (sensory signals) complement each other to better handle different models allowing interpolation between two already stored models. This facilitates accurate corrections during manipulations of new objects taking advantage of already stored models.

The associated journal article to this point is:

N. R. Luque, J. A. Garrido, R. R. Carrillo, O. J. M. D. Coenen, E. Ros, "Cerebellar Input Configuration Toward Object Model Abstraction in Manipulation Tasks". *IEEE Transaction on Neural Networks*, **22**(8), 1321-1328, 2011.

- ✓ As a natural evolution of this thesis, the next step focuses on evaluating the capability of the previously developed spiking cerebellar model when it is embedded in different loop architectures (recurrent, forward, and recurrent & forward architectures) to control a robotic arm (chapter 4 section 3). The implemented spiking network self-adapts and copes with perturbations in a manipulation scenario: changes in dynamics and kinematics of the simulated robot. Furthermore, the effect of several degrees of noise in the cerebellar input pathway (mossy fibers) was assessed depending on the employed control architecture. The implemented cerebellar model managed to adapt in the three control architectures to different dynamics and kinematics providing corrective actions for more accurate movements. However, according to the obtained results, coupling both

control architectures (recurrent & forward) provides benefits of the two of them and leads to a higher robustness against noise.

The associated journal article to this point is:

N. R. Luque, J. A. Garrido, R. R. Carrillo, S. Tolu, E. Ros, Adaptive Cerebellar Spiking Model Embedded In The Control Loop: "Context Switching And Robustness Against Noise", *Int. Journal of Neural Systems*, **21**(5), pp. 385-401, 2011.

- ✓ Once the primary cerebellar architecture and control loop is settled, it is time to evolve the achieved system according to not only an engineered point of view (machine-like systems that try to solve particular biological problems) but also taking into account physiological findings (chapter 4 section 4). As it was shown in contextualization chapter, in biological systems, instead of actual encoders at different joints, proprioception signals are acquired through distributed receptive fields. In robotics, a single and accurate sensor output per link (encoder) is commonly used to track the position and the velocity. Interfacing bio-inspired control systems with spiking neural networks emulating the cerebellum with conventional robots is not a straight forward task. Therefore it is necessary to adapt this one-dimensional measure (encoder output) into a multidimensional space (inputs of a spiking neural network) to connect, for instance, the spiking cerebellar architecture; i.e. a translation from an analog space into a distributed population coding in spike space. In this subsection it is analyzed how evolved receptive fields (optimized towards information transmission) can efficiently generate a sensori-motor representation that facilitates its discrimination from other "sensori-motor" states. This can be seen as an abstraction of the **Cuneate Nucleus** (CN) functionality in a robot-arm scenario. The CN is modeled as a spiking neuron population coding in time according to the response of realistic mechanoreceptors during a multi-joint movement in a robot joint space. An encoding scheme that takes into account the relative spiking time of the signals propagating from peripheral nerve fibers to second-order somatosensory neurons is proposed. Following the nature-inspired analogy, evolved configurations have shown to outperform simple hand-tuned configurations and other homogenized configurations based on the solution provided by the optimization engine (genetic algorithm).

  The associated journal article to this point is:

Luque, N. R.; Garrido, J. A.; Ralli, J.; Laredo, J. J.; Ros, E.: "From Sensors to Spikes: Evolving Receptive Fields to Enhance Sensory Motor Information in a Robot-Arm Scenario". *Int. Journal of Neural Systems*, **22**(4), pp. 0-20, 2012.

II. ALL ASSOCIATED PUBLICATION WITH THIS THESIS

The developed research has been done in the framework of two European projects; REALNET (IST-270434)/SENSOPAC (IST-028056) where different challenges have been addressed from different perspectives through synergies between neurophysiologists and engineers from different fields. This work has been evaluated in a framework of international conferences and scientific journals (with impact factor IF on JCR).

1. International Peer-review Journals

1. **Luque, N. R.**; Garrido, J. A.; Carrillo, R. R.; Coenen, O. J. M. D.; Ros, E: "Cerebellar-like corrective-model abstraction engine for robot movement control". *IEEE Transaction on system, man, and cybernetics - Part B: Cybernetics,* **41**(5), 2011. Impact Factor (JCR 2011): ***3.080. Quartile Q1 in categories: Automation & Control Systems, Computer Science, Artificial Intelligence and Computer Science, Cybernetics***

2. **Luque, N. R.**; Garrido, J. A.; Carrillo, R. R.; Coenen, O. J. M. D.; Ros, E: "Cerebellar input configuration towards object model abstraction in manipulation Tasks". *IEEE transaction on neural networks,* **22**(8), 1321-1328, 2011. Impact Factor (JCR 2011): ***2.952. Quartile Q1 in categories: Computer Science, Artificial Intelligence, Computer Science, Hardware & Architecture. Computer Science, Theory & Methods and Engineering, Electrical & Electronic.***

3. **Luque, N. R.**; Garrido, J. A.; Carrillo, R. R.; Tolu, S.; Ros, E.: "Adaptive cerebellar spiking model in a bio-inspired robot-control loop". *International Journal on Neural Systems*, **21**(5), 385-401, 2011. Impact Factor (JCR 2011): ***4.284. Quartile Q1 in category: Computer Science, Artificial Intelligence***.

4. **Luque, N. R*.**; Garrido, J. A*****.; Ralli, J.; Laredo, J. J.; Ros, E.: "From Sensors to Spikes: Evolving Receptive Fields to Enhance Sensory Motor Information in a Robot-Arm Scenario". *International Journal on Neural Systems*, **22**(4), 1-20, 2012. Impact Factor (JCR 2011): ***4.284. Quartile Q1 in category: Computer Science, Artificial Intelligence.***

   *****Both authors contributed equally to this work

5. Tolu, S.; Vanegas, M.; **Luque, N. R.**; Garrido, J. A.; Ros, E.: "Bio-Inspired Adaptive Feedback Error Learning Architecture for Motor Control". *Biological Cybernetics*, **106**(8-9), 507-522, 2012. Impact Factor (JCR 2011): ***1.586. Quartile Q1 in category: Computer Science, Cybernetics. Quartile Q4 in category: Neuroscience.***

6. Tolu, S.; Vanegas, M.; Garrido, J. A.; **Luque, N. R.**; Ros, E.: "Adaptive and Predictive Control of a Simulated Robot Arm" *International Journal on Neural Systems*, Accepted for publication. Impact Factor (JCR 2011): ***4.284. Quartile Q1 in category: Computer Science, Artificial Intelligence.***

2. International Peer-review Proceedings

1. Passot, J. B.; **Luque, N. R.**; Arleo, A.: "Internal models in the cerebellum: a coupling scheme for online and offline learning in procedural tasks". International Conference on Simulation of Adaptive Behavior, (SAB 2010). In Doncieux, S. et al., editors, LNAI Simulation of Adaptive Behavior, vol. 6226, pp 435-446, Springer-Verlag, (2010).

2. **Luque, N. R.;** Garrido, J. A.; Carrillo, R. R.; Ros, E.: "Cerebellar spiking engine: Towards object model abstraction in manipulation". International Joint Conference on Neural Networks (IJCNN 2010).

3. Garrido, J. A.; Carrillo, R. R.; **Luque, N. R.**; Ros, E.: "Event and time driven hybrid simulation of spiking neural networks". International Work-Conference on Artificial Neural Networks (IWANN 2011). Advances in Computational Intelligence. Lecture Notes in Computer Science, 6691, pp. 554-561. Springer, Heidelberg (2011).

4. **Luque, N. R.**; Garrido, J. A.; Carrillo, R. R.; Ros, E.: "A spiking cerebellum model in a multi-context robot control scenario for studying the granular layer functional role". International Work-

Conference on Artificial Neural Networks (IWANN 2011). Advances in Computational Intelligence. Lecture Notes in Computer Science, 6691, pp. 537-546. Springer, Heidelberg (2011).

5. Casellato, C.; Pedrocchi, A.; Garrido, J. A; **Luque, N. R.;** Ferrigno, G.; D'Angelo, E.; Ros, E.: "An integrated motor control loop of a human-like robotic arm: Feedforward, feedback and cerebellum-based learning". International Conference on Biomedical Robotics and Biomechatronics (BioRob), 2012 4th IEEE RAS\& EMBS .pp. 562-567(2012).

6. Garrido, J.A*.; **Luque, N.R*.**; D'Angelo, E.; Ros, E.; "Enhancing learning precision at parallel fiber-Purkinje cell connections through deep cerebellar nuclei LTD and LTP". Federation of European Neurosciences (FENS2012) (2012).* Both authors contributed equally to this work

III. SCIENTIFIC FRAMEWORK

This thesis has been developed in the framework of two European Projects:

- ✓ SENSOPAC (SENSOrimotor structuring of Perception and Action for emergent Cognition (FP6-IST-028056))
- ✓ REALNET (Realistic Real-time Networks: computation dynamics in the cerebellum (FP7-IST-270434)).

This fact has provided the perfect scenario to our research group for collaborating with different research groups at other European Universities and research institutions. The presented work represents just a part of the whole contribution the University of Granada has done in this two SENSOPAC/REALNET consortiums. In this scenario, the aims to be reached make a multidisciplinary approach mandatory.

This work mainly presents different results from a biological system point of view however this work involves other knowledge areas. Dealing with robotic systems using biological findings or implementing and evolving a realistic neural network simulator capable of running in different environments (task mostly developed by Jesús Alberto Garrido) are just a pair of examples of how difficult the research process was. It would not be fair to avoid the fact that all this effort has required a high collaborative and coordinated work with the working team.

IV. MAIN CONTRIBUTIONS

- A biologically relevant cerebellar model (embedded in a forward control loop with a crude inverse dynamics module) has been evolved and implemented. This model can effectively provide corrective torque to compensate deviations in the dynamics of a base plant model.

- It has been evaluated how a temporal-correlation kernel driving a specific error-related LTD and a compensatory non-specific LTP component (complementing each other) can achieve effective adaptation of the corrective cerebellar output. Both LTD and LTP need to be balanced with each other to achieve high performance adaptation capabilities and effective reduction of error in manipulation tasks with objects which significantly affect the dynamics of the base arm plant.

- In addition it has been studied how a temporal-correlation kernel can work even in the presence of sensorimotor delays. This cerebellar structure can adaptively generate any suitable output for each trajectory point codification; the delay of the sensorimotor pathways is not remarkably relevant.

- An evaluation of the input sensory signal influence over an evolved cerebellum architecture is presented (The granular layer is now added). Two input representations, context-related inputs (EC), and only actual sensory robot signals (IC) encoding the state during the experiments have been studied. The IC&EC cerebellar configuration takes advantage of both kinds of signals providing smoother inter-context transitions at a fast convergence speed, allowing the interpolation of new contexts based on previously acquired models and overcoming misleading external contextual information, thus making this cerebellar configuration robust against incongruent representations.

- This cerebellar architecture has been evaluated in different control loops (RR, FD, and FD&RR) in several noisy scenarios. The obtained results indicate that coupling both control loop architectures (FD&RR) leads to faster learning convergence, better accuracy gain and improved output stability in a noisy scenario.

- Moreover, it has been demonstrated that this (FD&RR) control architecture in context switching has the capability of inferring and storing different corrective models simultaneously under dynamic/kinematic modifications better than FD or RR configurations on their own. This proposed architecture is compatible with several neurophysiological findings.

- Finally, a general methodology (by means of using genetic algorithms) for efficiently representing joint encoder signals into spike patterns in a plausible robot scenario is presented.

These contributions covers the thesis objectives presented in the first chapter as follows: the first three points of this contribution section deal with the first objective. The next point corresponds to the second listed objective. The two last but one contribution points address the third objective. And the last contribution point corresponds to the last objective.

V. FUTURE WORK

As a future work there are two main research lines to be followed. On one hand it is necessary to evolve the whole cerebellar model in the framework of a control task by taking advantage of a larger number of biological processing characteristics of neurons and networks. Although there is not a straight connection between these neurophysiological properties and its final application in a particular control task scenario, the study of how these findings could improve a plausible cerebellar model requires a lot of research effort. It is mandatory to build a bridge between these apparently unrelated fields to better understand the architectural/functional/biological principles in the cerebellum. The inclusion of synaptic plasticity at most of the cerebellar synapses (as experimental studies have shown the existence of these mechanisms) will be our first step in this promising way. Achieving this distributed learning involves a powerful biological plausible control tool that automatically configures itself to match the surrounding environment just and to obtain the best possible performance. Adaptation mechanisms in connections such as MF→DCN or PC→DCN, together with the very well-known plasticity between GrC→PF→PC has been proven recently to have a strong impact in the learning consolidation [132].

It is also of high interest the IO→DCN connection; a biologically plausible Feedback Error Learning reinterpretation constitutes a prior research aim. This connection could play a key role to understand how a fast biological control in a real scenario could be possible without a classical PID controller (or

other classical controller strategies belonging to this control field) as functional approximations use such as CMAC, MPIM, LWPR or Fujita cerebellar inspired models.

More related with neural characteristics, an evolution of the granular layer with lateral inhibition in its neurons constitutes our incoming goal. By taking full advantage of this new feature, a better codification of input patterns will allow a better precision in terms of discrimination.

The second research line is related with the manipulation task. We are working on connecting the entire developed networks not just to a simulator but also to a real robot. We have to develop the way to interface in real time our cerebellar model with the real robot; we have to re-implement physical controllers which are able to modify point by point their actuation. We have to develop a methodology to validate different cerebellar model proposals in a manipulation task in terms of stability since classical mathematical tests such as Lyapunov stability test, Routh-Hurwitz criterion, Nyquist stability criterion etc do not fit well in these spiking cerebellar neural networks. Spiking cerebellar neural networks present an overwhelming dimensionality and complexity on the contrary classical mathematical tests are commonly applied to problems with lower levels of complexity and dimensionality where a perfect knowledge of the system is available. Indeed, when applying these classical mathematical tests, every single behavior is well known and restricted to certain boundaries where the whole system behaves deterministically and the computational test can be accomplished. These requirements are not available in a spiking neural network because of its own nature.

All these issues will be addressed in a recently started EU project (REALNET (IST-270434)).

CHAPTER 4

Methods & Results: Published and accepted papers

1. CEREBELLAR-LIKE CORRECTIVE-MODEL ABSTRACTION ENGINE FOR ROBOT MOVEMENT CONTROL.

Luque, N. R.; Garrido, J. A.; Carrillo, R. R.; Coenen, O. J. M. D.; Ros, E: "Cerebellar-like corrective-model abstraction engine for robot movement control". *IEEE Transaction on system, man, and cybernetics - Part B: Cybernetics,* **41**(5), 2011.

Status: Published

Impact Factor (JCR 2011): **3.080**

Subject Category:

- Automation & Control Systems. Ranking **2/58** , Quartile in Category: **Q1**
- Computer Science, Artificial Intelligence. Ranking **10/111**, Quartile in Category: **Q1**
- Computer Science, Cybernetics. Ranking **1/20**, Quartile in Category: **Q1**

2. CEREBELLAR INPUT CONFIGURATION TOWARDS OBJECT MODEL ABSTRACTION IN MANIPULATION TASKS.

Luque, N. R.; Garrido, J. A.; Carrillo, R. R.; Coenen, O. J. M. D.; Ros, E: "Cerebellar input configuration towards object model abstraction in manipulation Tasks". *IEEE transaction on neural networks,* **22**(8), 1321-1328, 2011.

Status: Published

Impact Factor (JCR 2010): **2.952**

Subject Category:

- Computer Science, Artificial Intelligence. Ranking **12/111** , Quartile in Category: **Q1**
- Computer Science, Hardware & Architecture. Ranking **1/50**, Quartile in Category: **Q1**
- Computer Science, Theory & Methods. Ranking **4/99**, Quartile in Category: **Q1**
- Engineering, Electrical & Electronic. Ranking **19/245**, Quartile in Category: **Q1**

3. ADAPTIVE CEREBELLAR SPIKING MODEL IN A BIO-INSPIRED ROBOT-CONTROL LOOP

Luque, N. R.; Garrido, J. A.; Carrillo, R. R.; Tolu, S.; Ros, E.: "Adaptive cerebellar spiking model in a bio-inspired robot-control loop". *International Journal on Neural Systems*, **21**(5), 385-401, 2011.

Status: Published

Impact Factor (JCR 2010): **4.284**

Subject Category:

- Computer Science, Artificial Intelligence. Ranking **4/111** , Quartile in Category: **Q1**

4. FROM SENSORS TO SPIKES: EVOLVING RECEPTIVE FIELDS TO ENHANCE SENSORY MOTOR INFORMATION IN A ROBOT-ARM SCENARIO

Luque, N. R.; Garrido, J. A.; Ralli, J.; Laredo, J. J.; Ros, E.: "From Sensors to Spikes: Evolving Receptive Fields to Enhance Sensory Motor Information in a Robot-Arm Scenario". Major revision in *International Journal on Neural Systems.*

Status: Published

Impact Factor (JCR 2010): **4.237**

Subject Category:

- Computer Science, Artificial Intelligence. Ranking **4/111** , Quartile in Category: **Q1**

CHAPTER 5

Introducción en Castellano

A día de hoy realizar una asociación entre cerebelo y diferentes características de control motor humano no es una asunción descabellada. De hecho, es de conocimiento general que el cerebelo desarrolla un rol fundamental en el control de movimientos rápidos y precisos. [1] [2] [3] [4]; El cerebelo es responsable de supervisar los llamados movimientos balísticos (movimientos extremadamente rápidos), siendo capaz de establecer la duración de dichos movimientos por adelantado (dirigiendo sus secuenciaciones temporales) y suministrando aquellos pares correctivos necesarios para su correcta ejecución [6] [7].

Todas estas características de secuenciación y control son llevadas a cabo correctamente gracias a la existencia de los diferentes mecanismos de realimentación presentes a lo largo de la estructura cerebelar [8] [9]. Haciendo uso de dichas estructuras de realimentación, el cerebelo es capaz de generar cierta elasticidad muscular en diferentes movimientos, ayudando así al sistema nervioso central a predecir el movimiento de cada una de las partes constitutivas de nuestro cuerpo [10]. Esta panoplia de características presentes en el cerebelo entroncan bien en el campo de la teoría de control y más concretamente en el campo de la robótica, en donde el cerebelo podría utilizarse como un controlador biológicamente plausible que pudiera orquestar apropiadamente la actividad motora del robot a controlar. [11] [12] [13] [14] [15] [16] [17] [18] [19].

Si bien, la relación existente entre el cerebelo y diferentes tipos de aprendizaje motor no es un campo del todo conocido con absoluta certeza, aún lo es menos la implicación del mismo en lo que es llamado "funciones de alto nivel" [20] [21]. A mediados de los ochenta, algunos descubrimientos experimentales en distintos campos de investigación empezaron a mostrar que el cerebelo no solo estaba implicado en tareas no motoras sino que también en la cognición espacial del individuo [22] [23] [24]. Los estudios de neuro-imagen han mostrado la activación del cerebelo en distintos procesos cognitivos tales como: generación de palabras [25], compresión y procesamiento semántico [26] [27], reconocimiento verbal y no verbal [28], memoria verbal inmediata [29], planificación cognitiva [30], imaginación motora [30], adquisición sensorial y discriminación [31] o atención cognitiva [32]. Por otro lado, también se han obtenido distintas evidencias de estos procesos cognitivos en distintos pacientes con lesiones focales [33] [34]: alteraciones en la velocidad de procesamiento en movimientos espaciales complejos y planificación operacional de tareas, generación de palabras en relación a una consigna, planificación y flexibilidad en razonamiento abstracto, memoria operativa o percepción y temporización motora. De

igual forma también se han observado cambios de personalidad, agratismo, disprosodia y dificultades ante cambios rápidos y precisos para llamar la atención.

Resulta pues evidente que durante la pasada década se han descubierto un conjunto importante de evidencias que reflejan el hecho de que el cerebelo está implicado en ciertas funciones cognitivas, sin embargo algunos investigadores presentan cierta actitud escéptica antes tales afirmaciones debido al hecho de que los experimentos llevados a cabo para demostrar estas implicaciones no están libres de toda duda [35] [36]. La activación cerebellar en ciertas tareas no permite asegurar directamente un rol fundamental del cerebelo en el proceso cognitivo bajo estudio debido a diferentes causas: los resultados clínicos presentan inconsistencias y contradicciones, no es fácil controlar los efectos de los problemas motores, las tareas son complejas y los déficits observados son difíciles de interpretar...etc. De cualquier manera, podemos asegurar que estamos ante uno de los campos de investigación más notables en neurofisiología.

Por lo tanto, teniendo en cuenta el comportamiento multitarea que el cerebelo presenta, y considerando:

- Que la organización sináptica uniforme que presenta el córtex cerebelar sugiere que tanto las funciones motores como cognitivas del mismo pudieran ser emuladas mediante los mismo principios computacionales.

- Y que un control robótico biológicamente plausible parece ser un buen candidato con el que trabajar para arrojar algo de luz sobre la funcionalidad cerebellar.

Es posible afirmar que una combinación de ambos campos (principios computacionales cerebelares y teoría de control) debería poder suministrar una herramienta útil para entender la funcionalidad cerebellar y cómo esta es llevada a cabo por los circuitos nerviosos. Estos dos puntos constituyen los pilares de esta tesis y serán desarrollados a lo largo de las siguientes secciones.

Como conclusión podemos afirmar que el principal objetivo de esta tesis consiste en progresar hacia la adquisición de un mejor conocimiento de los roles funcionales que el cerebelo presenta, bien sea en los procesos cognitivos motores, bien en los procesos espaciales, así como explorar el conjunto de fundamentos y reglas computacionales que nos permitan inferir el cómo dichos procesos pudieren establecerse en el cerebelo

I. EL PORQUÉ ES FUNDAMENTAL EL ESTUDIO DEL CEREBELO

El cerebelo es una región del cerebro que desempeña un papel relevante en el control motor. Dicho cerebelo además se encuentra relacionado con algunas funciones cognitivas tales como atención y lenguaje y probablemente algunas funciones de carácter emocional como fue previamente expuesto [41].

El cerebelo está inserto en un bucle de control motor que posibilita el ajuste del movimiento muscular [42] [43]. Cuando el córtex envía un comando motor hacia las neuronas motoras inferiores en el tronco encefálico y hacia la espina dorsal, a la misma vez se dirige una copia de esta información hacia el cerebelo. Concretamente, esta información motora se transporta desde las fibras piramidales en el córtex, en el tracto cortico-pontino-cerebelar, hacia el cerebelo. Junto a esta información motora, la información postural procedente de músculos, articulaciones y tendones alcanza también al cerebelo. [45]. Esta información permite al cerebelo determinar como de bien los comandos motores generados desde el córtex lo están haciendo y a su vez coordinar la actividad muscular para conseguir movimientos armoniosos y suaves mediante su conexión con los sistemas piramidales y extra piramidales y la formación reticular descendente [46] [47]. La principal consecuencia de este rol en la coordinación motora de movimientos precisos radica en el hecho de que el cerebelo pueda realizar una contribución importante en el control de movimientos musculares rápidos y alternos necesarios para obtener cierta velocidad.

El cerebro humano posee (estimado) unas cien mil millones de neuronas. Algunas fuentes defienden que el número ronda entre 10 and 100 mil millones [37] [38] ocupando el cerebelo sólo un 10% del volumen total del cerebro y poseyendo una estimación próxima al 50% de todas las neuronas del cerebro [39]. El cerebelo se muestra como una estructura independiente unida justo a la parte inferior del cerebro, localizado bajo los hemisferios cerebrales. Está revestido por una lámina intrincada de tejido llamada corteza cerebelosa, que contiene casi todas sus neuronas, donde las células de Purkinje y granulares resultan ser las de mayor relevancia [37] [39]. Tal cantidad de neuronas e interconexiones dotan al cerebelo de una gran capacidad de procesamiento de señales [40] (aun a pesar de que la mayoría de las salidas cerebelares se dirigen hacia un conjunto reducido de núcleos cerebelosos profundos localizados en el interior del cerebelo). Además, el cerebelo no sólo se ve implicado en el control motor, sino también está relacionado con varios tipos de aprendizaje motor, siendo el más relevante de ellos, el aprendizaje del ajuste a realizar sobre las primitivas sensoriomotoras [48]. A lo largo

de las últimas décadas se ha realizado un enorme esfuerzo en la construcción de modelos cerebelares teóricos para tratar de explicar dicho ajuste sensoriomotor en términos de plasticidad sináptica en el cerebelo (para una revisión más profunda se remite al lector al capítulo 2, sección 4). La mayoría de los modelos teóricos se basan en los primeros modelos formulados por Marr-Albus [49] [50], en donde cada célula Purkinje recibe dos tipos de entrada radicalmente diferentes: por un lado, miles de entradas provenientes de las fibras paralelas, cada una de ella individualmente muy débil, y por otro lado, la entrada de una sola fibra trepadora , que es, sin embargo, de acción tan fuerte que su actuación es capaz de dirigir la actividad de su célula Purkinje objetivo pudiendo ser artífice del disparo de un potencial de acción complejo. El concepto básico de la teoría de Marr-Albus reside en el hecho de que la fibra trepadora hace las veces de "señal de aprendizaje" [51], capaz de inducir un cambio a largo plazo en la eficacia sináptica de las fibras paralelas (actuando como entrada) que son activadas sincronizadamente [52]. Observaciones de (LTD) depresión a largo plazo en las fibras paralelas (reducción de la eficacia de la sinapsis neuronal.) son las principales artífices de la aparición de teorías de este tipo, sin embargo la validez de las mismas sigue siendo fuente de debate [53].

Se ha implementado y desarrollado un modelo teórico del cerebelo basado en una red neuronal de impulsos a lo largo de esta tesis. Dicho modelo y su evolución se desarrolla a lo largo de los artículos en revistas incluidos.

II. EL CEREBELO EN EL CONTROL MOTOR

Los sistemas de control biológico (los cuales son capaces de controlar sistemas biológicos no rígidos, tales como son las articulaciones superiores humanas) han evolucionado durante años convirtiéndose por derecho propio en un paradigma a seguir por los controladores robóticos actuales [54]. Se sabe que el cerebelo está implicado de alguna manera en la generación y aprendizaje de movimientos coordinados con cierta gracilidad [6]. Resulta por tanto evidente que, un conocimiento preciso y profundo sobre el cómo ésta avanzada máquina de control funciona, debería ser de ayuda en el proceso de control de robots biomorficos.

El brazo humano, entendido como manipulador mecánico, está compuesto por elementos rígidos; los huesos, los cuales están unidos con juntas flexibles (articulaciones), cuya flexibilidad se modifica en relación con el objeto a ser manipulado. Tanto huesos como uniones flexibles se encuentran articuladas por los músculos, músculos que actúan como efectores de alto rendimiento (poseen una alta relación

fuerza/masa). Estos efectores producen una contracción al recibir un estímulo nervioso, y se disponen en pares opuestos con el fin de permitir movimientos rotacionales bidireccionales en cada una de las articulaciones [55].

Todo el conjunto brazo-antebrazo-mano no posee una precisión mecánica extremadamente buena, por el contrario, sí que presenta una extraordinaria movilidad (27 grados de libertad en total donde cada dedo presenta 4 grados de libertad; 3 para extensión-flexión y 1 para abducción y aducción. El pulgar es un poco más complejo poseyendo 5 grados de libertad, quedando 6 grados de libertad para la rotación y traslación de la muñeca [56] más los 7 grados de libertad [57] del brazo) y una gran cantidad de sensores de esfuerzo para compensar esta falta de precisión ayudando así en las tareas de control. Nuestra gran capacidad de manipulación es consecuencia directa de la actuación del cerebelo como sistema de control capaz de desarrollar tareas de todo complejas con resultados hoy día inalcanzables por cualquier otro sistema de control actual.

En un escenario donde un sensor biológico detecta un contacto mecánico, el retardo de trasmisión del impulso generado desde el contacto del dedo con cualquier superficie hasta el córtex cerebellar está en torno a los 70ms, esto implica que, el ciclo de control presenta un retardo entre 100-150ms [58] (De hecho, los ciclos de control industriales no toleran este tipo de retardos en los canales de comunicación) [59]. Estos retardos en el canal de comunicación implican que nuestro brazo humano no es capaz de desarrollar tareas de contacto que requieran correcciones de pares con frecuencias mayores de entre 6 a 10 veces por segundo (entre unos 100-150ms de retardo). La respuesta a eventos de mayor rapidez se ve normalmente atenuada por la mano, sin embargo, cuando el contacto acaece con un elemento rígido del brazo, como pueda ser el puño, el error cometido resultante es alto [60].

Por lo tanto, la pregunta sería, ¿Cómo son capaces los seres humanos de desarrollar una extraordinaria habilidad manual cuando interaccionan en distintos escenarios? De hecho, el brazo (contacto prior), presenta una cierta rigidez modulada por los músculos. La activación simultanea del par de músculos complementarios permite aumentar la rigidez articular. Por ejemplo el codo puede incrementar su rigidez en un ratio de 200 a 1 [60], mediante la utilización del bíceps y el tríceps. La rigidez adecuada del brazo viene dada a priori por el conocimiento previo de la tarea a realizar; acto seguido, esta rigidez se modifica antes del contacto (antes de cometer un error los músculos modifican de nuevo la rigidez sin que el cerebro esté permanentemente implicado en esta acción) para así optimizar la tarea a realizar en términos de parámetros específicos de la propia tarea (posición, velocidad, aceleración, torques… etc).

A lo largo de esta tesis, se asume que los pares de músculos agonista-antagonistas son capaces de modificar la rigidez final del brazo, sin embargo desde un punto de vista más global, aquello que se modifica no es la rigidez en sí misma, sino la impedancia mecánica del brazo. En un escenario de control sencillo, podemos considerar que la impedancia del brazo tiene tres parámetros por grado de libertad: rigidez, masa y amortiguamiento. Por lo tanto, esta impedancia establece las relaciones estáticas y dinámicas entre fuerza y movimiento.

Está claro por tanto que una implementación de un control que modifica la impedancia mecánica del robot permitiría una aproximación más humana al comportamiento del brazo robótico. Con dicho objetivo, la tesis que aquí se presenta, ha evolucionado un controlador biológicamente plausible (ver sección anterior) embebido en un ciclo de control robótico, donde se trata de mimetizar la acción que un controlador motor biológico realiza sobre, por ejemplo, el brazo humano.

III. MOTIVACIÓN

La arquitectura cerebellar ha sido objeto de estudio durante más de un siglo, sin embargo su rol funcional y cognitivo aún sigue siendo un tema bajo estudio [21] [61]. Es bien sabido que el cerebelo juega un rol importante en el control motor, realizando una labor fundamental en la coordinación, precisión y temporización de movimientos primarios [62]. El cerebelo recibe entradas desde el sistema sensorial, de otras partes del cerebro y la espina dorsal, y las integra con los comandos motores para modular la actividad motora [46] [47]. Consecuentemente, tanto para explotar y clarificar cómo el cerebelo computa la información como para probar distintas hipótesis sobre su modo de operación, parece ser que las simulaciones del circuito nervioso central son la herramienta más apropiada. Aplicar distintas hipótesis cerebelares a una tarea de control motor compleja proporciona la posibilidad de explicar el cómo la información sensorimotora y cognitiva pudieran ser manipuladas por una arquitectura cerebelar computacional.

Debido a la alta dimensionalidad que una red neuronal realista presenta y las limitaciones y restricciones temporales inherentes a un entorno de control robótico en tiempo real, un simulador ultra-rápido de redes neuronales biológicas es a todas luces imprescindible. Las exigencias temporales demandan un simulador en tiempo real (EDLUT) [65] [66]. La combinación de ambos campos, arquitecturas biológicas y teoría de control, constituye un desafío excitante a la par que científicamente tremendamente relevante.

Para utilizar un modelo completo de cerebelo simulado, inserto en un ciclo de control donde se ha de manipular con precisión un brazo robótico, se necesita de un banco de pruebas apropiado para el testeo de los sistemas biológicos desarrollados. Para hacer frente a todos los inconvenientes surgidos de trabajar en medio de estos dos mundos, robótica y biología, se necesita una piedra de Rosetta que pueda establecer las pasarelas de comunicación entre ellos puesto que el procesamiento biológico se realiza en términos de impulsos eléctricos mientras que el procesamiento de control robótico se realiza en términos de señales analógicas. El cómo el impacto de una cierta actividad neuronal perteneciente a una estructura particular del cerebelo se ha de traducir a una tarea de control y viceversa no es una tarea trivial. Una vez establecido dicho diálogo entre impulsos y señales de control, los parámetros que permiten discernir entre las bondades de distintas arquitecturas constituye el siguiente paso a desarrollar.

Desde el punto de vista de la teoría de control, el mejor sistema sería aquel que consigue el mejor rendimiento en términos de precisión, velocidad y estabilidad. Esta idea puede ser extrapolada a la neurociencia, en el sentido de considerar el mejor sistema biológicamente inspirado a aquel que en una tarea de control consiga una mayor precisión, velocidad y estabilidad sin descuidar la fidelidad a los detalles biológicos. El mejor sistema biológicamente inspirado obtenido debiera suministrar un mejor y más profundo conocimiento sobre los sistemas biológicos reales.

IV. OBJETIVOS

El objetivo principal de este estudio es la implementación de un modelo funcional del cerebelo en un escenario de control robótico, explotando así las posibles capacidades que la arquitectura del cerebelo pudiera presentar. Esta implementación pretende contribuir a una mejor comprensión del sistema nervioso central (esencialmente el cerebelo) a partir de una aproximación computacional.

El diseño de un modelo integrado del cerebelo en un bucle de control no es un camino fácil y directo. Alcanzar este objetivo ha exigido y exige un proceso continuo de desarrollo el cual ha sido dividido en diferentes etapas (en relación a las publicaciones en revistas incluidas en este estudio) de manera que pueda darse una visión gradual de todo el trabajo desarrollado.

- ✓ En primer lugar, el primer sub-objetivo consiste en realizar el estudio de cómo un circuito cerebelar artificial integrado en un lazo de control sería capaz de crear modelos de corrección para compensar desviaciones en la trayectoria a ejecutar cuando la dinámica de la planta (el brazo en el caso de un operador humano) se viese alterada debido a la manipulación de objetos

pesados (cuya masa afecta significativamente a la dinámica del modelo base de la planta). El estudio tendría como finalidad entender cómo este modelo de corrección se infiere a través de un mecanismo de adaptación biológicamente plausible local utilizando una arquitectura cerebelar simplificada.

- ✓ El siguiente objetivo consiste en tratar de describir cómo una red neuronal de impulsos más realista (se añade la capa granular) que imita la micro-estructura cerebelar permite la abstracción de modelos correctivos internos. Mediante la adopción de una red inspirada en el cerebelo, se pueden explorar cómo las diferentes representaciones sensoriales poden ser utilizadas eficientemente con el fin de obtener un modelo de abstracción correctivo preciso para la manipulación de diferentes objetos. Esto se ha de llevar a cabo en dos fases:

    i. Se establece una tarea de relevancia biológica consistente en una manipulación precisa por parte de la planta base (brazo robótico) de objetos que por sus características afectan al modelo dinámico base de dicha planta (se ve afectado tanto su modelo cinemático como dinámico).

    ii. Se define e implementa un modelo aditivo de red neuronal cerebelar base para evaluar como diferentes propiedades de dicho modelo funcional afectan en la ejecución de la tarea previamente establecida.

- ✓ En tercer lugar se debe estudiar como el modelo cerebellar previo, el cual incluiría plasticidad en las fibras paralelas (depresión a largo plazo y potenciación a largo plazo de la transmisión sináptica), se pude embeber en distintos lazos de control (control recurrente, control antes del proceso: "forward", y una combinación de ambos modelos) para inferir modelos correctivos que compensen no solo las desviaciones en la trayectoria objetivo a causa de perturbaciones dinámicas o cinemáticas sino también causadas por el ruido (inherente a las señales de impulsos provenientes de los husos musculares) que se introduce a través de las fibras musgosas llegando al cerebelo. El principal objetivo debiera ser establecer una comparativa que evaluase estas arquitecturas de control para poder así mostrar la manera en la que una arquitectura recurrente y otra arquitectura de control antes del proceso puedan verse complementadas y la robustez que ambas presentasen ante la presencia de ruido.

- ✓ Finalmente se ha de estudiar cual sería la mejor manera de conseguir que la información sensorimotora en un entorno robótico genérico pudiera ser manipulada con objeto de obtener una codificación óptima en términos de información somatosensorial.

V. MARCO DE LOS PROYECTOS ASOCIADOS

Este trabajo se ha venido desarrollando en el marco de dos proyectos europeos; "estructuración sensorimotora de percepción y acción para la cognición emergente" (SENSOPAC) y "Redes realistas en tiempo real: la dinámica de la computación en el cerebelo" (REALNET (IST-270434)).

El primero de ellos, SENSOPAC (IST-028056), se extendió desde enero de 2006 a julio de 2010, donde se colaboró con 12 instituciones de 9 países diferentes. El proyecto SENSOPAC (IST-028056) combinaba tanto técnicas de aprendizaje automático como técnicas para el modelado de diversos sistemas biológicos con el fin de desarrollar una determinada estructura computacional que fuese capaz de abstraer conceptos cognitivos de las relaciones sensorimotoras durante las interacciones con su entorno, y a su vez también capaz de generalizar dicho conocimiento a situaciones nuevas. En particular, SENSOPAC (IST-028056) ha combinado distintos modelos de robot en una tarea de exploración táctil con el fin de comprender distintas relaciones causales de diferentes dinámicas sensoriales. Se han incorporado modelos neuronales detallados de áreas clave del cerebro en los modelos funcionales de percepción, toma de decisiones, planificación y control, con el fin de ampliar y mejorar el conocimiento que se tiene tanto en el campo de la Neurociencia como de la Ingeniería.

Más concretamente, se ha estado estudiando profundamente tanto la retroalimentación sensorial táctil como la realimentación de señales propioceptiva así como las fibras aferentes de los comandos motores. Dichos estudios se han s empleado en tareas de manipulación bajo diversos contextos permitiendo así estudiar la representación eficiente en la estructura neuronal, los mecanismos de codificación/decodificación de la información y las distintas abstracciones de conocimiento, tanto en la manipulación háptica humana, como los sistemas de sensores robóticos artificiales.

Nuestro grupo de investigación de la Universidad de Granada ha estado involucrado principalmente en el desarrollo del entorno de computación de neuronas y redes neuronales (EDLUT). Los hallazgos neurofisiológicos obtenidos, por ejemplo, a través de registros se han tratado de implementar en este simulador con el fin de diseñar sistemas de control más biológicos capaces de llevar a cabo eficientemente tareas de manipulación.

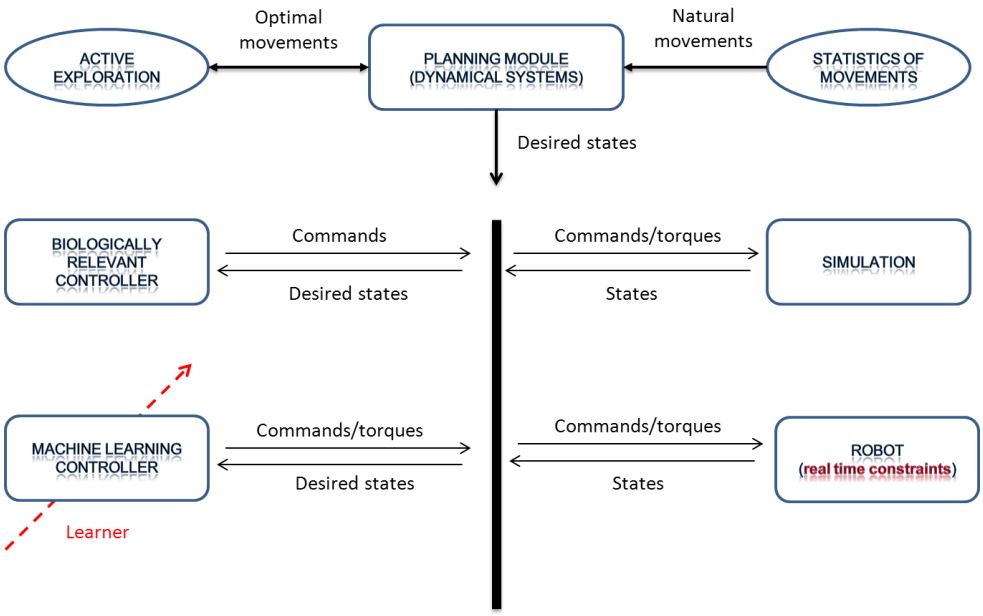

Figure 5.1. Organización de los Módulos en SENSOPAC

Nuestro trabajo como miembros en este proyecto se ha centrado en el estudio de tareas relevantes a nivel de control biológico así como en el conjunto de módulos de simulación necesarios para la integración entre neurofisiología y la teoría de control de sistemas robóticos.

Hoy en día, nuestro grupo de investigación está involucrado con el proyecto REALNET (IST-270.434) como continuación de SENSOPAC (IST-028056). REALNET (IST-270434) se inició en febrero de 2011 y se extenderá hasta febrero de 2014. El objetivo principal de este proyecto es comprender los circuitos cerebrales del sistema nervioso central desde su nivel funcional hasta su nivel molecular/neuronal. A fin de comprender el procesamiento cerebelar se necesita tomar un enfoque diferente; se necesita implementar redes neuronales realistas que hagan uso de comunicación por impulsos, inspiradas en el conjunto de registros neurofisiológicos experimentales obtenidos de verdadera actividad de la red cerebelar, para poder así investigar cuales debieran ser las bases teóricas de la computación del sistema nervioso central. Como punto de referencia de este proyecto se utiliza el circuito del cerebelo. Sobre la base de datos experimentales, este proyecto desarrollará la primera red realista en tiempo real del modelo de cerebelo. Este modelo de cerebelo se conectará a un sistema robótico biomorfico con el fin de evaluar su funcionamiento bajo condiciones de circuito de control realimentado. Los datos derivados de las grabaciones, las simulaciones a gran escala y los robots se

utilizan para explicar el funcionamiento de la circuitería cerebelar a través de la teoría del filtro adaptativo.

Debido a las necesidades de conocimiento multidisciplinar que estos proyectos requieren, cada uno de los miembros de nuestro grupo de investigación se ha visto obligado a centrar su investigación en un área particular. El presente trabajo presenta los resultados en los que una arquitectura cerebelar simulada se utiliza para manipular un brazo robótico. Este trabajo implica: tratar con sistema robóticos, desarrollar un simulador de brazo robótico, estudiar los lazos de control biológicamente plausibles, la conversión de señales de impulsos dadas por el simulador integrado EDLUT a señales utilizables en el lazo de control, estudio de relación impulso /señal analógica ... etc. Todos estos temas centran mi investigación, pero cabe señalar que todo este trabajo no habría sido posible sin el arduo trabajo de Jesús Alberto Garrido quien ha estado a cargo de la evolución del simulador EDLUT con el fin de simular estructuras biológicas más realistas y aumentar el rendimiento de las simulaciones.

VI. ORGANIZACIÓN POR CAPÍTULOS

Con el fin de facilitar la lectura y la utilización de esta tesis se hará una breve exposición de la información presentada en cada capítulo:

- ✓ En el capítulo 1 (este capítulo), se realiza una pequeña introducción del estado del arte en la neurociencia computacional aplicada en robótica. Se presenta la motivación de esta tesis y se resume el trabajo que se va a llevar a cabo.

- ✓ En el capítulo 2, se presenta una contextualización adecuada del área de investigación en la que se ha enmarcado esta tesis. A pesar de que los artículos en revistas son autocontenidos no hay duda de que una visión previa del campo de investigación tratado hace más fácil la tarea de adentrarse en los detalles a través de los artículos de revista.

- ✓ En el capítulo 3, se enumeran brevemente las principales aportaciones y se propone el trabajo futuro.

- ✓ Por último, en el capítulo 4, todos los artículos relacionados con la tesis se han incluido junto con una breve reseña indicando el factor de impacto que cada uno de ellos posee y el cuartil al

que pertenece. Además se han incluido distintas reseñas breves a diferentes publicaciones asociadas a este trabajo (ponencias y artículos en revistas con coautoría).

CHAPTER 6

Discusión y Conclusiones

En este capítulo se muestra un resumen de las principales contribuciones asociadas a los trabajos presentados, así como las futuras líneas de trabajo planteadas a partir de la labor descrita en esta memoria. De igual manera, se incluye un breve resumen de los resultados obtenidos así como una lista de las conferencias internacionales y revistas que este trabajo ha generado.

I. DISCUSIÓN

Como primer paso, esta tesis (capítulo 4, sección 1) presenta una arquitectura cerebelar sencilla capaz de inferir modelos de corrección en el marco de una tarea de control motor donde se manipulan objetos que afectan de manera significativa al modelo dinámico del sistema a controlar.

Esta aproximación primaria busca en primera instancia un enfoque bio-mimético, centrándose en el proceso de inferencia de modelos correctivos mediante un módulo cerebelar integrado en un ciclo de control. De igual forma se estudia cómo estos modelos de corrección internos se constituyen por medio de mecanismos sinápticos de adaptación biológicamente plausibles. Se muestra por tanto, como una ley de correlación temporal (que incluye depresión a largo plazo (LTD) y una potenciación a largo plazo (LTP) entre las fibras paralelas y sus células de Purkinje) es capaz de inferir dichos modelos correctivos. También se ha evaluado cómo esta ley de aprendizaje es capaz de correlacionar la actividad sensorial que llega a través de las fibras paralelas con las señales de aprendizaje (en función de las estimaciones de error) que llegan a través de las fibras trepadoras provenientes de la oliva inferior. Esta aproximación a un primer modelo funcional del cerebelo bioinspirado arroja un poco de luz sobre cómo estos componentes LTD y LTP deben estar bien equilibrados entre sí para lograr un aprendizaje preciso. Además, se ilustra cómo la ley de aprendizaje es responsable de la correlación temporal pudiendo trabajar en presencia de retrasos en la transmisión en las vías sensoriales.

Este tipo de investigaciones puede dar pistas sobre cómo la biología consigue un control preciso de las articulaciones no-rígidas de extremidades con actuadores de bajo consumo que implican sistemas de control con componentes de alta inercia.

El artículo asociado a esta parte es:

N. R. Luque, J. A. Garrido, R. R. Carrillo, O. J. M. D. Coenen, E. Ros, " Cerebellar-like Corrective Model Inference Engine for Manipulation Tasks ", *IEEE Transactions on Systems, Man, and Cybernetics, Part B: Cybernetics*, **41**(5), 2011.

- ✓ En segundo lugar este trabajo evalúa (capítulo 4 sección 2) la manera en la que una evolución de la arquitectura neuronal previamente señalada puede almacenar un modelo correctivo en la capa granular/molecular. Como fue señalado en el capítulo de contextualización, el cerebelo es uno de los centros nerviosos más importantes implicados en la corrección y refinamiento de movimientos planificados así como en la generación de correcciones apropiadas sobre la ejecución de dichos movimientos. Por lo tanto sería muy interesante no sólo estudiar la capacidad de almacenaje de la capa granular/molecular sino también como la microestructura cerebelar y la conexión de sus entradas puede apoyar eficientemente la abstracción de modelos correctivos que produzcan pares correctivos que incrementen la precisión al manipular diferentes objetos. En este trabajo se describe cómo las señales explícitas e implícitas de contexto (señales sensoriales) pueden complementarse entre ellas para mejorar la selección entre diferentes modelos correctores almacenados permitiendo incluso la interpolación entre dos modelos distintos ya establecidos. Se facilita así la generación de correcciones precisas durante la manipulación de nuevos objetos ayudándose de modelos correctores ya aprendidos.

  El artículo asociado a esta parte es:

  N. R. Luque, J. A. Garrido, R. R. Carrillo, O. J. M. D. Coenen, E. Ros, "Cerebellar Input Configuration Toward Object Model Abstraction in Manipulation Tasks". *IEEE Transaction on Neural Networks*, **22**(8), 1321-1328, 2011.

- ✓ Como evolución natural, el siguiente paso se centra en evaluar el comportamiento que el modelo cerebelar previamente descrito tiene cuando se inserta en diferentes ciclos de control (control recurrente, control antes del proceso: "forward", y una combinación de ambos) para controlar un brazo robótico (capítulo 4 sección 3). La red de impulsos se auto adapta frente a las perturbaciones en un escenario de manipulación de objetos donde existen cambios sobre la dinámica y cinemática

del modelo base del brazo robótico y junto a la presencia de distintos niveles de ruido en las entradas cerebelares (fibras musgosas). De acuerdo a los resultados obtenidos, acoplando ambas arquitecturas de control se obtienen los beneficios de ambas (mayor velocidad de convergencia y precisión) incrementándose además la robustez del sistema frente al ruido.

El artículo asociado a esta parte es:

N. R. Luque, J. A. Garrido, R. R. Carrillo, S. Tolu, E. Ros, Adaptive Cerebellar Spiking Model Embedded In The Control Loop: "Context Switching And Robustness Against Noise", *Int. Journal of Neural Systems*, **21**(5), pp. 385-401, 2011.

- ✓ Una vez que la arquitectura cerebellar primaria y el ciclo de control han sido establecidos llega el turno de evolucionar para conseguir un sistema que tenga no solo una aproximación desde un punto de vista tan ingenieril sino también que cada vez dicho sistema tome más en cuenta diferentes fuentes fisiológicas. (capítulo 4 sección 4). Como se mostró en el capítulo de contextualización, en los sistemas biológicos, en lugar de tener un codificador de posición por cada articulación, se tienen señales propioceptivas adquiridas a través de campos receptivos. En robótica, se utiliza una salida única y precisa de un sensor por eslabón para hacer un seguimiento de la posición y la velocidad. Realizar una interfaz entre un sistema de control bioinspirado con una red neuronal cerebelar de impulsos con un robot convencional no es algo directo y trivial. Por lo tanto se necesita adaptar esta medida unidimensional (salida del codificador de posición) a un espacio multidimensional (entradas de la red neuronal de impulsos) para conectar la arquitectura cerebelar de impulsos. En esta subsección se analiza cómo unos campos receptivos que han sido evolucionados para conseguir una mejor transmisión de información pueden generar una representación sensorimotora eficiente que facilite la discriminación entre distintos estados sensorimotores. Este proceso se puede entender como una abstracción del funcionamiento del núcleo cuneiforme. Este núcleo es modelado como un codificador en población mediante neuronas de impulsos en función de la respuesta de distintos mecanoreceptores. En nuestro caso las coordenadas del espacio articular de un robot son transformadas en patrones de impulsos susceptibles de ser procesados eficientemente por el siguiente módulo (el cerebelo). En concreto, el modelo de este núcleo presenta un esquema de codificación que toma en cuenta los tiempos relativos de los impulsos que se propagan desde las fibras nerviosas periféricas hacia las neuronas somatosensoras de segundo orden.

  El artículo asociado a esta parte es:

Luque, N. R.; Garrido, J. A.; Ralli, J.; Laredo, J. J.; Ros, E.: "From Sensors to Spikes: Evolving Receptive Fields to Enhance Sensory Motor Information in a Robot-Arm Scenario". *Int. Journal of Neural Systems*, **22**(4), pp. 0-20, 2012.

II. TODAS LAS PUBLICACIONES ASOCIADAS A ESTA TESIS

La investigación desarrollada se ha realizado en el marco de dos proyectos europeos; REALNET (IST-270434) / SENSOPAC (IST-028056), donde diferentes retos se han abordado desde diferentes perspectivas a través de las sinergias entre neurofisiólogos e ingenieros de diversas especialidades. Este trabajo ha sido evaluado en un marco de conferencias internacionales y publicaciones científicas (con factor de impacto (IF) en el JCR).

1. Revistas Internacionales con índice de impacto

1. **Luque, N. R.**; Garrido, J. A.; Carrillo, R. R.; Coenen, O. J. M. D.; Ros, E: "Cerebellar-like corrective-model abstraction engine for robot movement control". *IEEE Transaction on system, man, and cybernetics - Part B: Cybernetics,* **41**(5), 2011. Impact Factor (JCR 2010): 2.699. Quartile Q1 in categories: Automation & Control Systems, Computer Science, Artificial Intelligence and Computer Science, Cybernetics

2. **Luque, N. R.**; Garrido, J. A.; Carrillo, R. R.; Coenen, O. J. M. D.; Ros, E: "Cerebellar input configuration towards object model abstraction in manipulation Tasks". *IEEE transaction on neural networks,* **22**(8), 1321-1328, 2011. Impact Factor (JCR 2010): 2.633. Quartile Q1 in categories: Computer Science, Artificial Intelligence, Computer Science, Hardware & Architecture. Computer Science, Theory & Methods and Engineering, Electrical & Electronic.

3. **Luque, N. R.**; Garrido, J. A.; Carrillo, R. R.; Tolu, S.; Ros, E.: "Adaptive cerebellar spiking model in a bio-inspired robot-control loop". *International Journal on Neural Systems*, **21**(5), 385-401, 2011. Impact Factor (JCR 2010): 4.237. Quartile Q1 in category: Computer Science, Artificial Intelligence.

4. **Luque, N. R*.**; Garrido, J. A*****.; Ralli, J.; Laredo, J. J.; Ros, E.: "From Sensors to Spikes: Evolving Receptive Fields to Enhance Sensory Motor Information in a Robot-Arm Scenario". *International*

Journal on Neural Systems, **22**(4), 1-20, 2012. Impact Factor (JCR 2011): ***4.284. Quartile Q1 in category: Computer Science, Artificial Intelligence.***

*****Both authors contributed equally to this work

5. Tolu, S.; Vanegas, M.; **Luque, N. R.**; Garrido, J. A.; Ros, E.: "Bio-Inspired Adaptive Feedback Error Learning Architecture for Motor Control". *Biological Cybernetics*, **106**(8-9), 507-522, 2012. Impact Factor (JCR 2011): ***1.586. Quartile Q1 in category: Computer Science, Cybernetics. Quartile Q4 in category: Neuroscience.***

6. Tolu, S.; Vanegas, M.; Garrido, J. A.; **Luque, N. R.**; Ros, E.: "Adaptive and Predictive Control of a Simulated Robot Arm" *International Journal on Neural Systems*, Accepted for publication. Impact Factor (JCR 2011): ***4.284. Quartile Q1 in category: Computer Science, Artificial Intelligence***.

2. Conferencias Internacionales

1. Passot, J. B.; **Luque, N. R**.; Arleo, A.: "Internal models in the cerebellum: a coupling scheme for online and offline learning in procedural tasks". International Conference on Simulation of Adaptive Behavior, (SAB 2010). In Doncieux, S. et al., editors, LNAI Simulation of Adaptive Behavior, vol. 6226, pp 435-446, Springer-Verlag, (2010).

2. **Luque, N. R.;** Garrido, J. A.; Carrillo, R. R.; Ros, E.: "Cerebellar spiking engine: Towards object model abstraction in manipulation". International Joint Conference on Neural Networks (IJCNN 2010).

3. Garrido, J. A.; Carrillo, R. R.; **Luque, N. R**.; Ros, E.: "Event and time driven hybrid simulation of spiking neural networks". International Work-Conference on Artificial Neural Networks (IWANN 2011). Advances in Computational Intelligence. Lecture Notes in Computer Science, 6691, pp. 554-561. Springer, Heidelberg (2011).

4. **Luque, N. R**.; Garrido, J. A.; Carrillo, R. R.; Ros, E.: "A spiking cerebellum model in a multi-context robot control scenario for studying the granular layer functional role". International Work-Conference on Artificial Neural Networks (IWANN 2011). Advances in Computational Intelligence. Lecture Notes in Computer Science, 6691, pp. 537-546. Springer, Heidelberg (2011).

5. Casellato, C.; Pedrocchi, A.; Garrido, J. A; **Luque, N. R.;** Ferrigno, G.; D'Angelo, E.; Ros, E.: "An integrated motor control loop of a human-like robotic arm: Feedforward, feedback and cerebellum-based learning". International Conference on Biomedical Robotics and Biomechatronics (BioRob), 2012 4th IEEE RAS\& EMBS .pp. 562-567(2012).

6. Garrido, J.A*.; **Luque, N.R*.**; D'Angelo, E.; Ros, E.; "Enhancing learning precision at parallel fiber-Purkinje cell connections through deep cerebellar nuclei LTD and LTP". Federation of European Neurosciences (FENS2012) (2012).* Both authors contributed equally to this work

III. MARCO CIENTÍFICO

Esta tesis se ha desarrollado en el marco de dos proyectos europeos:

- ✓ SENSOPAC (estructuración sensoriomotora de la Percepción y la Acción para la cognición emergente (IST-028056))
- ✓ REALNET (redes realistas en tiempo real: la dinámica de la computación en el cerebelo (IST-270434)).)).

Este hecho ha proporcionado el escenario perfecto para que nuestro grupo de investigación pudiera colaborar con los diferentes grupos de investigación en otras universidades europeas e instituciones de investigación. El trabajo presentado representa sólo una parte de la contribución que la Universidad de Granada ha hecho en estos dos consorcios SENSOPAC / REALNET. En este escenario resulta imprescindible una aproximación multidisciplinar en el proceso de investigación.

Este trabajo presenta distintos resultados desde un punto de vista biológico, sin embargo, también implica otras áreas del conocimiento. Un ejemplo de la dificultad del proceso de investigación es el conjunto de frentes a atacar: desarrollo del sistema robótico, desarrollo de módulos computacionales biológicamente inspirados basados en datos neurofisiológicos y buscando posibles aplicabilidades en robótica o la evolución de un simulador realista de red neuronal capaz de funcionar en diferentes entornos son sólo un par de ejemplos. No sería justo obviar que todo este esfuerzo no ha sido único por mi parte sino que ha requerido de un trabajo de alta colaboración y coordinación con el equipo de trabajo.

IV. PRINCIPALES APORTACIONES

- Se ha presentado un modelo de cerebelo integrado en un lazo de control que incluye un modelo de cálculo aproximado de dinámica inversa. Este modelo puede proporcionar de manera efectiva pares correctores que compensan las desviaciones dinámicas de un modelo de la planta base (brazo robótico).

- Se ha evaluado cómo una ley de correlación temporal en fibras paralelas (que presenta depresión dirigida en los pesos sinápticos a largo plazo LTD y un componente de compensación de potenciación a largo plazo de pesos sinápticos LTP) puede alcanzar una adaptación eficaz de la salida correctiva del cerebelo. Tanto LTD como LTP han de ser equilibrados para alcanzar un buen rendimiento en la capacidad de adaptación. Un LTD bien equilibrado con la componente LTP asegura una reducción efectiva del error en las tareas de manipulación de objetos que pudieran afectar considerablemente a la dinámica de la planta base (brazo robótico).

- Se ha demostrado cómo dicha ley de correlación temporal puede trabajar en presencia de retardos sensoriales. Esta estructura cerebelar adaptativa puede generar la salida correctiva adecuada de manera adaptativa para cada punto de la trayectoria deseada, el retardo en las vías sensoriales ha demostrado no ser muy relevante.

- Se presenta una estudio de la influencia de las señales de entrada sensorial usando una evolución de la arquitectura cerebelar previamente desarrollada (se añade la capa granular). Se han estudiado dos representaciones posibles de entrada , señales sensoriales explícitas de contexto (CE) y señales sensoriales implícitas del contexto (IC). La configuración que utiliza ambas represen-taciones aprovecha las ventajas de ambas complementándolas entre sí. La configuración de entradas IC y EC ofrece transiciones más suaves entre contextos a una velocidad de convergencia mayor así como la capacidad de interpolación de nuevos contextos a partir de modelos previamente adquiridos. Además, es capaz de discernir información de contexto explícita engañosa, por lo que presenta cierta robustez ante representaciones incongruentes de contexto.

- La arquitectura cerebelar propuesta se ha evaluado en diferentes ciclos de control en un entorno robótico sometido a un escenario con presencia de distintos niveles de ruido. Los

resultados obtenidos indican que el acoplamiento de las arquitecturas de control recurrente y control antes del proceso: "forward", lleva a una convergencia más rápida del aprendizaje y a una ganancia de precisión y estabilidad en un entorno ruidoso mayor que si cada una de estas arquitecturas actuase por sí misma.

- Se ha demostrado que esta arquitectura de control acoplada tiene la capacidad de inferir y almacenar diferentes modelos de corrección cuando existen modificaciones dinámicas / cinemáticas sobre la planta base mejorando cada configuración desacoplada por si misma. Además esta arquitectura propuesta acoplada es compatible con varios hallazgos neurofisiológicos.

- Por último, se ha presentado una metodología general (mediante el uso de algoritmos genéticos) para representar de manera eficiente en términos de señales de entrada de impulsos los valores de los codificadores de posición de los diferentes eslabones que un manipulador robótico pudiera presentar.

V. TRABAJO FUTURO

Como trabajo futuro se presentan dos principales líneas de investigación a seguir:

Por un lado, se necesita evolucionar todo el modelo cerebelar en el marco de una tarea de control utilizando aquellas propiedades que los hallazgos de la neurociencia muestran. No hay una conexión directa entre estas propiedades neurofisiológicas y su aplicación final en un escenario de control de una tarea en particular. El estudio de cómo estos hallazgos podrían mejorar un modelo plausible del cerebelo requiere de un gran esfuerzo de investigación. Es necesario tender un puente entre estos campos (neurociencia e ingeniería) aparentemente tan poco relacionados para obtener una mejor comprensión de los principios arquitecturales, funcionales y biológicos que el cerebelo presenta. La inclusión de la plasticidad sináptica en la mayoría de las sinapsis neuronales cerebelares (diferentes estudios experimentales han demostrado la existencia de estos mecanismos en múltiples sinapsis) será nuestro primer paso en este prometedor camino. Este aprendizaje distribuido es una poderosa herramienta de adaptación en el control biológicamente plausible capaz de configurar la red neuronal automáticamente para obtener el mejor rendimiento posible. El aprendizaje localizado en conexiones

MF→DCN o PC→DCN junto con el bien conocido aprendizaje entre GrC→PF→PC se ha demostrado que tiene un fuerte impacto en la consolidación de aprendizaje en el cerebelo.

Hablando en el contexto de red, gran parte de la atención en nuestra investigación futura se centrará en la conexión IO→DCN. Esta conexión podría desempeñar un papel clave para entender cómo podría implementarse un control biológico de rápida respuesta sin hacer uso de un controlador PID clásico (o de otras estrategias de control clásico que pertenecen a este campo de control) ni usando aproximaciones funcionales tales como CMAC, MPIM, LWPR o el modelo cerebelar de Fujita.

Hablando en términos de conexiones neuronales, nuestro objetivo es evolucionar la capa granular, implementando la inhibición lateral neuronal. Esta característica podría permitir una mejor codificación de los patrones de entrada alcanzando una mayor precisión en términos de codificación en población. Diferentes grupos de neuronas responderían a determinados patrones de entrada logrando así una mejor diferenciación de estados.

La segunda línea de investigación está relacionada con la tarea de manipulación. Ahora mismo estamos trabajando en la interconexión de las redes neuronales desarrolladas no sólo con un simulador robótico, sino también con un robot real. Con este fin, tendremos que volver a re-implementar los controladores físicos para poder modificar su actuación punto a punto a lo largo de la trayectoria a seguir. Tenemos que desarrollar una metodología para validar diferentes hipótesis de modelos cerebelares en una tarea de manipulación en términos de estabilidad ya que los tests matemáticos clásicos tales como el criterio de estabilidad de Lyapunov, de Routh-Hurwitz, criterios de estabilidad de Nyquist, etc no encajan bien en estas redes neuronales de impulsos. Las redes neuronales de impulsos se caracterizan por poseer una complejidad y dimensionalidad extraordinaria, por el contrario los test matemáticos conocidos se aplican tradicionalmente a problemas de una mejor complejidad y dimensionalidad donde el comportamiento de cada uno de los elementos del sistema es perfectamente conocido dentro de unos ciertos límites dados donde es posible aplicar dichos tests.. Estos prerrequisitos no están disponibles en una red neural de impulsos debido a su propia naturaleza.

Todas estas cuestiones se abordarán en un proyecto europeo iniciado recientemente (REALNET (IST-270 434)).

BIBLIOGRAPHY

[1] J.B. Passot, N.R. Luque, and A. Arleo, "Internal models in the cerebellum: a coupling scheme," *LNAI*, vol. 6226, pp. 435-446, 2010.

[2] G. Holmes, "The Cerebellum of Man. Brain, ," *Brain*, vol. 62, no. 1, pp. 1–30, 1939.

[3] W.T. Thach, H.P. Goodkin, and J.G. Keating, "The cerebellum and the adaptive coordination of movement," *Annu. Rev. Neurosci.* , vol. 15, pp. 403-42, 1992.

[4] G. Z. Reckess, and H. Imamizu. R. C. Miall, "The cerebellum coordinates eye and hand tracking movements.," *Nat. Neurosci.* , vol. 4, no. 6, pp. 638–44, 2001.

[5] M. R. Delong and P.L. Strick, "Relation of Basal Ganglia, Cerebellum, and Motor Cortex," *Brain Res.*, vol. 71, pp. 327-35, 1974.

[6] J.R. et al. Flanagan, "Control of trajectory modifications in target-directed reaching," *J. Mot. Behav.*, vol. 25, pp. 140–52, 1993.

[7] G. Hinton, "Parallel computations for controlling an arm," *J. Mot.Behav.*, vol. 16, pp. 171–94, 1984.

[8] M. Desmurget and S. Grafton, "Forward modeling allows feedback control for fast reaching movements," *Trends Cog. Sci.*, vol. 4, no. 11, pp. 423-31, November 2000.

[9] M. Kawato and H. Gomi, "A computational model of four regions of the cerebellum based on feedback-error learning," *Biol.Cybern.* , vol. 68, pp. 95–103, 1992.

[10] A.M. Smith, "Does the cerebellum learn strategies for the optimal time-varaying control of joint stiffness," in *Motor learning and synaptic plasticity in the cerebellum.*: Cambridge university press, 1997, ch. 7, p. 198.

[11] N. R. Luque, J. A. Garrido, R. R. Carrillo, and E. Ros, "Cerebellar Spiking Engine: Towards Object Model Abstraction in Manipulation," in *IJCNN*, Barcelona, July 2010.

[12] N. R. Luque, J. A. Garrido, R. R. Carrillo, O. J. M. D. Coenen, and E. Ros, "Cerebellar Input Configuration Toward Object Model Abstraction in Manipulation Tasks," *Neural Networks, IEEE Trans.* , vol. 22, no. 8, pp. 1321-28, 2011.

[13] N. R. Luque, J. A. Garrido, R. R. Carrillo, S. Tolu, and E. Ros, "Adaptive Cerebellar Spiking Model Embedded In The Control Loop: Context Switching And Robustness Against Noise," *Int. Journal of Neural Systems*, vol. 21, no. 5, pp. 385-401, 2011.

[14] N. R. Luque, J. A. Garrido, R. R. Carrillo, O. J. M. D. Coenen, and E. Ros, "Cerebellarlike Corrective Model Inference

Engine for Manipulation Tasks," *Systems, Man, and Cybernetics, Part B: Cybernetics, IEEE Trans.*, vol. 41, no. 5, pp. 1299-312 , 2011.

[15] R.R. Carrillo, E. Ros, C. Boucheny, and O-J.M-D. Coenen, "A real time spiking cerebellum model for learning robto control," *Biosystems*, vol. 94, no. 1-2, pp. 18-27, 2008.

[16] J.S. Albus, "Data storage in the cerebellar model articulation controller (CMAC)," *J. Dyn. Syst. Meas. Contr. ASME*, vol. 3, pp. 228–33, 1975.

[17] J.C. Houk, J.T. Buckingham, and A.G. Barto, "Models of the cerebellum and motor learning," *Behav. Brain. Sci.*, vol. 19, no. 3, pp. 368–83, 1996.

[18] P. van der Smagt, "Cerebellar control of robot arms," *Connect. Sci.*, vol. 10, pp. 301–20, 1998.

[19] N. Schweighofer, "Computational Models of the Cerebellum in the Adaptive Control of Movements," *Ph.D. thesis*, 1995.

[20] W. T. Thach, "What is the role of the cerebellum in motor learning and cognition? ," *Trends in Cognitive Sciences* , vol. 2, no. 9, pp. 331-7, 1998.

[21] M. Glickstein and K. Doron, "Cerebellum: connections and functions ," *Cerebellum (London,England)*, vol. 7, no. 4, pp. 589–94, 2008.

[22] P. Brodal, "The corticopontine projection in the rhesus monkey.Origin and principles of organization.," *Brain* , vol. 101, pp. 251-83, 1978.

[23] M. Glickstein, J.G. May, and B.E. Mercier, "Corticopontine projection in the macaque: the distribution of labelled cortical cells after large injections of horseradish peroxidase in the pontine nuclei," *J. Comp. Neurol.*, vol. 235 , pp. 343-59, 1985.

[24] R. Bracke-Tolkmitt et al., "The cerebellum contributes to mental skills," *Behav.Neurosci.*, vol. 103, pp. 442-6, 1989.

[25] S.E. Petersen, P.T. Fox, M.I. Posner, M. Mintun, and M.E. Raichle, "Positron emission tomographic studies of the processing of single words," *J. Cogn. Neurosci.*, vol. 1, pp. 153-70, 1989.

[26] Petersen SE, Ojemann JG, Miezin FM, Squire LR,Raichle, L.E. Buckner RL, "Functional anatomical studies of explicit and implicit memory retrieval tasks," *J. Neurosci.* , vol. 15, pp. 12-29, 1995.

[27] J.E. Desmond, J.D. Gabrieli, and G.H. Glover, "Dissociation of frontal and cerebellar activity in a cognitive task: evidence for a distinction between selection and search," *Neuroimage*, vol. 7, pp. 368-76, 1998.

[28] J.A. Fiez and M.E. Raichle, "Linguistic processing," *Int. Rev. Neurobiol.*, vol. 41, pp. 233-54, 1997.

[29] N.C. Andreasen et al., "Short-term and long-term verbal memory: a positron emission tomography study," *Proc. Natl. Acad. Sci. U. S. A*, vol. 92, pp. 5111-5., 1995.

[30] M. Ito, "Movement and thought: identical control mechanisms by the cerebellum," *Trends Neurosci.*, vol. 16, pp. 448-50, 1993.

[31] L.Y. Shih et al., "Sensory acquisition in the cerebellum: an FMRI study of

cerebrocerebellar interaction during visual duration discrimination," *Cerebellum*, vol. 8, no. 2, pp. 116-26, Jun 2009.

[32] N.A. Akshoomoff and E. Courchesne, "A new role for the cerebellum in cognitive," *Behav. Neurosci.*, vol. 106, pp. 731-8, 1992.

[33] D. L. Harrington and K. Y. Haaland, "Neural Underpinnings of Temporal Processing: A Review of Focal Lesion, Pharmacological, and Functional Imaging Research," *Rev, Neurosci.*, vol. 10, no. 2, pp. 91–116, 1999.

[34] M. Molinari et al., "Cerebellum and procedural learning: evidence from focal cerebellar lesions," *Brain* , vol. 120, pp. 1753–62, 1997.

[35] M. Glickstein, "Motor skills but not cognitive tasks.," *TINS*, vol. 16, pp. 450-1, 1993.

[36] M. Gómez-Beldarrain and J.C. García-Moncó, "El cerebelo las funciones cognitivas ," *Revista Neuro.*, vol. 30, pp. 1273-6, 2000.

[37] E.R. Kandel, J.H. Schwartz, and T.M. Jessell,. New York: McGraw-Hill Professional Publishing, 2000, ch. 42.

[38] R. Carter, S. Aldridge, M. Page, and S. Parker, *The Human Brain Book.*: D.K. Publishing, 2009.

[39] R.R. Llinas, K.D. Walton, and E.J. Lang, "The Synaptic Organization of the Brain," in *CerebellumIn.*: New York: Oxford University Press, 2004, ch. 7.

[40] J.C. Eccles, M. Ito, and J. Szentágothai, *The Cerebellum as a Neuronal Machine*. New York: Springer-Verlag, 1967, vol. 53.

[41] H. C. Leiner, A. L. Leiner, and R. S. Dow, "Cognitive and language functions of the human cerebellum," *Trends in Neurosciences*, vol. 16, no. 11, pp. 444-447, November 1993.

[42] M. Ito, "Neurophysiological aspects of the cerebellar motor control system," *Int. J. Neurol.*, vol. 7, pp. 162–76, 1970.

[43] M. Ito, "Cerebellar circuitry as a neuronal machine," *Prog. Neurobiol.*, vol. 78, pp. 272-303, 2006.

[44] N. Rammani, "The primate cortico-cerebellar system: anatomy and function," *Nature Reviews*, vol. 7, pp. 511-522, 2006.

[45] A. Siegel and H.N. Sapru, *Essential Neuroscience,Revised First Edition.*: Lippincott Williams & Wilkins, October 24, 2007.

[46] N. Schweighofer, M.A. Arbib, and M. Kawato, "Role of the cerebellum in reaching movements in humans.I.Distributed inverse dynamics control," *European Journal of Neuroscience*, vol. 10, pp. 86-94, 1998a.

[47] N. Schweighofer, J. Spoelstra, M.A. Arbib, and M. Kawato, "Role of the cerebellum in reaching movements in human. II. A neural model of the intermediate cerebellum," *Eur.J. Neurosci.*, vol. 10, pp. 95-105, 1998b.

[48] E. Todorov and Z. Ghahramani, "Unsupervised Learning of Sensory-Motor Primitives," in *In Proceedings of the 25th Annual International Conference of the IEEE Engineering in Medicine and Biology Society*, 2003.

[49] D. Marr, "A theory of cerebellar cortex," *J. Physiol.*, vol. 202, pp. 437-70, 1969.

[50] J.S. Albus, "A theory of cerebellar function," *Math Biosci.*, vol. 10, pp. 25-61, 1971.

[51] M. Ito and M. Kano, "Long-lasting depression of parallel fiber-Purkinje cell transmission induced by conjunctive stimulation of parallel fibers and climbing fibers in the cerebellar cortex," *Neurosci. Letter*, vol. 33, pp. 253-58, 1982.

[52] M. Ito, "Long-term depression," *Annu. Rev. Neurosci*, vol. 12, pp. 85-102, 1989.

[53] M Schonewille et al., "Reevaluating the role of LTD in cerebellar motor learning," *Neuron*, vol. 70, no. 1, pp. 13-50, 2011.

[54] M. A. Arbib, G. Metta, and P. van der Smagt, "Neurorobotics: From Vision to Action," in *Springer Handbook of Robotics.*: Springer, 2008, ch. 62, pp. 1453-75.

[55] M. Kumamoto, T. Oshima, and T. Yamamoto, "Control properties induced by the existence of antagonistic pairs of bi-articular muscles.Mechanical engineering model analyses ," *Human Movement Science*, vol. 13, no. 5, pp. 611-34 , 1994.

[56] I. Albrecht, J. Haber, and H.P. Seidel, "Construction and animation of anatomically based human hand models," in *Proceedings of the 2003 ACM SIGGRAPH/Eurographics symposium on Computer animation* , San Diego, California, 2003.

[57] B. Tondu, S. Ippolito, J. Guiochet, and A. Daidie, "A Seven-degrees-of-freedom Robot-arm Driven by Pneumatic Artificial Muscles for Humanoid Robots," *J. Robotics Research*, vol. 24, no. 4, pp. 257-74 , 2005.

[58] T. Flash and N. Hogan, "The coordination of arm movements: an experimentally confirmed mathematical model," *J. Neurosci.*, vol. 5, no. 7, pp. 1688-1703, 1985.

[59] J. Nilsson, B. Bernhardsson, and B. Wittenmark, "Stochastic analysis and control of real-time systems with random time delays," *Automatica*, vol. 34, no. 1, pp. 57-64, 1998.

[60] T.E. Milner, "Contribution of geometry and joint stiffness to mechanical stability," *Exp. Brain. Res.*, vol. 143, pp. 515-9, 2002.

[61] W.T. Thach, "What is the role of the cerebellum in motor learning and cognition?," *Trends Cog. Sciences*, vol. 2, no. 9, pp. 331-7, 1998.

[62] R. B. Ivry and S.W. Keele, "Timing functions of the cerebellum," *J. Cog. Neurosci.*, vol. 1, pp. 136-52, 1989.

[63] D. M. Wolpert, R. C. Miall, and M. Kawato, "Internal models in the cerebellum," *Trends Cog. Sci.*, vol. 2, no. 9, pp. 338-47, 1998.

[64] R. C. Miall, D. J. Weir, D. M. Wolpert, and J. F. Stein, "Is the cerebellum a Smith predictor?," *J. Mot. Behav.*, vol. 25, pp. 203–16, 1993.

[65] E. Ros, R.R. Carrillo, E.M. E. M. Ortigosa, B. Barbour, and R. Agís, "Event-Driven Simulation Scheme for Spiking Neural Networks Using Lookup Tables to Characterize Neuronal Dynamics," *Neural Comp.*, vol. 18, pp. 2959-93, 2006.

[66] J.A. Garrido. (2012) Edlut official website. [Online]. http://edlut.googlecode.com.

[67] B.F. Skinner, "The operational analysis of psychological terms," *Behavioral and brain*

sciences, vol. 7, no. 4, pp. 547–81., 1984.

[68] W. Chaney, *Workbook for a Dynamic Mind*. Las Vegas: Houghton-Brace Publishing, 2006.

[69] E.J. Gibson, *Principles of perceptual learning and development*. New York: Appleton-Century-Crofts, 1969.

[70] E.R. Guthrie, *The psychology of learning*, Harper & Row, Ed. New York, 1952.

[71] D.M. Wolpert and J.R. Flanagan, "Motor learning," *Current Biol.*, vol. 20, no. 11, pp. 467-72, June 2010.

[72] J. Struyf and H. Blockeel, "Relational Learning," in *Encyclopedia of Machine Learning*, C. Sammut and Webb G.I., Eds.: Springer, 2010, pp. 851-857.

[73] E. C. Tolman, B. F. Ritchie, and D. Kalish, "Studies in spatial learning. I. Orientation and the short-cut.," *Journal of Experimental Psychology*, vol. 36, no. 1, pp. 13-24, Feb. 1946.

[74] E. C. Tolman, B. F. Ritchie, and D. Kalish, "Studies in spatial learning. II. Place learning versus response learning.," *Journal of Experimental Psychology*, vol. 36, no. 3, pp. 221-9, Jun. 1946.

[75] E. Tulving, "Precis of Elements of Episodic Memory," *Behavioural and Brain Sciences* , vol. 7, no. 2, pp. 223–68, 1984.

[76] A. Bandura, Grusec J.E., and Menlove F.L., "Observational learning as a function of symbolization and incentive set," *Child Development* , vol. 37, no. 3, pp. 499-506, Sep. 1966.

[77] A.W. Staats, *Behavior and Personality: Psychological Behaviorism*, Pamela Ritzer, Ed. New York, U.S.A: Springer Series on Behavior Therapy and Behaviral Medicine, 1996.

[78] C. Shaw, *Toward a theory of neuroplasticity*, Jill McEachern, Ed. London, England: Psychology Press, 2001.

[79] W. James, "Habit," in *The Principles of Psychology Vol:1.*, 1890, ch. 4.

[80] X. Benavent Garcia, "Modelización y control de sistemas dinámicos utilizando redes neuronales y modelos lineales. Aplicación al control de una plataforma de simulación," in *PhD Thesis*. Valencia, España, ch. 2.

[81] M. Ito, "The cerebellum and neural control," *New York, Raven Press*, 1984.

[82] M. Kawato, K. Furukawa, and R. Suzuki, "A hierarchical neural-network model for control and learning of voluntary movement," *Biol. Cybern.*, vol. 57, no. 3, pp. 169-85, 1987.

[83] R. M. C. Spencer, R.B. Ivry, and H.N. Zelaznik, "Role of the cerebellum in movements: control of timing or movement transitions?," *Exp. Brain res.*, vol. 161, pp. 383-96, 2005.

[84] B.R. Townsend, L. Paninski, and R.N. Lemon, "Linear encoding of muscle activity in primary motor cortex and cerebellum," *J. Neurophysiol.* , vol. 96, no. 5, 2006.

[85] J.R. Flanagan and A.M. Wing, "The role of internal models in motion planning and control: evidence from grip force adjustments," *J. Neurosci.*, vol. 17, pp. 1519–28, 1997.

[86] S. Keele, R. Ivry, and R. Pokorny, "Force control and its relation to timing," *J. Mot. Behav.*, vol. 19, pp. 96-114, 1987.

[87] M. Glickstein, *The Cerebellum: From Structure to Control,Mossy-fibre sensory input to the cerebellum*, C.I. De Zeeuw, P. Strata, and Voogd J., Eds.: Elsevier,Progress in Brain Research, 1997, vol. Volume 114,Chapter 14.

[88] J. Knierim. (1997, Jan) Neuroscience Online:an electronic texbook for neuroscience Chapter 5: Cerebellum. [Online]. http://neuroscience.uth.tmc.edu/

[89] K. A. Coffman, R.P. Dum, and P.L. Strick, "Cerebellar vermis is a target of projections from the motor areas in the cerebral cortex," in *J. Proceedings of the National Academy of Sciences of the United States of America*, 2011.

[90] E.J. Fine, C.C. Ionita, and L. Lohr, "The history of the development of the cerebellar examination," *Semin Neurol* , vol. 22, no. 4, pp. 375–84, 2002.

[91] J. R. Bloedel and J. Courville, *Handbook of Physiology, The Nervous System, Motor Control. Cerebellar Afferent Systems.*: John Wiley & Sons, Inc., 2011, vol. Supplement 2.

[92] M. Glickstein et al., "Visual pontocerebellar projections in the macaque.," *J. Comp. Neurol.*, vol. 349, no. 1, pp. 51-72, 1994.

[93] C.R. Legg, B. Mercier, and M. Glickstein, "Corticopontine projection in the rat: the distribution of labelled cortical cells after large injections of horseadish peroxidase in the pontine nuclei," *J. Comp. Neurol.*, vol. 286, no. 4, pp. 427-41, 1989.

[94] P. Brodal, "The corticopontine projection from the visual cortex in the cat. I. The total projection and the projection from area 17.," *Brain Res.*, vol. 39, no. 2, pp. 297-317, 1972.

[95] P. Brodal, "The corticopontine projection from the visual cortex in the cat.II.The projection from areas 18 and 19.," *Brain Res.*, vol. 39, no. 2, pp. 319-35, 1972.

[96] G. Nyberg and A Blomqvist, "The central projection of muscle afferent fibres to the lower medulla an upper spinal cord: an anatomical study in the cat withc the transganglionic transport method.," *J. Comp. Neurol.*, vol. 230, no. 1, pp. 99-109, 1987.

[97] van P. L. Kan, A.R. Gibson, and J.C. Houk, "Movement-related inputs to intermediate cerebellum of the monkey," *J. Neurophysiol.*, vol. 69, no. 1, pp. 74-94, 1993.

[98] P.D Mackie, J.W. Morley, and M.J. Rowe, "Signalling of static and dynamic features of muscle spindle input by external cuneate neurones in the cat," *J. Physiol.*, vol. 519, no. 2, pp. 559-69, 1999.

[99] J. Voogd and Glickstein. M., "The anatomy of the cerebellum," *Trends Neurosci.*, vol. 21, no. 9, pp. 370-5, 1998.

[100] R. Apps and R. Hawkes, "Cerebellar cortical organization: a one-map hypothesis," *Nat.Rev. Neurosci.*, vol. 10, no. 9, pp. 670–681, 2009.

[101] O. Oscarsson, "Spatial distribution of climbing and mossy fibre inputs into the cerebellarcortex," in *In Afferent and Intrinsic Organization of Laminated Structures in the Brain.* Berlin,creutzfeldt: Springer-Verlag, 1976,

pp. 34-42.

[102] G. Andersson and O. Oscarsson, "Projections to lateral vestibular nucleus from cerebellar climbing fiber zones," *Experimental Brain Research,* vol. 32, no. 4, pp. 549–64, 1978.

[103] C.F. Ekerot and B. Larson, "Branching of olivary axons to innervate pairs of sagittal zones in the cerebellar anterior lobe of the cat," *Experimental Brain Research*, vol. 48, no. 2, pp. 185-98, 1982.

[104] M. Ito, "Cerebellar long-term depression. Characterizations, signal transduction and functional roles," *Physiol. Rev.*, vol. 81, no. 3, pp. 1143-1195, 2001.

[105] M. Ito, "Control of mental activities by internal models in the cerebellum," *Brain Res*, vol. 886, no. 1-2, pp. 237-245, 2008.

[106] W. Wolpert and M. Kawato, "Multiple paired forward and inverse models for motor control," *Neural Networks*, vol. 11, pp. 1317-29, 1998.

[107] M. Fujita, "Adaptive filter model of the cerebellum," *Biol. Cybern.*, vol. 45, no. 3, pp. 195-206, 1982.

[108] P. Dean and J. Porril, "Adaptive filter Models of the Cerebellum. Computational Analysis," *The Cerebellum*, vol. 7, no. 4, pp. 567-571, 2008.

[109] P. Dean and J. Porrill, "The cerebellum as an adaptive filter: a general model?," *Funct. Neurol.*, vol. 25, no. 3, pp. 173-180, Jul-Sep 2010.

[110] P. Dean, J. Porrill, C.F. Ekerot, and H. Jörntel, "The cerebellar microcircuit as an adaptive filter: experimental and computational evidence," *Nat. Rev. Neurosci.*, vol. 11, pp. 30-4, 2010.

[111] T.J Sewjnowski, "Storing covariance with nonlinearity interacting neurons," *Journal of Mathematical Biology*, vol. 4, pp. 303-321, 1977.

[112] B. Winkelman and M. Frens, "Motor coding in floccular climbing fibers.," *Journal of Neurophysiology*, vol. 95, pp. 2342–2351, 2006.

[113] J.R. Bloedel and V. Bracha, "Current concepts of climbing fiber function," *Anat. Rec.*, vol. 253, pp. 118-126, 1998.

[114] C.I. De Zeeuw et al., "Microcircuitry and function of the inferior olive," *Trends in Neurosciences*, vol. 21, no. 9, pp. 391-400, 1998.

[115] A.R. Gibson, K.M. Horn, and M. Pong, "Activation of climbing fibers," *Cerebellum*, vol. 3, pp. 212-221, 2004.

[116] C. Boucheny, R.R. Carrillo, E. Ros, and O.J.-M.D Coenen, "Real-time spiking neural network: an adaptive cerebellar model," *LNCS*, vol. 3512, pp. 136–44, 2005.

[117] S. A. Heine, S. M. Highstein, and P. M. Blazquez, "Golgi Cells Operate as State-Specific Temporal Filters at the Input Stage of the Cerebellar Cortex," *The Journal of Neuroscience* , vol. 30, no. 50, pp. 17004-17014 , Dec 2010.

[118] J.W. Moore, J.E. Desmond, and N.E. Berthier, "Adaptively timed conditioned responses and the cerellum: a neural network approach.," *Biological Cybernetics*, vol. 62, pp. 17-28, 1989.

[119] D. Bullock, J.C. Fiala, and S. Grossberg, "A neural model of timed response learning in the cerebellum," *Neural Networks*, vol. 7, pp. 1101-1114, 1994.

[120] R. Brasselet, R. S. Johansson, and A. Arleo, "Quantifying neurotransmission reliability through metrics based information analysis," *Neural Comp.*, vol. 23, no. 4, pp. 852-81, 2011.

[121] T. Flash and T.J. Sejnowski, "Computational approaches to motor control," *Curr Opin Neurobiol.*, vol. 11, no. 6, pp. 655-62, Dec. 2001.

[122] R. Brasselet, R. S. Johansson, and A. Arleo, "Optimal context separation of spiking haptic signals by second-order somatosensory neurons," *Adv. Neural Information Processing System*, vol. 22, pp. 180-8, 2009.

[123] S. Wu, S. Amari, and H. Nakahara, "Population Coding and Decoding in a Neural Field: A Computational Study," *Neural Comp.*, vol. 14, pp. 999-1026, 2002.

[124] REALNET CONSORTIUM. (2012, Mar.) REALNET. [Online]. http://www.realnet-fp7.eu/

[125] R. Maex and E.D. Schutter, "Synchronization of golgi and granule cell granule cell layer," *Journal of neurophysiology*, vol. 80, no. 5, pp. 25-21, 1998.

[126] N. Wada et al., "Conditioned eyeblink learning is formed and stored without cerebellar granule cell transmission," *Proceedings of the National Academy of Sciences*, vol. 104, no. 42, pp. 16690-16695 , Oct 2007.

[127] S. Solinas, T. Nieus, and D'Angelo. E., "A realistic large-scale model of the cerebellum granular layer predicts circuit spatio temporal filtering properties," *Frontiers in Cellular Neuroscience*, vol. 4, no. 0, 2010.

[128] T. Yamazaki and S. Tanaka, "Neural modeling of an internal clock," *Neural Comp.*, vol. 17, no. 5, pp. 1032-58, 2005.

[129] W. Maass, T. Natschläger, and H. Markram, "Real-time computing without stable states: A new framework for neural computation based on perturbations ," *Neural Comp.*, vol. 14, no. 11, pp. 2531-60, 2002.

[130] T. Yamazaki and Tanaka. S., "Computational models of timing mechanisms in the cerebellar granular layer," *Cerebellum*, vol. 8, no. 4, pp. 423-32, Dec 2009.

[131] N. R. Luque, J. A. Garrido, R. R. Carrillo, and E. Ros, "Context Separability Mediated by the Granular Layer in a Spiking Cerebellum Model for Robot Control," *Lecture Notes in Computer Science* , vol. 6691, pp. 537-546, 2011.

[132] N. Masuda and Amari S., "A computational study of synaptic mechanisms of partial memory transfer in cerebellar vestibulo-ocular-reflex learning," *J. Comput. Neurosci.* , vol. 24, pp. 137-156, 2008.

[133] J.R. Anderson, "Classical Conditioning," in *Learning and memory; and integrated approach.* U.S.A: JOHN WILEY & SONS, INC., 2000, ch. 2, pp. 39-78.

[134] J.R. Anderson, "Instrumental conditioning," in *Learning and memory; and integrated approach.* U.S.A: JOHN WILEY & SONS, INC.,

2000, ch. 3, pp. 78-94.

[135] C.L. Heffner. (2001, April) web site Psychology 101: Section 3: Reinforcement and Reinforcement Schedules. [Online]. http://allpsych.com/psychology101/reinforcement.html

[136] J.C. Houk, Buckingham J.T., and Barto A.G., "Models of cerebellum and motor learning," *Behavioral and Brain Sciences*, vol. 19, no. 3, pp. 369-383, 1996.

Cerebellarlike Corrective Model Inference Engine for Manipulation Tasks

Niceto Rafael Luque, Jesús Alberto Garrido, Richard Rafael Carrillo, Olivier J.-M. D. Coenen, and Eduardo Ros

***Abstract*—This paper presents how a simple cerebellumlike architecture can infer corrective models in the framework of a control task when manipulating objects that significantly affect the dynamics model of the system. The main motivation of this paper is to evaluate a simplified bio-mimetic approach in the framework of a manipulation task. More concretely, the paper focuses on how the model inference process takes place within a feedforward control loop based on the cerebellar structure and on how these internal models are built up by means of biologically plausible synaptic adaptation mechanisms. This kind of investigation may provide clues on how biology achieves accurate control of non-stiff-joint robot with low-power actuators which involve controlling systems with high inertial components. This paper studies how a basic temporal-correlation kernel including long-term depression (LTD) and a constant long-term potentiation (LTP) at parallel fiber-Purkinje cell synapses can effectively infer corrective models. We evaluate how this spike-timing-dependent plasticity correlates sensorimotor activity arriving through the parallel fibers with teaching signals (dependent on error estimates) arriving through the climbing fibers from the inferior olive. This paper addresses the study of how these LTD and LTP components need to be well balanced with each other to achieve accurate learning. This is of interest to evaluate the relevant role of homeostatic mechanisms in biological systems where adaptation occurs in a distributed manner. Furthermore, we illustrate how the temporal-correlation kernel can also work in the presence of transmission delays in sensorimotor pathways. We use a cerebellumlike spiking neural network which stores the corrective models as well-structured weight patterns distributed among the parallel fibers to Purkinje cell connections.**

***Index Terms*—Adaptive, biological control system, cerebellum, learning, plasticity, robot, simulation, spiking neuron.**

I. Introduction

CONTROLLING fast non-stiff-joint robots accurately with low-power actuators is a difficult task which involves high inertia. Biological systems are, in fact, non-stiff-joint "plants" driven with relatively low-power actuators. However, in this case, control schemes require building accurate kinematic and dynamic models (dynamic models would not be required in the case of very stiff joint robots with inappreciable inertia). Even if the basic dynamics model is very accurate, manipulating tools and objects will affect this base model. This will lead to significant distortions along the desired movements, affecting the final accuracy. Therefore, these systems require adaptive modules for tuning the corrective models to specific object or tool manipulation. This challenge has been smartly solved by the biological systems by using the cerebellum as a force, stiffness, and timing control machine in every human movement. The cerebellar cortex performs a broad role in different key cognitive functions [1]. Three different layers constitute the cerebellar cortex—the molecular layer, the Purkinje layer, and finally, the granular layer. The cerebellar cortex seems to be well structured into microzones [2] related to a specific somatotopic organization in sensor and actuator areas. The human cerebellum involves about 10 000 000 Purkinje cells receiving excitatory inputs from parallel fibers (150 000 excitatory synapses at each Purkinje cell). Each parallel fiber synapses on about 200 Purkinje cells; these parallel fibers are granule cell axons. These granule cells are excited by mossy fibers (with afferent connections from the spinal cord, with sensory and motor estimates). Each Purkinje cell receives further excitatory synapses from one single climbing fiber. This connection is so strong that the activity from a single climbing fiber can drive the Purkinje cell to fire [3]. These spikes from the Purkinje cells generated by climbing fibers are called complex spikes, while the Purkinje cell spikes generated by the activity received from the parallel fibers are called simple spikes. Basket cells, being activated by parallel fiber afferents, can inhibit Purkinje cells. Finally, Golgi cells receive input from parallel fibers, mossy fibers, and climbing fibers, and inhibit granule cells. The output of a Purkinje cell is an inhibitory signal to the deep cerebellar nuclei [3] (Fig. 1). Granule cells and Purkinje cells play an important role in pattern recognition [4]. We can assume that the granular layer adaptation mechanism is essentially unsupervised [5] toward enhancing information transmission. In this layer, an efficient recoding of mossy fiber activity takes place, improving the learning capability in subsequent stages (granular cell-Purkinje cell synapse). The cerebellum seems to play a crucial role in model inference within manipulation tasks but the way this is supported by actual network topologies, cells, and adaptation properties is an open issue.

We have addressed the study of how this model inference task can be achieved in a local and distributed manner with a basic cerebellumlike architecture based on spiking neurons. Furthermore, we evaluate how spike-timing-dependent

Manuscript received November 4, 2010; revised March 3, 2011; accepted March 23, 2011. Date of publication May 2, 2011; date of current version September 16, 2011. This work was supported by EU Grant SENSOPAC (IST 028056) and the national projects DINAM-VISION (DPI2007-61683) and MULTIVISION (TIC-3873), and Spanish Subprograma Juan de la Cierva 2009 (MICINN). This paper was recommended by Associate Editor S. Hu.

N. R. Luque, J. A. Garrido, and E. Ros are with the Department of Computer Architecture and Technology, University of Granada, 18071 Granada, Spain (e-mail: nluque@atc.ugr.es; jgarrido@atc.ugr.es; eros@atc.ugr.es).

R. R. Carrillo is with the Department of Computer Architecture and Electronics, University of Almeria, 04120 Almería, Spain (e-mail: rcarrillo@atc.ugr.es).

O. J.-M. D. Coenen is with the Intelligent Systems Research Center, University of Ulster, Derry, BT48 7JL, Northern Ireland (e-mail: olivier@oliviercoenen.com).

Color versions of one or more of the figures in this paper are available online at http://ieeexplore.ieee.org.

Digital Object Identifier 10.1109/TSMCB.2011.2138693

1083-4419/$26.00 © 2011 IEEE

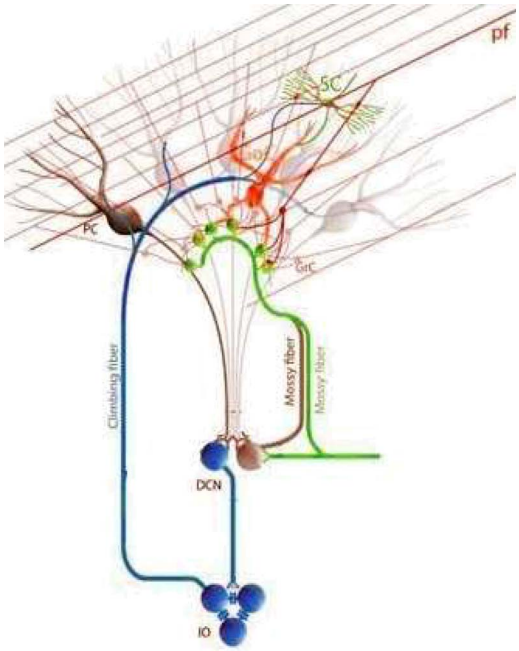

Fig. 1. **Scheme of the cerebellum organization** [6]. This scheme shows the most relevant connections within a cerebellar module. The cerebellar module presents different connections communicating different circuit elements in closed loops. Mossy fibers contact granule cells (GrC) and DCN cells which, in turn, receive inhibition from the same common set of Purkinje cells (PC). Moreover, the IO cells project climbing fibers that contact PC which also are projected to DCN cells.

plasticity (STDP) provides an efficient learning rule for this task. We do this by using a simple temporal-correlation kernel [long-term depression (LTD)] and a constant compensating long-term potentiation term (LTP) as the adaptation mechanism at the parallel fiber (PF)-Purkinje cell (PC) synapses. We explore how the LTP and LTD components of this learning rule need to be well balanced to achieve an acceptable performance. Although different systems that potentially compensate transmission delays have been proposed [7], [8]; in this paper, we explicitly avoid compensating them. The correlation kernel is able to correlate sensorimotor activity with error estimates without explicitly taking into account the transmission delays. This inferred model is therefore trajectory-specific. By means of a certain correlation kernel, the effect of several input spikes on plasticity is accumulated in a reduced number of variables without the necessity of storing spike times. This makes this correlation kernel computationally efficient for event-driven processing engines, as the one used in this paper, EDLUT [9]. In this paper, we explicitly evaluate how these corrective models are structured in a distributed manner among different synapses in the PF-PC connection space. The possibility of monitoring this spatio-temporal learned weight pattern represents a powerful tool to interpret how models are inferred to enhance the accuracy in a control task. We evaluate how this learning engine with specific (fixed gain) LTP and correlation-based LTD components can infer different corrective dynamic models corresponding to the manipulation of objects of different masses.

Control schemes of biological systems must cope with significant sensorimotor delays (100 ms approximately) [10]–[12]. Furthermore, actuators are very efficient but have a limited power and have to deal with viscoelastic elements. In order to deal with all these issues, biology has evolved efficient "model inference engines" to facilitate adaptive and accurate control of arms and hands [13]–[15]. A wide range of studies have proven the crucial role of the cerebellum in delivering accurate correcting motor actions to achieve high-precision movements even when manipulating tools or objects (whose mass or moment of inertia significantly affects the base dynamics models of the arm-hand) [15]–[17]. For this purpose, the cerebellum structure needs to infer the dynamics model of the tool or object under manipulation [18] and store it in a structured way that allows an efficient retrieval of corrective actions when manipulating this item. There are scientific evidences of synaptic plasticity at different sites of the cerebellum and the sensorimotor pathway. The synaptic connection between PFs and PCs seems to have a significant impact on the role of inferring models of sensorimotor correlations for delivering accurate corrective commands during control tasks in most cerebellar models [19]–[21]. Furthermore, the adaptation at this site seems to be driven by the activity coming from the inferior olive (IO) and by the way this activity correlates with the activity received through the PFs.

Within a cerebellarlike cell-based structure, the corrective model is inferred in a distributed way among synapses. Furthermore, this scheme based on distributed cell populations allows several models to be inferred in a non-destructive way by selecting a specific population each time.

The main goal of this paper is the study of how an adaptive cerebellumlike module embedded in the control loop can build up corrective models to compensate deviations in the target trajectory when the dynamics of the controlled plant (arm-hand-object in the case of a human operator) are altered due to manipulation of heavy objects (whose mass significantly affects the basic model dynamics). We address the study of how this corrective model is inferred through a biologically plausible local adaptation mechanism. To better illustrate this issue, we have simplified the cerebellum architecture.

Through this simple cerebellar structure, we have monitored how the weight's space adapts to a distributed stable model that depends on the basic network topology, the target trajectory, and model deviations.

The IO is an important paracerebellar center whose functional role is still an open issue [5], [6], [22]–[25]. Different research groups have studied its potential role in delivering a teaching signal during accurate movements [26]–[29]. The IO is the only source of cerebellar climbing fibers (CFs) which target the Purkinje cells (PC). Each PC receives a single CF which massively connects with this single neuron strongly driving its activity. When a spike of the IO reaches its target PC, the Purkinje cell fires a complex spike. Each CF connects approximately with ten PCs. Nevertheless, the IO fires at a very low frequency (between 1–10 Hz, average 1 Hz) and therefore, the amount of spikes coming from the CFs is almost negligible compared to the activity of the PCs generated by the parallel fibers (simple spikes) [30]–[33].

Neurophysiologic studies have revealed that there are many adaptation mechanisms at the cerebellum. Each of them may have a specific purpose (segmentation, maximization of information transference, correlation of sensorimotor signals, etc.) [34], [35]. In particular, the activity of the IO has a strong

impact on the PF-PC synaptic adaptation [36]. The adaptation of these synapses mediated by this activity seems to play a crucial role in correlating the sensorimotor activity with a "teaching signal" (arriving from the IO) [19], [20], [37], [38]. This teaching signal can be seen as an "intentional signal" that highlights, in time domain, the accuracy of the movement that is being performed. As proposed in [12], [39], this signal may be related to the error during a movement. But since the IO is only capable of very low-frequency output spikes (typically, output activity between 1 and 10 Hz), it does not encode the error quantity accurately in only one movement repetition, but rather provides a progressive estimate. Therefore, during repetitions of movements, its statistical representation may reproduce the error evolution more accurately [28], [40], [41] and thus, it can be a useful guide toward efficient error reduction to achieve accurate movements.

II. Materials and Methods

For extensive spiking network simulations, we have further developed and used an advanced event-driven simulator based on LookUp Tables [9], [42], [43]. EDLUT is an open-source tool [42], [43] which allows the user to compile the response of a predefined cell model (whose dynamics are driven by a set of differential equations) into lookup tables. Then, complex network simulations can be performed without requiring an intense numerical analysis. In this research, as a first approximation, neurons were evolved versions of leaky integrate-and-fire neuron models with the synapses represented as input-driven conductances.

For the experimental work, we have used a biomorphic robot plant, a simulated LWR (lightweight robot). This robot has been developed at DLR [44]. The LWR's arms are of specific interest for machine-human interactions in unstructured environments. In these scenarios, the use of low-power actuators prevents potential damage on humans in case of malfunctioning. Although a real impact on robotic applications is beyond the scope of this paper, the target application scenario of this robotic robot based on non-stiff low-power actuators shares certain characteristics with the daily manipulation tasks performed by humans. Therefore, we considered this robotic platform an appropriate tool for validating the cerebellar-based model inference engine under study.

For the sake of simplicity, in our simulations, we use a simulator of this robot in which we have fixed some joints to reduce the number of actual joints to three, limiting the number of degrees of freedom to three.

A. Training Trajectory

The described cerebellar model has been tested in a smooth pursuit task [45]–[47]. A target (desired target movement) moves along a repeated trajectory, which is composed of vertical and horizontal sinusoidal components. The target movement describes the "eight-shape" trajectories illustrated in Fig. 2, whose equations, in angular coordinates, are given by the following expressions (1). We have evaluated the learning capability performing a goal movement along this target trajectory.

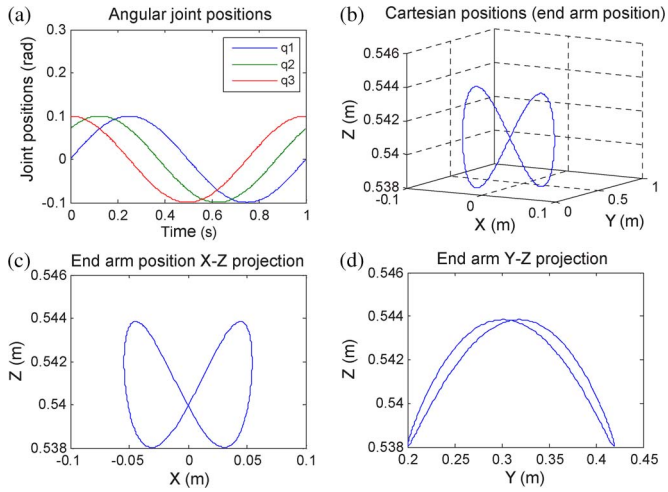

Fig. 2. **Three joint periodic trajectories describing eight-shape movements in joint coordinates. This trajectory implies movements of three joints.** (a) Cartesian coordinates of the eight-like trajectory. (b) 3-D view of the eight-like trajectory. (c) X- and Z-axes representation of this target trajectory. (d) Y and Z-axes representation of the eight-like target trajectory.

Each joint movement in our task is defined by q_1, q_2, and q_3, respectively,

$$\begin{aligned} q1 &= A_1 \sin(\pi t) + C_1 \\ q2 &= A_2 \sin(\pi t + \theta) + C_2 \\ q3 &= A_2 \sin(\pi t + 2\theta) + C_3. \end{aligned} \tag{1}$$

This trajectory with the three joints which are moving following sine shapes is shown in Fig. 2. We chose fast movements (1 s for the whole target trajectory) to study how inertial components (when manipulating objects) are inferred at the cerebellar structure. Slow movements would hide changes in the dynamics of the arm+object model, since they would not have significant impact when performing very slow movements.

Though for the sake of simplicity, we have used a single eight-like trajectory in each trial, consecutive eight-like trajectories have also been tested leading to similar results (provided that the corrective torque values do not get saturated along the global trajectory).

B. Control Loop. Interfacing the Cerebellum Model With a Simulated Robot

Some studies indicate that the brain may plan and learn to plan the optimal trajectory in intrinsic coordinates [14], [48]–[50]. The central nervous system is able to execute three major tasks—the desired trajectory computation in visual coordinates, the task-space coordinates translation into body coordinates, and finally, the motor command generation. In order to deal with variations of the dynamics of the operator arm, we have adopted an feedback error learning scheme [51] in conjunction with a crude inverse dynamic model. In this scheme, the association cortex provides the motor cortex with the desired trajectory in body coordinates, where the motor command is calculated using an inverse dynamic arm model. On one hand, the spinocerebellum—magnocellular red nucleus system provides an internal neural accurate model of the dynamics of the musculoskeletal system which is learned with practice by sensing the result of the movement. On the other hand, the

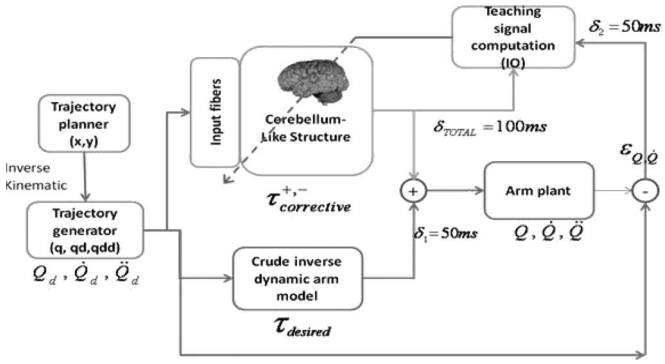

Fig. 3. Control loop. The adaptive module (cerebellarlike structure) contributes to the actual torques being received by the "crude inverse dynamics robot model" to enhance the accuracy of the movement.

cerebrocerebellum—parvocellular red nucleus system provides a crude internal neural model of the inverse dynamics of the musculoskeletal system which is acquired while monitoring the desired trajectory [51]. The crude inverse dynamic model works neck to neck with the dynamical model by updating the motor command by predicting a possible error in the movement. As it is illustrated in Fig. 3, the cerebellar pathways follow a feedforward architecture, in which only information about sensory consequences of incorrect commands can be obtained (i.e., the difference between actual and desired joint positions of the arm). The natural error signal for learning motor commands is the difference between actual and correct commands; this implies, for example, that if M muscles control N sensor dimensions involved in a task, then N-sensory errors must be converted into M-motor errors ($M \times N$ complexity). How to use this sensor information to drive motor learning is the so-called distal error problem [46], [52]. In order to overcome this motor error problem, (the cerebellum in our scheme provides torque corrections) the implemented spiking cerebellum used an adaptation mechanism described in Section II-D which can correlate the actual and desired states toward the generation of accurate corrective motor commands.

In our model, the cerebellum receives well-structured inputs encoding the planned trajectory. We assume that the errors occurred during the movement are encoded at the IO and transferred (at low firing rates) to the cerebellum through the climbing fibers.

We have built a module to translate a small set of signals (encoding the arm's desired state) into a sparse cell-based spike-timing representation (spatio-temporal population coding). This module has been implemented using a set of input fibers with specific receptive fields covering the working range of the different desired state variables (position and velocity of the different joints). In this way, the robot [analog domain consisting of trajectory planer, trajectory generator, crude inverse dynamic arm model, and arm plant (Fig. 3)] has been interfaced with the spiking cerebellar model (spiking domain).

In our control loop, the desired states (positions and velocities) that follow a certain trajectory are obtained from an inverse kinematic model computed by other brain areas [48] and then, they are translated into joint coordinates. These desired arm states are used at each time step by a crude inverse arm dynamics model to compute crude torque commands which are added to the cerebellum corrective torques. This control loop is illustrated in Fig. 3.

Fig. 3 illustrates how the trajectory planner module delivers desired positions and velocities for a target trajectory. The kinematics module translates the trajectory Cartesian coordinates into joint coordinates. The "crude inverse dynamics arm model" calculates the target torque in each joint which are necessary to roughly follow the target trajectory. But this crude arm model does not take into account modifications in the dynamics model due to object manipulation. Thus, if only these torque values are considered, the actual trajectory may significantly differ from the desired one. The adaptive cerebellar component aims at building corrective models to compensate these deviations, for instance, when manipulating objects.

In Fig. 3, the adaptive cerebellarlike structure delivers corrective actions that are added to compensate deviations in the base dynamics plant model when manipulating objects. In this feedforward control loop, the cerebellum receives a teaching error-dependent signal and the desired arm state so as to produce effective corrective commands. Total torque is delayed (on account of the biological motor pathways) and supplied to the robot plant δ_{total}. The difference between the actual robot trajectory and the desired one is also delayed $\delta_{1,2}$ and used by the teaching signal computation module to calculate the IO activity that is supplied to the cerebellum as a teaching input signal (for the computation of the cerebellar synaptic weighs). Using this control loop architecture, an accurate explicit model of the musculoskeletal arm inverse dynamics is not necessary. The cerebellum can infer corrective models tuned to different tools which may affect the dynamics of the plant (arm+object).

C. Cerebellum Model

The proposed cerebellarlike architecture, organized in cerebellar microzones [2] (somatotopic arrangement), tries to capture some cerebellum's functional and topological features [3], [53]. This cerebellum model consists of the following layers: (Fig. 4)

- Input layer (120 cells). This layer represents a simplification of the mossy and granular layers of the cerebellum and drives PCs and cells of the deep cerebellar nuclei (DCN). The goal of this simplification is to facilitate the study of how the sensorimotor corrective models are stored in adapted weights at the PF-PC connections. This input layer has been divided into six groups of 20-grouped cells which carry the desired joint velocity and position information (these desired position and velocity coordinates can be thought as efferent copies of the motor commands or "motor intention"); for the propioceptive encoding, three groups of cells encode the desired joint positions (one group per joint) and the other three encode the desired joint velocities. The analog position and velocity transformation into the fiber spike activity is carried out by using overlapping radial basis functions (RBF) (Fig. 5) [54] as receptive fields of the input-variable space, see (2) (joint-specific angular position)

$$I_{\text{mossy}_i} = e_i^{\frac{(\text{input variable}-\mu_i)^2}{2\sigma^2}} \quad 0 < i < n \quad \text{where} = \text{size of mossy group,} \tag{2.A}$$

where the mossy behavior is given by :

$$\tau_{m_i}\frac{dv_i}{dt} = -v_i(t) + R_i I_{\text{mossy}_i} \tag{2.B}$$

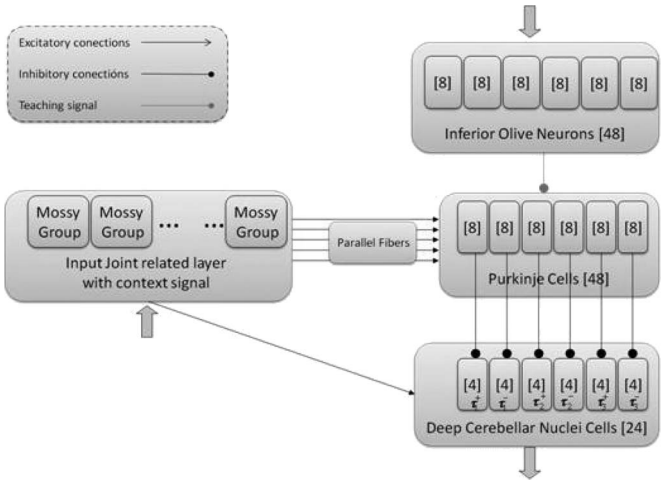

Fig. 4. **Cerebellum model diagram**. Inputs encoding the desired position and velocity (arm state) are sent (upward arrow) through the input layer which represents a simplification of the mossy fibers and granular layer. Inputs encoding the error are sent (upper downward arrow) through the inferior olive (IO). Outputs are provided by the deep cerebellar nuclei (DCN) (lower downward arrow). The DCN collects activity from the input layer (excitatory inputs which provide DCN with a basal activity when an input stimulus is presented) and the Purkinje cells (inhibitory inputs). The DCN activity represents the corrective torque generated by the cerebellum. This output activity is transformed into a proper analog torque signal by means of a buffer in which the DCN activity is accumulated. This activity buffer is used to compute an analog average value that acts as a corrective torque.

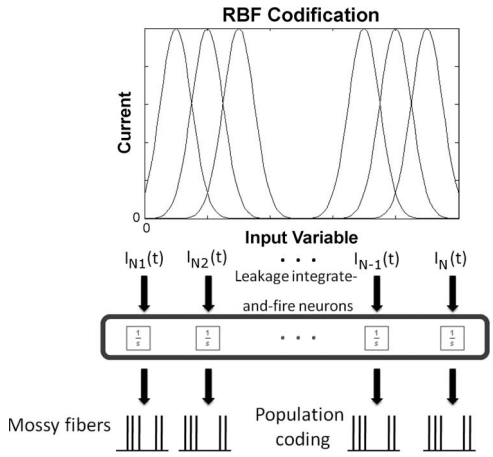

Fig. 5. **Encoding of cerebellar input signals**. Translation from joint-related analog variables (angular positions and velocities) into spike trains is carried out using overlapping RBFs as receptive fields in the analog domain. One-dimensional values are transformed into multidimensional current vectors (one for each RBF). Each current value is integrated using an integrate-and-fire (I & F) neuron model and determines the output activity of an input cell of the cerebellum model.

where μ_i is the mean and σ the standard deviation of i RBF. Related to the cell dynamics, τ_{m_i} is the resting time constant, v_i the membrane potential, I_{mossy_i} the input current, and R_i is related to the resting conductance of the membrane. For the sake of simplicity, in our model, we have not included a more detailed cellular structure (Golgi cells, interneurons, mossy fibers, etc.). We have adopted well-structured noise-free patterns to encode sensorimotor signals to partially embed potential roles typically performed in the granular layer [6], [55] (such as noise reduction, pattern separation, etc.). Parallel fibers are the output of this layer.

- Inferior olive cells (IO) (48 cells). This layer consists of six groups of eight cells. It translates the error signals into teaching spikes to the Purkinje cells. The IO output carries the teaching signal used for supervised learning (see STDP section).
- Purkinje cells (PC) (48 cells). They are divided into six groups of eight cells. Each input cell sends spikes through excitatory connections to PCs, which receive teaching signals from the IO. The PF-PC synaptic conductances are set to an initial average value (15 nS) at the beginning of the simulation and are modified by the learning mechanism during the training process.
- Cells of the DCN (24 cells). The cerebellum model output is generated by six groups of these cells (two groups of four cells per joint) whose activity provides corrective torques to the specified arm commands. The corrective torque of each joint is encoded by a couple of these antagonist groups, being one group dedicated to compensate positive errors and the other one to compensate negative errors. Each neuron group in the DCN receives excitation from every input layer cell and inhibition from the two corresponding PCs. In this way, the PC-DCN-IO sub circuit is organized in six microstructures (Fig. 4), three for positive joint corrections (one per joint) and three for negative joint corrections (one per joint).

We have used leaky integrate-and-fire (I&F) neurons with synapses modeled as variable conductances to simulate Purkinje cells and DCN cells. These models are a modified version of the spike response model [56]. These synaptic conductance responses were modeled as decaying exponential functions triggered by input spikes as stated by (3.A)–(3.C). Thus, these neuron models account for synaptic conductance changes (driven by pre-synaptic activity) rather than simply for current flows, providing an improved description over more basic I&F models. Table I contains the neuron model parameters of the Purkinje cells and DCN cells

$$g_{\text{exc}}(t) = \begin{cases} 0, & t < t_0 \\ g_{\text{exc}}(t_0) \cdot e^{-\frac{t-t_0}{\tau_{\text{exc}}}}, & t \geq t_0 \end{cases} \tag{3.A}$$

$$g_{\text{inh}}(t) = \begin{cases} 0, & t < t_0 \\ g_{\text{inh}}(t_0) \cdot e^{-\frac{t-t_0}{\tau_{\text{inh}}}}, & t \geq t_0 \end{cases} \tag{3.B}$$

$$C_m \frac{dV_m}{dt} = g_{\text{exc}}(t)(E_{\text{exc}} - V_m) + g_{\text{inh}}(t)(E_{\text{inh}} - V_m) + G_{\text{rest}}(E_{\text{rest}} - V_m) \tag{3.C}$$

where g_{exc} and g_{inh} represent the excitatory and inhibitory synaptic conductance (time constant) of the neuron. τ_{exc} and τ_{inh} represent the time constants of the excitatory and inhibitory synapses, respectively. Synaptic inputs through several synapses of the same type can simply be recursively summed when updating the total conductance if they have the same time constants, as indicated in (4). Membrane potential (V_m) is defined through (3.C) depending on the different reverse potentials and synaptic conductances

$$g_{\text{exc(post-spike)}}(t) = G_{\text{exc},j} + g_{\text{exc(pre-spike)}}(t) \tag{4}$$

$\boldsymbol{G}_{\text{exc},\boldsymbol{j}}$ is the weight of synapse j; a similar relation holds for inhibitory synapses.

TABLE I
NEURON MODEL PARAMETERS FOR THE SIMULATIONS [57]–[61]. IN THE TABLE, nS STANDS FOR NANOSIEMENS AND syn STANDS FOR SYNAPSES

	Purkinje cells	DCN cells
Refractory period	2ms	1ms
Membrane capacitance	500pF	2pF
Total excitatory peak conductance	1.3nS·175000syn.·10%	1nS·7syn.
Total inhibitory peak conductance	3nS·150syn.	30nS·1syn.
Firing threshold	-52mV	-40mV
Resting potential	-70mV	-70mV
Resting conductance	16nS	0.2nS
Mem. pot. time constant (τ_m)	20ms to 30ms	10ms
Exc. syn. time constant (τ_{exc})	1.2ms	0.5ms
Inh. syn. time constant (τ_{ihn})	9.3ms	10ms

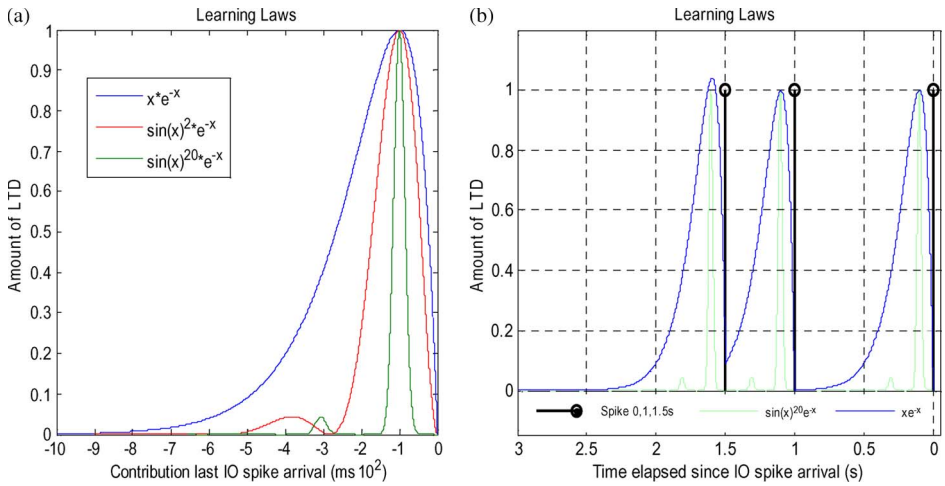

Fig. 6. **LTD integral kernel**. (a) Representation of a basic integral kernel $(x \cdot e^{-x})$ which has a rather wide peak that makes PC synaptic weights to decrease more prominently and a more complex integral kernel $(\sin(x)^{20}) \cdot e^{-x}$ which has a sharper peak. (b) This plot shows the amount of LTD at a particular synapse depending on the IO spike arrival time elapsed since the PF spikes for different integral kernels. The figure includes a comparison between the basic integral kernel $(x \cdot e^{-x})$ and a more complex integral kernel $(\sin(x)^{20}) \cdot e^{-x}$ which has a peak 100 ms after the input spike. The PC receives three spikes through a particular CF at times 0.0, 1, and 1.5 s.

D. STDP

The studied cerebellar model only includes synaptic plasticity at the PF-PC connections. The changes of the synaptic efficacy for each connection are driven by pre-synaptic activity (STDP) and are instantaneous.

In our model, since there are delays in the transmission of joint torque values and joint position measurements, the trajectory error measurements (which are used to calculate the teaching signal) reach the cerebellum with a 100-ms delay. This means that the learning mechanism must learn to provide corrective torque predictions.

This plasticity has been implemented including LTD and LTP mechanisms in the following way:

a) LTD produces a synaptic efficacy decrease when a spike from the IO reaches a PC, as indicated in (6.A). The amount of efficacy which decreases depends on the previous activity arrived through the PF (input of the cerebellar model). This previous activity is convolved with an integral kernel as defined by (5). This mainly takes into account those PF spikes which arrived 100 ms before the IO spike (see Fig. 6). This correction is facilitated by a time-logged "eligibility trace" [45], [47], [62], [63], which takes into account the past activity of the afferent PF. This trace aims to calculate the correspondence in time between spikes from IO (error-related activity) and the previous activity of the PF which is supposed to have provoked this error signal. The eligibility trace idea stems from experimental evidence showing that a spike in the climbing fiber afferent to a Purkinje cell is more likely to depress a PF-PC synapse if the corresponding PF has been firing between 50 and 150 ms before the IO spike (through CF) arrives at the PC [45], [47]

$$k(t) = e^{-(t-t_{\text{postsynapticspike}})} \sin(t - t_{\text{postsynapticspike}})^{20}. \quad (5)$$

b) LTP produces a fixed increase in synaptic efficacy each time a spike arrives through a PF to the corresponding PC as defined by (6.B). With this mechanism, we capture how an LTD process, according to neurophysiologists studies [64], can be inverted when the PF stimulation is followed by spikes from the IO or by a strong depression of the Purkinje cell membrane potential.

The strength of these two mechanisms needs to be tuned to complement and compensate each other. These biological LTP-LTD properties at PF-PC synapses have been tried to be emulated in different fields, i.e., in the adaptive filter [65] theory by

using the heterosynaptic covariance learning rule of Sejnowski [66] or in the adaptive control theory by using the least-mean-square learning rule [67]. Different alternative temporal kernels are shown in Fig. 6. The sharper the integral kernel peak is, the more precise the learning becomes. On the other hand, this leads us to a slower synaptic weight adaptation. However, LTP can lead the weight recruitment to be compensated by future IO activity. This situation drives us to faster synaptic weight saturation where LTP can hardly carry out the weight recruitment for future IO activity. After the main peak in the correlation kernel, a second marginal bump can be seen as a consequence of the mathematical model used for modeling the correlation engines. The chosen mathematical models of the kernel allow accumulative computation in an event-driven engine, avoiding the necessity of integrating the whole correlation kernel each time a new spike arrives. Therefore, these correlation models are computationally efficient in the framework of an event-driven simulation scheme, such as EDLUT [9], but they suffer this second marginal peak that can be considered noise in the weight integration engine.

This is indicated in the following (6):

$$LTD, \forall i, \Delta w_i = -\int_{-\infty}^{IO\text{spike}} k(t - t_{IO\text{spike}})\delta_{GR\text{spike}-i}(t)dt \tag{6.A}$$

$$LTP, \Delta w_i = \alpha. \tag{6.B}$$

E. Teaching Signal of the Inferior Olive

The crude inverse dynamics controller generates motor torque values for a rough control, but the long delays in the control loop prevent the online correction of the trajectory in a fast reaching task using a classical controller with a continuous feedback. In the studied control model, the trajectory error is used to calculate the teaching signal. This teaching signal follows (7)

$$\begin{aligned} \epsilon_{\text{delayed}_i} &= K_{pi} \cdot \epsilon_{\text{position}_i} + K_{vi} \cdot \epsilon_{\text{velocity}_i} \\ i &= 1, 2, 3, \ldots \text{joint} \\ \epsilon_{\text{position}_i} &= (q_{i\text{desired}} - q_{i\text{real}}) \left[(t + t_{\text{pred}})_i - t_i\right] \\ \epsilon_{\text{velocity}_i} &= (\dot{q}_{i\text{desired}} - \dot{q}_{i\text{real}}) \left[(t + t_{\text{pred}})_i - t_i\right] \end{aligned} \tag{7}$$

where $K_{pi} \cdot \epsilon_{\text{position}_i}$ represents the product of a constant value (gain) at each joint K_{pi} and the position error in this joint [difference between desired joint position and actual joint position $(q_{i\text{desired}} - q_{i\text{real}})$].

$K_{vi} \cdot \epsilon_{\text{velocity}_i}$ represents the product between a constant value (gain) at each K_{vi} joint and the velocity error in this joint [difference between desired joint velocity and actual joint velocity $(\dot{q}_{i\text{desired}} - \dot{q}_{i\text{real}})$].

The IO neurons synapse onto the PCs and contribute to drive the plasticity of PF-PC synapses. These neurons, however, fire at very low rates (less than 10 Hz), which appears problematic to capture the high-frequency information of the error signal of the task being learned. This apparent difficulty may be solved by their irregular or chaotic firing [13], [41], [68]. This is a very important property, which has the beneficial consequence of statistically sampling the entire range of the error signal over multiple trials (see below). Here, we implemented this irregular firing using a Poisson model [69] for spike generation. The weight adaptation was driven by the activity generated by the IO, which encoded the teaching signal into a low-frequency probabilistic spike train (from 0 to 10 Hz, average 1 Hz) [5], [41].

We modeled the IO cell responses with probabilistic Poisson process. Given the normalized error signal $\varepsilon(t)$ and a random number $\eta(t)$ between 0 and 1, the cell fired a spike if $\varepsilon(t) > \eta(t)$; otherwise, it remained silent [47]. In this way, on one hand, a single spike reported accurately timed information regarding the instantaneous error; and on the other hand, the probabilistic spike sampling of the error ensured that the whole error region was accurately represented over trials with the cell firing almost ten spikes per second. Hence, the error evolution is accurately sampled even at a low frequency [12]. This firing behavior is similar to the ones obtained in physiological recordings [41].

LTD and LTP play complementary roles in the model inference process. The LTP implemented at the PF-PC synapses was a non-associative weight increase triggered by each input cell spike [64]. The LTD was an associative weight decrease triggered by spikes from the inferior olive [26], [27]. This model of LTD uses a temporal kernel, shown in Fig. 6, which correlates each spike from the IO with the past activity of the parallel fiber [10], [45], [70]. Correlation-based LTD allows the adjustment of specific PF-PC connections to reduce the error according to the IO activity. When IO spikes are received, the synaptic weights of the PF-PC connections are reduced according to the temporal-correlation kernel and to the activity received through the PF. In this way, we reduce the probability of production of simple spikes by PC due to the activity coming from the PFs through these specific connections. Therefore, the IO effectively modulates the spatio-temporal corrective spike patterns. In this model, a learning state in the cerebellum (PF-PC weights) can be seen as a bidimensional function which relates each PF and PC combination with their corresponding synaptic weight [Fig. 7(c)].

Physiologically, the time matching of the desired and actual joint states can be understood by the fact that the trajectory error would be detected at the level of the spinal cord through a direct drive from the gamma motoneurons to the spinal cord [71].

III. Simulations and Results

We have carried out several simulations to study different issues: a) How LTD and LTP need to be balanced to optimize the adaptation performance; b) how the temporal-correlation kernel (integral kernel) works even in the presence of sensorimotor delays; and c) how the same learning mechanism can adapt the system to compensate different deviations in the basic model dynamics (due to manipulating objects of different weights).

A. LTD Versus LTP Trade-Off

At the beginning of the learning process (before the connection weights are adjusted), the spikes received from the input fibers excite the DCN cells, producing a "bias correction" term on the motor commands. The role of the cerebellar PF-PC-DCN loop is to specifically inhibit this bias term according to a spatio-temporal pattern that is inferred during

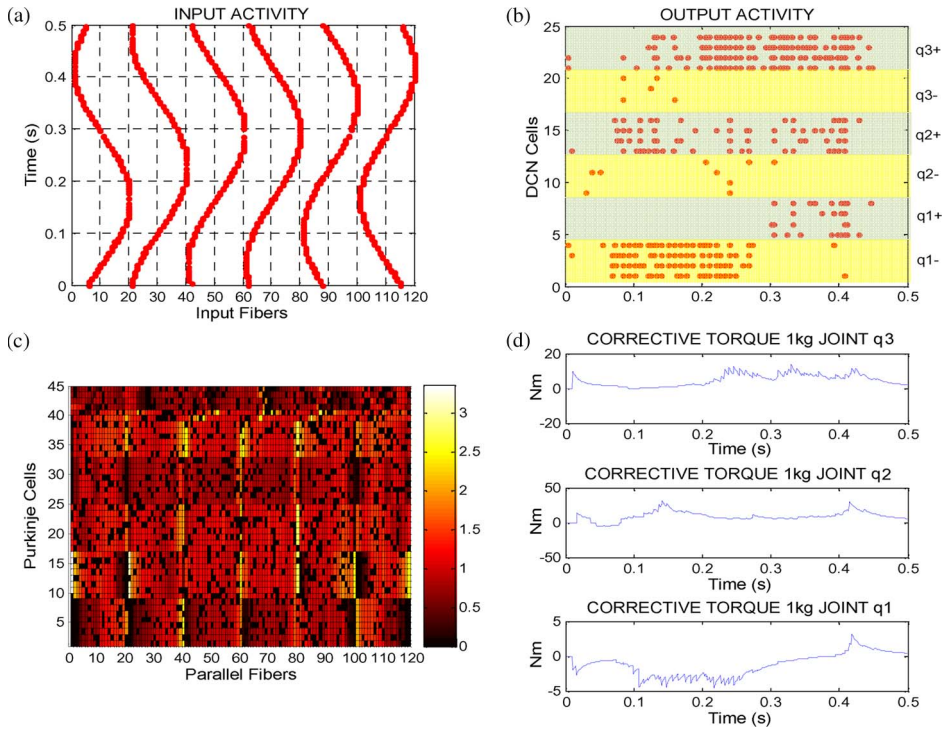

Fig. 7. **Cerebellum state after 300 trajectory learning iterations**. (a) Input activity at the cerebellum. The input layer produces a set of spikes after the transformation from analog domain into spike domain These spikes are transmitted directly by PF. This activity (desired positions and velocities) keeps on constant during all iterations. (b) DCN output activity generated by those synaptic weights. Error corrections are accomplished by changes in the activity of PCs that, in turn, influence the activity of the DCN [72], which afterward is translated into analog torque correction signals. Each group of four DCN cells encodes the positive or negative part of a joint corrective torque. The more activity the positive/negative group has, the higher/lower corresponding corrective torque is generated. (c) PC-PF synaptic weight representation. In x-axis, we can see the source cells (PFs). In y-axis, target cells (PCs) are shown. Dark colors represent lower synaptic weights, thus, the corresponding DCN cells are more active. We can see six well-defined rows, each row represents weights related with the positive and negative torque output of the three joints (q_3, q_2, and q_1), and six well-defined columns (related with the input activity of the PF corresponding to the desired position and velocity for the three joints). (d) Output torque after analog transformation from the DCN output spikes. These corrective torque curves have a profile strongly related with the number of DCN cells assigned per joint; thus, increasing the quantity of DCN per joint will generate a smoother corrective profile.

movement executions and to further compensate other deviations generated by the manipulation of different objects or other elements, affecting the dynamics of the initial "arm plant" (without object under manipulation). The PF-PC-DCN loop transmits an activity pattern which is adapted taking into account the teaching signals provided by the IO (described in the previous section).

In the first simulations, the arm is manipulating a 1-kg mass object. This mass significantly affects the dynamics of the arm+object. Therefore, the actual trajectory (without corrective support) deviates significantly from the target trajectory. We have studied how the cerebellar module compensates this deviation building a corrective model.

Fig. 7 illustrates how the corrective model is acquired through learning and structured in distributed synaptic weight patterns. When the arm moves along a target trajectory, different input cell populations are activated. They produce a temporal signature of the desired movement. Meanwhile, the IO continuously transfers trajectory error estimates (teaching signals) which are correlated with the input signature. In Fig. 7, the system adaptation capability is monitored. This helps to interpret how the corrective model is continuously structured. Similar monitoring experiments in much simpler scenarios and smaller scale cell areas are being conducted in neurophysiologic studies [6] to characterize the adaptation capability of neurophysiologic systems at different neural sites.

When manipulating heavy objects which do not properly fit the basic plant model, the followed trajectory drifts from the desired one before learning. This deviation is more prominent when the desired trajectory changes direction [see Fig. 7(a)] due to the arm's inertia. After learning, the cerebellum output counteracts this inertia, generating higher torques during these changes of the desired trajectory direction [see Fig. 7(d)]. The weight matrix learned by the cerebellum reflects the moments when higher corrective torque values are supplied. By looking at Fig. 7(b) and (d), we can see that the higher corrective torque is produced when the desired trajectory joint coordinates change direction. This occurs in the peaks of the sine waves describing the desired trajectory and corresponds to the activation of the higher and lower input fibers of each block [left and right side of the six weight columns of Fig. 7(c)]. To generate a high corrective torque, the cerebellum must unbalance the magnitude of the positive and negative parts of the joint corrective output [q+ and q− in Fig. 7(b)] which is calculated from the activity of the DCN cells. These DCN cells are grouped by joints. A higher activity affecting positive corrections in a joint produces higher corrective torque. Since PCs inhibit DCN cells, a low PC activity is required for a high DCN activity and vice versa. To obtain a low PC activity, low PF-PC weights are required, which corresponds to small dark squares in Fig. 7(c). Small light squares correspond to high values of the weights. Looking at both sides of the six

weight columns of Fig. 7(c), we can observe how the weight values alternate between high and low in adjacent rows which alternately encode the weights corresponding to the positive and negative parts of each joint corrective torque.

During the learning process, the corrective model is captured in the PF-PC connections. In this way, the movements become more accurate, the error decreases and therefore, also the activity of the IO is reduced. This allows the learned models to become stable once the error reaches appropriate values.

The learning performance is characterized by using four estimates calculated from the mean absolute error (MAE) curve [73]. For the calculation of the MAE of a trajectory execution, we have considered the addition of the error in radians produced by each joint independently.

1) accuracy gain (estimates the error reduction rate comparing the accuracy before and after learning). This estimate helps to interpret the adaptation capability of the cerebellum when manipulating different objects, since the initial MAE for each of these manipulated objects may be different

$$\text{Accuracy Gain} = MAE_{\text{initial}} - \left(\frac{1}{n}\sum_{i=0}^{n} MAE_{(\text{final}-i)}\right) \quad n = 30; \quad (8)$$

2) final error (average error over the last 30 trials)

$$\text{Final Error} = \left(\frac{1}{n}\sum_{i=0}^{n} MAE_{(\text{final}-i)}\right) \quad n = 30; \quad (9)$$

3) final error stability (average of standard deviation over the last 30 movement trials)

$$\text{Final Error Stability} = \frac{1}{n}\sum_{i=0}^{n}\left(\sigma\left(MAE_{(\text{final}-i)}\right)\right) \quad n = 30; \quad (10)$$

4) error convergence speed (number of samples to reach the final error average)

$$\text{Error Convergence Speed} = j; \text{ where } MAE_j \leq \left(\frac{1}{n}\sum_{i=0}^{n} MAE_{(\text{final}-i)}\right) \quad 0 < j \leq \text{final}. \quad (11)$$

We have carried out 70 simulations of a complete training process, where each training process consists of 400 trajectory executions and each trajectory execution is carried out in 1-s simulation time (i.e., the whole system is executed 28 000 times). During each of these training processes, the obtained error in each trajectory execution decreases until it reaches a final stable value. The obtained MAE of a single complete training process is shown in Fig. 8(a). We have tested this learning process with different LTD and LTP components to evaluate how they affect the adaptation capability of the system. From each of these training processes (with different LTD and LTP values), we obtain the performance estimates defined above (accuracy gain, final error, final error stability, and error convergence speed). These performance estimates characterize the adaptation mechanism capability.

As it is shown in Fig. 8(b) and (c), both LTP and LTD must be compensated. Low LTD values combined with high LTP values cause high weight saturation. This can be seen in Fig. 8(c), in which 3-D final normalized error values of the first figure are represented in a high flat surface corresponding to high errors. We also have a flat surface close to zero in Fig. 8(c) (3-D final normalized error stability figure); the cerebellum output is totally saturated. Therefore, when LTP-LTD tradeoff is unbalanced (LTP dominating LTD), the system adaptation capability is low, leading to high error estimators and useless high stability. On the other hand, when high LTD values are combined with low LTP values, this causes low weight saturation. In Fig. 8(c) 3-D plots, we see a good final average error and a good accuracy gain and convergence speed but very unstable output. This is also indicated by the error variance figure estimates which are high in this LTD-LTP area. A compensated LTD-LTP setting drives us to a high-accuracy gain and also, to a low and stable final error with high convergence speed. For instance, if our LTD choice is 0.075, our LTP must be lower than 0.015 to achieve a proper stable learning mechanism. In all the following simulations, we have fixed the LTD and LTP parameters to these values. Therefore, we illustrate how different model deviations (by different object manipulations) can be compensated with a fixed and balanced temporal-correlation kernel and how this correction loop works even in the presence of different sensorimotor transmission delays.

B. Learning Temporal-Correlation Kernel Allows Corrective Model Inference Even in the Presence of Sensorimotor Delays

The cerebellumlike structure previously described works even with sensorimotor delays by means of the temporal-correlation kernel which determines the amount of LTD to be applied. This is summarized in Fig. 9. The results (in Fig. 9) have been obtained after performing four simulations (each one for different delay setups) of 400 trajectory executions each. On the other hand, this temporal-correlation kernel remains robust not only with different unbalanced delays but also with a non-perfect matching between sensorimotor delays and the temporal correlation kernel peak, as it is shown in Fig. 10. These results have been obtained after performing five simulations (each one for a different time deviation) of 400 trajectory executions each.

This robustness is achieved because the scheme is using desired coordinates (positions and velocities) which remain stable across different trials. Nevertheless, with delays mismatching (between learning kernel inherent time shift and sensorimotor delays) over 70 ms, this scheme becomes unstable.

C. Learning Different Dynamic Models

The presented cerebellum microstructure and the long-term plasticity, side by side, facilitate internal model inference. The cerebellum model adapts itself to infer a new model by using error signals which are obtained when manipulating this new object. We study the ability of the cerebellar architecture to infer different corrective models for dynamics changes on a base manipulator model.

Under normal conditions, without adding any extra mass to the end of the effector (arm), the crude inverse dynamics

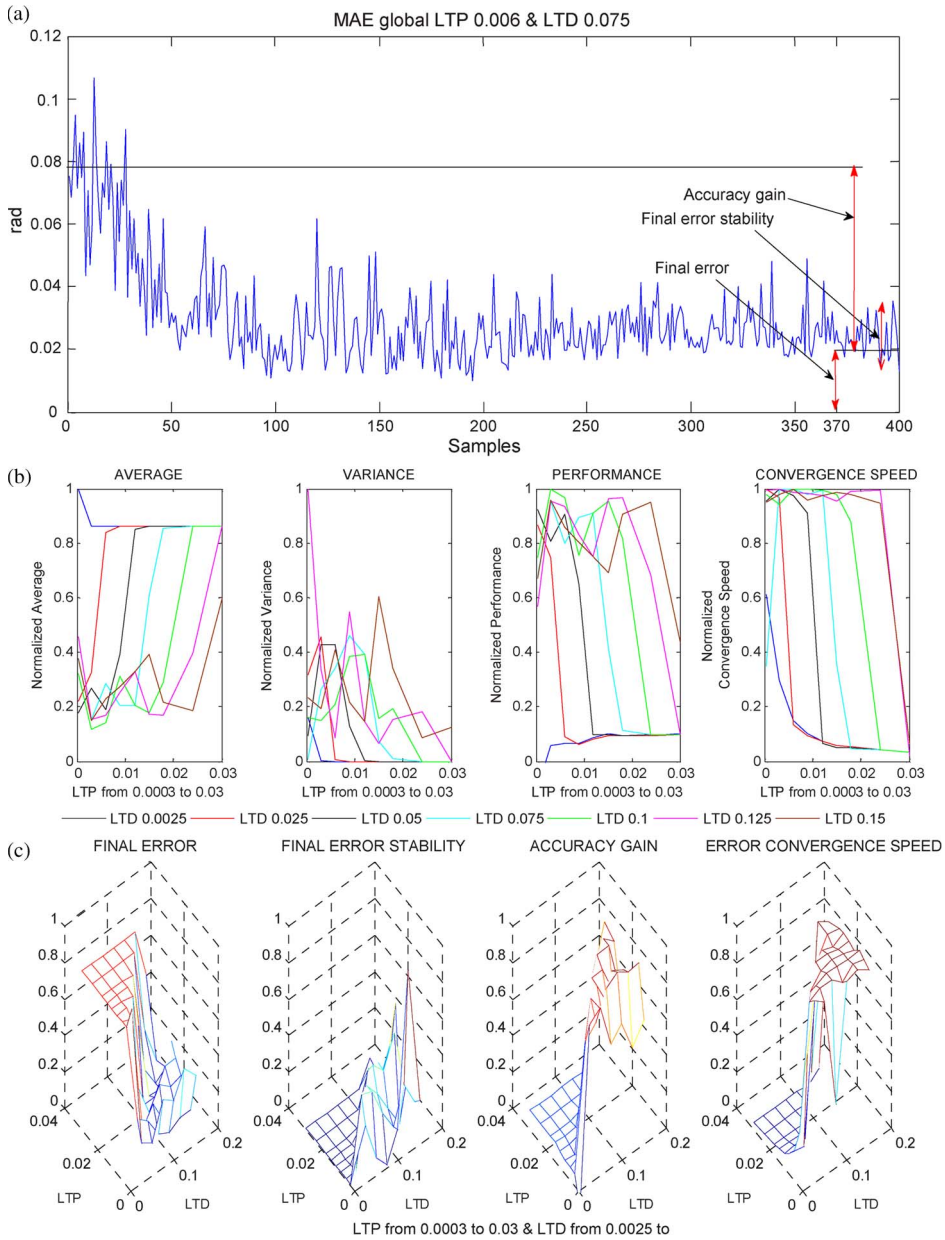

Fig. 8. **Learning characterization**. The error taken into account in this learning characterization is a global addition of the absolute joint errors in position from each link of our robot plant. (a) During the learning process, the movement error decreases along several iterative executions of trials of an eight-like trajectory benchmark. We evaluate the learning performance using four estimates extracted from the MAE curve: 1) accuracy gain; 2) final error; 3) final error stability; and 4) error convergence speed. (b) Using these four estimators, we can evaluate how LTP and LTD affect the learning process. We have conducted multiple simulations with different LTD-LTP tradeoffs to characterize the learning behavior. The goal of an appropriate learning process is to achieve a high-accuracy gain and a low and stable final error.

model calculates rough motor commands to control the arm plant. In contrast, under altered dynamics conditions, the motor commands are inaccurate to compensate for the new undergone forces (inertia, etc.), and this leads to distortions in the performed trajectories. During repeated trials, the cerebellum learns to supply the corrective motor commands when the arm plant model dynamics differs from the initial one. These corrective motor commands are added to the normal-condition motor commands. Then, improved trajectories are obtained as the learning process goes on. The cerebellum gradually builds up internal models by experience and uses them in combination with the crude inverse dynamics controller. This cerebellum adaptation is assumed to involve changes in the synaptic efficacy of neurons constituting the inverse dynamics model [74], as it is shown in our simulation results (Fig. 11).

The performance results of the followed trajectory have been evaluated during 400 trajectory executions manipulating different objects attached at the end of the last segment of the arm of 0.5, 1, 1.5, and 2 kg. Fig. 11 illustrates the performed trajectory for each simulation with an object of a different mass. Fig. 12 shows how the cerebellar model is able to learn/infer the corrective dynamics model for the different objects. The error curves of Fig. 12(a) (where each sample represents the error along one eight-like trajectory) show how the control loop with the adaptive cerebellar module is able to significantly reduce the error during the training process. Fig. 11 shows that

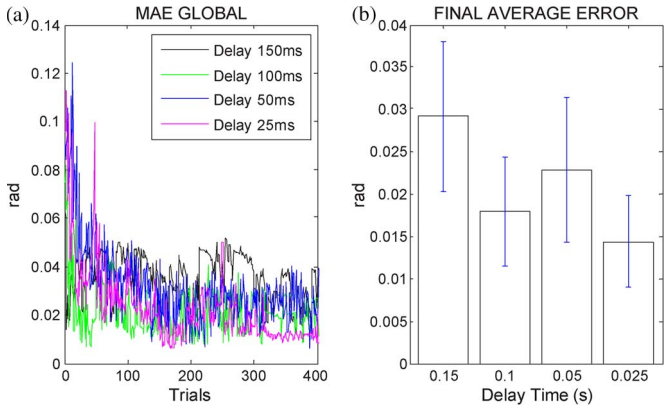

Fig. 9. **Temporal-correlation kernel for different sensorimotor delays (delays from 25 to 150 ms have been tested)**. We have adjusted the correlation kernel peak position to match (see Fig. 6) the sensorimotor delays of the control loop illustrated in Fig. 3. As it is shown, the delay value does not affect to a large extent the obtained performance. The final average error is nearly constant in these different simulations.

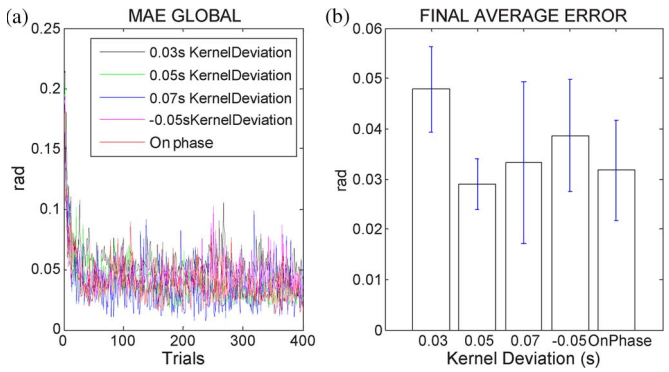

Fig. 10. **Temporal-correlation kernel behavior with different deviations between sensorimotor delays and the kernel peak (deviation from 50 to 70 ms have been tested)**. We have evaluated different deviations between the correlation kernel peak position (see Fig. 6) and the sensorimotor delays of the control loop illustrated in Fig. 3. As it is shown, despite the kernel peak does not exactly match with sensorimotor delays, the cerebellum still works and the final average error keeps on constant. The cerebellum is able to correlate the delayed sinusoidal inputs and the non-in-phase peak kernel.

manipulating heavier objects means that the starting error is higher, since the arm dynamics differ from the original one to a larger extent. Therefore, the cerebellum learns to supply higher corrective torques, which makes a bigger difference between the initial and final error. This makes the accuracy gain estimate higher than in the other cases. On the other hand, for improving the global accuracy gain, higher forces have to be counteracted to follow the desired trajectory.

IV. Discussion

This paper focuses on studying how a cerebellarlike adaptive module, operating together with a crude inverse dynamics model, can effectively provide corrective torque to compensate deviations in the dynamics of a base plant model (due to object manipulation). This is relevant to understand how the cerebellar structure embedded in a biologically plausible control loop can infer internal corrective models when manipulating objects which affect the base dynamics model of the arm. The spiking neural cerebellum connected to a biomorphic robot plant represents a tool to study how the cerebellar structure and learning kernels (including time shifts for compensating sensorimotor delays) provide adaptation mechanisms to infer dynamics correction models toward accurate object manipulation. Concretely, we have evaluated how a temporal-correlation kernel driving an error-related LTD and a compensatory LTP component (complementing each other) can achieve effective adaptation of the corrective cerebellar output. We have shown how the temporal-correlation kernel can work even in the presence of sensorimotor delays. However, considering the results obtained for several sensorimotor delays, we can state that the desired trajectory must be coded using a univocal population coding in each time step, that is, the codification of the desired position/velocity during the trajectory must be different for each point of the trajectory. And thus, as our cerebellar structure can adaptively generate any suitable output for each trajectory-point codification, the delay of the sensorimotor pathways is not remarkably relevant, even if this delay does not match the intrinsic compensatory delay of the learning integration kernel.

In this simple cerebellarlike structure, we have shown how the representation of the cerebellar weight matrix corresponding to the PF-PC connections can be interpreted in terms of the generated corrective torque (which, in turn, is a direct consequence of this representation). This allows us to study the performance of this corrective model storage and how the changes of the arm dynamics (manipulating different object) are inferred on different synaptic weight patterns.

We have also shown how LTD and LTP need to be balanced with each other to achieve high performance adaptation capabilities. We have studied the behavior of these two complementary adaptation mechanisms. We have evaluated how the learning behaves when they are balanced and also when they are in value ranges in which one of them dominates saturating the adaptation capability of the learning rule. We have evaluated how well-balanced LTD and LTP components lead to an effective reduction of error in manipulation tasks with objects which significantly affect the dynamics of the base arm plant.

We have used a simplified version of the cerebellum to focus on the way that the cerebellar corrective models are stored and structured in neural population weights. This is of interest to inform neurophysiologic research teams to drive attention to potential footprints of inferred models within the PF-PC connections.

As future work, we will study how to dynamically optimize the LTD-LTP integration kernel instead of a single, stable, and balanced LTD-LTP kernel, we will evaluate the capability of improving the adaptation mechanism, shifting this balance to acquire the corrective models faster and then, decrease the plasticity once an acceptable performance is reached. This approach can optimize the learning capability of the system.

We will also develop further real-time interfaces between analog signals and spiking neurons (between the robot and the EDLUT simulator) to perform simulations with real robots and new cerebellar architectures working in a manipulation task scenario in which granular layer, Golgi cells, and stellate cells will be included. This will be addressed in a starting EU project (REALNET).

The neuron models, cerebellar models, and adaptation mechanisms will be available at the EDLUT simulator site to facilitate the reproduction of the presented work.

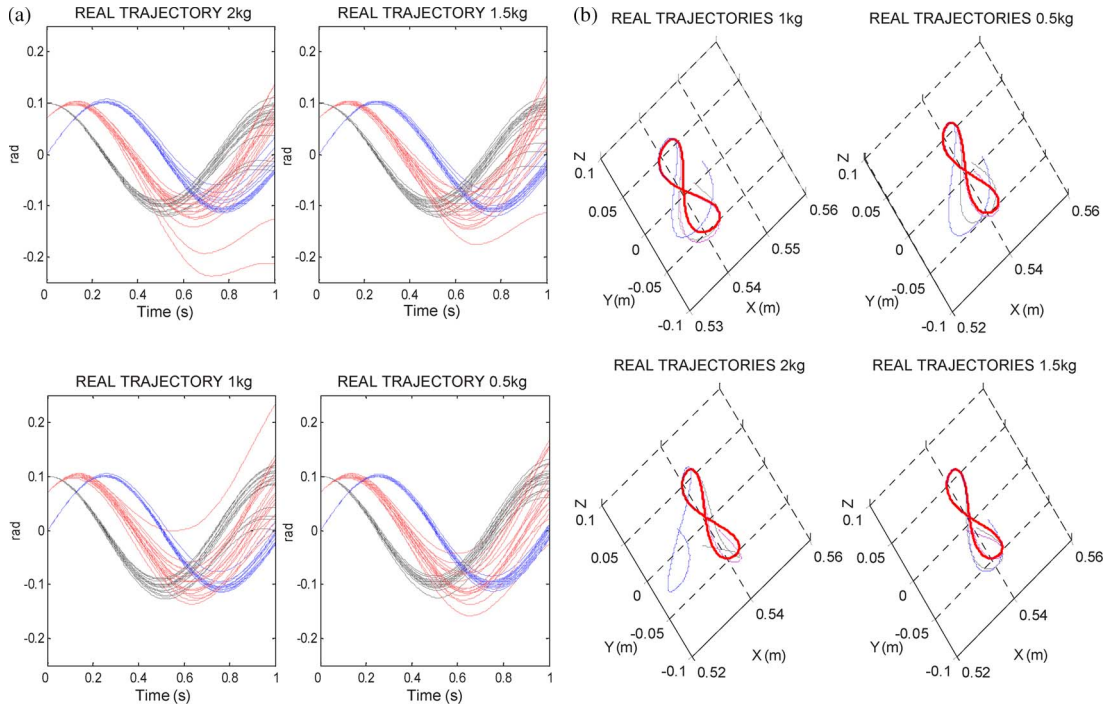

Fig. 11. **Learning the corrective models for the eight-like target trajectory when manipulating objects with different masses (2, 1.5, 1, and 0.5 kg)**. (a) three-joint value representation for the performed trajectory. The three joints are shown. The followed trajectory is shown each 25 trials during a 400-trial complete learning process. (b) 2-D representation of the performed trajectory (Desired trajectory in red; in blue. initial trial; in black, trial number 200; and in cyan, final trial). **Improvement in %: 0.5 kg** 200-trial 40.4% 400-trial 49%; **1 kg** 200-trial 64.6% 400-trial 64.5%; **1.5 kg** 200-trial 72.5% 400-trial 74.4%; **2 kg** 200-trial 78.6% 400-trial 79.3%. **Stability improvement in %** (average std over 0–30 trials/17–200 trials/370–400 trials). **0.5 kg** 170–200-trials 82% compared to initial 0–30-trials, 370–400-trials 60.1% comparing to initial 0–30-trials. **1 kg** 170–200-trials 49.6% compared to initial 0–30 trials, 370–400-trials 42.1% compared initial 0–30-trials. **1.5 kg** 170–200 trials 46.1% compared to initial 0–30 trials, 370–400-trials 26.4% compared to initial 0–30-trials. **2 kg** 170–200 trials 26.4% compared to initial 0–30-trials, 370–400 trials 25.1% compared to initial 0–30 trials.

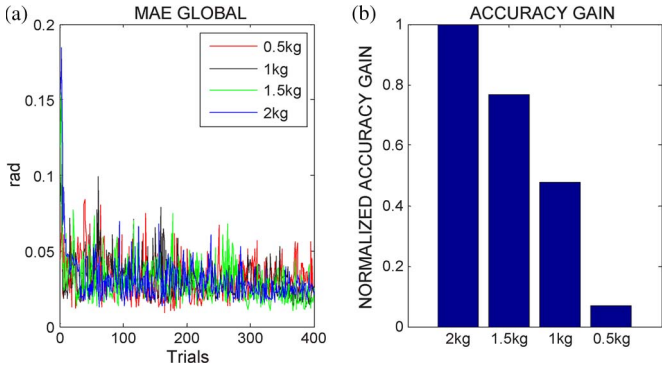

Fig. 12. **Learning performance when manipulating different objects (0.5, 1, 1.5, and 2 kg) during 400-trial learning processes**. (a) MAE evolution. Learning occurs on a continuous basis providing incremental adaptability throughout the simulation time. (b) Accuracy gain.

ACKNOWLEDGMENT

The authors would like to thank the German aerospace center DLR/Institute of Robotics and Mechatronics, particularly Dr. P. van der Smagt, Head of Bionics Group, for his help.

REFERENCES

[1] H. C. Leiner, A. L. Leiner, and R. S. Dow, "Cognitive and language functions of the human cerebellum," *Trends Neurosci.*, vol. 16, no. 11, pp. 444–447, Nov. 1993.

[2] P. Dean, J. Porrill, C. F. Ekerot, and H. Jörntel, "The cerebellar microcircuit as an adaptive filter: Experimental and computational evidence," *Nat. Rev. Neurosci.*, vol. 11, no. 1, pp. 30–43, Jan. 2010.

[3] E. R. Kandel, J. H. Schwartz, and T. M. Jessell, *Principles of Neural Science*. New York: McGraw-Hill, 2000, ch. 42.

[4] D. Philipona and O. J.-M. D. Coenen, "Model of granular layer encoding in the cerebellum," *Neurocomputing*, vol. 58–60, pp. 575–580, Jun. 2004.

[5] N. Schweighofer, K. Doya, H. Fukai, J. V. Chiron, T. Furukawa, and M. Kawato, "Chaos may enhance information transmission in the inferior olive," *Proc. Nat. Acad. Sci.*, vol. 101, no. 13, pp. 4655–4660, Mar. 2004.

[6] E. D'Angelo, S. K. Koekkoek, P. Lombardo, S. Solinas, E. Ros, J. Garrido, M. Schonewille, and C. I. De Zeeuw, "Timing in the cerebellum: Oscillations and resonance in the granular layer," *Neuroscience*, vol. 162, no. 3, pp. 805–815, Sep. 2009.

[7] S. G. Massaquioi and J. J. E. Stoline, "The intermediate cerebellum may function as a wave-variable processor," *Neurosci. Lett.*, vol. 215, no. 1, pp. 60–64, Aug. 1996.

[8] V. Steuber, D. Willshaw, and A. Van Ooyen, "Generation of time delays. Simplified models of intracellular signaling in cerebellar Purkinje cells network," *Comput. Neural Syst.*, vol. 17, no. 2, pp. 173–191, Jun. 2006.

[9] E. Ros, R. Carrillo, E. M. Ortigosa, B. Barbour, and R. Agís, "Event-driven simulation scheme for spiking neural networks using lookup tables to characterize neuronal dynamics," *Neural Comput.*, vol. 18, no. 12, pp. 2959–2993, Dec. 2006.

[10] J. L. Raymond and S. G. Lisberger, "Neural learning rules for the vestibulo-ocular reflex," *J. Neurosci.*, vol. 18, no. 21, pp. 9112–9129, Nov. 1998.

[11] H. Voicu and M. D. Mauk, "Parametric analysis of cerebellar LTD in eyelid conditioning," *Neurocomput. Comput. Neurosci. Trends Res.*, vol. 69, no. 10–12, pp. 1187–1190, Jun. 2006.

[12] R. R. Carrillo, E. Ros, C. Boucheny, and O.-J. M.-D. Coenen, "A real time spiking cerebellum model for learning robot control," *Biosystems*, vol. 94, no. 1/2, pp. 18–27, Oct.–Nov. 2008.

[13] M. Kawato, "Brain controlled robots," *HFSP J.*, vol. 2, no. 3, pp. 136–142, Jun. 2008.

[14] J. C. Houk, J. T. Buckingham, and A. G. Barto, "Models of cerebellum and motor learning," *Behav. Brain Sci.*, vol. 19, no. 3, pp. 368–383, 1996.

[15] P. Van der Smagt, "Cerebellar control of robot arms," *Connect. Sci.*, vol. 10, no. 3/4, pp. 301–320, Dec. 1998.

[16] R. C. Miall, "The cerebellum, predictive control and motor coordination," in *Proc. Novartis Found. Symp.*, 2007, vol. 218, Sensory Guidance of Movements, pp. 272–290.
[17] S. Khemaissia and A. Morris, "Use of an artificial neuroadaptive robot model to describe adaptive and learning motor mechanisms in the central nervous system," *IEEE Trans. Syst., Man, Cybern. B, Cybern.*, vol. 28, no. 3, pp. 404–416, Jun. 1998.
[18] D. M. Wolpert, R. C. Miall, and M. Kawato, "Internal models in the cerebellum," *Trends Cognit. Sci.*, vol. 2, no. 9, pp. 338–347, Sep. 1998.
[19] J. S. Albus, "A theory of cerebellar function," *Math Biosci.*, vol. 10, no. 1/2, pp. 25–61, Feb. 1971.
[20] M. Ito, "Cerebellar circuitry as a neuronal machine," *Progr. Neurobiol.*, vol. 78, no. 3–5, pp. 272–303, Feb.–Apr. 2006.
[21] P. Dean and J. Porril, "Adaptive filter models of the cerebellum. Computational analysis," *Cerebellum*, vol. 7, no. 4, pp. 567–571, 2008.
[22] G. A. Jacobson, D. Rokni, and Y. Yarom, "A model of the olivo-cerebellar system as a temporal patterm generator," *Trends Neurosci.*, vol. 31, no. 12, pp. 617–625, Dec. 2008.
[23] G. A. Jacobson, I. Lev, Y. Yarom, and D. Cohen, "Invariant phase structure of olivo-cerebellar oscillations and putative role in temporal pattern generation," *Proc. Nat. Acad. Sci.*, vol. 106, no. 9, pp. 3579–3584, Mar. 2009.
[24] C. I. De Zeeuw, J. I. Simpson, C. C. Hoogenraad, N. Galjart, S. K. Koekkoek, and T. J. Ruigrok, "Microcircuitry and function of the inferior olive," *Trends Neurosci.*, vol. 21, no. 9, pp. 391–400, Sep. 1998.
[25] A. Mathy, S. S. Ho, J. T. Davie, I. C. Duguid, B. A. Clark, and M. Häusser, "Encoding of oscillations by axonal bursts in inferior olive neurons," *Neuron*, vol. 62, no. 3, pp. 388–399, May 2009.
[26] M. Ito and M. Kano, "Long-lasting depression of parallel fiber-Purkinje cell transmission induced by conjunctive stimulation of parallel fibers and climbing fibers in the cerebellar cortex," *Neurosci. Lett.*, vol. 33, no. 3, pp. 253–258, Dec. 1982.
[27] M. Ito, "Cerebellar long-term depression: Characterizations, signal transduction and functional roles," *Physiol. Rev.*, vol. 81, no. 3, pp. 1143–1195, 2001.
[28] N. Schweighofer, J. Spoelstra, M. A. Arbib, and M. Kawato, "Role of the cerebellum in reaching movements in human. II. A neural model of the intermediate cerebellum," *Eur. J. Neurosci.*, vol. 10, no. 1, pp. 95–105, Jan. 1998.
[29] J. Simpson, D. Wylle, and C. I. De Zeeuw, "On climbing fiber signals and their consequences," *Behav. Brain Sci.*, vol. 19, no. 3, pp. 368–383, 1996.
[30] I. Raman and B. P. Bean, "Ionic currents undelying spontaneous action potentials in isolated cerebellar Purkinje neurons," *J. Neurosci.*, vol. 19, no. 5, pp. 1663–1674, Mar. 1999.
[31] E. Bauswein, F. P. Kolb, B. Leimbeck, and F. J. Rubia, "Simple and complex spike activity of cerebellar Purkinje cells during active and passive movements in the awake monkey," *J. Physiol.*, vol. 339, pp. 379–394, Jun. 1983.
[32] J. L. Gardner, S. N. Tokiyama, and S. G. Lisberger, "A population decoding framework for motion after effects on smooth pursuit eye movement," *J. Neurosci.*, vol. 24, no. 41, pp. 9035–9048, Oct. 2004.
[33] R. Soetedjo and A. F. Fuchs, "Complex spike activity of Purkinje cells in the oculomotor vermis during behavioral adaptation of monkey saccades," *J. Neurosci.*, vol. 26, no. 29, pp. 7741–7755, Jul. 2006.
[34] E. D'Angelo, T. Nieus, M. Bezzi, A. Arleo, and O. J.-M. D. Coenen, "Modeling synaptic transmission and quantifying information transfer in the granular layer of the cerebellum," *Lecture Notes Comp. Sci.*, vol. 3512, pp. 107–114, 2005a.
[35] M. Kawato and H. Gomi, "A computational model of four regions of the cerebellum based on feedback-error learning," *Biol. Cybern.*, vol. 68, no. 2, pp. 95–103, 1992.
[36] C. D. Hansel, D. J. Linden, and E. D'Angelo, "Beyond parallel fiber LTD: The diversity of synaptic and non-synaptic plasticity in the cerebellum," *Nat. Neurosci.*, vol. 4, no. 5, pp. 467–475, May 2001.
[37] D. Marr, "A theory of cerebellar cortex," *J. Physiol.*, vol. 202, no. 2, pp. 437–470, Jun. 1969.
[38] M. Ito, *The Cerebellum and Neural Control*. New York: Raven, 984.
[39] J. Spoelstra, M. A. Arbib, and N. Schweighofer, "Cerebellar adaptive control of a biomimetic manipulator," *Neurocomputing*, vol. 26/27, pp. 881–889, Jun. 1999.
[40] D. M. Wolpert and Z. Ghahramani, "Computational principles of movement neuroscience," *Nat. Neurosci.*, vol. 3, no. Suppl., pp. 1212–1217, Nov. 2000.
[41] S. Kuroda, K. Yammoto, H. Miyamoto, K. Doya, and M. Kawato, "Statistical characteristics of climbing fiber spikies necessary for efficient cerebellar learning," *Biol. Cybern.*, vol. 84, no. 3, pp. 183–192, Mar. 2001.
[42] E. Ros, E. M. Ortigosa, R. Agís, R. Carrillo, and M. Arnold, "Real-time computing platform for spiking neurons (RT-spike)," *IEEE Trans. Neural Netw.*, vol. 17, no. 4, pp. 1050–1063, Jul. 2006.
[43] R. Agís, J. Díaz, E. Ros, R. R. Carrillo, and E. M. Ortigosa, "Hardware event-driven simulation engine for spiking neural networks," *Int. J. Electron.*, vol. 94, no. 5, pp. 469–480, May 2007.
[44] J. Butterfaß, M. Grebenstein, H. Liu, and G. Hirzinger, "DLR hand II: Next generation of a dextrous robot hand," in *Proc. IEEE Int. Conf. Robot. Automat.*, 2001, pp. 109–114.
[45] R. E. Kettner, S. Mahamud, H.-C. Leung, N. Sitkoff, J. C. Houk, B. W. Peterson, and A. G. Barto, "Prediction of complex two-dimensional trajectories by a cerebellar model of smooth pursuit eye movement," *J. Neurophysiol.*, vol. 77, no. 4, pp. 2115–2130, Apr. 1997.
[46] A. Haith and S. Vijayakumar, "Robustness of VOR and OKR adaptation under kinematics and dynamics transformations," in *Proc. 6th IEEE ICDL*, London, U.K., 2007, pp. 37–42.
[47] C. Boucheny, R. R. Carrillo, E. Ros, and O. J.-M. D. Coenen, "Real-time spiking neural network: An adaptive cerebellar model," *LNCS*, vol. 3512, pp. 136–144, 2005.
[48] E. Nakano, H. Imamizu, R. Osu, Y. Uno, H. Gomi, T. Yoshioka, and M. Kawato, "Quantitative examinations of internal representations for arm trajectory planning. Minimum commanded torque change model," *J. Neurophysiol.*, vol. 81, no. 5, pp. 2140–2155, May 1999.
[49] E. J. Hwang and R. Shadmehr, "Internal models of limb dynamic and the encoding of limb state," *J. Neural Eng.*, vol. 2, no. 3, pp. S266–S278, Sep. 2005.
[50] E. Todorov, "Optimality principles in sensorimotor control (review)," *Nat. Neurosci.*, vol. 7, no. 9, pp. 907–915, Sep. 2004.
[51] M. Kawato, K. Furukawa, and R. Suzuki, "A hierarchical neural-network model for control and learning of voluntary movement," *Biol. Cybern.*, vol. 57, no. 3, pp. 169–185, 1987.
[52] J. Porrill, P. Dean, and J. V. Stone, "Recurrent cerebellar architecture solves the motor-error problem," *Proc. Biol. Sci.*, vol. 271, no. 1541, pp. 789–796, Apr. 2004.
[53] B. B. Andersen, L. Korbo, and B. Pakkenberg, "A quantitative study of the human cerebellum with unbiased stereological techniques," *J. Comp. Neurol.*, vol. 326, no. 4, pp. 549–560, Dec. 1992.
[54] C. Assad, S. Dastoor, S. Trujillo, and L. Xu, "Cerebellar dynamic state estimation for a biomorphic robot arm," in *Proc. Syst., Man. Cybern.*, Oct. 2005, vol. 1, pp. 877–882.
[55] E. D'Angelo, P. Rossi, D. Gall, F. Prestori, T. Nieus, A. Maffei, and E. Sola, "LTP of synaptic transmission at the Mossy Fiber-Granule cell relay of the cerebellum," *Progress in Brain Research*, vol. 128, pp. 69–80, 2005.
[56] W. Gerstner and W. Kistler, *Spiking Neuron Models: Singleneurons, Populations, Plasticity*. Cambridge, U.K.: Cambridge Univ. Press, 2002.
[57] D. Jaeger, "No parallel fiber volleys in the cerebellar cortex: Evidence from cross-correlation analysis between Purkinje cells in a computer model and in recordings from anesthetized rats," *J. Comput. Neurosci.*, vol. 14, no. 3, pp. 311–327, May/Jun. 2003.
[58] A. Roth and M. Häusser, "Compartmental models of rat cerebellar Purkinje cells based on simultaneous somatic and dendritic patch-clamp recordings," *J. Physiol.*, vol. 535, pp. 445–472, Sep. 2001.
[59] S. Solinas, R. Maex, and E. De Schutter, "Synchronization of Purkinje cell pairs along the parallel fibre fiber axis: A model," *Neurocomputing*, vol. 52–54, pp. 97–102, Jun. 2003.
[60] D. Jaeger, E. De Schutter, and J. Bower, "The role of synaptic and voltage-gated currents in the control of Purkinje cell spiking: A modeling study," *J. Neurosci.*, vol. 17, no. 1, pp. 91–106, Jan. 1997.
[61] M. Häuser and B. Clarck, "Tonic synaptic inhibition modulates neuronal output pattern and spatiotemporal synaptic integration," *Neuron*, vol. 19, no. 3, pp. 665–678, Sep. 1997.
[62] R. S. Sutton and A. G. Barto, "Toward a modern theory of adaptive networks: Expectation and prediction," *Psychol. Rev.*, vol. 88, no. 2, pp. 135–170, Mar. 1981.
[63] A. G. Barto, R. S. Sutton, and C. W. Anderson, "Neuronlike adaptive elements that can solve difficult learning control problems," *IEEE Trans. Syst., Man., Cybern.*, vol. SMC-13, no. 5, pp. 934–846, Sep./Oct. 1983.
[64] V. Lev-Ram, S. B. Meht, D. Kleinfeld, and R. Y. Tsien, "Reversing cerebellar long term depression," *Proc. Nat. Acad. Sci.*, vol. 100, no. 26, pp. 15 989–15 993, Dec. 2003.
[65] M. Fujita, "Adaptive filter model of the cerebellum," *Biol. Cybern.*, vol. 45, no. 3, pp. 195–206, 1982.
[66] T. J. Sewjnowski, "Storing covariance with nonlinearity interacting neurons," *J. Math. Biol.*, vol. 4, no. 4, pp. 303–321, Oct. 1977.
[67] B. Widrow and S. D. Stearns, *Adaptive Signal Processing*. Englewood Cliffs, NJ: Prentice-Hall, 1985.

[68] J. G. Keating and W. T. Thach, "Nonclock behavior of inferior olive neurons. Interspike interval of Purkinje cell complex spike discharge in the awake behaving monkey is random," *J. Neurophysiol.*, vol. 73, no. 4, pp. 1329–1340, Apr. 1995.
[69] A. Linares-Barranco, M. Oster, D. Cascado, G. Jiménez, A. Civit, and B. Linares-Barranco, "Inter-spike-intervals analysis of AER Poisson-like generator hardware," *Neurocomputing*, vol. 70, no. 16–18, pp. 2692–2700, Oct. 2007.
[70] J. Spoelstra, N. Schweighofer, and M. A. Arbib, "Cerebellar learning of accurate predictive control for fast-reaching movements," *Biol. Cybern.*, vol. 82, no. 4, pp. 321–333, Apr. 2000.
[71] J. L. Contreras-Vidal, S. Grossberg, and D. Bullock, "A neural model of cerebellar learning for arm movement control: Cortico-spino-cerebellar dynamics," *Learn. Memory*, vol. 3, no. 6, pp. 475–502, Mar./Apr. 1997.
[72] D. Purves, G. J. Augustine, and D. Fitzpatrick, *Neuroscience*, 2nd ed. Sunderland, MA: Sinaver Associates Inc., 2001.
[73] C. J. Willmott and K. Matsuura, "Advantages of the mean absolute error (MAE) over the root mean square error (RMSE) in assessing average model performance," *Clim. Res.*, vol. 30, no. 1, pp. 79–82, Dec. 2005.
[74] M. Kawato and D. M. Wolpert, "Internal models for motor control," in *Proc. Novartis Found. Symp.*, 1998, vol. 218, pp. 291–307.

Niceto Rafael Luque received the B.S. degree in electronics engineering and the M.S. degree in automation and industrial electronics from the University of Córdoba, Córdoba, Spain, in 2003 and 2006, respectively, and the M.S. degree in computer architecture and networks from the University of Granada, Granada, Spain, in 2007.

He is currently participating in an EU project related to adaptive learning mechanisms and bio-inspired control. His main research interests include biologically processing control schemes, lightweight robot, and spiking neural networks.

Jesús Alberto Garrido received the M.S. degree in computer science and the M.S. degree in computer architecture and networks from the University of Granada, Granada, Spain, in 2006 and 2007, respectively.

He is currently participating in an EU project related to adaptive learning mechanisms and bio-inspired control. His main research interests include biologically processing control schemes, lightweight robots, and spiking neurons.

Richard Rafael Carrillo received the Ph.D. degree in computer and electronics engineering from the University of Cagliari, Cagliari, Italy, in 2008, and in computer science from the University of Granada, Granada, Spain, in 2009.

He is currently a Researcher in the Department of Computer Architecture and Electronics, University of Almeria, Almeria, Spain. He is interested in efficient implementations for the simulation of spiking neural networks and models of neural circuits which could be used in engineering (e.g., robot control).

Olivier J.-M. D. Coenen received the Ph.D. degree jointly from the Department of Physics, Physics/Biophysics Program, University of California at San Diego (UCSD), La Jolla, and Computational Neurobiology Laboratory, Howard Hughes Medical Institute, The Salk Institute for Biological Studies, La Jolla, CA, in 1998.

His research interests include developing theories and models of neural networks.

Eduardo Ros received the Ph.D. degree from the University of Granada, Granada, Spain, in 1997.

He is currently Full Professor in the Department of Computer Architecture and Technology, University of Granada, where he is currently the responsible Researcher of two European projects related to bio-inspired processing schemes. His research interests include simulation of biologically plausible processing schemes, hardware implementation of digital circuits for real-time processing in embedded systems, and high-performance computer vision.

This article has been accepted for inclusion in a future issue of this journal. Content is final as presented, with the exception of pagination.

Brief Papers

Cerebellar Input Configuration Toward Object Model Abstraction in Manipulation Tasks

Niceto R. Luque, Jesus A. Garrido, Richard R. Carrillo, Olivier J.-M.D. Coenen and Eduardo Ros

***Abstract*— It is widely assumed that the cerebellum is one of the main nervous centers involved in correcting and refining planned movement and accounting for disturbances occurring during movement, for instance, due to the manipulation of objects which affect the kinematics and dynamics of the *robot-arm plant model*. In this brief, we evaluate a way in which a cerebellar-like structure can store a model in the granular and molecular layers. Furthermore, we study how its microstructure and input representations (context labels and sensorimotor signals) can efficiently support model abstraction toward delivering accurate corrective torque values for increasing precision during different-object manipulation. We also describe how the explicit (object-related input labels) and implicit state input representations (sensorimotor signals) complement each other to better handle different models and allow interpolation between two already stored models. This facilitates accurate corrections during manipulations of new objects taking advantage of already stored models.**

***Index Terms*— Adaptive, biological control system, cerebellum architecture, learning, robot, spiking neuron.**

I. Introduction

In the framework of a control task, many successful approaches which use different kinds of "learning" (adaptation mechanisms) in the control loop have been developed: reinforcement learning [1], where systems can learn to optimize their behavior making use of rewards and punishments, genetic algorithms [2], where control systems are evolved over many generations mimicking the process of natural evolution, recurrent artificial neural networks [3], and also, recently approaches based on biologically realistic spiking neural networks (SNNs) [4], [5]. Most of the works focused on SNNs addressing issues such as computational complexity and real-time feasibility [6], biologically plausible models of different complexity [7], effects of biological learning rules [8], etc. This brief represents a multidisciplinary research effort in which SNNs adopting a cerebellar-like neural topology are used with biologically plausible neural models. We evaluate how the topology of a biological neuronal circuit is specifically related with its potential functionality, starting from electrophysiological recordings (validating the cell models) to a proposed biologically plausible spiking control solution.

More concretely, in this brief, we describe how a SNN mimicking a cerebellar micro-structure allows an internal corrective model abstraction. By adopting a cerebellar-like network, we explore how different sensor representations can be efficiently used for a corrective model abstraction corresponding to different manipulated objects. When a new object is manipulated and the system detects that significant trajectory errors are being obtained, the abstracted internal model adapts itself to match the new model (kinematic and dynamic modifications of a base arm plant model). The stored models to be used can be selected by explicit object-related input signals (as specific input patterns generated for instance from the visual sensory pathway) or implicit signals (such as a haptic feedback). This can be seen as a "cognitive engine" that abstracts the inherent object features through perception-action loops and relates them with other incidental properties, such as color, shape, etc. The cognition process that relates both properties is important because it allows the inference of inherent properties just by activating explicit perceived primitives making possible to build up models of the environment that describe how it will "react" when interacting with it.

In the framework of a robot control task, manipulating objects that significantly affect the base kinematic and dynamic model with bio-inspired schemes is an open issue [5], [9], [10]. Biology seems to have developed (evolved) a scalable control system capable of abstracting new models in an incremental way in real time. This requires a smart model abstraction engine which is believed to be largely based on the cerebellum [11]. State-of-the-art simulation tools [12] and also hardware platforms [13], [14] allow cell-based simulation of nervous centers of certain complexity in the framework of biologically relevant tasks. This allows addressing studies in which the function and structure of nervous centers are conjointly evaluated to better understand how the system operation is based on cell and network properties.

The working hypothesis and methodology of this brief can be briefly described as follows:

1) we address a biologically relevant task which consists in an accurate manipulation of objects which affect a base (kinematic and dynamic) model of the base plant using low power actuators;

Manuscript received May 10, 2011; revised May 11, 2011; accepted May 11, 2011. This work was supported in part by the European Union Sensorimotor Structuring of Perception and Action for emergent Cognition Project, under Grant IST 028056 and the national projects, MULTIVISION under Project TIC-3873 and ITREBA Project TIC-5060.

N. R. Luque, J. A. Garrido, and E. Ros are with the Department of Computer Architecture and Technology, University of Granada, Granada 18071, Spain (e-mail: nluque@atc.ugr.es; jgarrido@atc.ugr.es; eduardo@atc.ugr.es).

R. R. Carrillo is with the Department of Computer Architecture and Electronics, University of Almeria, Almeria 4120, Spain (e-mail: rcarrillo@atc.ugr.es).

O. J.-M. D. Coenen is with the Intelligent Systems Research Center, University of Ulster, Londonderry, Ireland (e-mail: olivier@oliviercoenen.com).

Color versions of one or more of the figures in this paper are available online at http://ieeexplore.ieee.org.

Digital Object Identifier 10.1109/TNN.2011.2156809

1045–9227/$26.00 © 2011 IEEE

This article has been accepted for inclusion in a future issue of this journal. Content is final as presented, with the exception of pagination.

2) we define and implement a spiking-neuron-based cerebellum model to evaluate how different properties of the cerebellar model affect the functional performance of the system.

II. Material and Methods

A. Experimental Setup. Interfacing the Cerebellum Model with a Robot

1) Robot Plant: For the robot plant simulation, we have implemented an interface between the simulator of the light-weight-robot (LWR) developed at DLR [15] and the control loop including the cerebellum module. The LWR robot is a 7-DOF arm composed of revolute joints. For the sake of simplicity, in our experiments, we used the first (we will refer to it as q_1), third (q_2) and fifth joints (q_3), keeping the other ones fixed, limiting the number of degrees of freedom.

2) Training Trajectory: The described cerebellar model has been tested on a task of smooth pursuit, in a similar way to the one adopted by other authors [16]: a target moves along a repeated trajectory, which is a composition of sinusoidal components (this represents the desired trajectory). In previous works, we evaluated a simpler cerebellar model in a target-reaching task [5], [10] and a simple smooth pursuit task. After these preliminary works, in this brief, we study context switching capability, generalization-interpolation capability, and different input sensorimotor representations.

We use an 8-like trajectory defined by in (1). The trajectories of the individual joints have enough variation so that a sufficiently rich movement is executed allowing dynamic robot arm features to be revealed [17]. A multi-joint movement is more complex from a mechanical standpoint than a summed combination of single-jointed movements. This is due to the interaction torque values generated by one linkage moving on another. In this framework, the cerebellum role on the control task becomes more complex

$$q1 = A\sin\pi t,\ q2 = A\sin(\pi t+\theta),\ q3 = A\sin(\pi t+2\theta). \tag{1}$$

3) Control Loop: It is largely assumed that the cerebellum plays a major role in motor control [18]–[20]. Based on this hypothesis, a wide range of cerebellar motor-control-system approaches have been proposed in the literature (for a review, the reader is referred to [21]). The central nervous system (CNS) executes three relevant tasks. The desired trajectory computation in visual coordinates, the task-space coordinate translation into body coordinates, and finally, the motor command generation. As in [22], in this brief, we have adopted the feedback-error learning (FEL) scheme in order to deal with variations in the dynamics of the robot-arm [22] in connection with a crude inverse dynamic model. But in contrast with the adaptation modules used by Miller *et al.* [20], we use a biologically plausible neural model as described in the next section. Using FEL, the association cortex supplies the motor cortex with the desired trajectory in body coordinates, where the motor command is generated using an inverse dynamic arm model.

Kawato *et al.* [22] relate different components of the control scheme with the biological counterpart. As described in [22], the spinocerebellum-magnocellular red nucleus system provides an accurate internal neural model of the dynamics of the musculoskeletal system which is learned by sensing the result of the movement. The cerebrocerebellum-parvocellular red nucleus system provides a crude internal neural model of the inverse-dynamics of the musculoskeletal system which is acquired while monitoring the desired trajectory.

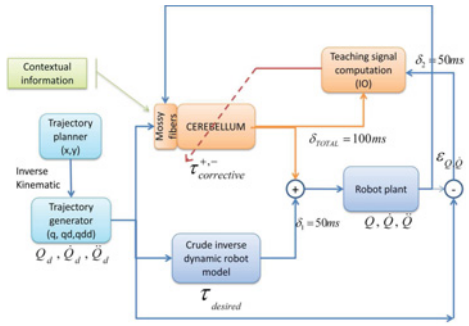

Fig. 1. Control loop.

The crude inverse dynamic model and the dynamical model work together by means of updating the motor command and predicting possible errors in the movement. As illustrated in Fig. 1, the cerebellar pathways are structured in a feedforward architecture, in which only information about sensory consequences of incorrect commands is obtained (i.e., the difference between actual and desired joint positions of the arm). We developed our cerebellar-based control loop according to this model as illustrated in Fig. 1.

We have also built a module to translate a small set of analog signals into a sparse cell-based spike-timing representation (spatio-temporal population coding). They encode the arm's desired and actual states (position and velocity) as well as contextual information. This module has been implemented using a set of mossy fibers (MFs) with specific receptive fields covering the working range of the different state variables.

B. Cerebellum Model

For extensive spiking network simulations, we have further developed and used an advanced event-driven simulator based on lookup Tables EDLUT [23]. EDLUT is an open-source tool [5] which accelerates the simulation of SNNs by compiling the dynamic response of pre-defined cell models into lookup tables before the actual network simulation. The proposed cerebellar architecture (Fig. 2) consists of the following layers:

1) MFs: MFs carry both contextual information and sensory joint information. A MF is modeled by a leaky I & F neuron, whose input current is calculated using overlapping radial basis functions as receptive fields in the value space of the input signals.

2) Granular Layer (1500 Cells): This layer represents a simplified cerebellar granular layer. The information given by MFs is transformed into a sparse representation in the granule layer [24]. Each granular cell (GR) has four excitatory input connections: three of them from randomly chosen joint-related MF groups and another one from a context-related MF. Parallel fibers (PFs) are the output of this layer.

This article has been accepted for inclusion in a future issue of this journal. Content is final as presented, with the exception of pagination.

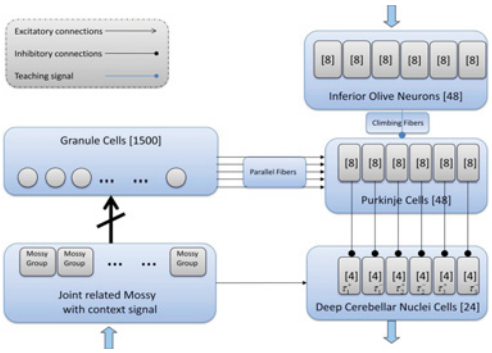

Fig. 2. Cerebellum configuration inputs encoding the movement (desired arm states, actual sensorimotor signals and context-related signals) are sent (upward arrow) through the PFs. Error-related inputs are sent (upper downward arrow) through the CFs. Outputs are provided by the DCN cells (lower downward arrow).

3) Climbing Fibers (CFs) (48 CFs): This layer is composed of six groups of eight *CF*s each. It carries the IO output which encodes teaching spike trains (related to the error) for the supervised learning in the PF–PC connections.

4) Purkinje Cells (PC) (48 Cells): They are divided into six groups of eight cells. Each GR is connected to 80% of the PCs. Each PC receives a single teaching signal from a CF. PF–PC synaptic conductances are modified by the learning mechanism during the training process.

5) Deep Cerebellar Nuclei Cells (DCN) (24 Cells): The cerebellum model output is generated by six groups of these cells. The corrective torque value of each joint is encoded by a couple of these groups, one group is dedicated to compensate positive errors (agonist) and the other one is dedicated to compensate negative errors (antagonist). Each neuron group in the DCN receives excitation from every MF cell and inhibition from the two corresponding PCs. In this way, the subcircuit PC–DCN–IO is organized in six microzones, three of them for joint positive corrections (one per joint) and the other three of them for joint negative corrections (one per joint). The DCN outputs are added as corrective activity in the control loop.

The MFs encode input representation in a rather specific way and the granular cells integrate information from different MFs. These characteristics partially embed functional roles of the inhibitory loop driven by the Golgi cells. Therefore, although Golgi cells have not been explicitly included, part of their functional roles has been integrated into the system.

C. Learning Process

It is well known that the cerebellum not only learns sequences of pre-defined voluntary movements but also adapts itself to external influences. This behavior seems to be very difficult to analyze, but the cerebellum presents a regular structured architecture that facilitates the study of how learning may take place in our context-driven scenario using this topology.

Although there seems to be an adaptation process at many sites within the cerebellar structure [25], the main synaptic adaptation driven by teaching or temporal signals (from the IO) seems to take place at the PF–PC synapses. We have adopted a plasticity mechanism that drives the modification of the PF–PC synapses in the cerebellar model, based on the concept of "eligibility trace" [16]. This trace aims to relate spikes from IO error-related activity and the previous activity of the PF that is supposed to have generated this error signal. The eligibility trace idea stems from experimental evidence showing that a spike in the CF afferent to a PC is more likely to depress a PF–PC synapse if the corresponding PF has been firing between 50 and 200 ms before the CF spike arrives at the PC [16], [26]. This is indicated in (3) [5] where the integration kernel $k(t)$ is defined in (2). A marginal peak occurs in the learning rule (around 450 ms after spike arrival) due to the event-driven simulation scheme (mathematical expression based on exponential functions modulating a periodic kernel, this presents a little hump), its impact in the global learning amount is negligible (4%) and can be considered as non-specific noise. In comparison with the previous learning schemes [5], [10] in similar cerebellum structures, this one allows to shift the maximum peak independently from the peak width. Therefore, we can tune the control loops to different sensorimotor delays and can narrow the maximum peak to allow more specific learning.

We have used a simplified spiking cerebellar neural network with spike-timing dependent plasticity (STDP). This plasticity has been implemented including long-term depression (LTD) and long-term potentiation (LTP) mechanisms in the following.

1) LTD produces a synaptic efficacy decrease when a spike from the IO reaches a PC. The IO output activity is interpreted as an error signal [18], [21], triggering a weight depression mechanism in synapses (PF–PC connections) depending on the received activity from the PFs. To calculate this amount of decrease, this previous activity is convolved with an integral kernel as defined by (2). Different expressions can be used for the learning rule [8]. This kernel mainly takes into account all the PF spikes which arrived 100 ms before the IO spike to overcome the effect of transmission delays of this range on sensory and motor signals (see Fig. 1). After this mechanism is repetitively activated, when the same pattern of PFs appears, the PC will not fire, in such a way, they will not inhibit its corresponding DCN cells [16], [27].
2) LTP produces a fixed increase in synaptic efficacy each time a spike arrives through a PF at the corresponding PC as defined by (2). For the sake of synaptic conductance equilibrium, LTD is accompanied by the opposite process (LTP), which takes place at this same synaptic site [28].

$$\begin{aligned} LTD: \forall i, \Delta w_i &= -\int_{-\infty}^{IOspiketime} k\left(t - t_{IOspike}\right) \\ LTP: \Delta w_i &= \alpha \end{aligned} \tag{2}$$

$$k(t) = e^{-(t-tpost\,synaptic\,spike)} \times \sin\left(t - t_{post\,synaptic\,spike}\right)^{20}. \tag{3}$$

These two learning rule components need to be tuned complementing each other to be able to efficiently reduce

This article has been accepted for inclusion in a future issue of this journal. Content is final as presented, with the exception of pagination.

action errors in the framework of a control task. In biological systems, sensors (for instance, skin sensors and proprioceptors) are not directly connected to the cerebellum. They pass through the cuneate nucleus [29] and other centers along the sensory pathway where signals seem to be efficiently organized to better address the cerebellar processing engine. In this brief, we investigate how the cerebellum model can take advantage of different cerebellar input representations during object manipulation.

D. Mossy Layer Configuration in the Cerebellar Model

Different mossy layer configuration models have been proposed in order to improve the cerebellum storage capability.

1) *Base "Desired-proprioceptive configuration."* It consists of 120 joint-related fibers, the MF layer has been divided into six groups of 20 fibers, three groups of fibers encoding joint positions (one group per joint) and the other three, encoding joint velocities.
2) Encoding Approach (EC) model. *Explicit Context* EC (16 context-related fibers plus 120 joint-related fibers): This mossy layer configuration uses the base desired-proprioceptive configuration adding 16 context-related fibers. The contextual information is coded by two groups of eight fibers. An external signal (related to the "label or any captured property" of the object, for instance assuming information captured through visual sensory system) feeds these dedicated-eight-grouped fibers.
3) IC model. *Implicit Context* EC (240 joint-related fibers): The MF layer consists of 12 groups of 20 fibers and delivers the actual and desired joint velocity and position information. It uses the base-desired proprioceptive configuration and adds three groups of fibers encoding actual joint positions and other three groups encoding actual joint velocities. The implicit contextual information is conveyed using these six groups of fibers. The actual position and velocity "helps" the cerebellum to recognize where and how far from the ideal (desired) situation it is. These deviations implicitly encode a "context-like" representation based on sensorimotor complexes.
4) EC & IC. *Explicit and Implicit Context* encoding approach (16 context-related fibers plus 240 joint-related fibers): It uses the base desired proprioceptive and incorporates also IC and EC architectural specifications. Thus, this MF layer is a combination of the EC and IC models described above.

The main aim of searching a proper mossy layer configuration is to exploit the capability of the granule layer for generating a sequence of active neuron populations without recurrence. This sequence is able to efficiently represent the passage of time (representation of different time passages are related with different input signals). Our system takes advantage of this spatiotemporal discrimination of input signals for learning different contexts.

As indicated in Section II-B, afferent MFs are randomly connected to granule cells, on average, four MFs [30] per

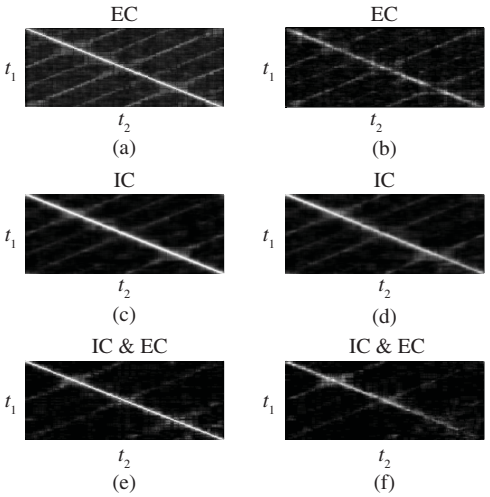

Fig. 3. Similarity indices for a spatiotemporal activity between two activity patterns using EC, IC, and IC & EC configurations. The values of indices are represented in gray scale; black 0, white 1. (a), (c), (e) Left side panels show a white diagonal band indicating a proper generation of a time-varying granular activity population. EC presents a mean gray value of 0.18, IC leads to a mean gray level of 0.101, and IC & EC leads to a mean gray value of 0.074. (b), (d), (f) Right side panels show similarity indices for two contexts. The darker the matrix is, the better uncorrelated activity patterns are. EC presents a mean gray value of 0.024, IC leads to a mean gray value of 0.096, and IC & EC achieves 0.044.

granule cell. When an input signal pattern arrives at the MFs, a spatiotemporal activity pattern is generated and the population of active neurons in the granule layer changes in time according to this received input. In order to evaluate the non-recurrence in this activation train, the following correlation function (4) is used [31]:

$$C(t_1, t_2) = \frac{\sum_i f_i(t_1) f_i(t_2)}{\sqrt{\sum_i f_i^2(t_1)} \sqrt{\sum_i f_i^2(t_2)}} \tag{4}$$

where f_i corresponds to the instantaneous frequency of the n_i neuron (frequency measured within a 20-ms time window). The numerator calculates the inner product of the population vector of active neurons at times t_1 and t_2, and the denominator normalizes the vector length. $C(t_1, t_2)$ takes values from 0 to 1, 0 if two vectors are complementary, 1 if two vectors are identical. To facilitate the production of accurate corrective terms, different input signals shall generate different spatiotemporal activity patterns. The following correlation function is used to evaluate this point as indicated in (5):

$$C(t_1, t_2) = \frac{\sum_i f_i^{(1)}(t_1) f_i^{(2)}(t_2)}{\sqrt{\sum_i f_i^{(1)2}(t_1)} \sqrt{\sum_i f_i^{(2)2}(t_2)}} \tag{5}$$

where $f_i^{(1)}$ and $f_i^{(2)}$ denote the activities of the n_i neuron at time t under different input signals (1 and 2, respectively).

The left panels in Fig. 3(a), (c) and (e) shows the similarity index using a $t_1 \times t_2$ matrix within the active granular population at t_1 and t_2. A wide white band, surrounding the main diagonal, points out that the index decreases monotonically

This article has been accepted for inclusion in a future issue of this journal. Content is final as presented, with the exception of pagination.

as the distance [t_1–t_2] increases. That means a one-to-one correspondence between the active neuron population and time. This implies that a dynamically active neuron activity changing can represent the passage of time.

The right panels in Fig. 3(b), (d) and (f) show how different input signals can be discriminated by different activity patterns. The values of the similarity index are small suggesting that the two represented activity patterns are independent of the other one. Actual and desired entries of the IC configuration vary during time leading to a richer codification within a single context, while EC only uses desired entries varying along the trajectory execution. On the other hand EC gives a better granular activity codification between contexts by using its specific contextual signals. IC has no specific entries helping to distinguish activity patterns when using two different contexts. IC & EC takes advantages from both configurations, it uses the context and the position/velocity entries to produce a better time-varying granular activity population.

E. Experimental Methods

We have carried out several experiments to evaluate the capability of cerebellar architecture to select and abstract models using different cerebellar topologies. In these experiments, objects which significantly affect the dynamics and kinematics of the base plant model have been manipulated to evaluate the performance of different cerebellar configurations. Finally, we have also studied how interpolation/generalization can be naturally done for different plant + object models which have not been used during the training process. We divided the experiments into the following groups.

1) Cerebellar input configuration including only context-related signals (and desired arm states) (EC).
2) Cerebellar input configuration including only sensorimotor representation (IC) (i.e., desired and actual arm states).
3) Cerebellar input configuration including conjointly sensorimotor and context-related signals (IC & EC).

For this purpose, we have used a set of benchmark trajectories that we repeat in each iteration and evaluate how learning adapts the GR-PC weights to tune accurate corrective actions in the control loop (Fig. 1).

F. Quantitative Performance Evaluation

The learning process performance is characterized by using three estimates calculated from the mean absolute error (MAE) curve. The accuracy gain estimates the error reduction rate comparing the accuracy before and after learning. This estimate helps to interpret the adaptation capability of the cerebellum when manipulating different objects, provided that the initial error is different

$$Accuracy\ Gain = MAE_{initial} - \left[\frac{1}{n}\sum_{i=0}^{n} MAE_{(final-i)}\right]; \quad n = 30. \qquad (6)$$

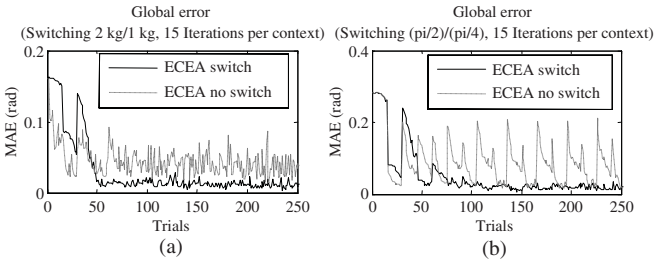

Fig. 4. Multi-context simulation with changes in dynamics and kinematics using EC cerebellar input. Each sample represents the MAE evolution (sum of error at different joints) for a trajectory execution (trial) during learning with no context-related signals and with explicit context-related signals. (a) Manipulating two different loads with and without context signals. Explicit context signals reduce 68.31% the final average error and 70.73% the final standard deviation. (b) Equivalent end-segment of the arm has been rotated in certain angles $\pi/2$ and $\pi/4$. The corrective torque values should compensate these different deviations in each context (with and without activated context signals). Explicit context switching signals reduce 62.04% the final average error and 26% the final standard deviation.

The final error (average error over the last 30 trials)

$$Final\ Error = \left[\frac{1}{n}\sum_{i=0}^{n} MAE_{(final-i)}\right]; \quad n = 30. \qquad (7)$$

The final error stability (standard deviation over the last 30 movement trials)

$$Final\ Error\ Stability = \left[\frac{1}{n}\sum_{i=0}^{n} \sigma\left(MAE_{(final-i)}\right)\right]; \quad n = 30. \qquad (8)$$

III. Experimental Results

A. EC Cerebellar Input

The explicit context EC uses a set of MFs to explicitly identify the context, assuming that they carry information provided by other areas of the CNS (such as vision which helps to identify the correct model to be used) or even cognitive signals. Therefore, a specific group of context-based MFs become active when the corresponding context is present. In this way, when a certain context becomes active, a GR population is pre-sensitized due to the specific context-related signals. We have randomly combined the sensor signals (desired position and velocity) of the different joints and the context-related signals (in the MF to GR connections) allowing granule cells to receive inputs from different randomly selected MFs (at the network-topology definition stage). In order to explicitly evaluate the capability of these signals to separate neural populations for different object models, each granule cell has four synaptic input connections: three random MF entries which deliver joint-related information and one MF which delivers context-related signals. In this case, we have evaluated the capability of the cerebellum model to efficiently use these context-related signals to learn to separate models when manipulating objects of different weights or different kinematics (deformation in the robot-plant end-segment) (Fig. 4).

This article has been accepted for inclusion in a future issue of this journal. Content is final as presented, with the exception of pagination.

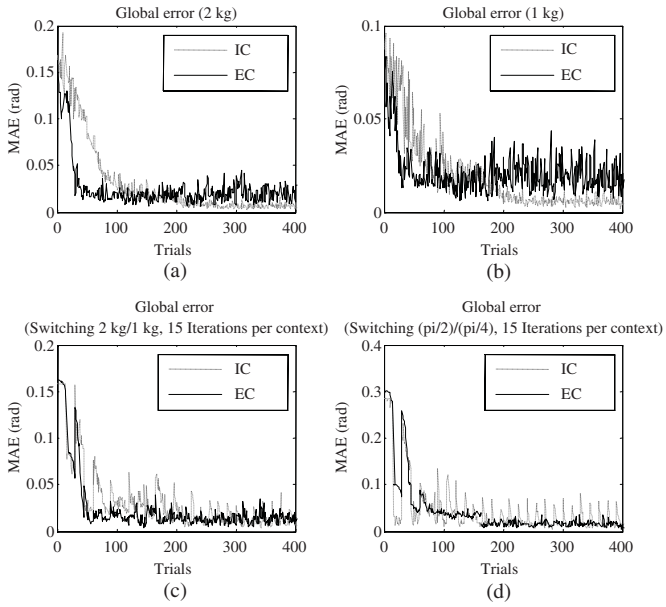

Fig. 5. Single-context simulation using EC and IC cerebellar input and multi-context simulation with changes in kinematics and dynamics using IC cerebellar input. (a) and (b) Manipulation of objects of different loads (2 kg/1 kg) without context signals. Each sample represents the MAE for a trajectory execution (trial). (c) MAE evolution during the learning process in EC and IC with dynamics-changing contexts. Two contexts with different loads are manipulated, switching every 15 trials. (d) MAE evolution for EC and IC configurations and two contexts with different ending deformation (kinematics change), switching every 15 trials.

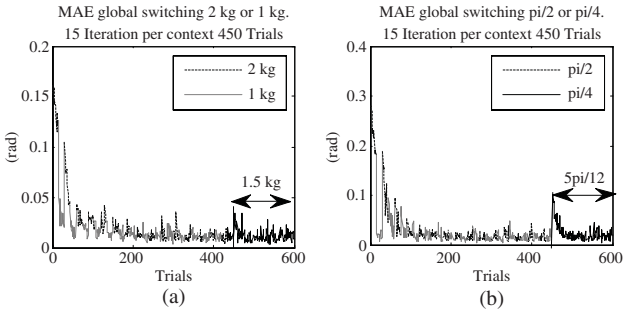

Fig. 6. Multi-context simulation with changes in kinematics and dynamics using IC cerebellar input. Interpolation capability. (a) After 450 trials of 15 iterations per context (2 kg/1 kg added alternatively to the robot arm), a new 1.5 kg context is presented to the cerebellum. (b) After 450 trials of 15 iterations per context (the end-segment of the robot arm includes different rotations: $\pi/2$ and $\pi/4$ angles alternatively), a new $5\pi/12$ context is presented to the cerebellum.

B. IC Cerebellar Input

In this section, we define an implicit context encoding approach (IC), where no context-identifying signals are used. The sensor signals (actual position and velocity of the robot) implicitly encode (through MFs) the context during object manipulation. We have randomly combined the sensor signals (position and velocity) of the different joints (in the MF to GR connections) allowing granule cells to receive four inputs from different randomly selected MFs. The context models are distributed along cell populations. These cell populations are dynamically changing during the learning process (because the actual trajectory changes as corrective torque values are learned and integrated). Each time a new context is activated, the specific neural population is tuned due to the slightly different sensorimotor signals during the trajectory execution. The context switching in IC is done automatically and learning is carried out in a non-destructive manner, learned contexts are not destroyed (Fig. 5).The fact that IC transitions do not need explicit contextual information may indicate that this configuration allows interpolation between different learned contexts. This capability is explored by making the cerebellum learn two contexts alternately and then, presenting a new intermediate context (Fig. 6).

As shown in Fig. 5, although EC has a faster convergence speed, IC presents a lower final error (0.007 rad. average final error in IC against 0.018 rad. in EC) and a more stable behavior (0.002 rad. of standard deviation in IC against 0.006 rad. of standard deviation in EC) after the learning process.

Accuracy gain, final error average and final standard deviation are similar in IC and EC. EC develops a better inter-context transition. Comparing EC with IC in a dynamic context switching experiment, we obtain context switching error discontinuities 47.6% larger and a standard deviation 24.7% higher in the EC explicitly canceling context switching signals than in the IC configuration [Figs. 4(a) versus 5(c)]. This highlights the importance of actual sensorimotor signals efficiently used in the IC configuration, compared to EC which only used desired states during manipulation.

Finally, comparing EC with IC in a kinematic context switching experiment, we obtain context switching error discontinuities 32.85% larger and a final standard deviation 16.71% higher in the EC without activating context switching signals than in the IC configuration [Figs. 4(b) versus 5(d) explicit context signals are efficiently used in EC configuration].

C. IC Plus EC Cerebellar Input

In this section, we evaluate how the previous EC and IC input representations are complementary. In this case, the cerebellar architecture includes both inputs. The MFs arriving in the cerebellum encode the desired states, the actual states (positions and velocities), and also, context signals which identify the current contexts.

In Fig. 7(c) IC & EC uses the pre-learned synaptic weights obtained in previous contexts to deal with a new payload. Nevertheless, sensorimotor state signals feeding MFs drive fast to a new contextual adaptation. The kinematics interpolation is not efficient [Fig. 7(d)], interpolation across kinematics changes is not an easy task (not linear).

IC & EC configuration also becomes robust against incongruent external context-related signals (for instance, extracted from vision). As shown in Fig. 7(e), during each epoch, the external context signal changes do not match the actual object switching (i.e., the external context signal does not remain constant while manipulating a 2 kg object and it does not do it either when using a 1 kg object). Thus, *context* 1 value in the first 2 kg-415-trial-context equals A and *context* 2 value in the first 1 kg-15-trial-contexts equals B.

This article has been accepted for inclusion in a future issue of this journal. Content is final as presented, with the exception of pagination.

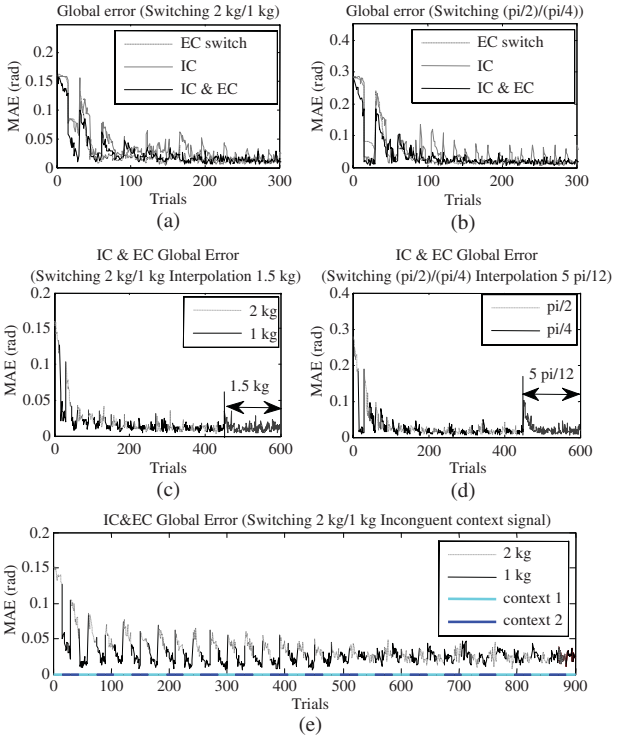

Fig. 7. Multi-context simulation with changes in kinematics and dynamics using EC, IC, and IC & EC cerebellar input. Interpolation of a new context and robustness against incongruent contextual input signals. (a) Dynamics correction task with different loads in the robot arm. (b) Kinematics correction task with different deviations in the end-segment of the robot arm. (c) 1.5 kg load is fixed to the end-segment of the robot. (d) $5\pi/12$ rotation in the end-segment of the robot is presented. (e) IC & EC configuration is able to avoid non-congruent contextual signals. Context-related input signals are indicated with highlighted colors in the x-axis of the plot.

In the following 15-trial-context switching trials, values A and B are interchanged. The incoming external contextual information is not congruent but, thanks to sensorimotor state signals (actual position and velocity of IC configuration), the cerebellum is able to deal with these "misleading" external signals.

IV. Conclusion

We have proposed a new simple biologically plausible cerebellar module which can abstract models of manipulated objects that significantly affect the initial dynamics and also kinematics of the plant (arm + object), providing corrective torque values toward more accurate movements. The results are obtained from object manipulation experiments. This new cerebellar approach, with two representations, receiving context-related inputs (EC) and actual sensory robot signals (IC) encoding the context during the experiments, has been studied. The IC & EC cerebellar configuration takes advantage of both configurations which complement each other. Smoother inter-context transitions are achieved at a fast convergence speed. It allows the interpolation of new contexts (different loads under manipulation) based on previously acquired models. Moreover, a good learning curve profile in long-term epochs can be achieved and finally, the capability of "overcoming" misleading external contextual information, making this cerebellar configuration robust against incongruent representations (Fig. 7), is remarkable. Furthermore, the results obtained with this kind of cerebellar architecture are coherent with the experiments [32], [33]. Therefore, when both representations congruently encode the context, they shall complement each other, while when they are incongruent, they interfere with each other. This is so because in the implemented cerebellar architecture, context classification and model abstraction tasks are carried out in a distributed manner. No pre-classification process is executed to disambiguate incongruent context identification. In our approach, we have also evaluated how sensorimotor representation can overcome incongruent incidental context-related signals (i.e., sensorimotor representation dominating a context-related incongruent signal).

In a classical machine learning approach, disambiguation is usually explicitly done through a classification module (decision making) that can be tuned to adopt a winner-takes-all strategy and leads to a single context model to be recalled even in this incongruent context representation. In biological systems, this kind of pre-classification (disambiguation) mechanisms may be processed in other nervous centers, although it may reduce the interpolation and generalization capabilities of the cerebellar model presented.

References

[1] A. G. Barto and M. Sridhar, "Recent advances in hierarchical reinforcement learning," *Discr. Event Dyn. Syst.*, vol. 13, no. 4, pp. 341–79, 2003.

[2] D. A. Linkens and H. O. Nyongesa, "Learning systems in intelligent control: An appraisal of fuzzy, neural and genetic algorithm control applications," *IEEE Proc. Control Theory Appl.*, vol. 143, no. 4, pp. 367–386, Jul. 1996.

[3] K. J. Hunta, D. Sbarbaroa, R. Z. Bikowskia, and P. J. Gawthropa, "Neural networks for control systems—A survey," *Automatica*, vol. 28, no. 6, pp. 1083–112, Nov. 1992.

[4] S. Ghosh-Dastidar and H. Adeli, "Spiking neural networks," *Int. J. Neural Syst.*, vol. 19, no. 4, pp. 295–308, 2009.

[5] R. R. Carrillo, E. E. Ros, C. Boucheny, and O. Coenen, "A real-time spiking cerebellum model for learning robot control," *Biosystems*, vol. 94, nos. 1–2, pp. 18–27, Oct.–Nov. 2008.

[6] M. J. Pearson, A. G. Pipe, B. Mitchinson, K. Gurney, C. Melhuish, I. Gilhespy, and M. Nibouche, "Implementing spiking neural networks for real-time signal-processing and control applications: A model-validated FPGA approach," *IEEE Trans. Neural Netw.*, vol. 18, no. 5, pp. 1472–1487, Sep. 2007.

[7] E. M. Izhikevich, "Simple model of spiking neurons," *IEEE Trans. Neural Netw.*, vol. 14, no. 6, pp. 1569–1572, Nov. 2003.

[8] W. Gerstner and W. Kistler, *Spiking Neuron Models: Single Neurons, Populations, Plasticity*. Cambridge, U.K.: Cambridge Univ. Press, 2002.

[9] M. A. Arbib, G. Metta, and P. van der Smagt, "Neurorobotics: From vision to action," in *Handbook of Robotics*. New York: Springer-Verlag, 2008, ch. 62, pp. 1453–1475.

[10] C. Boucheny, R. R. Carrillo, E. Ros, and O. J.-M. D. Coenen, *Real-Time Spiking Neural Network: An Adaptive Cerebellar Model* (Lecture Notes in Computer Science), vol. 3512. New York: Springer-Verlag, 2005, pp. 136–144.

[11] D. M. Wolpert, R. C. Miall, and M. Kawato, "Internal models in the cerebellum," *Trends Cog. Sci.*, vol. 2, no. 9, pp. 338–347, Sep. 1998.

[12] R. Brette, M. Rudolph, T. Carnevale, M. Hines, D. Beeman, J. M. Bower, M. Diesmann, A. Morrison, P. H. Goodman, and F. C. Harris, "Simulation of networks of spiking neurons: A review of tools and strategies," *J. Comput. Neurosci.*, vol. 23, no. 3, pp. 349–398, 2007.

[13] E. Ros, E. M. Ortigosa, R. Agís, R. Carrillo, and M. Arnold, "Real-time computing platform for spiking neurons (RT-spike)," *IEEE Trans. Neural Netw.*, vol. 17, no. 4, pp. 1050–1063, Jul. 2006.

This article has been accepted for inclusion in a future issue of this journal. Content is final as presented, with the exception of pagination.

[14] M. J. Pearson, A. G. Pipe, B. Mitchinson, K. Gurney, C. Melhuish, I. Gilhespy, and M. Nibouche, "Implementing spiking neural networks for real-time signal-processing and control applications: A model-validated FPGA approach," *IEEE Trans. Neural Netw.*, vol. 18, no. 5, pp. 1472–1487, Sep. 2007.

[15] J. Butterfaß, M. Grebenstein, H. Liu, and G. Hirzinger, "DLR-hand II: Next generation of a dextrous robot hand," in *Proc. IEEE Int. Conf. Robot. Autom.*, vol. 1. 2001, pp. 109–114.

[16] R. E. Kettner, S. Mahamud, H.-C. Leung, N. Sitkoff, J. C. Houk, B. W. Peterson, and A. G. Barto, "Prediction of complex 2-D trajectories by a cerebellar model of smooth pursuit eye movement," *J. Neurophysiol.*, vol. 77, no. 4, pp. 2115–2130, Apr. 1997.

[17] H. Hoffmann, G. Petckos, S. Bitzer, and S. Vijayakumar, "Sensor-assisted adaptive motor control under continuously varying context," in *Proc. Int. Conf. Inf. Control, Autom. Robot.*, Angers, France, 2007, pp. 1–8.

[18] M. Ito, *The Cerebellum and Neural Control*. New York: Raven, 1984.

[19] E. Todorov, "Optimality principles in sensorimotor control (review)," *Nat. Neurosci.*, vol. 7, pp. 907–915, Aug. 2004.

[20] L. E. Miller, R. N. Holdefer, and J. C. Houk, "The role of the cerebellum in modulating voluntary limb movement commands," *Arch. Ital. Biol.*, vol. 140, no. 3, pp. 175–183, 2002.

[21] M. Ito, "Cerebellar circuitry as a neuronal machine," *Prog. Neurobiol.*, vol. 78, nos. 3–5, pp. 272–303, Feb.–Apr. 2006.

[22] M. Kawato, K. Furukawa, and R. Suzuki, "A hierarchical neural-network model for control and learning of voluntary movement," *Biol. Cybern.*, vol. 57, no. 3, pp. 169–185, 1987.

[23] E. Ros, R. Carrillo, E. M. Ortigosa, B. Barbour, and R. Agís, "Event-driven simulation scheme for spiking neural networks using lookup tables to characterize neuronal dynamics," *Neural Comput.*, vol. 18, no. 12, pp. 2959–2993, Dec. 2006.

[24] E. D'Angelo, T. Nieus, M. Bezzi, A. Arleo, and O. J.-M. D. Coenen, *Modeling Synaptic Transmission and Quantifying Information Transfer in the Granular Layer of the Cerebellum* (Lecture Notes in Computer Science), vol. 3512. Berlin, Germany: Springer-Verlag, 2005, pp. 107–113.

[25] C. D. Hansel, D. J. Linden, and E. D'Angelo, "Beyond parallel fiber LTD: The diversity of synaptic and non-synaptic plasticity in the cerebellum," *Nat. Neurosci.*, vol. 4, no. 5, pp. 467–475, May 2001.

[26] R. R. Llinás, "Inferior olive oscillation as the temporal basis for motricity and oscillatory reset as the basis for motor error correction," *Neuroscience*, vol. 162, no. 3, pp. 797–804, Sep. 2009.

[27] M. Ito, M. Sakurai, and P. Tongroach, "Climbing fibre induced depression of both mossy fibre responsiveness and glutamate sensitivity of cerebellar Purkinje cells," *J. Physiol.*, vol. 324, pp. 113–134, Jan. 1982.

[28] R. R. Carrillo, E. Ros, B. Barbour, C. Boucheny, and O. J.-M. D. Coenen, "Event-driven simulation of neural population synchronization facilitated by electrical coupling," *Biosystems*, vol. 87, nos. 2–3, pp. 275–280, Feb. 2007.

[29] P. E. Roland, "Sensory feedback to the cerebral cortex during voluntary movement in man," *Behav. Brain Sci.*, vol. 1, no. 1, pp. 129–171, 1978.

[30] E. Mugnaini, R. L. Atluri, and J. C. Houk, "Fine structure of granular layer in turtle cerebellum with emphasis on large glomeruli," *J. Neurophysiol.*, vol. 37, no. 1, pp. 1–29, Jan. 1974.

[31] T. Yamazaki and S. Tanaka, "The cerebellum as a liquid state machine," *Neural Netw.*, vol. 20, no. 3, pp. 290–297, Apr. 2007.

[32] A. F. Hamilton, D. W. Joyce, J. R. Flanagan, C. D. Frith, and D. M. Wolpert, "Kinematic cues in perceptual weight judgement and their origins in box lifting," *Physiol. Res.*, vol. 71, no. 1, pp. 13–21, 2007.

[33] A. A. Ahmed, D. M. Wolpert, and J. R. Flanagan, "Flexible representations of dynamics are used in object manipulation," *Current Biol.*, vol. 18, no. 10, pp. 763–768, May 2008.

International Journal of Neural Systems, Vol. 21, No. 5 (2011) 385–401
© World Scientific Publishing Company
DOI: 10.1142/S0129065711002900

World Scientific
www.worldscientific.com

ADAPTIVE CEREBELLAR SPIKING MODEL EMBEDDED IN THE CONTROL LOOP: CONTEXT SWITCHING AND ROBUSTNESS AGAINST NOISE

N. R. LUQUE[*,‡], J. A. GARRIDO[*,§], R. R. CARRILLO[†,¶], S. TOLU[*,‖] and E. ROS[*,**]

[*]*Department of Computer Architecture and Technology*
CITIC, University of Granada
Periodista Daniel Saucedo s/n, Granada, Spain

[†]*Department of Computer Architecture and Electronics*
University of Almería, Ctra. Sacramento s/n
La Cañada de San Urbano, Almería, Spain

[‡]*nluque@atc.ugr.es*
[§]*jgarrido@atc.ugr.es*
[¶]*rcarrillo@atc.ugr.es*
[‖]*stolu@atc.ugr.es*
[**]*eros@atc.ugr.es*

This work evaluates the capability of a spiking cerebellar model embedded in different loop architectures (recurrent, forward, and forward&recurrent) to control a robotic arm (three degrees of freedom) using a biologically-inspired approach. The implemented spiking network relies on synaptic plasticity (long-term potentiation and long-term depression) to adapt and cope with perturbations in the manipulation scenario: changes in dynamics and kinematics of the simulated robot. Furthermore, the effect of several degrees of noise in the cerebellar input pathway (mossy fibers) was assessed depending on the employed control architecture. The implemented cerebellar model managed to adapt in the three control architectures to different dynamics and kinematics providing corrective actions for more accurate movements. According to the obtained results, coupling both control architectures (forward&recurrent) provides benefits of the two of them and leads to a higher robustness against noise.

Keywords: Cerebellum; STDP; robot simulation; learning; biological control system; noise.

1. Introduction

The efficiency and complexity of animal movement suggest that the biological motor controller does not consider the articulated animal limbs as strings of independent linked bodies. The necessary force for coordinated animal movements, such as reaching and walking, is smartly and conjointly determined for each joint. Due to the nonlinear relationship between joint forces and limb movements and the need to satisfy certain constraints on a movement in different controlling scenarios, biology seems to use advanced controlling mechanisms of interest also to advanced robotics.

Although numerous details of cerebellar microcircuitry have been determined, the functional contribution of the cerebellum to the motor system function remains an open issue. The complexity and the sophistication of the primate motor control system are overwhelming. This motor control is highly multi-dimensional and non-linear, making its characterization troublesome.[1] However, the cerebellum is commonly supposed to be responsible for timing, fine-tuning, and coordinating the motor system.[2–4] It is fair to think that emulating the functionality of the cerebellar microcircuitry would allow the control of non-stiff-joint "robotic arms" properly driven

with relatively low-power actuators (as is the case of biological counterparts).[5] Very diverse models have been proposed and evaluated.[6–11] The cerebellum is usually divided into three parts. One region that is mainly associated with the vestibular system, another part related with the brainstem and spinal cord, and a third region, the cerebrocerebellum, that has extensive interconnections with the cerebral cortex and is likely to be involved in motor coordination.[12] However, this knowledge about the cerebellar cortex has not been used in robotics as successfully as in biology.

The control function of any individual region of the cerebellum relies both on its internal microcircuitry and on the way it is connected with other parts of the motor system.[13,14] These connections and their functionality still remain an open issue.[15]

The cerebellum is involved in a feedback loop for muscle control. When the cortex sends a message for motor movement to the lower motor neurons in the brain stem and to the spinal cord, it also sends a copy of this message to the cerebellum. This is transmitted from the pyramidal fibers in the cortex on the cortico-pontine-cerebellar tract to the cerebellum. Additionally, the cerebellum also receives information from muscle spindles, joints and tendons.[16] Therefore, the cerebellum receives motor commands and also, actual sensory signals. This allows the extraction of corrective models on the "manipulating arm" for accurate movements. Traditionally, when considering the control system, it is assumed that the efference copy of motor commands predicts the sensory consequences of actions, including the sensorimotor pathways delays (the spinal cord inverse model transforms the torques into muscle tension) and also allowing its integration with the sensory information related with the actual state.[17] The concept of internal feedback from an internal model of the arm (or body)[18–20] has been extensively accepted (known as the forward model and formed in the cerebellum via the cerebrocerebellar communication loop).

Furthermore, a wide range of cerebellar motor-control-system approaches has been developed. This is a very active research field (for a review, please, refer to Ref. 10).

By using a forward model combined with an inverse dynamics model, the efference copy of the motor command output from the inverse model can be used as an input for a forward model. A forward dynamics transformation is able to predict the dynamics of the muscles from the state of the system and therefore, can be used to compute a controller output.

On the other hand, it has been recently suggested that cerebellar microzones typically receive mossy fiber (MFs) inputs that are related to the outputs of those microzones.[21] This configuration leads to a rather modular scheme. This modularity seems to facilitate the potential role of the cerebellum in adding corrective signals on the sensory space rather than onto motor signals. There are biological evidences that suggest that motor cortex functionality is heterogeneous allowing both control possibilities (addition of corrective terms in both the sensory and motor space).[22] The cerebellum computing corrective terms in the sensory space have motivated some authors to suggest a different cerebellar control loop which is called recurrent model.[14,21]

This biologically inspired cerebellar architecture based on the cerebellar connectivity can deal with the so-called distal error problem. The natural error signal for learning motor commands is the difference between actual and correct commands ('motor error'). However, in autonomous systems, the correct command is typically unknown. Only information about the sensory consequences of incorrect commands is available, which leads to an error representation (based on sensory signals). This is related to the motor error; however, this relation may be complex. Therefore, sensory-based error estimations are called 'distal errors'. How to use this information to drive motor learning is the distal error (or motor error) problem.

These two cerebellar architectures have been proposed as biologically-inspired approaches. Thus, it is fair to think that both architectures may co-exist and work together in the cerebellum developing a complementary functionality (see Fig. 1). This is the main issue under study in this paper.

The configuration illustrated in Fig. 1 has remarkable analogies with the classical inner loop/outer loop control architecture (see Fig. 2).

The inner loop/outer loop architecture groups many classical robot-control strategies from the literature.[23,24] This separation of the inner loop and outer loop terms is important for several reasons; in

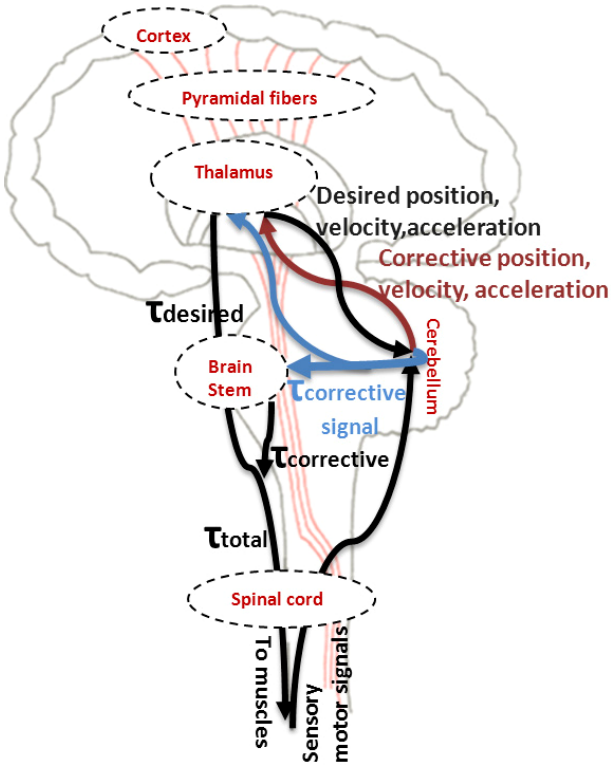

Fig. 1. Biological circuitry projection of the recurrent-forward control loops.

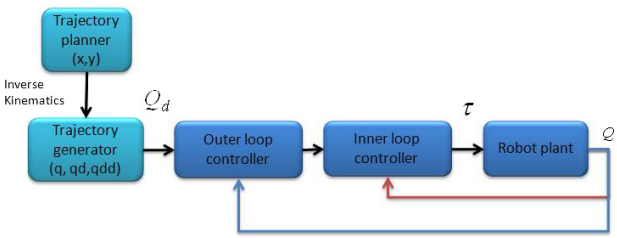

Fig. 2. Inner/outer control loop.

the inner loop, the calculation of the torque commands (non-linear terms) is computed to achieve a better precision and computation speed. Besides, the structure of the inner loop control remains fixed; what control designers may modify more freely to customize the control system architecture is mainly in the outer loop. Thus, the outer loop can be totally modified without restrictions to achieve several other goals without the need to modify the dedicated inner loop control. For instance, additional compensation terms may be included in the outer loop to enhance robustness to parametric uncertainty, unknown dynamics, and external disturbances or tracking of task space trajectories instead of joint space trajectories, regulating both motion and force. Drawing an analogy between the inner/outer control loop and the presented composed control architecture, the inner loop corresponds to the forward architecture that supplies the torque corrections and the outer control loop corresponds to the recurrent architecture that supplies the position/velocity corrections.

This paper studies how an adaptive spiking cerebellum-like module which includes long-term depression (LTD) and long-term potentiation (LTP) at parallel-fiber to Purkinje-cell synapses (PF-PC) is embedded in diverse control loops (forward, recurrent, and a combination of both architectures) to infer corrective models which compensate deviations in the robot trajectory when the dynamics and kinematics of the controlled robotic arm are altered and noise (related to the inherent noise of the muscle spindle signal) is introduced in the cerebellar input (MFs).[25,26] The main goal of this work is a comparative evaluation of these control architectures which shows how forward and recurrent architectures complement each other in the framework of a manipulation task and how robustly they behave in the presence of noise.

2. Methods

As was exposed in the *introduction section*, nowadays, biologically inspired neural processing is an open issue where spiking neural networks play a fundamental role.[27–36] For a comprehensive review on spiking neural networks, please, refer to Ref. 37.

For extensive spiking network simulations, an advanced event-driven simulator based on lookup tables (EDLUT) has been further developed and used.[38,39]

For the robot plant simulation and the evaluated control loops, an interface between the EDLUT and the simulator of the LWR (Light-Weight Robot) developed at DLR (German Aerospace Center)[40] has been implemented. In this way, we were able to evaluate robotic movements of the LWR manipulating different objects that significantly affected the dynamics and kinematics of the robotic arm.

2.1. *Robotic arm simulator*

Different control loops have been integrated within the robot plant simulator of the LWR.[40] The

simulated-robot-plant physical characteristics can be dynamically modified to match different contexts. The LWR robot is a 7-Degrees-of-Freedom (DOF) arm consisting of revolute joints. For the sake of simplicity, in our experiments, the number of actual joints (degrees of freedom) has been reduced to three. Specifically, the first (we will refer to it as Q_1), second (Q_2), and fifth joint (Q_3) have been used and the others have been kept fixed. This robot is especially suited for interactions with humans. In this scenario, the use of robots based on low-power actuators in order to reduce danger for humans in case of malfunctioning is of special interest. Furthermore, the accuracy in position and trajectory is not fully exploitable because of the dynamically changing interaction characteristics (non-static and structured scenario as is the case in other robotic control application fields). Figure 3 includes a simple scheme of the robot arm indicating the three non-fixed joints used in our experiments.

2.2. *Control scheme*

Lee Miller in Ref. 41 proposes a cerebellar control system based on a predictive signal (supplied by the cerebellum) with the aim of giving progressive and proper motor control commands. According to this approach, our first cerebellar control-loop model has been developed as a forward (FD) cerebellar control.

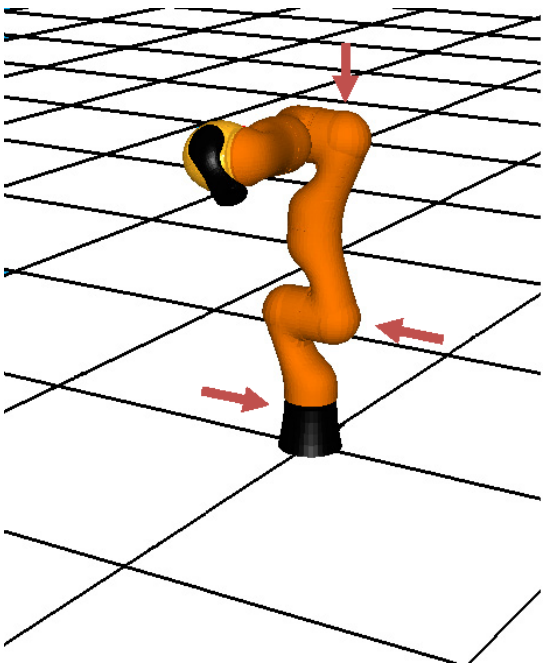

Fig. 3. LWR robot-arm. The three joints used in our experiments are explicitly indicated, all other joints are fixed.

In this control loop (see Fig. 4(a)), the desired arm states (robot end-effector position at each time) are generated by the trajectory planner to follow the desired trajectory. This trajectory in Cartesian coordinates is translated into joint coordinates (positions (Q), velocities ($\dot{Q}$), and accelerations ($\ddot{Q}$)) by the trajectory generator that consists of a crude inverse kinematic model representing the output of the motor cortex and other motor areas (while motor cortex provides a basic command which is appropriate for slow single-joint movements, the cerebellum provides the necessary correction for multi-joint movements).[26] In our experiment, the robot follows the trajectory described in Eq. (1) (see Fig. 5).

$$Q_1 = 0.1\sin(\pi t), \quad Q_2 = 0.1\sin(\pi t + \theta), \quad Q_3 = 0.1\sin(\pi t + 2\theta). \tag{1}$$

In the forward architecture, these desired arm states in joint coordinates are used at each time step to compute crude torque commands (crude inverse dynamic robot model). They are also used together with the contextual information (which could be obtained through visual, haptic information or cognitive "labels" as model profiles) related to the manipulated object, as input to the cerebellum model which produces the predictive corrective commands ($\tau_{\text{corrective}}$) that are added to these crude torque commands (τ_{desired}). Total torque (τ) is delayed (on account of delays of the biological motor pathways, this is δ_1 in Fig. 4) and supplied to the robot plant. The difference (ε) between the actual robot trajectory and the desired one is also delayed (δ_2 in Fig. 4) and used by the teaching signal computation module to calculate the inferior olive (IO) activity that reaches the cerebellum through the climbing fibers. This signal will be used by the cerebellum to adapt its output as described in the learning process section.

On the other hand, the presented recurrent architecture helps the cerebellum to find out temporal regularities in trajectory distortions. In this way, the cerebellum is able to compute predictive corrective position and velocity commands to compensate the deviation caused by the dynamic and kinematic modifications on the base-robot arm.

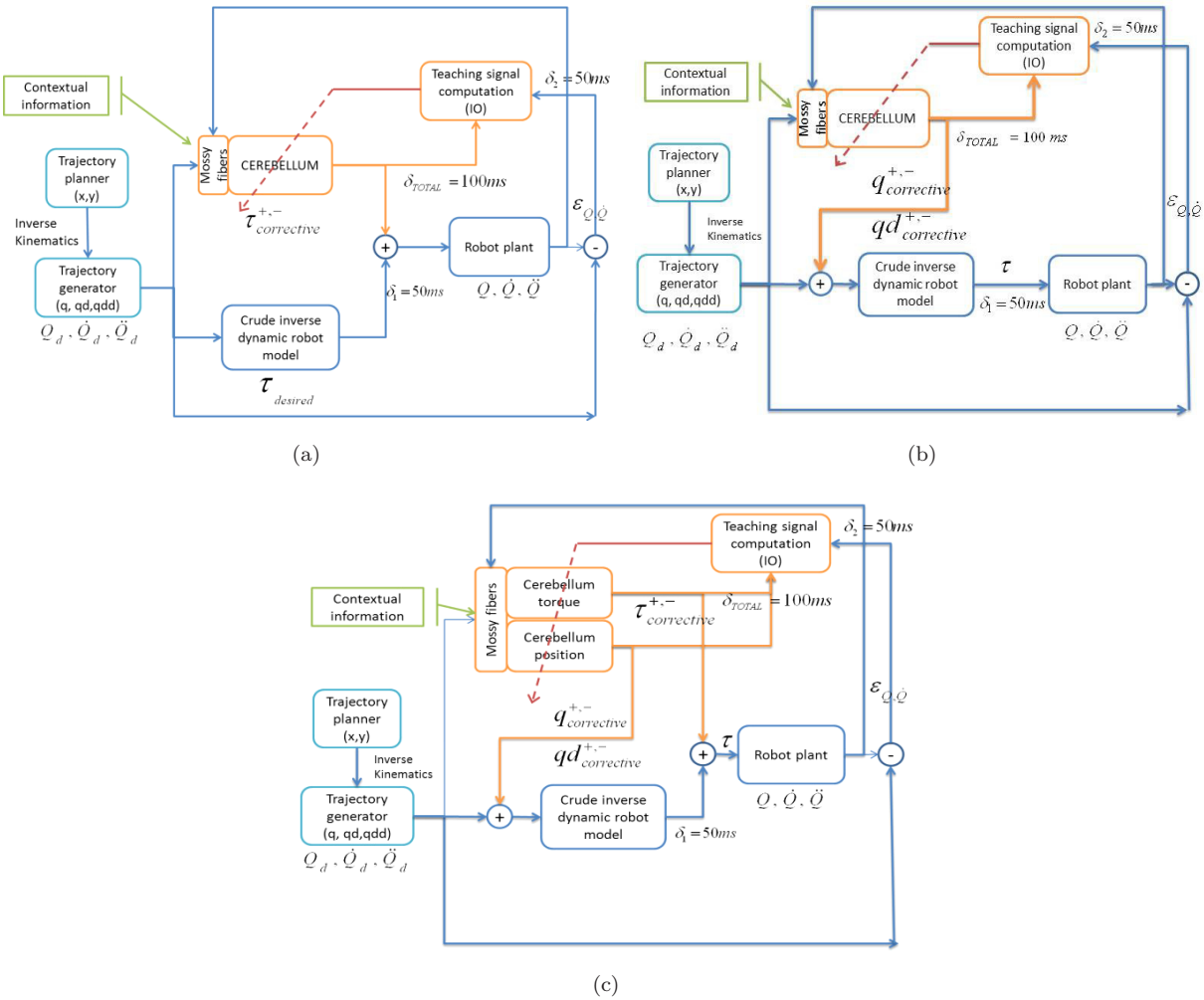

Fig. 4. Forward (FD), recurrent (RR), and forward&recurrent control loop (FD&RR). (a) In this FD control loop, the adaptive cerebellar module is embedded in the forward control loop and delivers add-on corrective torques to compensate deviations in the base dynamics and kinematics of the robotic arm model when manipulating different objects. (b) Recurrent control loop, the adaptive cerebellar model infers a model from the error signal related to a sensorimotor input to produce effective corrective position and velocity add-on terms. In this way, instead of propagating data from input to output as the forward architecture does, the recurrent architecture also propagates data from later processing stages to earlier ones. (c) FD&RR control loop delivers add-on corrective actions to compensate deviations in the base dynamic and kinematic robotic arm model when manipulating objects. In this forward&recurrent control loop, the adaptive cerebellar modules infer a model of effective corrective position, velocity, and torque add-on terms from the error signal related to sensorimotor input.

According to this hypothesis and based on the control loop described in Ref. 14, the recurrent control architecture shown in Fig. 4(b) has been developed.

In the recurrent architecture (RR), the arm states in joint coordinates are also used together (joint related information) with the contextual information (related to the manipulated object) as input to the cerebellum which produces the predictive corrective position and velocity commands ($q_{\text{corrective}}$, $qd_{\text{corrective}}$) which are added to the desired position and velocity trajectory commands. The final total torque computed by the crude inverse dynamics and the error signal are handled in the same way as the previously-presented forward architecture.

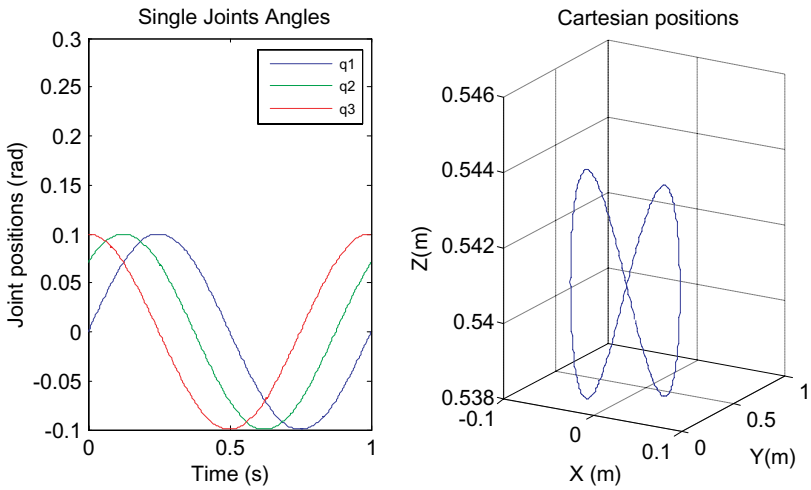

(a) (b)

Fig. 5. Three-joint periodic trajectory describing 8-shaped movements: (a) Angular coordinates of each joint of the Light Weight Robot, (b) 3D view of the robot end-effector trajectory in Cartesian coordinates. This 8-like trajectory ensures a sufficiently rich movement that allows robot arm dynamics to be revealed.[42] The interaction torque values generated in a multi-joint movement demand a more complex cerebellar control task than a summed combination of single-jointed movements.

These two cerebellar architectures have been proposed as biologically-inspired approaches; thus, it is interesting to study their potential complementary role in a control correcting scenario. Therefore, the developed forward&recurrent (FD&RR) architecture as presented in Fig. 4(c) will be evaluated.

Under normal conditions, without extra mass added to the robot end effector, the "crude inverse dynamic robot" module calculates rough motor commands to control the robotic arm. Under altered dynamics conditions, in contrast, the rough motor commands are very inaccurate to compensate for the new undergone forces (inertia, etc.), and this leads to distortions in the performed trajectories. During repeated trials, the cerebellar model is able to learn a corrective dynamics model for each manipulated object and supplies:

(a) Corrective motor torques in FD architecture.
(b) Corrective trajectory positions and velocities in RR architecture.
(c) Corrective motor torques and corrective trajectory position and velocities in FD&RR architecture.

2.3. *EDLUT: Spiking neuron simulator*

EDLUT is an open software platform which allows fast event-driven simulation of relatively-complex neural networks through an innovative method: the neural network[43] simulations are split into the two stages; Cell behavior characterization: each neural model included in the network (usually defined by a set of differential equations which govern the neural state) is simulated for every possible neural state and the consequent evolution of each neural state variable is stored in lookup tables. Then, in a second stage, when a simulation of a network containing these models is required, it can be performed without requiring a computationally-costly numerical procedure for solving the differential equations defining the neural model. EDLUT is used for the simulation of the embedded cerebellar module.

2.4. *Neural models*

The simulated spiking network consists of two different integrate-and-fire (I&F) cell types.[43] The used cell models are a modified version of the spike-response model (SRM) with synapses modeled as input-driven conductance.[44,45] Thus, the neuron models account for dynamic synaptic conductance rather than simply for constant current flows, providing an improved description over simpler I&F models.[46]

The synaptic conductance follows a decaying exponential function triggered by input spikes as

stated in Eq. (2):

$$g_{\text{exc}}(t) = \begin{cases} 0, & t < t_0 \\ g_{\text{exc}}(t_0)e^{-\frac{(t-t_0)}{\tau_{\text{exc}}}} & t \geq t_0 \end{cases} \quad (2a)$$

$$g_{\text{inh}}(t) = \begin{cases} 0, & t < t_0 \\ g_{\text{inh}}(t_0)e^{-\frac{(t-t_0)}{\tau_{\text{inh}}}} & t \geq t_0 \end{cases} \quad (2b)$$

where g_{exc} and g_{inh} represent the excitatory and inhibitory synaptic conductance. τ_{exc} and τ_{inh} represent the corresponding synaptic time constants. Finally t_0 represents the last spike time arrival (already computed).[38] This exponential representation has several advantages. Firstly, it is an effective representation of realistic synaptic conductance. Secondly, each synapse type requires only a single state variable per neuron, because the effect of input spikes through several synapses of the same type can simply be recursively summed when updating the total conductance if they have the same time constants. Therefore, when an input spike is received at time t, for example, through an excitatory synapse, its corresponding conductance $g_{\text{exc(pre-spike)}}(t)$ is abruptly incremented in a term $G_{\text{exc},j}$ as described in Eq. (3):

$$g_{\text{exc(post-spike)}}(t) = G_{\text{exc},j} + g_{\text{exc(pre-spike)}}(t). \quad (3)$$

$G_{\text{exc},j}$ is the weight of synapse j (a similar relation holds for inhibitory synapses) and $g_{\text{exc(pre/post-spike)}}$ represents the excitatory synaptic conductance before (*pre*) and after (*post*) the spike arrival, respectively.

In our simulations, the synaptic parameters have been chosen to represent excitatory AMPA-receptor-mediated synapse time constants and inhibitory GABAergic synapse time constants of cerebellar granule cells.[47–51] Note that different cells might have different parameters (Table 1).[52–55]

The neuron membrane potential V_m at time t is defined by differential Eq. (4).

$$C_m \frac{dV_m}{dt} = g_{\text{exc}}(t)(E_{\text{exc}} - V_m) + g_{\text{inh}}(t)(E_{\text{inh}} - V_m) + G_{\text{rest}}(E_{\text{rest}} - V_m). \quad (4)$$

Where the conductance values $g_{\text{exc}}(t)$ and $g_{\text{inh}}(t)$ integrate all the contributions received through individual excitatory and inhibitory synapses respectively, G_{rest} represents the resting conductance, and E_{exc}, E_{inh}, and E_{rest} represent the corresponding reversal potentials. Equation (4) is amenable to numerical analysis. In this way, V_m, g_{exc}, and g_{inh}, can be calculated for a given time after a previous neural state or input spike allowing the event-driven simulation scheme. The firing time (t_f) is the time when the membrane potential (V_m) reaches the firing threshold (V_{th}) and an output spike is emitted. It can be calculated from the membrane potential evolution.

Table 1. Parameters of the cell types.

Parameter	Granule cell	Purkinje cell
Refractory period	1 ms	2 ms
Membrane capacitance	2 pF	400 pF
*Total excitatory peak conductance	1 nS · 100	1.3 nS· ·175000 · 10%*
Total inhibitory peak conductance	1 nS · 200	3 nS · 150
Threshold	−40 mV	−52 mV
Resting potential	−70 mV	−70 mV
Resting conductance	0.2 nS	16 nS
Resting time constant (τ_m)	10 ms	25 ms
Excitatory-synapse time constant (τ_{exc})	0.5 ms	0.5 ms
Inhibitory-synapse time constant (τ_{inh})	10 ms	1.6 ms

Note: Parameters obtained from the following papers: Granule cell (GrC)[47–51] and Purkinje cell (PC)[52–55]. *Where 10% means the ratio of active connections PF-PC (out of the total 175000 PFs).

Table 1 shows the equation parameters corresponding to the two neural models used in the simulated cerebellum.

2.5. *Cerebellum model*

Two different cerebellar module configurations based on the scheme of Fig. 6 have been used. The first one corresponds to the previously called forward control architecture providing corrective torque terms and the second one corresponds to the recurrent control architecture providing corrective terms in the sensory space. Here we briefly indicate the different cerebellar module layers:

(i) *Mossy fibers* (256 *fibers*) (*MFs*): Mossy fibers carry both contextual information and joint sensory information related to desired and actual positions and velocities. An MF is modeled as a

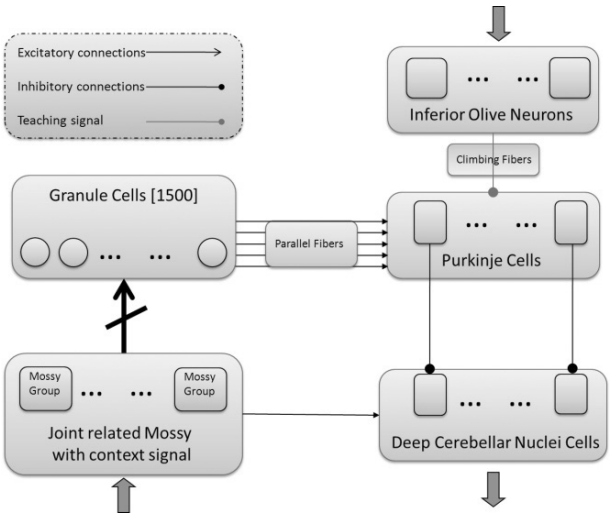

Fig. 6. Cerebellum model scheme. In FD and RR configurations, the cerebellar input, which encodes both the desired and actual position and velocity of each joint during the trajectory, is conveyed (upward arrow) through the mossy fibers (MFs) to the granular layer (crossed arrow indicates a random connectivity, i.e. each Granular cell receiving four randomly chosen MFs). Inputs encoding the error are sent (upper downward arrow) through the inferior olive (IO). Cells of the deep cerebellar nuclei (DCN) collect activity from the MFs (excitatory inputs) and the Purkinje cells (inhibitory inputs) and provide the cerebellar outputs (lower downward arrow). The DCN output is added as a corrective activity in the control loop. In the forward-architecture the output is added as corrective torques to the control torques (Fig. 4(a)). In the recurrent-architecture cerebellum configuration, the output is added as trajectory corrections (in position and velocity) in the control loop (Fig. 4(b)). Both outputs work complementarily in Fig. 4(c).

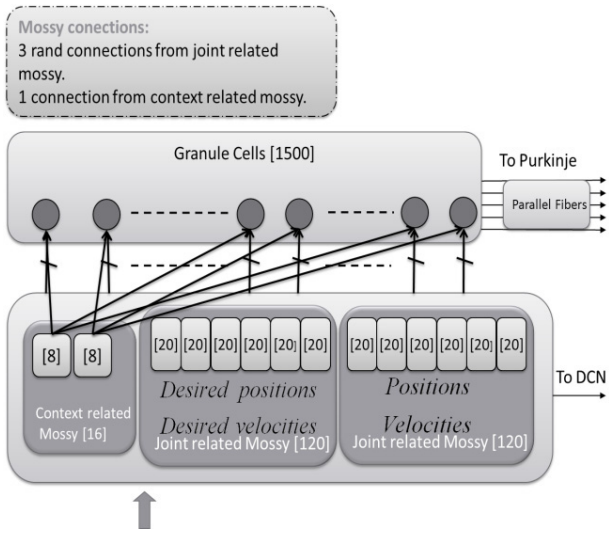

Fig. 7. Granular layer model. Explicit and Implicit context encoding approach.[59] Each granule cell receives excitation from an explicit-context-encoding fiber and three other randomly chosen MFs from the current and desired position and velocity groups.

leaky I&F neuron, whose input current is calculated using overlapping Gaussian functions as receptive fields on the input-variable value space.[39] This is carried out by modeling the contribution received from muscle or skin related afferents at a high level of abstraction. This cerebellar input layer (MFs) has been divided into 14 groups of fibers: 12 groups of twenty-grouped fibers encode both actual and desired joint velocity and position sensor information; the other 2 groups encode the context. The explicit contextual information is encoded by these 2 groups of eight-grouped cells (16 context input fibers). These MFs encode information assumed to be received through other sensory systems (such as vision). Each different context (object under manipulation) activates differently this population of neurons. Figure 7 illustrates this input connectivity.

(ii) *Granular layer* (1500 *cells*) (*GR*): A simplified granular layer of the cerebellum has been designed with the purpose of obtaining suitable signals at parallel fiber (PF) signals. The information provided by MFs is transformed into a sparse representation that facilitates discrimination of very similar inputs in the large granule cell (GR) layer,[56] in which each cell receives four excitatory connections: three connections from randomly chosen joint-related MFs groups and the other one, from a context-related MF group. PFs are the output of this layer. The sensorimotor corrective models are learned and stored as weight values at the PF-PC connections.

(iii) *Climbing fibers* (*CF*) (48 *climbing fibers in forward architecture,* 96 *climbing fibers in recurrent architecture*): This layer consists of 6 groups of CFs. In recurrent architecture, each group is composed by 16 CFs (each of them is subdivided in 2 subgroups of 8 CFs). In the forward architecture, each group is composed by 8 CFs. Each CF carries the teaching spikes (obtained from error signals) from the IO to a Purkinje cell.

(iv) *Purkinje Cells* (*PC*) (48 *Purkinje cells in forward architecture*) (96 *Purkinje cells in recurrent architecture*): In the forward architecture, this layer is divided into 6 groups of 8 cells. In the recurrent architecture, this layer is composed by 6 groups of 16 PCs; each group is also subdivided into 2 subgroups of 8 Purkinje cells. Each granule layer cell is connected to 80 per cent of PCs. Each PC receives the teaching signals used for the synaptic plasticity from a CF. Every two PCs; a cell of the deep-cerebellar-nuclei is inhibited. The PF-PC synaptic conductances are set to an initial value (15nS) at the beginning of the simulation, and are modified by the learning mechanism during the training process. This value is significantly lower in the corresponding rat cerebellum synapses.[57] However, a reduced version of the cerebellum (1500 GRs) is being modeled; therefore, each PC only receives activity from 1200 PFs (80% of GR). In a full model of the cerebellum, each PC should receive activity from 150000 PFs.[58] Therefore, PF-PC weight values have been scaled in order to obtain a similar PC excitation.

(v) *Deep Cerebellar Nucleus cells* (*DCN*) (24 *DCN cells in forward architecture*) (48 *DCN cells in recurrent architecture*): In the forward model, the cerebellum output is generated by 6 groups of these cells (2 groups per joint) whose activity provides corrective actions to the specified arm commands. Each neuron group in the DCN receives excitation from every MF and inhibition from the two corresponding PCs. In this way, the sub circuit PC-DCN-IO is organized in six microzones. In the forward architecture, the cerebellar corrective output (torque) for each joint is encoded by a couple of these groups. One group is dedicated to compensate for negative errors (agonist) and the other one is dedicated to compensate for positive errors (antagonist). In the case of the recurrent architecture, the cerebellum output is generated by 6 groups of these cells; 3 groups correspond to the joint–position corrections (one group per joint) and the other three groups correspond to the joint–velocity corrections. Each group is subdivided into 2 subgroups (of 4 cells); one subgroup handles positive error corrections and the other one handles negative error corrections.

2.6. *Learning process*

Although there seems to exist adaptation processes at several sites within the cerebellar circuitry,[60,61] one of the main synaptic adaptation mechanisms (induced by CF activity) seems to be the long-term depression (LTD) at PF-PC synapses[62,63] that has been correlated to cerebellar motor learning.[64] Therefore, the IO output (CF activity) is interpreted as an error-related signal [65–68] which drives this plasticity. When the conductivity of a PF-PC synapse becomes very low by this adaptation, the corresponding PC will not inhibit its corresponding deep cerebellar nucleus cells.[56,69] Another type of plasticity, long-term potentiation (LTP), which occurs at the same site, does not require the activation of CF[70] and compensates the effect of LTD.

Spike-timing-dependent plasticity (STDP) mechanisms to reproduce these adaptation processes have been implemented.[71] Since LTD synaptic plasticity requires the co-activation of PF and CF input, every time a CF spike is received by a PC, the conductance of all PF synapses corresponding to that PC are decreased according to Eq. (6a). That is, the past spike activity received through each PF is convolved with the integral kernel defined by Eq. (5) and the result is used to obtain the corresponding conductance decreases. This integral kernel, which correlates the IO and PF activity, was designed in such a way that it shows a peak at 100 milliseconds[72–74]; which makes the PF activity that was received 100 ms before the CF spike relevant. This time delay matches the sensorimotor delays of our system (see Fig. 4). After this mechanism is repetitively activated, when the same pattern of PF activation appears, the PC will not become active and the corresponding DCN will produce activity recognizing the learned pattern. The opposite adaptation process (LTP) is implemented by increasing the weight of a PF-PC synapse each time it transmits a spike as defined in Eq. (6b).[39,43,68,71]

$$k(t) = e^{-(\frac{t-t_0}{\tau})} \sin\left(2\pi\left(\frac{t-t_0}{\tau}\right)\right)^{20}. \tag{5}$$

$$LTD : \forall i, \quad \Delta w_i = \beta \int_{-\infty}^{\text{IOspike}} k(t_{\text{IOspike}} - t)\delta(t)_{\text{PF}_i} dt. \tag{6a}$$

$$LTP : \Delta w_i = \alpha. \tag{6b}$$

Where t_0 is a time constant determined by the biological path delay which is fixed to 100 ms and τ is a time reference which is set to 1 s in order to normalize the arguments in the learning rule. Δw_i represents the synaptic weight increment at the ith PF reaching that PC, t_{IOspike} stands for the time in which the corresponding CF transmits a spike, $\delta(t)_{PFi}$ is a Dirac delta function which represents the activity in the ith PF (1 when the PF carries a spike, 0 when it does not). Finally α and β are constant values that modulate the synaptic weight changes at PF-PC synapses ($\alpha = 0.005$ and $\beta = -0.1$).

2.7. *The error signal drives teaching signal*

The trajectory position/velocity error is used to calculate the teaching signal. This teaching signal follows Eq. (7).

$$\begin{aligned}\varepsilon_{\text{position}_i} &= (Q_{\text{desired}_i} - Q_{\text{actual}_i})[(t + t_{\text{delays}}) - t_i].\\ \varepsilon_{\text{velocity}_i} &= (\dot{Q}_{\text{desired}_i} - \dot{Q}_{\text{actual}_i})[(t + t_{\text{delays}}) - t_i].\\ &\qquad i = 1, 2, \ldots n, \quad \text{joints}\end{aligned} \tag{7}$$

And the computed error in the forward and recurrent architectures is given by Eq. (8).

$$\begin{aligned}FD\varepsilon_{\text{delayed}_i} &= k_{pi} \cdot \varepsilon_{\text{position}_i} + k_{vi} \cdot \varepsilon_{\text{velocity}_i};\\ RR\varepsilon_{p\text{delayed}_i} &= k_{pi} \cdot \varepsilon_{\text{position}_i};\\ RR\varepsilon_{v\text{delayed}_i} &= k_{vi} \cdot \varepsilon_{\text{velocity}_i}\\ &\quad i = 1, 2 \ldots n, \quad \text{joints.}\end{aligned} \tag{8}$$

Where $k_{pi} \cdot \varepsilon_{\text{position}i}$ represents the product of a constant value (gain) at each joint and the position error in this joint (difference between desired joint position and actual joint position ($Q_{\text{desired}} - Q_{\text{actual}}$)).

$k_{vi} \cdot \varepsilon_{\text{velocity}i}$ represents the product between a constant value (gain) at each joint and the velocity error in this joint (difference between desired joint velocity and actual joint velocity ($\dot{Q}_{\text{desired}} - \dot{Q}_{\text{actual}}$)).

Position/velocity error signals are delayed to align them in time according to biological delay pathways (t_{delays} represents the signal delays in the control loop). Biologically speaking, this time-matching of the desired and actual joint states can be explained by the fact that the trajectory error would be detected at the level of the spinal cord, through a direct drive from the gamma motoneurons to the spinal cord.[75]

IO cells respond with probabilistic Poisson process encoding the teaching signal into a low frequency probabilistic spike train (from 0 to 10 Hz, average 1 Hz).[76]

2.8. *Decoding the cerebellar output*

The output variables $\tau_{\text{corrective}}$ (in the FD configuration) or $(q, \dot{q})_{\text{corrective}}$ (in the RR configuration) are extracted from the firing rates of the DCN belonging to the related population, Eq. (9).

$$\tau^{+/-}_{\text{corrective}}/(q, \dot{q})^{+/-}_{\text{corrective}} = \sum_{j=1}^{4} \bar{v}_j(t). \tag{9}$$

Where $\bar{v}_j(t)$ is the firing rate of neuron j at time t, and the over-line indicates that the measures are averaged over a sliding time window of 100 ms, inspired by the low frequency filtering performed by motoneurons.

2.9. *Experimental methods*

Firstly, the behavior of different control architectures has been studied in a noisy scenario by using a Gaussian/uniform additive white noise on MF input signals. Table 2 indicates the different tested levels of noise.

The MFs signals are driven when an animal performs different activities. When an arm is moved along a learned trajectory, this arm movement is accompanied by predictable changes occurring primarily in MFs inputs reporting kinesthetics of this movement. Noise on the produced neural control signal (which may vary the firing time of motor neurons) will cause deviation in actual trajectories from the desired ones: $Q(t) = Q_{\text{desired}}(t) + \varepsilon(t)$ where Q_{desired} represents the desired trajectory/velocities to be followed. We have studied how the system behaves against two noise models (Table 2): (a) ε is a random signal with uniform distribution and a non-repeatable seed, (b) ε is a random signal with Gaussian distribution and zero mean. Although Golgi cells

Table 2. Noise levels on mossy fiber signals.

$SNR = 10 \log \frac{\mathrm{E}[x^2(n)]}{\varepsilon^2(n)}$	Uniform distribution	Gaussian distribution
Noise 1x	32 dB	23 dB
Noise 2x	18 dB	15.5 dB
Noise 4x	4 dB	8 dB

seem to play a crucial role in removing noise,[77] the evaluated cerebellar circuitry may help to accomplish this task.

Different added noise levels were checked. The used Signal-to-Noise-Ratio can be seen in Table 2.

In addition, different experiments have been also carried out to evaluate how different biologically-inspired control architectures work by abstracting models and switching between different contexts with a suitable cerebellar configuration.

3. Results

3.1. *Noise on MF input*

The learning process is evaluated by using the Mean Absolute Error (MAE) curve. For the calculation of the MAE of a trajectory execution, the addition of the error in radians produced by each joint independently along the whole trajectory has been used. 800 trials of the defined 8-shaped trajectory using the FD, RR, and FD&RR control-loop architectures have been executed. The robot end effector was loaded with 2 kg to increase the inertia (thus, the initial dynamics model needs to be corrected through learning).

Figure 8 shows the global mean absolute error (MAE) evolution obtained from the robot joint coordinates in radians. The noise was set to 1x, 2x, and 4x and was generated from a uniform distribution (a, b, and c plots, respectively) and a Gaussian distribution (d, e, and f plots).

As it is shown in Fig. 8, FD&RR architecture remains more stable against random noise than FD and RR architectures used independently. When the random noise level is 1x, FD and FD&RR responses are similar, but the more noise there is, the better response is obtained in FD&RR compared to RR and FD. In Figs. 8(b) and 8(c), it is easy to see that the convergence speed and output stability is better in FD&RR. FD&RR uses both configurations in a complementary way, to support FD with the corrections provided by RR. This causes FD&RR to have more stability and better performance when the noise is higher.

White Gaussian noise (Figs. 8(a)–8(c)) allows a good precision in the cerebellum output correction (torque predictions); prediction errors remain highly delimited around mean values. The probability density function has its maximum value at the mean, that is, during the learning process, the generated noise values tend to accumulate around the mean, the cerebellum learns this tendency and compensates it. In contrast, white uniform noise (Figs. 8(d)–8(f)) makes prediction torques less accurate since its probability density function does not have a single maximum value (thus, this is a harder task). The generated noise values do not tend to accumulate around any specific value therefore; the cerebellum cannot easily abstract any tendency information.

3.2. *Context switching between two dynamic/kinematic models*

Firstly, a set of experiments have been executed to study the capability of the cerebellar model to infer different corrective models when the dynamics of the robotic arm is modified by manipulating different objects using FD, RR, and FD&RR architectures. During a first learning process, the robot was loaded with a 1kg weight and executed 450 trials of the 8-like trajectory (Fig. 9(a)). During a second learning process, the robot was loaded with a 2 kg weight (Fig. 9(b)).

As shown in Figs. 9(a) and 9(b), FD&RR architecture takes advantage of both configurations; it uses the cerebellar corrections in torques and in positions and velocities to provide a better profile in the obtained MAE curves.

In order to evaluate the ability of the cerebellar module to infer and store different corrective models simultaneously using different control-loop architectures, an experiment in which the dynamics of the robotic arm is changed during the learning process every 15 trials has been carried out. The context alternates between manipulating a 2 kg object and a 1 kg object (Fig. 9(c)). The context-related cerebellar input is supplied with different signals in each context to enable the cerebellum to differentiate both contexts allowing different models (contexts) to be efficiently learned and retrieved in a non-destructive manner. Finally, the three different proposed control architectures (RR, FD, and FD&RR) are compared in a kinematic context switching scenario (Fig. 9(d)). This kinematic context switching scenario consists of a deformation of the end-effector (angle).

In RR architecture, the relationship between the produced robot-arm state error and the cerebellar output is direct, the cerebellum receives the position and velocity error-related signals, which are properly

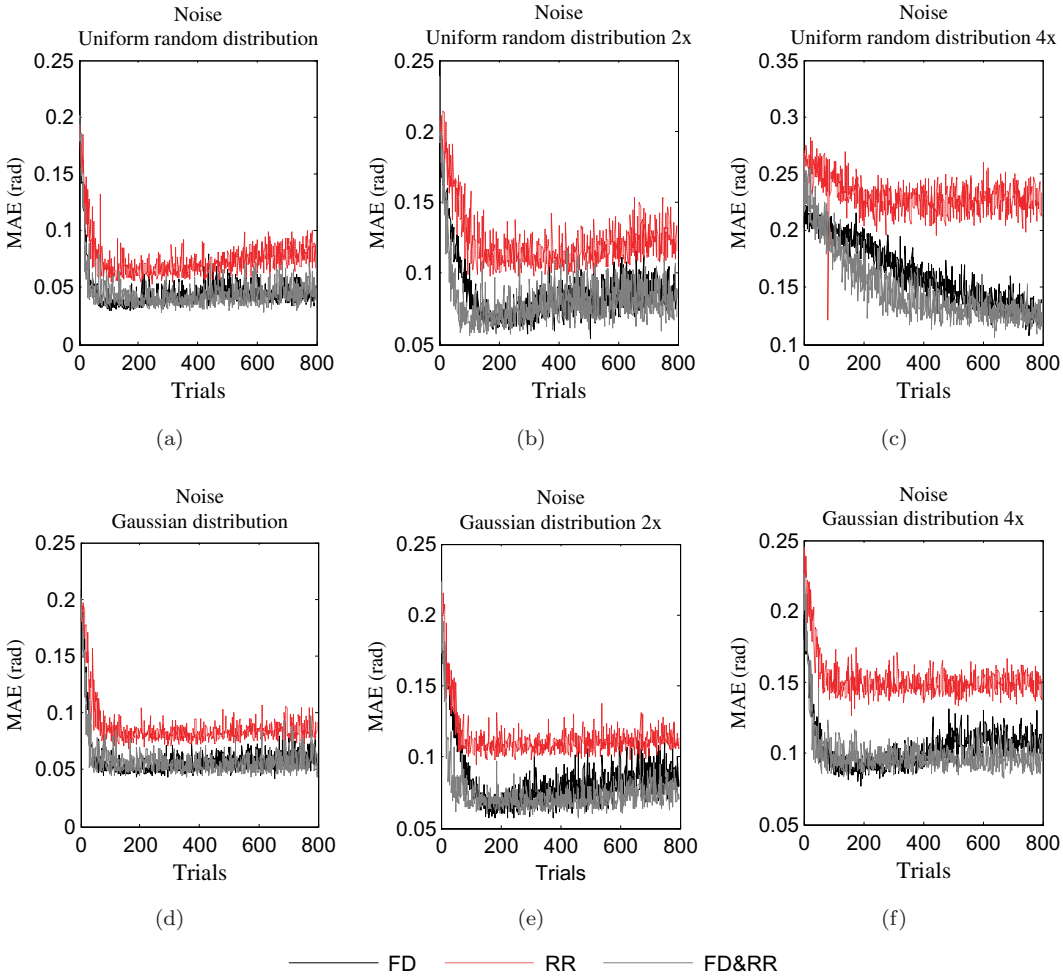

Fig. 8. Accuracy evolution of the three control architectures (FD, RR, and FD&RR) when introducing noise on input signals of MFs. Mean absolute error (MAE) of the joint coordinates in radians of the robot loaded with a 2 kg weight using forward, recurrent, and FD&RR architectures during a learning process of 800 trials of the 8-like trajectory execution. (a), (b), and (c) correspond to 1x, 2x, and 4x additive noise respectively using a uniform distribution. (d), (e), and (f) correspond to 1x, 2x, and 4x additive noise respectively using a Gaussian distribution.

provided by CFs, and cerebellar outputs consist of trajectory corrections of position and velocity, being these input and output dimensions equivalent. Therefore, the cerebellum does not need to implement a complex model representation translation. With this dimension matching, the cerebellum is able to learn and provide a quick response (a faster convergence is obtained in RR than in FD in Figs. 9(a) and 9(b)). Nevertheless, our crude inverse dynamic robot models need to be fed with clean and continuous corrected inputs in order to supply accurate torque values which command the robotic arm properly. Due to these required input characteristics of this dynamic model, the final torque commands in RR architecture are not as good as the ones delivered by the FD architecture (the RR MAE error curve is less stable than the FD case). The accuracy of the cerebellum corrective output involves making a trade-off between number of cells and simulation time.

In the FD architecture, the accuracy is not improved by correcting the input of the robot crude inverse dynamics; the cerebellum supplies torque command corrections almost directly to the robotic arm (see Fig. 4(a)). However, in the FD architecture, the relationship between the produced robot-arm state error and the cerebellar output is not straightforward. The position and velocity error signal is

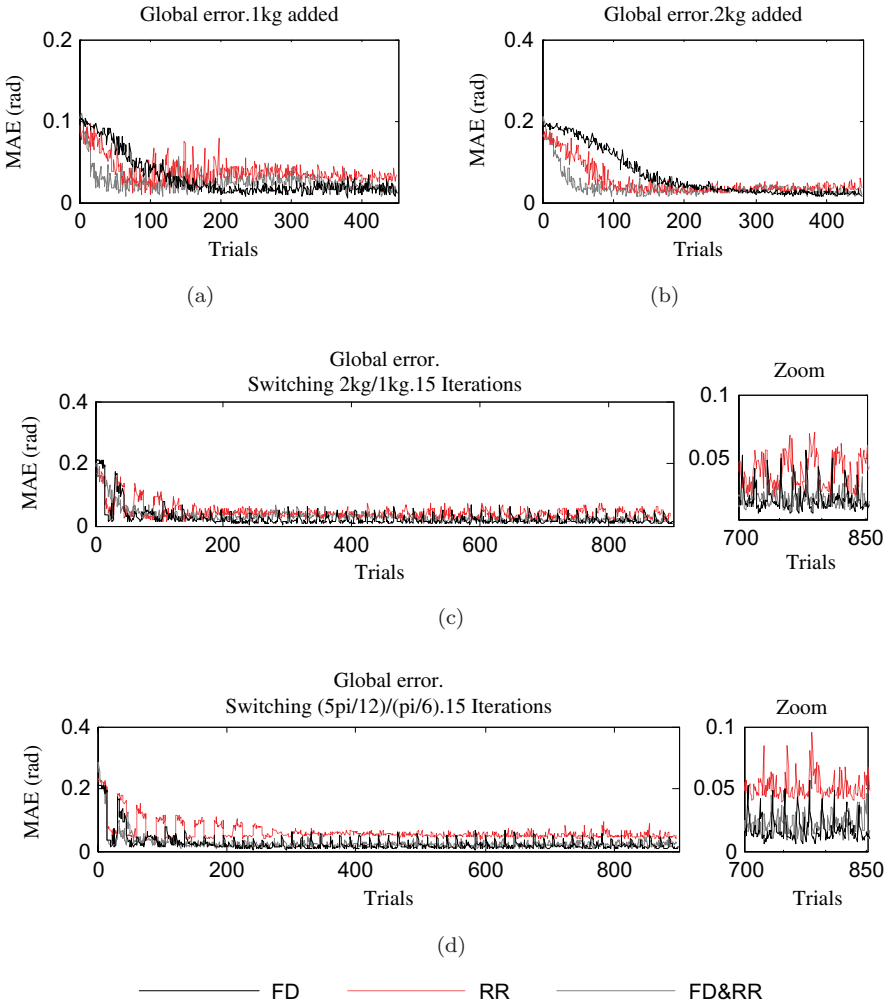

Fig. 9. Accuracy evolution of the three control architectures with and without context switching. Mean absolute error (MAE) of the robot joint coordinates in radians using FD, RR, and FD&RR architectures executing the 8-like trajectory. (a) and (b) The context is not changed: The robot manipulates a 1 kg object and a 2 kg object respectively during a 450-trial learning process. (c) The dynamics of the robotic arm is alternately changed between the two contexts every 15 trials. In the first context, the end segment of the robot arm is loaded with a 2 kg object. In the second one, it is loaded with a 1kg object. (d) The kinematics of the plant is alternately changed between two contexts every 15 trials: in the first context, the robot must follow the trajectory using an end segment which is deformed $5\pi/12$ radians. In the second one, the robot end segment is deformed $\pi/6$ radians (this corresponds to kinematics changes that may be caused by manipulating an object of a certain length).

conveyed by CFs while cerebellar output supplies torque corrections. These input and output dimensions are not equivalent, the cerebellum learning task is of higher complexity. Thus, the learning convergence is slower but the command torques are more precise (FD MAE error curve is more stable than the one of the RR architecture).

Again, FD&RR combines the advantages of both the RR and the FD architectures. It has a high convergence speed and good output stability after learning. FD&RR uses the position and velocity corrections given by RR to facilitate the FD torque correction task, and they mutually complete each other.

Figure 9(c) shows the MAE evolution of a 900-trial learning process. It is shown that the learning is performed in a non-destructive manner since once the final error for each context is reached, this error value is maintained stable when the context changes (therefore, the previously-learned context model was

not destroyed). This feature relies on the separation capability of the granular layer for sensory signals related to different contexts. Again, FD&RR reaches a better behavior compared to RR and FD architectures (Fig. 9(c)). FD&RR allows better inter-context transitions (error peaks between two different contexts are almost negligible because of its superior convergence speed (thanks to the RR loop)) and it also achieves a better final stability.

The MAE evolution of a 900-trial learning process is shown in Fig. 9(d). The results are similar to the dynamics context-switching scenario, in single-context learning (as we have within 15 iterations), high convergence speed, and good performance learning curve profile in the long term seem to be desirable aims. RR makes the transition between contexts softer; in the long term, no transition peaks are observed. When the kinematics of the robotic plant changes, no inertia tensors are involved, so the "crude inverse dynamic robot model" module has an easier task in computing the proper new torques. On the other hand, FD provides a better curve performance than RR (no crude inverse dynamic robot model is involved in processing the cerebellum output). As shown in Fig. 9(d), FD&RR configuration takes advantage of both loops obtaining smoother transitions between contexts and a good learning curve profile in long the term.

4. Conclusions

This work has focused on studying biologically-inspired robot-arm control architectures under dynamic and kinematic perturbations of the manipulation scenario. Furthermore, it has evaluated different control loops (RR, FD, and FD&RR) in several noisy scenarios. A cerebellar adaptive module embedded in these loops could effectively provide torque/position&velocity corrections to compensate for deviations in the dynamics/kinematics of a base robotic arm model (due to the manipulation of different objects and deformations of the end effector) increasing the movement accuracy.

The cerebellar model included an input representation which encodes context-specific inputs and current sensory signals encoding the actual arm states during the experiment.

It has been evaluated how a temporal-correlation kernel driving an error-related LTD and a compensatory LTP component (which complement each other) can achieve an effective adaptation of the corrective cerebellar output.

The obtained results indicate that coupling both control loop architectures (FD&RR) leads to a high robustness against noise. Employing the recurrent architecture (RR) to ensure a faster convergence in learned profile curve dynamics has been combined with exploiting the fact that the forward architecture (FD) provides a better accuracy gain and output stability in a noisy scenario.

In the same way, the results demonstrate that the composite control architecture in context switching has the capability to infer and store different corrective models simultaneously under dynamic/kinematic modifications better than FD or RR configurations on their own.

The assumption that the cerebellum is involved in forward modeling for motor control is familiar in the literature.[78,79] Our results suggest that both FD and RR loops could be present in the biological motor control in order to achieve a better performance. In fact, this proposed architecture (FD&RR) is compatible with several neurophysiological findings. Firstly, several studies have reported relations between motor cortex activity and various kinematic parameters of the motor output such as distance and speed[80–82] as well as parameters related to the dynamics of the movement.[22] As the motor cortex has been described as one of the targets of the cerebellar output,[83] the cerebellar output could influence these kinematic (RR loop) and dynamic parameters (FD loop). And secondly, results of virus tracing studies have shown that the regions of the cerebellar cortex that receive input from the motor cortex are the same as those that project to the motor cortex.[84] These observations suggest that several closed-loop circuits may be present in the cerebrocerebellar circuits as it occurs in the FD&RR architecture.

As future work, the scalability of these cerebellar configurations, the potential role of new nervous circuits, such as the cuneate nucleus and Golgi cells in noisy scenarios, other kinds of plasticity, and cell features and finally, scalability on the number of robot-plant joints will be studied.

Acknowledgments

This work has been supported by the EU grants SENSOPAC (IST 028056) and REALNET (IST-270434), the Spanish national project ARC-VISION (TEC2010-15396), and Spanish *Subprograma Juan de la Cierva 2009* (MICINN).

References

1. S. J. Blakemore, D. M. Wolpert and C. D. Frith, Central cancellation of self-produced tickle sensation, *Nat. Neurosci.* **1**(7) (1998) 635–640.
2. R. B. Ivry and S. W. Keele, Timing functions of the cerebellum, *J. Cog. Neurosci.* **1** (1989) 136–152.
3. M. Kawato and H. Gomi, A computational model of four regions of the cerebellum based on feedback-error learning, *Biol. Cybern.* **68**(2) (1992) 95–103.
4. R. C. Miall, D. J. Weir, D. M. Wolpert and J. F. Stein, Is the cerebellum a Smith predictor? *J. Mot. Behav.* **25** (1993) 203–216.
5. A. M. Smith, Does the cerebellum learn strategies for the optimal time-varying control of joint stiffness? *Behav. Brain Sci.* **19**(3) (1996) 339–527.
6. J. S. Albus, A theory of cerebellar function, *Math Biosci.* **10** (1971) 25–61.
7. D. Marr, A theory of cerebellar cortex, *J. Physiol.* **202** (1969) 437–470.
8. J. Porrill, P. Dean and J. V. Stone, Recurrent cerebellar architecture solves the motor-error problem, *Proceedings in Biol. Sci.* **271**(1541) (2004) 789–796.
9. A. Haith and S. Vijayakumar, Robustness of VOR and OKR adaptation under kinematics and dynamics transformations, in: *Proceedings of 6th IEEE (ICDL '07)*, London (2007).
10. M. Ito, Cerebellar circuitry as a neuronal machine, *Prog. Neurobiol.* **78** (2006) 272–303.
11. C. Assad, S. Dastoor, S. Trujillo and L. Xu, Cerebellar dynamic state estimation for a biomorphic robot arm, *Syst. Man Cybern. IEEE Trans.* (2005) 877–882.
12. E. O'Hearn and M. E. Molliver, Organizational principles and microcircuitry of the cerebellum, *International Review of Psychiatry* **13**(4) (2001) 232–246.
13. J. Porrill and P. Dean, Cerebellar motor learning: when is cortical plasticity not enough? *PLoS Computational Biology* **3** (2007a) 1935–1950.
14. J. Porrill and P. Dean, Recurrent cerebellar loops simplify adaptive control of redundant and nonlinear motor systems, *Neural Computation* **19**(1) (2007b) 170–193.
15. N. Ramnani and C. Miall, Expanding cerebellar horizons, *Trends Cog. Neurosci.* **5** (2001) 135–136.
16. F. Colin, L. Ris and E. Godeaux, in *The Cerebellum and its Disorders*, ed. M. U. Manto (Cambridge University Press, Cambridge, 2002).
17. S. J. Blakemore, C. D. Frith and D. M. Wolpert, The cerebellum is involved in predicting the sensory consequences of action, *NeuroReport* **12**(9) (2001) 1879–1885.
18. M. Ito, The cerebellum and neural control, *New York, Raven Press* (1984).
19. M. Kawato and D. M. Wolpert, Internal models for motor control, *Novartis Foundation Symp.* **218** (1998) 291–307.
20. R. C. Miall, The cerebellum, predictive control and motor coordination, in *Novartis Foundation Symposium. Sensory Guidance of Movements* **218** (2007) 272–290.
21. P. Dean, J. Porrill, C. F. Ekerot and H. Jörntel, The cerebellar microcircuit as an adaptive filter: Experimental and computational evidence, *Nat. Rev. Neurosci.* **11** (2010) 30–34.
22. L. E. Sergio, C. Hamel-Pâquet and J. F. Kalaska, Motor cortex neural correlates of output kinematics and kinetics during isometric-force and arm-reaching tasks, *J. Neurophysiol.* **94** (2005) 2353–2378.
23. W. S. Levine, *The Control Handbook* (CRC Press, Boca Raton, 1996), pp. 1339–1368.
24. C. Ott *et al.*, A humanoid two-arm system for dexterous manipulation, *IEEE-RAS International Conference on Humanoid Robots* (2006) 276–283.
25. N. Schweighofer, J. Spoelstra, M. A. Arbib and M. Kawato, Role of the cerebellum in reaching movements in human. II. A neural model of the intermediate cerebellum, *European J. Neuroscience* **10** (1998a) 95–105.
26. N. Schweighofer, M. A. Arbib and M. Kawato, Role of the cerebellum in reaching movements in human. I. Distributed Inverse dynamics control, *European J. Neuroscience* **10** (1998b) 86–94.
27. J. L. Rossello, V. Canals, A. Morro and J. Verd, Chaos-based mixed signal implementation of spiking neurons, *Int. J. Neural Syst.* **6**(16) (2009) 465–471.
28. S. P. Johnston, G. Prasad, L. Maguire and T. M. McGinnity, An FPGA Hardware/Software Co-Design Towards Evolvable Spiking Neural Networks for Robotics Application, *Int. J. Neural Syst.* **20**(6) (2010) 447–461.
29. E. Nichols, L. J. McDaid and N. H. Siddique, Case study on a self-organizing spiking neural network for a robot navigation, *Int. J. Neural Syst.* **20**(6) (2010) 501–508.
30. S. Ghosh-Dastidar and H. Adeli, Improved spiking neural networks for EEG classification and epilepsy and seizure detection, *Integr. Comput-Aid E.* **14**(3) (2007) 187–212.
31. S. Ghosh-Dastidar and H. Adeli, A new supervised learning algorithm for multiple spiking neural networks with application in epilepsy and seizure detection, *Neural Networks* **22**(10) (2009) 1419–1431.
32. J. Iglesias and A. E. P. Villa, Emergence of preferred firing sequences in large spiking neural networks

during simulated neuronal development, *Int. J. Neural Syst.* **18**(4) (2008) 267–277.
33. S. Soltic and N. Kasabov, Knowledge extraction from evolving spiking neural networks with rank order population coding, *Int. J. Neural Syst.* **20**(6) (2010) 437–445.
34. T. J. Strain, L. J. McDaid, L. P. Maguire and T. McGinnity, An STDP training algorithm for a spiking neural network with dynamic threshold neurons, *Int. J. Neural Syst.* **20**(6) (2010) 463–480.
35. S. Schliebs, N. Kasabv and M. Defoin-Platel, On the probabilistic optimization of spiking neural networks, *Int. J. Neural Syst.* **20**(6) (2010) 481–500.
36. R. Acharya, E. C. P. Chua, K. C. Chua, L. C. Min and T. Tamura, Analysis and automatic identification of sleep stages using higher order spectra, *Int. J. Neural Syst.* **20**(6) (2010) 509–521.
37. S. Ghosh-Dastidar and H. Adeli, Spiking neural networks, *Int. J. Neural Syst.* **4**(19) (2009).
38. E. Ros, R. R. Carrillo, E. M. Ortigosa, B. Barbour and R. Agís, Event-driven simulation scheme for spiking neural networks using lookup tables to characterize neuronal dynamics, *Neural Comp.* **18** (2006) 2959–2993.
39. R. R. Carrillo, E. Ros, C. Boucheny and O. J.-M. D. Coenen, A real-time spiking cerebellum model for learning robot control, *Biosystems* **94**(1–2) (2008) 18–27.
40. J. Butterfaß, M. Grebenstein, H. Liu and G. Hirzinger, DLR Hand II: Next generation of a dextrous robot hand, *IEEE ICRA* (2001) 109–114.
41. L. E. Miller, R. N. Holdefer and J. C. Houk, The role of the cerebellum in modulating voluntary limb movement commands, *Archives Italiennes de Biologie* **140** (2002) 175–183.
42. H. Hoffmann, G. Petckos, S. Bitzer and S. Vijayakumar, *Sensor-Assisted Adaptive Motor Control Under Continuously Varying Context*, presented at ICINCO, Automation and Robotics (2007).
43. W. Gerstner and W. Kistler (eds.), *Spiking Neuron Models: Singleneurons, Populations, Plasticity* (Cambridge University, 2002).
44. F. J. Pelayo, E. Ros, X. Arreguit and A. Prieto, VLSI implementation of a neural model using spikes, *Analog Integr. Circ. S.* **13**(1–2) (1997) 111–121.
45. E. Ros *et al.*, Stimulus correlation and adaptive motion detection using spiking neurons, *Int. J. Neural Syst.* **9**(5) (1999) 485–490.
46. J. Feng, Is the integrate-and-fire model good enough? A review, *Neural Networks* **14** (2001) 955–975.
47. Z. Nusser, S. CullCandy and M. Farrant, Differences in synaptic GABA(A) receptor number underlie variation in GABA mini amplitude, *Neuron* **19** (1997) 697–709.
48. D. J. Rossi and M. Hamann, Spillover-mediated transmission at inhibitory synapses promoted by high affinity alpha(6) subunit GABA(A) receptors and glomerular geometry, *Neuron* **20** (1998) 783–795.
49. R. A. Silver, D. Colquhoun, S. G. CullCandy and B. Edmonds, Deactivation and desensitization of non-NMDA receptors in patches and the time course of EPSCs in rat cerebellar granule cells, *J. Physiol.* **493** (1996) 167–173.
50. S. Tia, J. F. Wang, N. Kotchabhakdi and S. Vicini, Developmental changes of inhibitory synaptic currents in cerebellar granule neurons: Role of GABA(A) receptor alpha 6 subunit, *Journal of Neuroscience* **16** (1996) 3630–3640.
51. E. D'Angelo, G. Defilippi, P. Rossi and V. Taglietti, Synaptic activation of $Ca2^{+}$ action potentials in immature rat cerebellar granule cells *in situ*, *J. Neurophysiol.* **78**(3) (1997) 1631–1642.
52. E. D'Angelo, T. Nieus, A. Maffei, S. Armano and P. Rossi, Theta-frequency bursting and resonance in cerebellar granule cells: experimental evidence and modeling of a slow K^{+}-dependent mechanism, *J. Neurosci.* **21** (2001) 759–770.
53. E. D'Angelo, G. Defilippi, P. Rossi and V. Taglietti, Ionic mechanism of electroresponsiveness in cerebellar granule cells implicates the action of a persistent sodium current, **80** (1998) 493–503.
54. E. D'Angelo, P. Rossi and V. Taglietti, Different proportions of N-Methyl-D-Aspartate and Non-N-Methyl-D-Aspartate receptor currents at the mossy fiber granule cell synapse of developing rat cerebellum, *Neurosci.* **53** (1993) 121–130.
55. T. Nieus, E. Sola, J. Mapelli, E. Saftenku and P. Rossi, LTP regulates burst initiation and frequency at mossy fiber-granule cell synapses of rat cerebellum: Experimental observations and theoretical predictions, *J. Neurophysiol.* **95** (2006) 686–699.
56. E. D'Angelo, T. Nieus, M. Bezzi, A. Arleo and O. J.-M. D. Coenen, Modeling synaptic transmission and quantifying information transfer in the granular layer of the cerebellum, *LNCS* **3512** (2005) 107–113.
57. P. Isope and B. Barbour, Properties of unitary granule cell− >Purkinje cell synapses in adult rat cerebellar slices, *J. Neurosci.* **22**(22) (2002) 9668–9678.
58. N. Brunel, V. Hakim, P. Isope, J. P. Nadal and B. Barbour, Optimal information storage and the distribution of synaptic weights: Perceptron versus Purkinje cell, *Neuron* **43** (2004) 745–757.
59. N. R. Luque, J. A. Garrido, R. R. Carrillo, O. J.-M. D. Coenen and E. Ros, Cerebellar input configuration towards object model abstraction in manipulation tasks, *Neural Network, IEEE Trans.* DOI: 10.1109/TNN.2011.2156809 (2011).

60. T. V. Bliss and T. Lomo, Long-lasting potentiation of synaptic transmission in the dentate area of the anaesthetized rabbit following stimulation of the perforant path, *J. Physiol.* **232** (1973) 331–356.
61. C. D. Hansel, D. J. Linden and E. D'Angelo, Beyond Parallel Fiber LTD: The diversity of synaptic and non-synaptic plasticity in the cerebellum, *Nat. Neurosci.* **4** (2001) 467–475.
62. M. Ito and M. Kano, Long-lasting depression of parallel fiber-Purkinje cell transmission induced by conjunctive stimulation of parallel fibers and climbing fibers in the cerebellar cortex, *Neurosci. Letter* **33** (1982) 253–258.
63. G. Bi and M. Poo, Synaptic modifications in cultured hippocampal neurons: Dependence on spike timing, synaptic strength, and postsynaptic cell type, *J. Neurosci.* **18** (1998) 10464–10472.
64. C. I. De Zeeuw and C. H. Yeo, Time and tide in cerebellar memory formation, *Curr. Opin. Nuerobiol.* **15** (2005) 667–674.
65. D. Jaeger, No parallel fiber volleys in the cerebellar cortex: Evidence from cross-correlation analysis between Purkinje cells in a computer model and in recordings from anesthetized rats, *J. Comp. Neurosci.* **14** (2003) 311–327.
66. A. Roth and M. Häusser, Compartmental models of rat cerebellar Purkinje cells based on simultaneous somatic and dendritic patch-clamp recordings, *J. Physiol* **535** (2001) 445–472.
67. S. Solinas, R. Maex and E. De Schutter, Synchronization of Purkinje cell pairs along the parallel fibre-fiber axis: A model, *Neurocomputing* **52–54** (2003) 97–102.
68. R. R. Carrillo, E. Ros, B. Barbour, C. Boucheny and O. J.-M. D. Coenen, Event-driven simulation of neural population synchronization facilitated by electrical coupling, *Biosystems* **87**(2–3) (2007) 275–280.
69. D. Jaeger, E. De Schutter and J. Bower, The role of synaptic and voltage-gated currents in the control of Purkinje cell spiking: A modeling study, *Journal of Neuroscience* **17** (1997) 91–106.
70. P. A. Salin, R. C. Malenka and R. A. Nicoll, Cyclic AMP mediates a presynaptic form of LTP at cerebellar parallel fiber synapses, *Neuron* **16** (1996) 797–803.
71. N. R. Luque, J. A. Garrido, R. R. Carrillo, O. J.-M. D. Coenen and E. Ros, Cerebellar-like corrective model inference engine for manipulation tasks, *Syst Man Cybern., IEEE Transactions*, DOI: 10.1109/TSMCB.2011.2138693 (2011).
72. R. E. Kettner *et al.*, Prediction of complex two-dimensional trajectories by a cerebellar model of smooth pursuit eye movement, *J. Neurophysiol.* **77**(4) (1997) 2115–2130.
73. J. Spoelstra, M. A. Arbib and N. Schweighofer, Cerebellar adaptive control of a biomimetic manipulator, *Neurocomputing* **26–27** (1999) 881–889.
74. J. L. Raymond and S. G. Lisberger, Neural learning rules for the vestibulo-ocular reflex, *J. Neurosci.* **18**(21) (1998) 9112–9129.
75. J. L. Contreras-Vidal, S. Grossberg and D. A. Bullock, A neural model of cerebellar learning for arm movement control. Cortico-spino-cerebellar dynamics, *Learn. Memory* **3**(6) (1997) 475–502.
76. C. Boucheny, R. R. Carrillo, E. Ros and O. J.-M. D. Coenen, Real-time spiking neural network: An adaptive cerebellar model, *LNCS* **3512** (2005) 136–144.
77. D. Philipona and O. J.-M. D. Coenen, Model of granular layer encoding in the cerebellum, *Neurocomputing* **58–60** (2004) 575–580.
78. D. M. Wolpert and R. C. Miall, Forward models for physiological motor control, *Neural Netw.* **9** (1996) 1265–1279.
79. M. Kawato *et al.*, Internal forward models in the cerebellum: FMRI study on grip force and load force coupling, *Prog. Brain Res.* **142** (2003) 171–188.
80. J. Ashe and A. P. Georgopoulos, Movement parameters and neural activity in motor cortex and area 5, *Cereb. Cortex* **4** (1994) 590–600.
81. G. A. Reina, D. W. Moran and A. B. Schwartz, On the relationship between joint angular velocity and motor cortical discharge during reaching, *J. Neurophysiol.* **85** (2001) 2576–2589.
82. Q. G. Fu, D. Flament, J. D. Coltz and T. J. Ebner, Temporal encoding of movement kinematics in the discharge of primate primary motor and premotor neurons, *J. Neurophysiol.* **73** (1995) 836–854.
83. P. J. Orioli and P. L. Strick, Cerebellar connections with the motor cortex and the arcuate premotor area: An analysis employing retrograde transneuronal transport of WGA-HRP, *J. Comp. Neurol.* **288**(4) (1989) 612–626.
84. R. M. Kelly and P. L. Strick, Cerebellar loops with motor cortex and prefrontal cortex of a nonhuman primate, *J. Neurosci.* **23**(23) (2003) 8432–8444.

International Journal of Neural Systems
©World Scientific Publishing Company

FROM SENSORS TO SPIKES: EVOLVING RECEPTIVE FIELDS TO ENHANCE SENSORIMOTOR INFORMATION IN A ROBOT-ARM

NICETO R. LUQUE*, JESÚS A. GARRIDO*, JARNO RALLI, +JUANLU J. LAREDO AND EDUARDO ROS

Department of Computer Architecture and Technology, CITIC
University of Granada, Periodista Daniel Saucedo s/n, Granada, Spain
E-mail: {nluque, jgarrido, jarnor, eros}@atc.ugr.es
+ juanlu@geneura.ugr.es

In biological systems, instead of actual encoders at different joints, proprioception signals are acquired through distributed receptive fields. In robotics, a single and accurate sensor output per link (encoder) is commonly used to track the position and the velocity. Interfacing bio-inspired control systems with spiking neural networks emulating the cerebellum with conventional robots is not a straight forward task. Therefore, it is necessary to adapt this one-dimensional measure (encoder output) into a multidimensional space (inputs for a spiking neural network) to connect, for instance, the spiking cerebellar architecture; i.e. a translation from an analog space into a distributed population coding in terms of spikes. This paper analyzes how evolved receptive fields (optimized towards information transmission) can efficiently generate a sensorimotor representation that facilitates its discrimination from other "sensorimotor states". This can be seen as an abstraction of the Cuneate Nucleus (CN) functionality in a robot-arm scenario. We model the CN as a spiking neuron population coding in time according to the response of mechanoreceptors during a multi-joint movement in a robot joint space. An encoding scheme that takes into account the relative spiking time of the signals propagating from peripheral nerve fibers to second-order somatosensory neurons is proposed. Due to the enormous number of possible encodings, we have applied an evolutionary algorithm to evolve the sensory receptive field representation from random to optimized encoding. Following the nature-inspired analogy, evolved configurations have shown to outperform simple hand-tuned configurations and other homogenized configurations based on the solution provided by the optimization engine (evolutionary algorithm). We have used artificial evolutionary engines as the optimization tool to circumvent non-linearity responses in receptive fields.

Keywords: Receptive Field, Evolutionary Algorithm, Parallelism, Population Coding, Cuneate Nucleus, Spiking Neural Network, Robot.

1. Introduction

There is an active interdisciplinary field called Neurobotics in which actual robots are controlled by bio-inspired neural processing engines. Besides other potential applications, this kind of set ups are important for understanding neurobiological computational principles (system neuroscience), specifically, some issues under study are how sensorimotor representations are integrated and efficiently used in accurate manipulation tasks,[1-3] how spike timing based on different sensory representations can help to enhance information transmission[4,5] and be efficiently used by biologically plausible neural systems [6-12] (such as cerebellar-like structures).[13]

It is well known that the cerebellum constitutes a fundamental part in motor systems.[13-17] The cerebellum is fed by inputs from the cerebellar cortex, providing a contribution in *fast and precise movements*.[18] This is crucial in the fine control of the temporal evolution of fast ballistic movements,[19] that is, extremely fast movements that are impossible to be modified by feedback circuits because the complete movement muscle sequence control has to be planned in advance.[20,21]

Furthermore, taking a look at the current research in robot labs, a new trend in constructing and controlling light-weight compliant robot arms [22-24] which mimic human arms can be seen. Such new robotic features pursue the search of new ways of control. In fact, controlling the dynamics of any of these kinds of robot arms is an open issue (there is no general established methodology developed yet).[25] Since the cerebellum combines sensory information with the physical current state to generate motor signals, it is a proper candidate

*These authors contributed equally to this work

for studying how these controlling problems are solved by nature. In that sense, cerebellum architecture, as a control scheme, has received much attention in the literature and different cerebellum computational models have been developed. Among others, the Cerebellar Model Articulation Controller (CMAC),[26] the Adjustable Pattern Generator (APG),[27] the Schweighofer-Arbib Model,[28] or the Multiple Paired Forward-Inverse Model[29,30] represent good state-of-the-art examples. All these models have something in common: they try to mimic the functionality of the cerebellum by making an abstraction of the cerebellum structure while keeping robotic control theory in mind. As a result, the approximations mentioned above configure their sensorimotor inputs to enhance their control aims.

The cerebellum *supervises and supplies corrective adjustments in motor commands*[31,32] which are generated in other encephalon zones. It receives continuous information from peripheral body parts (position, movement rhythm, interacting external forces, etc…) and, according to *sensorial information*, compares the physical state of each body part against the desired state which the motor system is trying to achieve.[33-35] In the framework of errors (detected through this continuous comparison), proper corrective signals are transmitted to the motor system increasing or decreasing specific muscle activity.[36] The cerebellar *sensorial input* is carried by mossy fibers[37] (MFs), which constitute one of the major cerebellar afferent systems.[38] MFs carry information from different sources; MFs from the pontine nuclei report on motor and sensory areas of the cerebellar cortex,[39-43] MFs from cells in the CN handle information from forelimb muscle spindles[44] related to position and movement,[45,46] MFs from collaterals of cortical fibers carry a copy of descending motor commands to the cerebellum, and finally, MFs from the visual cortex supply information about movements in the visual space.[47] Therefore, different kinds of MFs drive detailed information related to the external world and the desired/actual body movements/positions. As a result of that, it can be postulated that sensorial *cerebellum inputs play a critical role in cerebellum functionality.*

Our system uses neural population coding[48] for sensorimotor representation. Each neuron presents a distribution of responses over some set of inputs, and the responses of many neurons are combined to determine some information about the input state.[48,49] Using this kind of coding, each input stimulus is represented by a set of spikes. However, the occurrence of these spikes strongly depends on the current generated by sensors and on which spikes subsequently reach the first-layer cells.

In a reaching movement, the arm direction is encoded by means of neurons whose input current changes with the cosine of the difference between the stimulus angle and the cell's preferred direction[50] (Cosine tuning). Each population vector cell contributes a vector in the direction of its preferred direction in relation to its current. Nevertheless, a simple reaching movement involves extracting spatial information including visual acquisition of the target, coordination of multi-modal proprioceptive signals, and a proper motor command generation to drive proper motor response towards the target.[51] Usual reaching movements towards a target that we have already seen involve an internal representation of the target and limb positions, and also a coordinate transformation between different internal reference frames. A spiking population coding seems to be the best way to encode sensorial information to be consistent with biological control requirements.[52, 53] This is also important to allow system level studies for the evaluation of the cerebellum functionality in the framework of accurate movement experiments. [1,2]

However, the integration of computational models with neurophysiologic observations in order to understand the main problems in motor control requires not only the cerebellum functionality to be considered (as is done in the CMAC, APG, and other approaches) but also, its biological architecture (cell-network) has to be taken into account. A necessary translation from analog domain sensor signals into spike based patterns compatible with a spiking cerebellar network needs to be developed.

This paper tries to reveal the best way in which sensorimotor information in a common robot scenario can be handled to investigate an optimal encoding in terms of somatosensory information.

To that aim, the followed methodology can be briefly described at the following points:

(i) Firstly, we consider the execution of a biologically relevant reaching movement in a robot arm scenario. With that purpose, different trajectories are defined over a joint space. A biologically plausible translation from joint position/velocity measures to their corresponding spike train representation has been defined. Population coding

and tuning curves are used to be consistent with reaching arm movements.

(ii) In order to make previous codifications more accurate, a bio-inspired Evolutionary Algorithm (EA) which optimizes the receptive fields towards maximizing sensorimotor information and state discrimination has been used. The combinatorial space to be explored towards an optimization is enormous; the EA seems to be the proper tool that unifies biology evolution and an optimization procedure.[54]

(iii) Finally, the performance of the sensorial representations using different measures that take into account metrical properties of the spike train space has been evaluated.

Therefore, the paper uses a new methodology in which an EA is used as an optimization engine towards reaching an efficient sensory representation to be further processed at the spiking based cerebellum. As a result, in this case, an EA is used for reverse engineering an abstraction of a biologically plausible model. Rather than finding an optimal fitness value of the cost function, the goal is to arrive at an efficient solution in terms of receptive fields in the sensory space. The cost function includes actual trajectories, which makes the experimental set up heavier but also more informative, enhancing the usefulness of the searching methodology carried on by the EA.

2. Materials and methods

This section describes the principles of the proposed methodology. An answer to different issues explicitly indicating what/why/how and the basis of the proposed approach is given.

2.1. *Target reaching trajectories*

Anthropomorphic robotic arms, mimicking human arms, usually consist of three links (arm, forearm, and hand) which are connected with each other using motorized joints (shoulder, elbow, and wrist). Reaching involves bringing the endpoint of the robot arm to a desired target position. Therefore, the aim is to "connect" two points, the initial point, defined by the actual endpoint robot arm position and the final point, defined by the endpoint robot arm target position. The control system leads the sequence of motor actions to achieve the target. In a robotic arm (due to the redundancy in the degrees of freedom), there is an infinite number of possible trajectories that allow the arm to reach any given target point. A specific approach will be provided by a planner module. But even focusing on a single joint workspace (see Fig. 1) (shoulder, elbow, wrist), the movement can be performed in different ways, in smoother or abrupt movements (as indicated in Fig. 1).

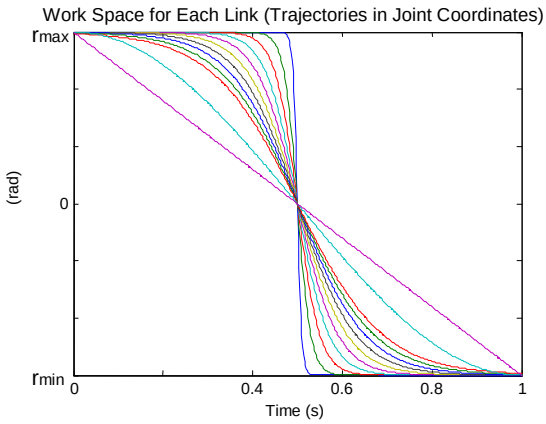

Fig. 1. Trajectory benchmark. Within a single joint workspace (as shown in this plot) the actual movement can be done also in different ways, through different position/velocities profiles. r_{max} and r_{min} represent the maximum and the minimum values of the joint angle.

Taking into account both the ability of humans to generalize motor learning skills with a changeable duration/amplitude in a common workspace and the possibility of reaching a target point in infinite different ways, we designed a set of different trajectories (Fig. 1) that allows us to properly explore the workspace in a very simplified scenario. An optimal evolution of receptive fields in this workspace may provide us a generalized solution, i.e. a solution for this kind of movements.

These trajectories are realistic both in terms of robotics (cubic polynomials, linear segments with parabolic blends[55]) and biological plausibility (smooth trajectories with a bell-shaped velocity profile (with different smooth profiles and different trajectory ranges)).[56,57]

2.2. *From analog signals to spike patterns: Receptive fields*

When interacting with the real world, a representation of the external environment and the internal state of our body is supplied by the somatosensory system to the central nervous system. The afferent (sensory) information signals are propagated from peripheral nerve

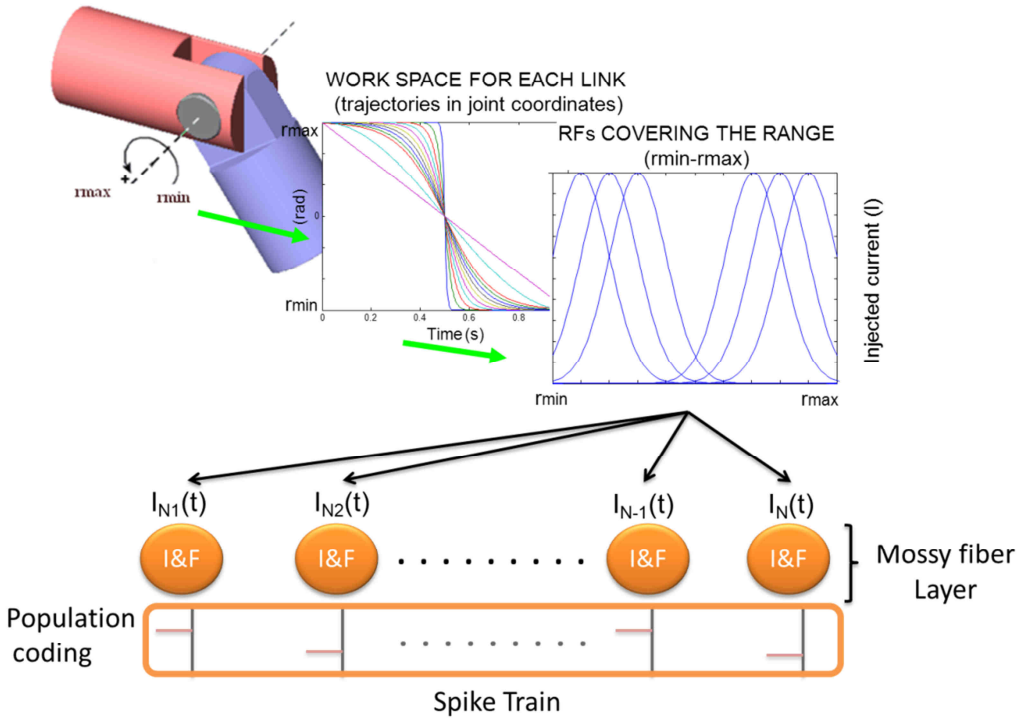

Fig. 2. Population coding of receptor (proprioceptors) signals. The position of a revolute joint given by an encoder along a trajectory is translated into a population coding by means of a set of tuning curves which represent the current injected to Integrate & Fire (I&F) neurons by different sensory receptors (propioceptors). Tuning proprioceptor curves are overlapped mimicking peripheral nerve receptive fields in the human arm. Each value of a proprioceptor output signal (I current) is integrated using an I&F neuron whose output spikes represent the activity provided by the mossy fibers. At the end, in each step time, a spike train is obtained from the mossy fibers that represent the sensory inputs to the cerebellum module.

fibers to the central nervous system (spinal cord and brain).[58] Each region of the skin is related to an individual cutaneous sensory nerve fiber (or a population of them). These skin regions are called receptive fields. Therefore, each nerve fiber has its associated receptive field, which overlaps with other receptive fields from other fibers. This overlapping is not fixed; the average overlapping degree between receptive fields is related to its body-location.[58]

When a target reaching movement is executed, different body-parts, as muscles, tendons, and joints are articulated depending on their body-location along the followed trajectory. Sensory receptors (proprioceptors) are activated according to movement; thus, a time-varying set of stimuli is produced, and its corresponding neural population varying activity is generated. In contrast, in a robot scenario, the only available sensory information is the one supplied by a single encoder for each link. That involves a translation between the joint position/velocity measures to a time-varying set of stimuli. This is illustrated in Fig. 2. At this point, to find out an optimal biologically plausible encoding scheme that allows "biological decoders" to take advantage of the codification is a non-trivial point. It is assumed that the firing rate of an individual sensory receptor follows a neural response which is characterized by Eq. (1) (also equivalent to a cosine tuning curve, that is, neurons' firing rate varies as the angle between a sensory receptors' preferred direction or angle varies). [59] Therefore, a reaching movement execution will be represented with a sparse population of active cells which are changing with time. This coding mechanism facilitates the representation of the current sensorial state during the trajectory execution in an unambiguous way.

The output of each receptive field (RF) in Fig. 2 is given by Eq. (1):

$$I_{Ri}(t) = r_{min} + r_{max} \sum_{n} e^{-\left(\theta - \theta_{pref_i} - 2\pi n\right)^2 / 2\sigma_i^2}. \quad (1)$$

Where $[r_{min}, r_{max}]$ is the joint range in radians, θ is the actual position, θ_{pref} is the RF preferred direction which in this work is simplified by the RF centroid (RF responses maximally during a trajectory execution near this centroid, and its response decreases when the trajectory execution increasingly differs from the preferred direction or RF centroid in this case), σ is the width of the RF, i is the identifier of each RF (each one is linked to its corresponding mossy fiber), $2\pi n$ is a subtractive term used to refer the actual position to the first-360-degrees (the maximal range of any revolute joint is ideally 360º), and finally, I_{Ri} is the input current from the corresponding RF_i.

RFs are distributed along the range of each joint (Fig. 2) and they have certain overlap (as in the case of peripheral nerve receptive fields).

Each value of a proprioceptor output signal is integrated using a leaky integrate-and-fire neuron model shown in Eq. (2), which determines the output activity that drives the cuneate nucleus activity in the same way as the mossy fiber activity from cells in the CN handles information from forelimb muscle spindles.

$$\tau_{mi} \frac{dv_i}{dt} = -v_i(t) + R_i I_{Ri}. \quad (2)$$

Related to the integrated and fire cell dynamics, [60] τ_{mi} is the resting time constant, v_i, the membrane potential, I_{Ri}, the input current from the corresponding receptive field, and R_i is related to the resting conductance of the membrane. Finally, the i sub-index term defines the identifier of the related mossy fiber. Therefore, the mossy fiber layer will consist of a group of leaky I&F neurons connected to their corresponding target granule cells.

At this point, the problem in this population coding scheme is not only how to distribute propioceptors (centroid and width) along the workspace, but also how many RFs should be used in order to enhance the information transfer between sensor signals and their spike representation.

2.3. *The evolutionary algorithm as optimization engine*

The distribution of peripheral nerve receptive fields in a human arm is the result of a continuous test and trial process of biological evolution through millions of years. Taking a look around our surrounding environment, there are many examples of well-adapted organisms (in fact, as many as living forms), pointing out that evolution is a universal solver which overcomes difficulties presented by nature. Hence, evolutionary algorithms[61] seem to be a proper tool to optimize the receptive fields of our cerebellum architecture according to artificial evolution and keeping the analogy (though at a very high abstraction level) with the way in which nature solved the biological problem.

Strictly speaking, evolutionary algorithms are a set of bio-inspired techniques for optimization based in the Darwinian process of natural selection. As in the evolution of species, those individuals (solutions) showing to be the fittest ones are preferentially selected for mating, so that their offspring will inherit their genes through the course of generations. Iteratively, selection acts as a filter for genes and just those belonging to the best solutions are able to overcome the selection pressure and recombine forming higher order solutions. It is within that process where the stochastic based search of an evolutionary algorithm has been shown to succeed in many optimization problems.[62,63] A genetic algorithm (i.e. a sub-class of an evolutionary algorithm) is used to obtain, through evolution, a near-optimal peripheral nerve receptive field distribution.

In Table 1, the pseudo-code of an evolutionary algorithm where a population of plausible solutions (P) is iteratively improved from random is shown. This

Table 1. Pseudo code of a Generational EA

```
/* The initial population is a random sampling of the search
landscape*/
P <= Randomly generated initial population
Fitness(P)
    /*For a number of predefined generations*/
Repeat until termination
    /*Every generation, we create a new population (P_aux) of
evolved individuals*/
  Repeat P times
    Ind1 Ind2 <= Select 2 of the fittest individuals in P
    New_Ind1 New_Ind2 <= Crossover(Ind1,Ind2)
    New_Ind1 <= Mutate(New_Ind1)
    New_Ind2 <= Mutate(New_Ind2)
    P_aux.add(New_Ind1,New_Ind2)
  End Repeat
   /* Evaluate individuals in population P_aux */
  Fitness(P_aux)
   /* To keep elitism, we replace the worst individual in P_aux with
the best individual in P */
  P_aux(individual_worst) <= P(individual_best)
  P <= P_aux
End Repeat
```

evolvable population (P) consists of Individuals *(Ind)* as indicated in Eq. (3).

$$P = \{Ind_1, Ind_2, \ldots, Ind_j\}, where\ j = 1, \ldots Ind_{max}. \quad (3)$$

Where the candidate solutions (Individuals) are encoded by Eq. (4).

$$Ind = \{RF_{max}, \{e_1, e_2, \ldots, e_i\}\}, where\ i = 1, \ldots RF_{max}. \quad (4)$$

And finally, e is a receptive field defined in Eq. (5).

$$e = (\theta, \sigma). \quad (5)$$

Where θ represents the centroid of the receptive field along the sensory space (preferred coordinate of receptive field e) and σ, the width of the receptive field (Fig. 3). Therefore, according to Fig. 2, each candidate solution presents a spike train response in time when a trajectory is executed. A set of executed trajectories produce a set of spike train responses. R denotes the set of spiking responses of a possible candidate solution along the followed trajectories as expressed in Eq. (6).

The heuristic based search consists in projecting each individual encoding (*Ind*) into the problem space (i.e. using the *Fitness* function). Then, the fittest

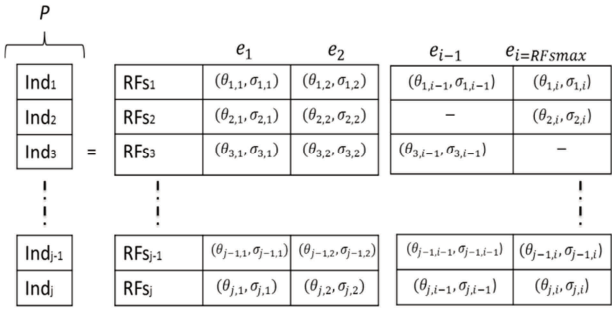

Fig. 3. Visual interpretation of the Population (P) to be evolved. Each individual consists of a vector containing a variable number of RFs defined by their own preferred coordinate θ_{pref} and the width of the receptive field associated.

individuals are selected for recombination. As in the case of natural reproduction, *crossover* applies to a couple of individuals (Ind_1 and Ind_2), merging their encodings to produce descendants (New_{Ind1} and New_{Ind2}). Furthermore, there are also small *mutations* in descendants in order to escape from local-optima attracting regions. Within this process, the best solution in every iteration (known as *epoch*) is preserved for the next one.

2.4. *Van Rossum distance based fitness function. Metrics for evaluating information transfer*

At this point, it is necessary to define a metric (goal function) to measure whether a solution A is better than a solution B. This is intimately related to the functionality assumed by the system. To that end, a metrical information transfer measure which is employed in order to assess the fitting of an evolved peripheral nerve receptive field distribution has been chosen. We have found no previous approach related to information transfer (Shannon's mutual information, for instance) that takes into account the whole metrics of the spike response space.[64] In order to determine the quantity of information transmission carried on by a large population of spikes (taking into consideration their metrical properties), a new entropy definition based on Ref. 65 is used. That facilitates the comparison between different spike populations generated by different receptive field distributions, as shown by Eq. (6).

$$H^*(R) = -\sum_{r \in R} \frac{1}{card(R)} log\left(\sum_{r' \in R} \frac{1}{card(R)} \alpha(r, r')\right). \quad (6)$$

Where R is the set of spiking responses of a possible configuration of receptive fields along the followed trajectories, *card(R)* is the cardinal number of R, and finally, α is a similarity real function between the responses *(r, r')*. We use as a similarity function between two spike trains the van Rossum distance[66] D_{vr} defined in Eq.(8). The van Rossum based Real function *α(r, r')* will take values in the interval [0, 1] as a response to r, r' stimuli, as shown in Eq. (7).

$$\alpha(r, r') = 1 \leftrightarrow r = r'$$
$$otherwise \quad \alpha(r, r') = {D_{vr}}^{-1} \quad (7)$$

Eq. (6) means that the quantity of entropy in a system is proportional to the logarithm of possible different microstates presented by this system. Maximizing the entropy involves maximizing the quantity of possible microstates in the system. Keeping in mind this concept and looking backwards to our previously defined receptive field system, some relevant points can be clarified:

(a) Each set of evolvable receptive fields produces a set of spiking stimuli for the previously described trajectory benchmark.
(b) A population coding that represents the different sensorial states in an unambiguous way when each of the trajectories belonging to the benchmark is executed is desirable (Fig. 4).
(c) Maximizing the number of possible population coding microstates improves the representation of different sensorial states. Each microstate might be unambiguously represented in just one single way.
(d) In order to differentiate a couple of spike train sets, van Rossum distance is used. If two sets of spike trains are equal, the entropy is zero, the more difference between both sets, the higher the entropy will be, i.e. the number of microstates representing different sensorial states increases in proportion with the entropy. According to Eq. (6), entropy depends on α, and α depends on van Rossum distance as well. Therefore, an optimal representation will be ensured only if we evolve receptive fields to maximize the minimal distance between any of two single spike based states of the whole generated set of spike trains for any benchmark trajectory.

2.4.1. Similarity function

As it was previously indicated, we have chosen a similarity function based on the van Rossum distance. [66] This function is related to the distance introduced by Victor and Purpura, [67,68] but is computationally more efficient, Eq. (8), and has a more natural physiological interpretation.

$$D_{vr}^2(r,r')_{tc} = \frac{1}{t_c}\int_0^{\infty}[r(t)-r'(t)]^2\,dt. \qquad (8)$$

Where our spike train *(r)* is defined by a set of first spikes generated along a certain time window by the implemented spiking neural network. It is assumed that all spikes generated by the spiking neural network are identical; being the timing of its spikes the key information in a spike train. Therefore, it is reasonable to model a spike train as a sequence of identical, instantaneous Dirac delta functions ($\delta(t)$), representing individual spikes as expressed in Eq. (9.A).

$$r(t) = \sum_i^M \delta(t - t_i). \qquad (9.A)$$

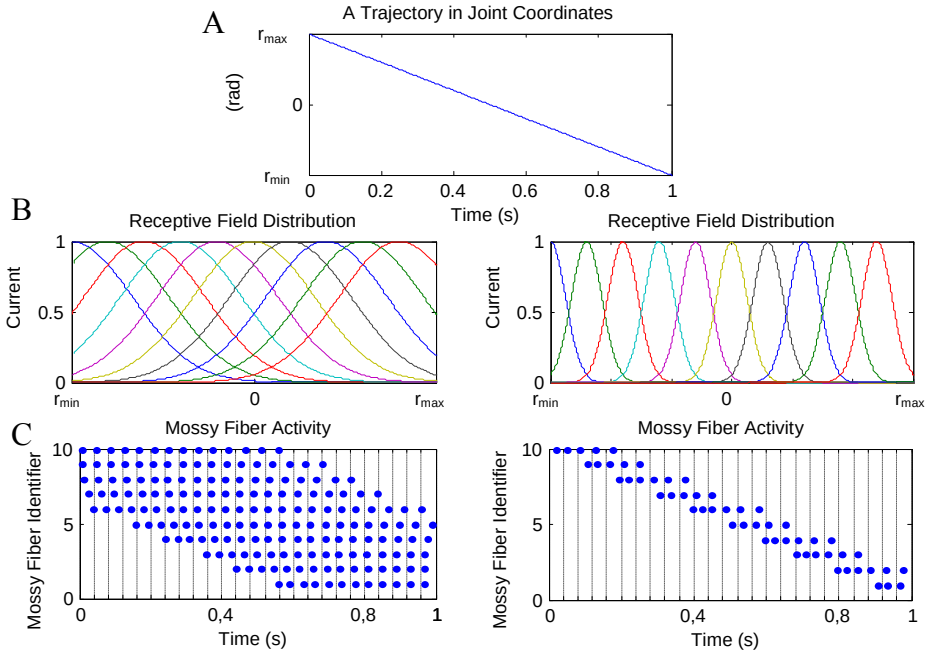

Fig. 4. Different mossy activities corresponding to two different receptive fields when a rectilinear trajectory is followed. A) Trajectory which is followed by a link of a robot-arm. B) Two configurations of receptive fields mapping the analog joint coordinate. C) Two spike populations (population coding) representing each sensorial state (vertical columns) along the executed trajectory. Each sensorial state highly depends on the input receptive field distribution.

$$r(t)=\sum_{i}^{M} H(t-t_i)\cdot e^{-(t-t_i)/t_c}. \qquad (9.B)$$

In Eq. (9.B), each Dirac delta function Eq. (9.A) is substituted by an exponential function $e^{-(t-t_i)/t_c}$. H is the Heaviside step function (*H(x) = 0 if x<0 and H(x) =1 if x≥0*) and *M* is the number of events in the spike train. In Eq. (8), distance D_{vr} is calculated as the integration of the difference between *r* and *r′*, which are spike-driven functions with exponential terms, as indicated in Eq. (9.B). Note that the resulting distance and, indeed, its interpretation depends upon the exponential decay constant, t_c in Eq. (9.B). The distance also depends upon the number of spikes in the trains; it can be normalized dividing the number of spikes by M.

2.4.2. Similarity measure

The previously introduced similarity function D_{vr} depends on the t_c parameter, (van Rossum cost parameter).[66] This parameter determines the penalization cost of two spikes when calculating the distance between them; if the distance is higher than t_c, the penalty will be one, the lower the distance is, the lower the penalty will be. According to Ref. 64, 65, the CN population code is able to discriminate different stimuli around 35ms after the first afferent spike; therefore, a t_c value of 40ms is assumed. The codification has to respond in less than 40ms to be consistent with biology, larger values shall be punished in the spike metric measure using this decay constant. Human micro-neurography recordings[52,53,64] (for distribution latencies of the first afferent spike, see Figs. 3 and 4 in Ref. 52) show that generated spike trains from different continuous stimuli have time lengths around 35ms on average. Hence, in order to be biologically coherent, a spike train (microstate) is generated for each 40ms time window providing sensor estimates through a spike-based pattern (Fig. 4.C). The goal function to be calculated per executed trajectory is given by Eq. (10).

$$\Phi_{min}=\min_{\substack{i\neq j\\ i,j}}\left(D_{vr}(r_i,r_j)\right), r\in R \text{ and } i,j\in N^{+}$$
$$R=\{r_n\}, \text{where } n=\text{number of trajectories}. \qquad (10)$$

Where r_i and r_j represent a pair of spike trains as a response to two different stimuli. A 40ms time window activity after the stimulus presentation is taken into account to determine the stimulus response (i.e. in a 1 second trajectory, 25 time windows of 40ms are obtained; therefore, consequently 25 spike trains corresponding to 25 microstates are obtained too). *R* is the whole set of spike patterns $\{r_n\}$ generated when following *n* trajectories. D_{vr} (r_i, rj) represents the inter-stimulus distances between responses of two different stimuli. We try to find out the minimal distance between any pair of spikes in the whole set of time windows Φ_{min}. This process is implemented one by one in each benchmark trajectory Φ^{n}_{min} obtaining Eq. (11):

$$\frac{1}{n}\sum_{1}^{n}\left(\Phi^{n}_{min}\right), \text{where } n=\text{number of trajectories}. \qquad (11)$$

On the other hand, to be consistent with biology, intra-stimulus distance has been implemented by means of using a slightly stochastic threshold voltage in integrated and fire neurons (Eq. 2). This means that the same stimulus may lead to a slightly different response (Fig. 5). The same input (trajectory) is presented three times to our receptive field; the whole obtained spike set is used in Eq. (11). Therefore, the effect of firing

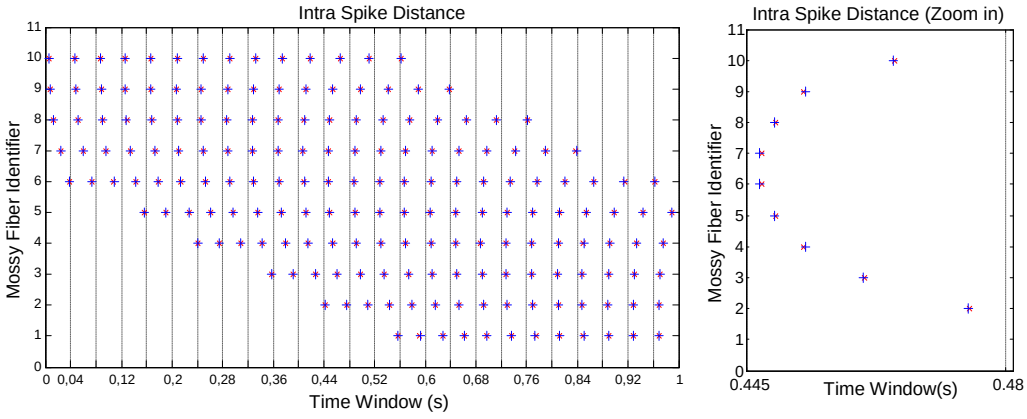

Fig. 5. Intra-Stimulus Distance. A 40ms length time window showing two slightly different responses (cross and star markers) of the receptive field configurations shown in 4.B (left side) for the same input due to stochasticity in the neural model.

probability in stochastic leaky I&F neurons is compensated in the cost function.

2.4.3. Fitness function

The target problem, the spike representation to be used, and how to measure the fitness of a particular solution (receptive field distribution) have been defined. Hence, the final global fitness function to be optimized is given by Eq. (12).

$$fitness = max\left(\frac{1}{n}\sum_{1}^{n}\left(\Phi_{min}^{n}\right)\right), n = number\ of\ trajectories. \quad (12)$$

2.5. *Experimental setup*

As it was explained in the previous section, the optimization criterion is to find a combination of receptive fields capable of maximizing Eq. (12). That translates into a hard combinatorial and deceptive problem in which a good solution can be found near a poor region of the searching landscape. Specifically, up to 30 receptive fields are considered, each having 6000 positions (i.e. each vector element that goes from r_{min}=-6rad to r_{max}= 6rad in steps of 0.002rad is considered as a possible centroid's position) and different coverage width (i.e. each value from σ =0.02 to σ=10 in steps of 0.001 is considered as a possible width of the associated receptive field). That is, the combinatorial space can be roughly estimated to be around 10^{169}.

Furthermore, the time to simulate the fitness of a single solution is computationally expensive and can last several seconds even in current processors. Therefore, to alleviate the burden of a deterministic exploration of the combinatorial space, we have used an evolutionary algorithm in which receptive fields are represented using three vectors; the first one encodes the number of receptive fields to be used, the second one contains the position of the receptive fields covering the range that can be achieved by the joint, and the last one contains the width of the respective receptive fields. An initial random solution (in terms of the number of receptive fields, their position over the defined range of possible values per joint, and their width) is supplied to the evolutionary algorithm. Through evolution, the evolutionary algorithm drives the population to promising regions of the searching space towards near-optimal solutions.

It is remarkable that an evaluation of a single trajectory takes 0.645s in an Intel Core Quad Q6600 2.4 GHz 4 GB RAM (the evaluation has been performed using MATLAB). An evaluation of the previously described benchmark takes 7.75 seconds; the evaluation of the whole population of 100 individuals takes almost 13 minutes. An evaluation of such a population of over 300 or more epochs/generations will take days. That means that finding an optimal solution in a reasonable time becomes a problem. Fortunately, the nature of the evolutionary algorithm is inherently suited to be parallelized, offering a straightforward way to be scaled up improving performance in terms of convergence time.[69,70] The main idea is to speed-up the execution times by sharing the workload of the individuals among a pool of processors. To overcome the issue of computational time, a global parallel evolutionary algorithm has been implemented. This approach takes advantage of the parallelism at an evaluation level in the case of a very demanding fitness evaluation function (as is the case in this work). Global parallelization consists in the parallel evaluation of the individuals (i.e. candidate solutions),[71] usually following a master-slave model. The algorithm runs on the master node and the individuals are sent for evaluation to the slaves. Additionally, the master is responsible for collecting the results and applying the genetic operators.

In order to conduct the experiments, a 14 node computer cluster has been used. Each node has two Xeon E5320 processors at 1.86GHz, with four nuclei and 4 GBs of RAM at each node.

3. Results

This Results section is focused in how to validate this new proposed methodology. Therefore, this section is structured in different steps showing how this methodology should be applied when it is particularized for a certain experiment.

Towards this aim, firstly, a predictable trajectory has been used, that is, a rectilinear trajectory (Fig. 4). If the results of the evolved set of receptive fields, obtained with this simplified problem, are suitable and consistent, it will be possible to extrapolate the followed methodology to an extension of the problem over different trajectories.

At this point, it is important to define specific metrics to evaluate how good a solution is. The Metrical Discrimination Analysis plays a fundamental role in the

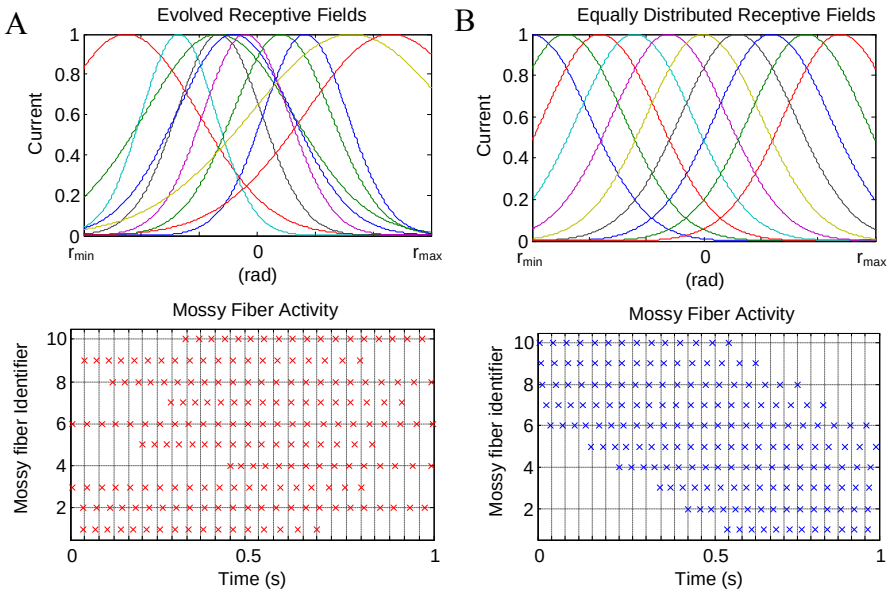

Fig. 6. Ten Evolved Receptive Fields vs. Ten Equally distributed Receptive Fields. The trajectory represented in Fig. 4.A is used as an input of the evolvable receptive fields whose final configuration is driven by the genetic algorithm (GA). A) Evolved receptive fields generate a population coding that ensures a maximal fitness of Eq. (12). (Fitness 0.0434 instead of 0.0 in the equidistant solution). A none zero D_{vr} means that we have a set of spikes that represent the coding of the executed trajectory in unambiguous way (each time window has its own unique spike train representation that implies that any spike train can be distinguished from any other). The higher the fitness is, the more separated representation we have (a spike train is distanced from any other spike train of the whole set as much as possible). This involves that we can distinguish a spike train from any other sooner and more robustly in the presence of noise.

interpretation of the results (in terms of spike generation) and therefore, the evaluation of the obtained solutions. We have included a subsection with the Metrical Discrimination Analysis within the Results section to make the reading more understandable.

3.1. *Metrical analysis*

In order to abstract the strategy behind the evolved values of the receptive fields, we work in a scenario in which D_{vr} (r_i, r_j) is linear. In this case, if D_{vr} (r_i, r_j) were linear, the way in which spikes would be distributed to maximize the distance between each other should be equidistant. An optimal distribution under linear assumption of the "cost" function D_{vr} in the mossy fiber number 1 of the Fig. 6.A. would be a single spike in each time window (0.04s) with a relative separation of 0.0016 second (time window/number of windows) from the previous time window spike time. The optimal relative distance between spikes in mossy fiber 1 would be 0.0016s. This process should be repeated trough the other mossy fibers obtaining a value of 0.0016 · number of mossy fibers (in our case 0.0016·10). Translating this value into van Rossum distance (t_c=*TimeWindow*); the obtained intra-stimulus-value is D_{vr} $(s_0, s_{0.0016})$ = 0.0392 · number of mossy fibers. As it was previously established, this result would correspond to a linear cost function, but D_{vr} is essentially an exponential cost function, which means that the obtained result cannot be used as an accurate optimum but, at least, it can be used as a non-feasible upper bound for the fitness value the evolutionary algorithm could achieve.

The trajectory shown in Fig. 4.A is used as the only input that feeds the evolvable receptive fields. The evolutionary algorithm, after 1500 epochs/generations of evolution using a population of 100 individuals, obtains a feasible near-optimal distribution (Fig. 6.A.). As it is shown, receptive fields which are placed near range extremes [r_{max}-r_{min}] have a wider tail in comparison to equally distributed receptive fields (general solution) in which receptive fields around range extremes are under-utilized. The evolutionary algorithm optimizes the width of the receptive field at the extremes with two purposes;

to cover a wider area and to provide a spike contribution in a more extended range. The evolutionary algorithm also distributes central receptive fields in an equally distributed way but with different widths; equally distributed central fields ensure proper range coverage in a rectilinear trajectory, different widths make distances between different stimuli not linearly related with the estimation being encoded.

3.1.1. Metrical discrimination analysis

In order to validate the previously presented EA optimization process, a metrical analysis is needed to have a proper tool for discerning a good solution from a bad one.

A metrical discrimination analysis allows us to numerically measure the main features of a given solution. As was established in Section 2.4, the desirable objective to achieve, broadly speaking is to generate a spike population set over time that represents the current sensorial state in an unambiguous way. That is, each sensorial state (trajectory state) should have a sole spike train representation which differentiates it from others. Consequently, it is necessary to prove that the evolved solution presents this discrimination feature between spike trains. Numerically, the EA maximizes the fitness function to enhance inter-stimulus distance. As a result, a given number representing this fitness is obtained, but, how does this inter-stimulus distance behave over time? How long does the discrimination between spike trains take? How can we evaluate that we have obtained an unambiguous spike train representation?

The metrical discrimination analysis of Eq. (13) gives answer to these questions.

$$\left[\Phi_{max|min}\right]_{i_{(1,1)},j_{(i+1,1)}}^{i_{(nTimeWindow-1,nStep)},j_{(nTimeWindow,nStep)}}. \quad (13)$$

Where *j* and *i* are the sub-indexes that indicate the pair of selected spike trains to calculate the van Rossum distance D_{vr} (r_i, r_j). *nStep* is the integration step number within a time window. For instance, a time window of 40ms, assuming an integration step of 1ms, has 40 steps, i.e. *nStep* runs from 1 to 40. Finally, n*TimeWindow* is the index within the number of time windows into which a certain trajectory can be divided. For instance, a 1s trajectory can be divided in 25 time windows of 40ms each (thus, *nTimeWindow* runs from 1 to 25). As an example, $r_i=(1,1)$ value corresponds to the set of spikes belonging to the first spike train of the first time window

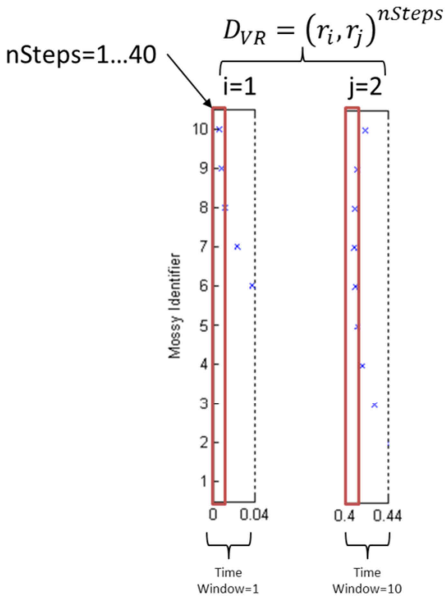

Fig. 7. Metrical discrimination analysis. Van Rossum distance is calculated between two spike trains (r_i, r_j) of different time windows (i, j) along *n* integration Steps within their corresponding time windows.

(0s to 0.04s) that are located in the first integration step (0s to 0.001s) (Fig. 7).

Since the stimulus changes along the trajectory, we can measure the inter-stimulus-distance in each time window. The first spike train belonging to the first 0.04s time window is compared with the second spike train belonging to the second 0.04s time window. The first spike train is then compared consecutively with the third spike train, then with the fourth, and so on. After this, the second spike train is compared successively with the third, the fourth, the fifth spike train, and so on. And this is repeated for each spike train, thus making an exhaustive comparison process.

As a result, a *minimal-inter-stimulus-distance* curve is obtained. As it is shown in Fig. 8.A, Eq. (13) is applied to the EA solution (Fig. 6.A). We can see the *minimal-inter-stimulus-distance* behavior. Considering a 40ms time window, we can ensure that it takes 34ms (first non-zero value for minimal-inter-stimulus-distance) to distinguish any two spike trains (i.e. the actual state –joint angle- in the trajectory) of the generated spike set when a rectilinear trajectory is performed and the state variables (joint angle in these experiments) are translated into spikes through the evolved receptive fields given by the EA. A non-zero value for minimal-inter-stimulus-distance means a

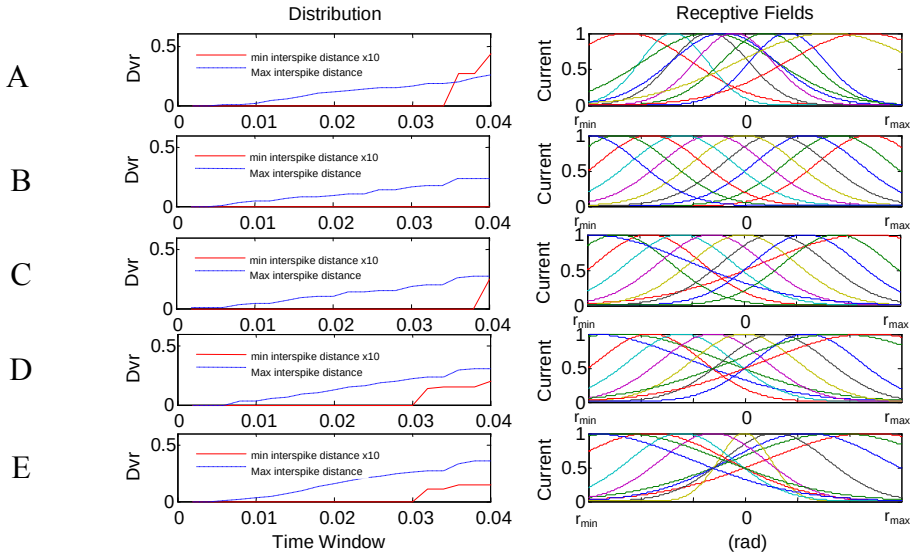

Fig. 8. Inter-stimulus distribution function for different receptive fields illustrates the discrimination capability of the system (a 10 scale factor has been used to better plot the *minimal-inter-stimulus-distance* in the left panels). A) Evolved receptive fields. B) Equally distributed receptive fields. C) and D) Equally distributed receptive fields with a better coverage at both ends of the range. E) Equally distributed receptive fields with a decreasing coverage of the range from the ends to the center.

perfect discrimination. The earlier this non-zero value is obtained, the sooner it is possible to distinguish a spike train from any other. That means that we can ensure a perfect discrimination between any two spike trains over any 40ms time window because discrimination actually takes time before 34 ms.

We can also verify that the *maximum minimal-inter-stimulus-distance* is 0.0434 and it is achieved around 40ms. This maximum value represents an estimate of how easy the discrimination between different stimuli becomes in different time windows (sensory states).

To establish a comparison, this solution has been compared against other four solutions; an equally distributed receptive field solution (Fig. 8.B), two different equally distributed receptive field solutions with a better coverage at both ends of the range (Fig. 8.C and 8.D), and finally, an equally distributed receptive field solution with a decreasing coverage of the range from the ends of the range to the center. The second solution is a hand-calibrated solution; the third and fourth solutions try to emulate the behavior of the solution obtained by the EA. Receptive fields placed near both ends of the range are modified in order to ensure a better response to initial and final trajectory segments and the fifth solution not only tries to mimic the behavior of the EA solution at both ends of the range and also the behavior at central range positions, the receptive field width is modified from the range of extreme positions to the center position; the higher the distance of the receptive field center from the range center value, the wider receptive field is used. Different widths covering center range values ensure quite different responses to slightly different entries.

As is shown in Fig. 8.A, in order to distinguish any two spike trains (microstates) of the generated set, it takes over 0.034s. A maximum of 0.434 (0.0434 · numMossyFibers) in the *minimal-intra-stimulus-distance* is achieved (this value is consistent with the result obtained by the EA solution). Fig. 8.B shows a constant zero *minimal-inter-spike-distance*; equally, distributed receptive fields are not able to properly discriminate two spike trains of the generated spike set.

On the other hand, although solutions of Fig. 8.C and Fig. 8.D really do a discrimination between spike trains (*minimal-inter-stimulus-distance* does not remain constantly zero) even sooner than the evolved solution (Fig. 8.D at 0.03s), neither of them achieves a maximum value of the *minimal-inter-stimulus-distance* near 0.434. The obtained maximum values are around 50% lower, so a better coverage of the whole range is implemented by the evolved solution.

Finally, the last solution (Fig. 8.E) shows the same problem as the previous one, whereas a discrimination is possible even sooner than the evolved solution and the

maximal-inter-stimulus-distance is better than Fig. 8.C and Fig. 8.D (blue dashed curve), the maximum value of the *minimal-inter-stimulus-distance* is 66% less than the evolved solution. The evolved solution still represents a better way to cover the whole range of joint angles; the evolved solution not only ensures a perfect discrimination between spike stimuli but also ensures a maximal distance between their spike representations (Fig. 9).

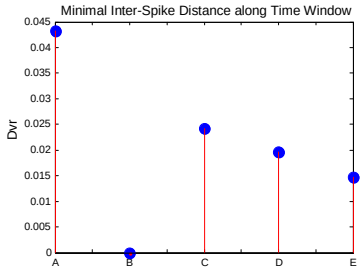

Fig. 9. Minimal-inter-stimulus-distances (D_{vr}) achieved at time 0.04s by different by different receptive field distribution solutions. Cases A, B, C, D, and E corresponding to the respective A, B, C, D, and E solutions illustrated in Fig. 8.

3.2. *Analysis of evolved receptive fields in multiple trajectories*

Once the proposed methodology has been shown to succeed in a single-trajectory scenario, now the EA based optimization methodology is generalized to different trajectories. All the trajectories illustrated in Fig. 1 are used.

In this scenario, the solutions will not be easily compared to manually handcrafted ones capturing the essence of the evolved solutions. The EA has been set to manage up to 30 possible receptive fields to be conjointly evolved. After the EA evolves a population of 100 individuals over 2000 epochs, a final evolved solution is obtained as is shown in Fig. 10. Fig. 10.C shows the resulting receptive fields after the optimization process.

We can see that the EA has concentrated the receptive field distribution in the $[2/3r_{max}\text{-}2/3r_{min}]$ range. In this range region, the majority of the trajectories have sharp changes in their values; having a pretty concentrate centroid distribution right in $[2/3r_{max}\text{-}2/3r_{min}]$ values of the range ensures a proper population of sensitized neurons (their base current forces neurons to be closer to their firing state) to fast changes in the input value. That is, fast changes in trajectory values involve very different generated spike trains, which is what we are looking for in this area.

On the other hand, at the end of the range values, the EA has increased the width of the receptive fields providing a sparse distribution of them. Placing those wide receptive fields at the ends of the range is a way to distinguish the extreme areas in the spiking code. This involves that, at least, immediately, one neuron is firing in this area, being accompanied by the rest of firing neurons with certain delays no longer than 40ms (time windows) due to the width of the central receptive fields. Central receptive fields are wide enough to be sensitive

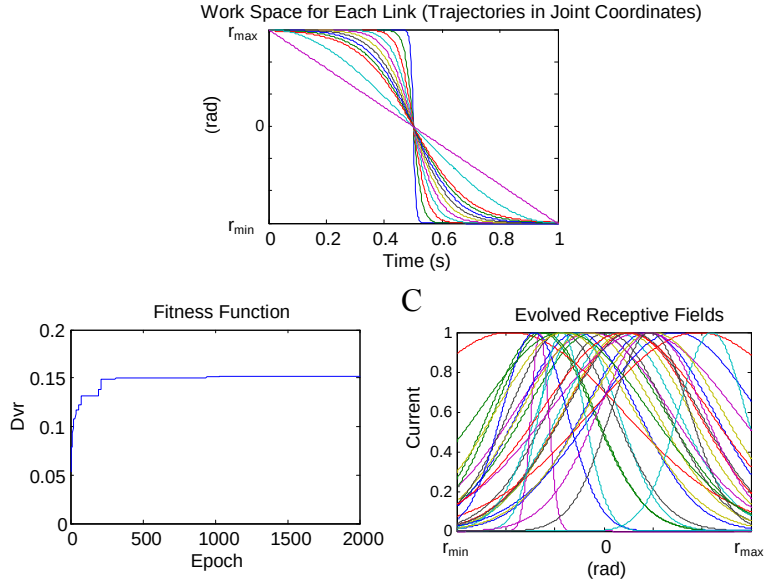

Fig. 10. Evolved receptive field solution. A) The EA uses the multiple trajectory benchmark to cover the defined workspace $[r_{max}-r_{min}]$. Through evolution, the EA obtains a receptive field distribution that ensures discrimination between any spike-train mossy fiber produces (Fig. 2). B) Fitness evolution. Fitness curve converges properly after 1000 epochs. C) Final evolved distribution of the receptive fields.

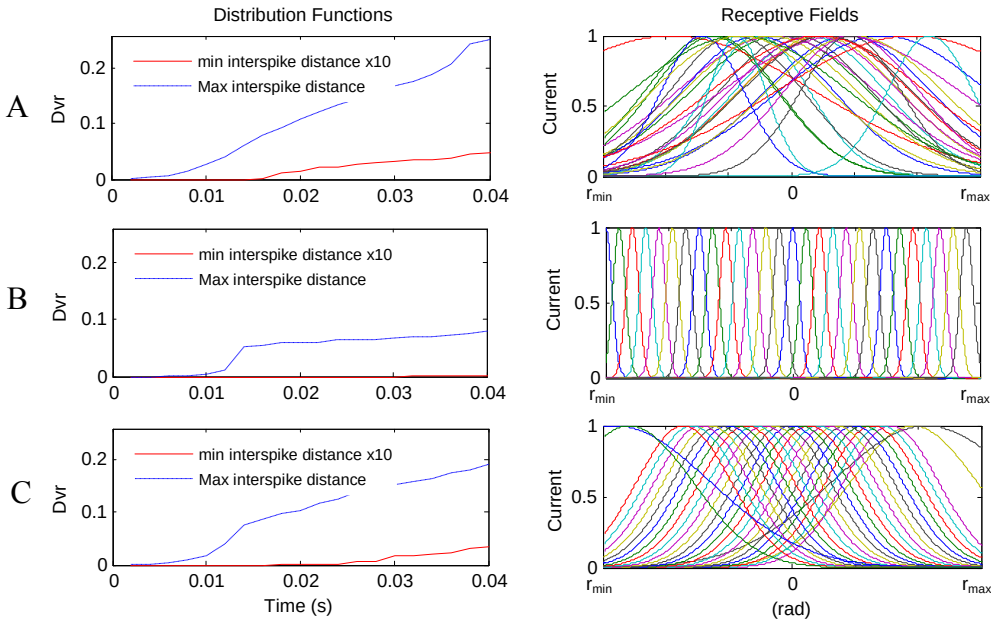

Fig. 11. Inter-stimulus distribution obtained by the EA using the whole set of benchmark trajectories. A) Evolved receptive fields. B) Equally distributed receptive fields. C) Equally distributed receptive fields with a better coverage at both ends and in interval [$2/3r_{max}$-$2/3r_{min}$] of the range.

to input values belonging to both ends of the range areas.

3.2.1. Metrical discrimination analysis

The metrical discrimination analysis extended to the multiple trajectories benchmark is given by Eq. (14).

$$\frac{1}{n}\sum_{1}^{n}\left[\Phi_{max|min}\right]_{i_{(1,1)},j_{(i+1,1)}}^{i_{(nTimeWindow-1,nStep)},j_{(nTimeWindow,nStep)}}. \quad (14)$$

Where j and i are the sub-indexes that indicate the pair of selected spike trains to calculate the van Rossum distance D_{vr} *(*r_i*,* r_j*)*. As previously described, *nStep* is the integration step number within a time window. *nTimeWindow* is an index within the number of time windows in which a certain trajectory can be divided into, and finally, *n* is the number of the trajectories of the benchmark. This equation is computed once in every trajectory obtaining a set of curves (a curve per trajectory). Each curve represents the behavior of the *minimal-inter-stimulus-distance* over each 0.04ms time window along the trajectory (using the receptive field solution given by the EA). As it was done in Section 3.1, the spike train set generated by a trajectory is computed according to Eq. (13). As a result, a *minimal-inter-stimulus-distance* curve is obtained per trajectory.

A final mean curve is calculated using this set of minimal-inter-stimulus-distance curves applying Eq. (14). As it is shown in Fig. 11, the evolved solution has been compared against a designed solution which consists of equally distributed receptive fields (other equally distributed solutions with different RF widths were tested but these experiments did not provide any new further information) and also, to a solution manually implemented which tries to emulate the EA solution. This illustrates how the EA solution itself can be used, or how it is also possible to try to emulate it (after interpreting it) towards designing efficient hand-crafted solutions based on the EA guidance.

Fig. 11.A shows the evolved solution and its performance. The discrimination condition between any pair of spike trains from the generated spike set using evolved receptive fields is possible after 0.014s in average with a maximum at the *minimal-inter-stimulus-distance* of D_{vr}=0.0476. In contrast, the equally distributed receptive field standard solution presents a maximum value at *minimal-inter-stimulus-distance* of D_{vr}=0.00138. The discrimination between any pair of spike trains is possible after 0.032s on average. These values are clearly improved by the evolved solution. Finally, equally distributed receptive fields with a better

coverage at both ends and in interval [$2/3r_{max}$ -$2/3r_{min}$] of the range are able to discriminate any pair of spike trains from the generated spike set after 0.018s on average. The maximum value of the *minimal-inter-stimulus-distance* at each time window is D_{vr} =0.0356. This maximum value of the *minimal-inter-stimulus-distance* is larger in the evolved solution than in the others; therefore, the discrimination process is not only executed sooner, but also with higher *inter-stimulus-distance* values (which represent a larger margin that is useful in the case of noise in the sensory signal estimation). The EA solution not only ensures an earlier discrimination between spike trains, but also increases the distance between any pair of spike trains.

4. Conclusions

A methodology for efficiently representing incoming encoder signals from different links in terms of spikes in a plausible robot scenario is presented. Several approaches in controlling robots with cerebellum-like networks have been proposed in the literature[26-29] (all of them keeping classical control theory in mind). Little attention has been given to efficient sensory representation in these approaches. To that aim, an evolutionary algorithm as an optimization engine has been proposed in this contribution. In this way, a goal function that captures how sensory information can be efficiently represented in terms of spike trains was defined, maximizing the *minimal-inter-stimulus-distance* when performing movements (benchmark trajectories). In the framework of experiments with cerebellar based robot control[1-3,13,72,73] or other bio-inspired experiments, [74,75] the presented contribution will allow at initial stages of the adaptation mechanisms of the cerebellum to distinguish more accurately specific instants along the trajectories in which potential corrections or actions need to be performed.

The receptive fields in our sensory input layer have been evolved. We focus on the way in which these receptive fields have to be distributed both to encode each sensorial state in an unambiguous way and to enhance information transfer (in terms of entropy) between mechanoreceptor signals and their spike representations. The receptive field configuration task is carried out by the aforementioned Evolutionary Algorithm. Such an algorithm evolves receptive fields along the robot-link work space according to a goal function that takes into account the metrical properties of the spike train space.

Beyond this specific contribution, this work also presents a general methodology of using EAs for optimization purposes when addressing reverse engineering of biological systems. In this scenario, it is important to implement a goal function that captures the essence of attributed properties of the system which is being optimized. In our case, the goal function is the optimization of sensory representation in terms of spikes with inter-spike discrimination capability along movement trajectories. This required the definition of a metric to allow the evaluation of the different candidate solutions, in order to derive a final fitness function for the EA. The definition of a fitness function that allows convergence through an EA is not straight forward; it required a preliminary experimental stage in which preliminary simulations where done with a single trajectory in which the results (and obtained solutions in terms of receptive field configuration) were easy to interpret. The searching space in this kind of problems and the computational cost of spike train distances may require the parallelization of the EA, as it has been done in this work.

This technique will be included into robotic experiments with cerebellar like modules as corrective engines to evaluate how an optimal sensory representation facilitates an effective adaptation at the cerebellum. Thus, it will be applied to object manipulation experiments with an adaptive cerebellar-like module. In previous experimental studies[76-78], the translation from analog robotic sensory signals to spike trains has been done manually (through a manually designed receptive filter configuration) to facilitate an easy discrimination when performing different trajectories.

We will also apply the presented technique to tactile sensors[79-82] to maximize information transmission as discrimination between microstates in the framework of sensing tasks.

We will also study the possibility of introducing an STDP[83] law that increases the performance of the evolved system in such sensing task frameworks. Furthermore, we will apply other parallel optimization schemes[84,85] in order to scale up the complexity of the representations that can be studied.

Acknowledgements

This work has been supported by the EU grant REALNET (FP7-IST-270434) and national projects ARC-VISION (TEC2010-15396), MULTIVISION (TIC-3873), and ITREBA (TIC-5060).

References

1. R.R. Carrillo, E. Ros, C. Boucheny and O.J.–M.D. Coenen, A Real-time Spiking Cerebellum Model for Learning Robot Control, *Biosystems* **94** (1-2) (2008)18–27.
2. R.R. Carrillo, E. Ros, B. Barbour, C. Boucheny and O.J.–M.D. Coenen, Event-driven Simulation of Neural Population Synchronization Facilitated by Electrical Coupling, *Biosystems* **87** (2-3) (2007) 275–80.
3. C. Boucheny, R.R Carrillo, E. Ros and O.J.–M.D. Coenen, Real-time Spiking Neural Network: an Adaptive Cerebellar Model, *LNCS* **3512** (2005) 136–44.
4. E. Nichols, L.J. McDaid and N.H. Siddique, Case Study on Self-organizing Spiking Neural Networks for Robot Navigation, *Int. J. Neural Syst.* **20** (6) (2010) 501–8.
5. S.P. Johnston, G. Prasad, L. Maguire and T.M. McGinnity, An FPGA Hardware/software Co-design Methodology Towards Evolvable Spiking Networks for Robotics Application, *Int. J. Neural Syst.* **20** (6) (2010) 447–61.
6. S. Ghosh-Dastidar and H. Adeli, Spiking Neural Networks, *Int. J. Neural Syst.* **19** (4) (2009) 295–308.
7. S. Ghosh-Dastidar and H. Adeli, Improved Spiking Neural Networks for EEG Classification and Epilepsy and Seizure Detection, *Integr. Comput-Aid E.* **14** (3) (2007) 187–212.
8. S. Ghosh-Dastidar and H. Adeli, A New Supervised Learning Algorithm for Multiple Spiking Neural Networks with Application in Epilepsy and Seizure Detection, *Neural Networks* **22** (10) (2009) 1419–31.
9. J. Iglesias and A.E.P. Villa, Emergence of Preferred Firing Sequences in Large Spiking Neural Networks During Simulated Neuronal Development, *Int. J. Neural Syst.* **18** (4) (2008) 267–77.
10. S. Soltic and N. Kasabov, Knowledge Extraction from Evolving Spiking Neural Networks with Rank Order Population Coding, *Int. J. Neural Syst.* **20** (6) (2010) 437–45.
11. A. Vidybida, Testing of Information Condensation in a Model Reverberating Spiking Neural Network, *Int. J. Neural Syst*. **21** (3) (2011) 187–98.
12. A.F. Jahangiri and D.M. Durand, Phase Resetting of Spiking Epileptiform Activity by Electrical Stimulation in the CA3 Region of the Rat Hippocampus, *Int. J. Neural Syst*. **21** (2) (2011) 127–38.
13. J.B. Passot, N. R. Luque and A. Arleo, Internal Models in the Cerebellum: a Coupling Scheme, *LNAI* **6226** (2010) 435–46.
14. M. Ito, The Cerebellum and Neural Control, *New York, Raven Press* (1984).
15. M. Kawato, K. Furukawa and R. Suzuki, A Hierarchical Neural-Network Model for Control and Learning of Voluntary Movement, *Biol. Cybern.* **57** (3) (1987) 169–85.
16. D.M. Wolpert, R.C. Miall and M. Kawato, Internal Models in the Cerebellum, *Trends Cog. Sci.* **2** (9) (1998) 338–47.
17. R. M. C. Spencer, R.B. Ivry and H.N. Zelaznik, Role of the Cerebellum in Movements: Control of Timing or Movement Transitions?, *Exp. Brain res.* **161** (2005) 383–96.
18. M. Desmurget and S. Grafton, Forward Modeling Allows Feedback Control for Fast Reaching Movements, *Trends Cog. Sci.* **4** (11) (2000) 423–31.
19. M.R. Delong and P.L. Strick, Relation of Basal Ganglia, Cerebellum, and Motor Cortex, *Brain Res.* **71** (1974) 327–35.
20. G. Hinton, Parallel Computations for Controlling an Arm, *J. Mot.Behav.* **16** (1984) 171–94.
21. J.R. Flanagan, *et. al.*, Control of Trajectory Modifications in Target-Directed Reaching, *J. Mot. Behav.* **25** (1993) 140–52.
22. J. Butterfaß, M. Grebenstein, H. Liu and G. Hirzinger, *DLR Hand II: Next Generation of a Dextrous Robot Hand*, (ICRA, 2001).
23. A. Albu-Schäffer, *et al.*, The DLR Lightweight Robot: Design and Control Concepts for Robots in Human Environments, *Int. J. Ind. Robot* **34** (5) (2007) 376–85.
24. A. De Luca and B. Siciliano, Closed-Form Dynamic Model of Planar Multilink Lightweight Robots, *Syst. Man and Cybern., IEEE Trans.* **21** (4) (1991) 826–39.
25. P. van der Smagt, F. Groen and K. Schulten, Analysis and Control of a Rubbertuator Arm, *Biol. Cybern.***75** (5) (1996) 433–40.
26. J. S. Albus, Data Storage in the Cerebellar Model Articulation Controller (CMAC), *J. Dyn. Syst. Meas. Contr. ASME* **3** (1975) 228–33.
27. J.C. Houk, J.T. Buckingham and A.G. Barto, Models of the Cerebellum and Motor Learning, *Behav. Brain. Sci.* **19** (3) (1996) 368–83.
28. N. Schweighofer, Computational Models of the Cerebellum in the Adaptive Control of Movements. *Ph.D. thesis* (1995).
29. P. van der Smagt, Cerebellar Control of Robot Arms, *Connect. Sci.* **10** (1998) 301–20.
30. P. van der Smagt, Benchmarking Cerebellar Control, *Robot. Auton. Syst.* **32** (2000) 237–51.
31. J. R. Flanagan and A.M. Wing, The Role of Internal Models in Motion Planning and Control: Evidence from Grip Force Adjustments, *J. Neurosci.* **17** (1997) 1519–28.
32. S. Keele, R. Ivry and R. Pokorny, Force Control and Its Relation to Timing, *J. Mot. Behav.* **19** (1987) 96–114.
33. R. C. Miall, D.J. Weir, D.M. Wolpert and J.F. Stein, Is the Cerebellum a Smith Predictor?, *J. Mot. Behav.* **25** (1993) 203–16.
34. M. Ito, Neurophysiological Aspects of the Cerebellar Motor Control System, *Int. J. Neurol.* **7** (1970)162–76.
35. M. Kawato and H. Gomi, A Computational Model of Four

Regions of the Cerebellum Based on Feedback-Error Learning, *Biol.Cybern.* **68** (1992) 95–103.

36. N. Schweighofer, M.A. Arbib and M. Kawato, Role of the cerebellum in reaching movements in human. I. Distributed Inverse dynamics control, *European J. Neurosci.* **10** (1998) 86–94.
37. M. Glickstein, *The Cerebellum: From Structure to Control, Mossy-fibre Sensory Input to the Cerebellum* (Elsevier, Progress in Brain Research, 1997).
38. J. R. Bloedel and J. Courville, *Handbook of Physiology, The Nervous System, Motor Control. Cerebellar Afferent Systems* (John Wiley and Sons, Inc., 2011).
39. M. Glickstein *et al.*, Visual Pontocerebellar Projections in the Macaque, *J. Comp. Neurol.* **349** (1) (1994) 51–72.
40. C. R. Legg, B. Mercier and M. Glickstein, Corticopontine Projection in the Rat: the Distribution of Labelled Cortical Cells after Large Injections of Horseradish Peroxidase in the Pontine Nuclei, *J. Comp. Neurol.* **286** (4) (1989) 427–41.
41. P. Brodal, The Corticopontine Projection from the Visual Cortex in the Cat. I. The Total Projection and the Projection From Area 17, *Brain Res.* **39** (2) (1972) 297–317.
42. P. Brodal, The Corticopontine Projection from the Visual Cortex in The Cat. II. The Projection from Areas 18 and 19, *Brain Res.* **39** (2) (1972) 319–35.
43. M. Glickstein, J.G. 3er May and B.E. Mercier, Corticopontine Projection in the Macaque: The Distribution of Labelled Cortical Cells after Large Injections of Horseradish Peroxidase in the Pontine Nuclei, *J. Comp. Neurol.* **235** (3) (1985) 343–59.
44. G. Nyberg and A. Blomqvist, The Central Projection of Muscle Afferent Fibres to the Lower Medulla an Upper Spinal Cord: An Anatomical Study in the Cat with the Transganglionic Transport Method, *J. Comp. Neurol.* **230** (1) (1987) 99–109.
45. v. P. L. Kan, A. R. Gibson and J.C. Houk, Movement-Related Inputs to Intermediate Cerebellum of the Monkey, *J. Neurophysiol.* **69** (1) (1993) 74–94.
46. P.D. Mackie, J.W. Morley and M.J. Rowe, Signalling of Static and Dynamic Features of Muscle Spindle Input by External Cuneate Neurons in the Cat, *J. Physiol.* **519** (2) (1999) 559–69.
47. J. Baker, A. Gibson, M. Glickstein and J. Stein, Visual Cells in the Pontine Nuclei of the Cat, *J. Physiol.* **255** (2) (1976) 415–33.
48. S.Wu, S. Amari and H. Nakahara, Population Coding and Decoding in a Neural Field: A Computational Study, *Neural Comp.* **14** (2002) 999–1026.
49. A. Pouget, P. Dayan and R. Zemel, Information Processing with Population Codes, *Nature Rev. Neurosci.* **1** (2000) 125–32.
50. T. Flash and T.J. Sejnowski, Computational Approaches to Motor Control, *Curr. Opin. Neurobiol.* **11** (6) (2001) 655–62.
51. B. Amirikian and A.P. Georgopoulos, Directional Tuning Profiles of Motor Cortical Cells, *Neurosci.* **36** (2000) 73–9.
52. R. S. Johansson and I. Birznieks, First Spikes in Ensembles of Human Tactile Afferents Code Complex Spatial Fingertip Events, *Nature. Neurosci.* **7** (2004) 170–7.
53. R. S. Johansson and J. R. Flanagan, Coding and Use of Tactile Signals from the Fingertips in Object Manipulation Tasks, *Nature Reviews Neurosci.* **10** (2009) 345–59.
54. S. Schliebs, N. Kasabv and M. Defoin-Platel, On the Probabilistic Optimization of Spiking Neural Networks, *Int. J. Neural Syst*. **20** (6) (2010) 481–500.
55. J.J. Craig, *Introduction to Robotics, Mechanics and Control*, 3rd ed. (Pearson Education, Inc., New Jersey, 2005).
56. D.M. Wolpert, Z. Ghahramani and M.I. Jordan, An Internal Model for Sensorimotor Integration, *Science* **269** (1995) 1880–2.
57. S. J. Goodbody and D.M. Wolpert, Temporal and Amplitude Generalization in Motor Learning, *J. Neurophysiol.* **79** (1998) 1825–38.
58. D.R. Boff and J.E. Lincoln, *Engineering Data Compendium: Human Perception and Performance.* (AAMRL, 1988).
59. N.V. Swindale, Orientation Tuning Curves: Empirical Description and Estimation of Parameters, *Biol. Cybern.* **78** (1) (1998) 45–56.
60. W. Gerstner and W. Kistler, *Spiking Neuron Models* (Cambridge University, Cambridge, 2002).
61. A.E. Eiben and J.E. Smith, *Introduction to Evolutionary Computing* (Springer Verlag, 2003).
62. E. Alfaro-Cid, et al., Comparing Multiobjective Evolutionary Ensembles for Minimizing Type I and II Errors for Bankruptcy Prediction (*IEEE Congress on Evol. Comp*., 2008).
63. L. Trujillo and G. Olague, Automated Design of Image Operators that Detect Interest Points, *Evol. Comp.* **16** (2008) 483–507.
64. R. Brasselet, R.S. Johansson and A. Arleo, Optimal Context Separation of Spiking Haptic Signals by Second-Order Somatosensory Neurons, *Adv. Neural Information Processing System* **22** (2009) 180–8.
65. R. Brasselet, R.S Johansson and A. Arleo, Quantifying Neurotransmission Reliability Through Metrics Based Information Analysis, *Neural Comp.* **23** (4) (2011) 852–81.
66. M.C.W. van Rossum, A Novel Spike Distance, *Neural Comp.* **13** (2001) 751–63.
67. J.D. Victor and K.P. Purpura, Nature and Precision of Temporal Coding in Visual Cortex: A Metric-Space Analysis, *J. Neurophysiol.* **76** (1996) 1310–26.
68. J.D. Victor and K.P. Purpura, Metric-Space Analysis of spike Trains: Theory, Algorithms, and Application, *Network* **8** (1997) 127–64.
69. E. Alba and M. Tomassini, Parallelism and Evolutionary Algorithms, *Evol. Comp., IEEE Trans.* **6** (5) (2002) 443–62.
70. M., Tomassini, *Spatially Structured Evolutionary*

Algorithms (Springer, 2005).

71. E. Cantu-Paz, A Survey of Parallel Genetic Algorithms, Calculateurs Paralleles*, Reseaux et Systems Repartis* **10** (2) (1998)141–71.
72. J. Porrill, P. Dean and J.V. Stone, Recurrent Cerebellar Architecture Solves the Motor-Error Problem, *Proc. Biol. Sci.* **271** (1541) (2004) 789–96.
73. M. Fujita, Adaptive Filter Model of the Cerebellum, *Biol. Cybern.* **45** (3) (1982) 195–206.
74. T. Yamazaki and S. Tanaka, The Cerebellum as a Liquid State Machine, *Neural Networks* **20** (2007) 290–7.
75. T. Yamazaki and S. Tanaka, Neural Modeling of an Internal Clock, *Neural Comp.* **17** (5) (2005) 1032–58.
76. N. R. Luque, J. A. Garrido, R.R. Carrillo, O.J.–M.D. Coenen and E. Ros, Cerebellar Input Configuration Toward Object Model Abstraction in Manipulation Tasks, *Neural Networks IEEE Trans.* **22** (8) (2011) 1321–8.
77. N. R. Luque, J.A. Garrido, R.R. Carrillo, O. J.–M.D. Coenen and E. Ros, Cerebellar-Like Corrective-Model Abstraction Engine for Robot Movement Control. *Syst. Man and Cybern., IEEE Trans. – Part B* **41** (5) (2011) 1299–312.
78. N.R. Luque, J.A. Garrido, R.R. Carrillo, S. Tolu and E. Ros, Adaptive Cerebellar Spiking Model Embedded in the Control Loop: Context Switching and Robustness Against Noise, *Int. J. Neural Syst.* **21** (5) (2011) 385–401.
79. F. Vidal-Verdú, M.J. Barquero, J. Castellanos-Ramos, R. Navas-González, J.A. Sánchez, J. Serón and A. García-Cerezo, A Large Area Tactile Sensor Patch Based on Commercial Force Sensors, *Sensors* **11** (2011) 5489–507.
80. F. Vidal-Verdú, O. Oballe-Peinado, J.A. Sánchez-Durán, J. Castellanos-Ramos and R. Navas-González, Three Realizations and Comparison of Hardware for Piezoresistive Tactile Sensors, *Sensors* **11** (3) (2011) 3249–66.
81. J. Castellanos-Ramos, B. Navas-González, H. Macicior, T. Sikora, E. Ochoteco and F. Vidal-Verdú, Tactile Sensors Based on Conductive Polymers, *Microsyst. Technol.* **5** (2010) 765–76.
82. R. Maldonado-López, F. Vidal-Verdú, G. Liñán and A. Rodríguez-Vázquez, Integrated Ciruitry to Detect Slippage Inspired by Human Skin and Artificial Retinas. *Circuits-I, IEEE Trans.* **56** (2009) 1554–65.
83. T.J. Strain, L.J. McDaid, L.P. Maguire, and T.M. McGinnity, An STDP Training Algorithm for a Spiking Neural Network with Dynamic Threshold Neurons, *Int. J. Neural Syst.* **20** (6) (2010) 463–480.
84. J.L. Redondo, I. García and P.M. Ortigosa, Parallel Evolutionary Algorithms Based on Shared Memory Programming Approaches, *J. Supercomp*. 1 (2009) 1–10.
85. J.L. Redondo, B. Pelegrín, P. Fernández, I. García, and P.M. Ortigosa, Finding Multiple Global Optima for Unconstrained Discrete Location Problems, *Optim. Methods Softw.* **26** (2) (2011) 207–24.